Designing of Biospecific Nanoparticles for Advanced Drug Delivery Applications

Y.M.Thasneem

Ph.D. THESIS
2014

SREE CHITRA TIRUNAL INSTITUTE FOR MEDICAL
SCIENCES AND TECHNOLOGY
THIRUVANANTHAPURAM
INDIA

Designing of Biospecific Nanoparticles for Advanced Drug Delivery Applications

A THESIS PRESENTED BY

Y.M. Thasneem

TO

SREE CHITRA TIRUNAL INSTITUTE FOR MEDICAL
SCIENCES AND TECHNOLOGY
THIRUVANANTHAPURAM
INDIA

IN PARTIAL FULFILMENT OF THE REQUIREMENTS
FOR THE AWARD OF
DOCTOR OF PHILOSOPHY

2014

DECLARATION

I, Y.M.Thasneem, hereby certify that I had personally carried out the work depicted in the thesis entitled, ***"Designing of Biospecific Nanoparticles for Advanced Drug Delivery Applications"***. No part of the thesis has been submitted for the award of any other degree or diploma prior to this date.

Thiruvananthapuram **Y.M.Thasneem**

9-10-2014 Reg No: PhD/2010/08

SREE CHITRA TIRUNAL INSTITUTE FOR MEDICAL SCIENCES & TECHNOLOGY, TRIVANDRUM

Thiruvananthapuram – 695011, INDIA
(An Institute of National Importance under Govt. of India)
Phone-(91)0471-2520248 Fax-(91)0471-2341814
Email: jayabalan@sctimst.ac.in Web site – www.sctimst.ac.in

CERTIFICATE

This is to certify that **Mrs. Y.M.Thasneem**, in the Biosurface Technology Division of this institute has fulfilled the requirements prescribed for the Ph. D. degree of the Sree Chitra Tirunal Institute for Medical Sciences and Technology, Thiruvananthapuram. The thesis entitled, ***"Designing of Biospecific Nanoparticles for Advanced Drug Delivery Applications"*** was carried out under my direct supervision. No part of the thesis was submitted for the award of any degree or diploma prior to this date.

* Clearance was obtained from the Institutional Ethics Committee/ Institutional Animal Ethics Committee for carrying out the study.

Thiruvananthapuram
9-10-2014

Dr. Chandra P Sharma PhD
(Research Supervisor)
Former Senior Scientist G & Head
Biomedical Technology Wing
SCTIMST
Thiruvananthapuram

The thesis entitled

"Designing of Biospecific Nanoparticles for Advanced Drug Delivery Applications".

Submitted by

Thasneem Y.M.

for the degree of

Doctor of Philosophy

Of

SREE CHITRA TIRUNAL INSTITUTE
FOR MEDICAL SCIENCES AND TECHNOLOGY,
THIRUVANANTHAPURAM - 695011

is evaluated and approved by

…….	……..
Dr. Chandra P Sharma	Examiner
(Research Supervisor)	

In love of my mother

and father .....

ACKNOWLEDGEMENT

In the name of Almighty, I begin and to whom I should return.

My thesis reflects the kind help and support of many individuals along with my humble efforts. I would like to extend my sincere thanks to all of them.

First of all, I express my gratitude towards my advisor, Dr. Chandra P Sharma, Senior Scientist G and Head, Division of Biosurface Technology-BMT Wing, SCTIMST. Dr. Sharma was a constant source of admiration, inspiration and encouragement throughout. He has initiated the urge within me to become an independent researcher. He has always welcomed my ideas, provided me the freedom to research and enriched me with his worldly wisdom and knowledge. It was only because of his kindness and support, I completed my Ph.D programme.

I am grateful to the former and present Director of SCTIMST and the present Head and the previous Heads, BMT Wing for all support provided during the course of my work.

No amount of words can adequately express the debt I owe to Dr. Sajeesh S, who taught me the basics of nanotechnology. He was always there to answer any question, no matter how trivial and provided solutions during critical events. I value his support immensely.

My deep respect and gratitude to my dear Madam, Dr. Rekha M.R. It was my honour to work with a scientist like her. Her dedication to science, her attention to minute details and her ethics in general has helped to shape myself as a researcher and as a good person.

The suggestions and advices of my advisor, Dr, Sharma, Dr. Sajeesh S and Dr. Rekha M.R. would be the guiding light through my research path and beyond.

I thank members of the doctoral advisory committee, Dr. Ramesh P, (Scientist F, Polymer Processing Laboratory), Dr. Annie John, (Scientist F, Transmission Electron Microscopy Lab) and Dr. Rekha M.R. (Scientist D, Biosurface Technology Division) for their timely suggestions and useful comments.

I am thankful to Dr. Sundar Jayasingh, Deputy Registrar, Dr. Prabha D. Nair, Associate Dean for PhD affairs, Dean, and all members of academic division and Director's office for their administrative support.

I am thankful to Dr. Lissy Krishnan and Mr. Ranjith Kartha for FACS analysis, Dr. T.V. Kumari, Dr. Anilkumar P.R and Ms. Deepa for providing L929 cell lines, Dr. H K Varma, Mr. Suresh, Mr. Nishad K V for FTIR analysis, Dr. Annie John and Ms. Susan for TEM analysis, Dr. Roy Joseph and Mr. Hari for providing lyophilisation facility, Dr. Jayabalan, Dr. Sunita Prem Victor, Dr. Anilkumar T V, Dr. Umashankar and Dr. Mira Mohanty for their kind help during the evaluations. Special regards to Mr. Willi Paul for AFM, DSC analysis and many other technical details.

I thank all my seniors, colleagues, juniors and friends from our laboratory and institute, for all their help and support. I cherish those discussions, laughter and togetherness all through my life.

Thanks to the staff of various administrative departments and library of the Institute and fellow students in the campus for their lively companionship.

I am thankful to UGC, DST and FADDS for fellowships and travel grant.

I would like to thank my ummy, Y. Mumtaz, for being there always, my papa, Y. Mujahid, for being my role model, my little brother, Y.M. Abdul Rahiman, for being my strength, my mother-in law, Nafeesa P, for being an ideal person whom I look upon. The faces of my loving grandparents, dear and near family members and my respectable teachers come to my mind. Without their blessings, prayers, support and encouragement, I could never accomplish this step in my life.

I further thank many, who directly or indirectly helped me to prepare this thesis.

Last but by no means least, I thank my husband, Jahfar Ali, for being my best friend and foe.

My humble prostration before Almighty, for providing me the right circumstances, the right people and the right opportunities. I thank HIM for enriching my life with the good and bad experiences.

Y.M. Thasneem

Contents

List of Figures

List of Tables

List of Abbreviations

ABC transporters	ATP-binding cassette transporters
ADP	Adenosine di phosphate
ASTM	American Society for Testing and Materials
BAX	Bcl-2- associated X protein
BCL-2	B-cell lymphoma-2
BCS	Biopharmaceutics Classification System
CD 11 b	Cluster of differentiation molecule 11 b
CVD	Cardiovascular disease
DCC	N,N'- Dicyclohexylcarbodiimide
DMEM	Dulbecco's modified eagle medium
DMF	Dimethylformamide
DMSO	Dimethyl sulfoxide
DNA	Deoxyribonucleic acid
DSC	Differential scanning calorimetry
EDC	1-Ethyl-3-(3-dimethylaminopropyl)carbodiimide
ELISA	Enzyme-linked immuno sorbent assay
EPR	Enhanced permeability and retention effect
FACS	Fluorescence activated cell sorting

FBGC	Foreign body giant cells
F_C receptor	Fragment, crystallisable receptor
F_C• R	Fragment, crystallisable gamma receptor
FDA	Food and Drug Administration
FTIR	Fourier Transform Infra Red Spectroscopy
GPIIB/IIIA	GlycoproteinIIB/IIIA
GTPase	Guanosine triphosphatase
HDL	High density lipoprotein
^{1}H NMR	Proton nuclear magnetic resonance
HRP	Horseradish peroxidase
IgA	Immunoglobulin A
IgG	Immunoglobulin G
IgM	Immunoglobulin M
IL-1•	Interleukin-1-beta
IL-18	Interleukin-18
ISO	International Organisation for Standardisation
kDa	Kilo Dalton
Mac-1	Macrophage-1 antigen
MAPK	Mitogen activated protein kinase
MDR	Multi drug resistance
MEM	Minimal essential medium

MEND	Multifunctional envelope- type nano device
MPS	Mononuclear phagocyte system
MTT	(3-(4,5-Dimethyl thiazol-2-yl)-2,5-Diphenyl Tetrazolium Bromide)
NHS	N-Hydroxysuccinimde
PAA	Polyacrylic acid
PEG	Polyethylene glycol
Pgp	Permeability glycoprotein
PEO	Polyethylene glycol
PHEMA	Polyhydroxyethylmethacrylate
PLA	Polylactic acid
PMP	Platelet microparticles
PEO-PPO	Polyethylene oxide and Polypropylene oxide block copolymer
PSGL	Platelet-selectin glycoprotein ligand-1
PVA	Polyvinyl alcohol
RBC	Red blood cell
RES	Reticuloendothelial system
RGD	Arginine-Glycine-Aspartate
SAMs	Self assembled monolayers
SDS	Sodium dodecyl sulfate
TMB	3,3’,5,5’- Tetramethyl benzidine

TXA2	Thromboxane A2
UV	Ultra Violet
W	Watt
WBC	White blood cell

Synopsis

The drug resistant nature of cancer remains as a formidable challenge for the effectiveness of chemotherapy. Nanoparticle mediated drug delivery has been considered as a promising way of bypassing the chemo resistance. Injectable biodegradable and biocompatible copolymers of lactic and glycolic acid constitute an important advanced drug delivery system for week to month controlled release of both hydrophobic and hydrophilic drugs that display poor bioavailability. In fact, PLGA has the greatest clinical impact among the various controlled release polymer technologies. Thus, the need of the hour is the precise engineering of PLGA for encapsulating different therapeutics and thereby rendering them suitable for parenteral administration. Hence, facilitate the delivery and enhanced bioavailability of various drugs. However, before developing an effective nanoparticle based drug carrier system for biomedical applications, an evaluation of several criteria including the precise control between biological, chemical and physical properties are necessary. Hence, the central dogma of drug delivery is to steer therapeutic carriers to target tissues or cells to achieve maximal therapeutic efficacy with minimal toxic effects. The success of each nanoparticle in meeting the clinical expectation is directly dependent on its hemocompatibility and the ability to overcome the host defence mechanism, the mononuclear phagocytic system. Despite the numerous advantages, PLGA suffers from several well characterised

shortcomings that necessitated the surface modification of the polymer. In this context, we emphasized on the potentiality of thiol, glucose and mucin as the surface modifiers that promoted the compatibility of PLGA nanoparticles, both in terms of physical and biological interactions. The dual role of thiol, glucose and mucin functionalities in bestowing the PLGA nanoparticles with adequate hemocompatibility parameters without compromising the ability to penetrate the cancer cells has been established. This enhanced compatibility cum cell penetrating capacity of the modified PLGA matrixes, prompted us to determine its therapeutic potential when compared to unmodified PLGA nanoparticles, following chemotherapeutic drug encapsulation. Hence, we have investigated the anti cancer activities of surface modified PLGA nanoparticles after encapsulating the chemotherapeutic drugs doxorubicin, curcumin and betulinic acid respectively. Three different chemotherapeutics of increasing hydrophobicity namely doxorubicin, curcumin and betulinic acid were chosen to analyse the interactions of these drugs to the hydrophobic core of PLGA matrix. The rationale for selecting doxorubicin, curcumin and betulinic acid for encapsulation inside PLGA and modified PLGA nanoparticles was based on the fact that nanoformulations are therapeutically active than the respective free drugs and also inhibit the development of MDR leading to increased antiproliferative activity in C6 cell lines. In their free form, frequent systemic administration of large doses of curcumin, betulinic acid and doxorubicin is necessary to achieve even a minimal therapeutic potential owing to the poor bioavailability and short half lives. Hence, the PLGA based nanoencapsulation of curcumin, betulinic acid and doxorubicin were attempted to determine the chemotherapeutic effectiveness of these

different drug-nanoparticle combinations on exposure to glioma cells, C6 in vitro, after rendering the PLGA surface to varying hydrophilicity.

First of all, drug encapsulated nanoparticles were synthesised. Then the effect of surface modification on encapsulation efficiency and release kinetics of drugs from PLGA nanoparticles were considered. Afterwards we studied the cellular uptake and cytotoxic potential of drug loaded PLGA nanoparticles on C6 cell lines, in correlation to the surface modification. Finally, based on these characteristics, we have identified the most effective drug-particle combination in terms of in vitro chemotherapeutic activity following the surface modification of PLGA nanoparticles.

List of Abbreviations

ABC transporters	ATP-binding cassette transporters
ADP	Adenosine di phosphate
ASTM	American Society for Testing and Materials
BAX	Bcl-2- associated X protein
BCL-2	B-cell lymphoma-2
BCS	Biopharmaceutics Classification System
CD 11 b	Cluster of differentiation molecule 11 b
CVD	Cardiovascular disease
DCC	N,N'- Dicyclohexylcarbodiimide
DMEM	Dulbecco's modified eagle medium
DMF	Dimethylformamide
DMSO	Dimethyl sulfoxide
DNA	Deoxyribonucleic acid
DSC	Differential scanning calorimetry
EDC	1-Ethyl-3-(3-dimethylaminopropyl)carbodiimide
ELISA	Enzyme-linked immuno sorbent assay
EPR	Enhanced permeability and retention effect
FACS	Fluorescence activated cell sorting
FBGC	Foreign body giant cells
F_C receptor	Fragment, crystallisable receptor
F_C• R	Fragment, crystallisable gamma receptor
FDA	Food and Drug Administration

FTIR	Fourier Transform Infra Red Spectroscopy
GPIIB/IIIA	GlycoproteinIIB/IIIA
GTPase	Guanosine triphosphatase
HDL	High density lipoprotein
^{1}H NMR	Proton nuclear magnetic resonance
HRP	Horseradish peroxidase
IgA	Immunoglobulin A
IgG	Immunoglobulin G
IgM	Immunoglobulin M
IL-1•	Interleukin-1-beta
IL-18	Interleukin-18
ISO	International Organisation for Standardisation
kDa	Kilo Dalton
Mac-1	Macrophage-1 antigen
MAPK	Mitogen activated protein kinase
MDR	Multi drug resistance
MEM	Minimal essential medium
MEND	Multifunctional envelope- type nano device
MPS	Mononuclear phagocyte system
MTT	(3-(4,5-Dimethyl thiazol-2-yl)-2,5-Diphenyl Tetrazolium Bromide)
NHS	N-Hydroxysuccinimde
PAA	Polyacrylic acid
PEG	Polyethylene glycol

Pgp	Permeability glycoprotein
PEO	Polyethylene glycol
PHEMA	Polyhydroxyethylmethacrylate
PLA	Polylactic acid
PMP	Platelet microparticles
PEO-PPO	Polyethylene oxide and Polypropylene oxide block copolymer
PSGL	Platelet-selectin glycoprotein ligand-1
PVA	Polyvinyl alcohol
RBC	Red blood cell
RES	Reticuloendothelial system
RGD	Arginine-Glycine-Aspartate
SAMs	Self assembled monolayers
SDS	Sodium dodecyl sulfate
TMB	3,3’,5,5’- Tetramethyl benzidine
TXA2	Thromboxane A2
UV	Ultra Violet
W	Watt
WBC	White blood cell

Chapter 1

INTRODUCTION

1 INTRODUCTION

1.1 Controlled Drug Delivery Systems Based on Nanoparticles

Synergistic innovations in material science and nanotechnology has provided significant momentum for the design of controlled drug delivery systems with improved performance and extended patent life (Zhang et al., 2013). Packaging an existing drug into nanocarriers that are biocompatible, biodegradable, targeting and stimulus responsive can realise temporal and spatial distribution of drug inside the body. Since the original discovery by Folkman and Long in 1964, polymeric materials, with their diverse chemistry, topology and dimension have occupied a central status in the fabrication of controlled drug delivery systems (Qiu and Bae, 2006). A vast array of polymers, ranging from synthetic, natural to hybrid has been investigated for the formulation of biodegradable polymeric nanoparticles. The structure and properties of the polymer used and the mode of nanoparticle preparation specifies the optimal formulation for every particular drug delivery applications. Aliphatic polyesters like poly lactic co glycolide have been most extensively used in controlled release technology owing to their biodegradable and low toxic profile (Lü et al., 2009). Poly (lactic-co-glycolic acid) (PLGA) is one of the most commercially used biodegradable polymer because of its long clinical experience, favourable degradation characteristic and possibility for sustained drug release (Danhier et al., 2012a). The different reasons behind the success story of PLGA family of polymers are many

- Biodegradable and biocompatible chemistry
- Approval of FDA and European Medicine Agency as drug delivery systems for parenteral administration in humans
- Tunable physico chemical characteristics
- Formulation techniques well adapted to encapsulate various types of drugs by controlling the relevant parameters such as polymer molecular weight, ratio of lactide to glycolide and drug content
- Drug is well protected from degradation
- Release profile in a sustained manner
- Possibility of surface modification to provide stealthness and/or better interaction with biological materials
- Possibility of target specific delivery of nanoparticles to specific organs or cells.

The PLGA based technology project new dimensions in tissue engineering applications and for the treatment of diseases such as CVD and cancer. However, a thorough evaluation of biocompatibility criteria is mandatory before the widespread use of nanoparticles in drug delivery systems, for ensuring appropriate safety precautions regarding human health (Gaspar and Duncan, 2009). The manner in which a benign coexistence of biomaterials and tissues are developed and retained has been the foundation of the subject biocompatibility (Ratner et al., 2013). The dynamic physicochemical characteristics of nanoparticles while interacting with the cells and extracellular environment can trigger a sequence of biological events that determine the biocompatibility of the system as a whole. As such Williams has reviewed the biocompatibility concept in 1986 as “the ability of a material to perform

with an appropriate host response in a specific situation." (Williams, 2008). Later, in 1993 Ratner defined biocompatibility as the body s acceptance of a material, i.e., the ability of an implant surface to interact with the cells and fluids of the biological system and to elicit reactions analogous to the body tissues (Ratner, 1993). As a general rule, high degree of biocompatibility is achieved when material interacts within the host without eliciting unwanted toxic, immunogenic, carcinogenic and thrombogenic complications. However the limitations and the relative nature of the biocompatibility criteria demand a case by case and tissue and application specific evaluation of the matter. Generally, the assessment of the material biocompatibility progresses through in vitro and in vivo phases with a predictive correlation data. The term biocompatibility encompasses material properties that include toxicity, tissue compatibility and hemocompatibility that enables screening in terms of in vitro cytotoxicity and hemocompatibility parameters. In summary, biocompatibility comprises two elements, biosafety, appropriate host response at both systemic and localised levels and biofunctionality i.e., the ability of the material to perform the specific task for which it is intended (Naahidi et al., 2013). In, 1992, the international standards organisation adopted and published a multipart international standard on the biological evaluation of medical devices ISO 109939. Among the different tests mentioned in ISO 109939, hemocompatibility evaluation forms an important criteria for applications of nano enabled drug delivery platforms (Dobrovolskaia et al., 2008a). The hemocompatibility and subsequent cytocompatibility and the resulting biological behaviour are largely dictated by the process of nanoparticle interface to the blood, cells and tissues after an intravenous injection. Multiple factors are

involved in the complex blood material interactions including chemical composition, charge, flexibility, wettability and conditions of blood flow (Wang et al., 2004).

1.2 Factors Mediating the Biocompatibility

The basic factors that govern the compatibility of biomaterials are not fully elucidated. The chemical structure and surface properties together influence the design of biocompatible surfaces through the

- Interfacial free energy
- Balance between the hydrophilicity and hydrophobicity
- Chemical structure and the functional groups
- Type and density of surface charges
- Molecular weight of the polymer
- Conformational flexibility of the polymer
- Surface topography and roughness

1.2.1 Interfacial Free Energy

Once the biomaterial comes in contact with the blood, a new interface gets established between the fluid and cellular components of the blood. According to the laws of thermodynamics, a driving force acts at the interface to minimise the interfacial free energy. The formation and configuration of the plasma – protein corona around the material is driven by the magnitude of this thermodynamic quantity called interfacial free energy. Accordingly, the minimum interfacial free energy of biocompatibility was proposed by Andrade (Andrade, 1973). In order to achieve the minimum interfacial free energy, the biomaterial must obtain a free energy close to that of water (50.8dyne/cm), as blood plasma is largely aqueous in nature. Although such a high surface free energy is virtually impossible for a

synthetic surface, a minimal magnitude of 1-3dyne/cm is suggested for acquiring long term biocompatibility. Hence the techniques like radiation grafting, plasma discharge, chemical etching, glow discharge and mimicking or adsorbing hydrophilic moieties attempt to modulate the cell/tissue interactions by increasing the surface free energy.

1.2.2 Balance between hydrophilicity and hydrophobicity

The evolutionary ancient alert system of our body recognises any hydrophobic portions on biological surfaces as a universal signal of danger to initiate innate immunity (Fadeel, 2012). Therefore incorporating hydrophilic surfaces on to a biomaterial seems to enhance the blood compatibility of materials. In addition, the hydrophilic surfaces in absence of ionic groups are thought to suppress the platelet adhesion and activation (Higuchi et al., 2002). To name a few hydrophilic polymers, we have PEG, PAA and PHEMA to be biocompatible in nature.

1.2.3. Chemical Structure and Functional Groups

Functional groups on polymer surface constitute another important determinant of biocompatibility. The results from various groups have confirmed that the compatibility and cell growth are enhanced in the order of CO(OH)> CO(NH2)=OH=NH2<CH3 (Tidwell et al., 1997). An inhibitory effect of negatively charged surfaces on complement and platelet activation has been confirmed. The in vivo spreading of macrophages and their subsequent fusion into giant foreign body cells were decreased with an increase in the presence of negative charges.

1.2.4. Types and Density of Charges in Polymer

As a general rule, polycations are more cytotoxic when compared to neutral charges and polyanions. Consequently an increase in the number of cationic charges per monomer unit correlates to the increase in cytotoxicity (Fischer et al., 2003). As most proteins bear a net negative charge they get repelled upon approaching an anionic surface.

Biocompatibility may also be influenced by various properties of the polymer like its molecular weight, surface topography, porosity and conformational flexibility. Correlating the properties of nanomaterials like the size, shape, chemical functionality, surface charge and composition with the nano-bio interactions would help us to predict the behaviour of nanomaterials in complex biological systems (Naahidi et al., 2013).

1.3 Physicochemical Characteristics of Nanoparticles that Influence the Biocompatibility

1.3.1 Size

The majority of in vivo functions of drug carriers such as circulation time, extravasation, targeting, immunization, internalisation, intracellular targeting, clearance and uptake mechanisms depend on the most prominent physicochemical characteristic termed size (Albanese et al., 2012). Increase in particle diameter can propel the capture by reticuloendothelial system in the midst of their transport and adhesion to blood vessels. Optimal phagocytosis occurs within a size range of 1-3μm in diameter (Bertrand and Leroux, 2012). Microparticles are trapped by the Kupffer cells in liver while nanoparticles below 100nm exocytose through the fenestrations in the endothelial lining. Opsonisation also depends on the

size related curvature of spheres. Particles less than 10 nm are filtered by the glomeruli of kidney and undergo short circulatory half life and quick clearance from the body. However particles larger than 10nm would be more efficiently captured by the reticuloendothelial system and cause emboli in the liver and lungs. Hence an optimum size range around 100 nm is desirable for intravenal applications (Moghimi et al., 2001).

1.3.2. Shape

Notably, the shape of the particle seems critical in mitigating cellular responses. To be more specific, the geometry of the particle at the point of contact of a macrophage can dictate the initiation of cellular internalisation. Disc shaped, cylindrical and hemi spherical particles would evade the phagocytosis more efficient than the spherical ones (Liu et al., 2012b). Targeting strategies to endothelium make use of oblate particles instead of spherical particles of the same volume.

1.3.3. Surface Microstructure, Texture and Porosity

The nano/micro topography of surfaces is a critical factor that determines the cell morphology, adhesion and motility. Depending on the surface structures particle would undergo directed differentiation, or apoptosis.

1.3.4. Hydrophobicity, Roughness and Rigidity

Hydrophobicity of the particle surface has an active role in mediating the cellular uptake as hydrophobicity promote cellular uptake. Opsonisation also occurs maximally on the hydrophobic surfaces.

Surface roughness can also influence cellular binding of nanoparticles. Protrusions and depressions on the particle surface leads to surface

roughness and minimises the repulsive force between the particles and cell surfaces. Surface roughness can be modulated to influence cellular differentiation and growth. Particle rigidity is a determining factor of the in vivo biodistribution profile as more flexible the nanoparticles are, more easily traverse through narrow capillaries and pores.

1.4 Nano-Bio Interface

The nano bio interface consists of three dynamically inter-related components

- The surface of the nanoparticle characterised by the physicochemical composition
- The blood-particle interface and the interactions with the surrounding blood components
- The blood-particle contact zone with the biological substrates.

The major physicochemical characteristics that determine the surface properties of nanoparticle within any biological media are the material's chemical composition, surface functionalisation, shape, angle of curvature, porosity, surface crystallinity, heterogeneity, roughness and hydrophobicity or hydrophilicity. Some other properties such as effective surface charge, state of dispersion, stability, biodegradability, dissolution characteristics, hydration and valence of the surface layer are influenced by the properties of the suspending media including the ionic strength, pH, temperature and presence of organic molecules like proteins or detergents (Nel et al., 2009). The interactions between the nanoparticle and the medium are promoted through

- The adsorption of ions, proteins, natural and organic materials and detergents
- Double layer formation
- Dissolution
- Minimising free energy by surface restructuring.

This in turn determines the forces that operate at the particle medium interface. In short the nano-bio interface comprises the dynamic physicochemical interactions, kinetics and thermodynamic exchanges between the nanomaterial surfaces and the surfaces of the component (Nel et al., 2009).

1.4.1 Forces at the nano-bio interface

The nano-bio interactions are characterised by the same principles applied for colloidal particles such as VDW, electrostatic, solvation, solvophobic and depletion forces but with special consideration for events occurring at the nanoscale. The positioning of the relatively few surface atoms of nanoparticle and their standard bulk permittivity function increases the complexity while interfacing biological systems. In addition, the high ionic strength of the biological medium can obscure the electrostatic forces and the zero frequency contribution of the VDW forces. The solvation and hydrophobic-hydrophilic forces determine the stability or aggregation of particles dispersed in the biological media. The cell differs from any other material surface by virtue of

- A non rigid compliant membrane that can deform as a result of the fluidity and thermodynamics of the membrane
- Patchiness or surface charge heterogeneity of the cell surface that alters the energy of inter particle interactions even between two ideal particles
- Time dependent dynamicity

- The major forces that influence the nano-bio interface are mentioned in the Table I.

Table I: Major forces governing the interfacial interactions between nanomaterials and biological systems (Nel at al. 2009)

Force	Range (nm)	Possible impact on the interface
Hydrodynamic Interactions	10^3-10^6	Increase the frequency of collisions between nanoparticles and other surfaces responsible for transport
Electrodynamic Interactions	1 to 100	Universally attractive in aqueous media: substantially smaller for biological media and cells owing to high water content
Electrostatic Interactions	1 to 100	Overlapping double layers are generally repulsive as most materials acquire negative charge in aqueous media but can be attractive for oppositely charged materials
Solvent Interactions	1 to 10	Lyophilic materials are thermodynamically stable in the solvent and do not aggregate
Steric Interactions	1 to 100	Increase the stability of individual
Polymer Bridging Interactions	1 to 100	Promote aggregation or deposition

1.5. Formation of the protein corona

Protein adsorption is the initial event that occurs when the nanoparticle enters a biological fluid like blood, plasma or interstitial fluid. Following adsorption, the proteins may undergo conformational changes, leading to the exposure of new epitopes, altered function or avidity effects. This protein corona further shapes the surface properties, charges, resistance to aggregation and hydrodynamic size of the nanoparticles (Karmali and Simberg, 2011). The kinetics of nanoparticle-protein association and dissociation depends on the dynamic exchanges with other proteins in the media. This in turn determines the particle's interaction with other biological surfaces and receptors on cells that may influence cellular uptake, inflammation, accumulation and degradation and clearance rate within the body. The physicochemical characteristics of nanoparticles, including their surface hydrophobicity/hydrophilicity, size, radius of curvature, charge and surface coatings have a prominent role on deciding their interactions with proteins and cells. The plasma protein corona generally consists of a hard corona of slowly exchanging proteins that are surrounded by an outer reversible collection of weakly interacting and rapidly exchanging soft corona (Hlady and Buijs, 1996). Over time, in the absence of cellular interactions the composition of the adsorbed layer will gradually change as faster diffusing molecules are displaced by proteins with a higher affinity for the surface, often referred to as the Vroman effect. The more abundant proteins like albumin and fibrinogen may initially occupy the surface and get subsequently displaced by other low abundant proteins with higher affinities.

The kinetics of protein adsorption on the nanoparticle surface is influenced by

- Amount of proteins available to interact with the nanoparticle surface
- Affinity of the proteins towards the nanoparticle surface
- Ability of proteins to completely occupy the nanoparticle surface
- Physiochemical characteristics of nanoparticle e.g., curvature of nanoparticle decides the flexibility and surface area available to adsorbed protein molecules

The major forces that lead to protein adsorption could include electrostatic and hydrophobic interactions in combination with the gain in entropy following the conformational alteration of adsorbed proteins.

1.6. OPSONINS

Opsonins are proteins which are present in the plasma that after adsorption to a particle surface would augment their recognition, uptake and phagocytosis via cells of the reticuloendothelial system (Dufort et al., 2012). On the contrary proteins, such as albumin, that inhibit this recognition constitute the dysopsonins. The complexity of the human plasma proteome is attributed to almost 100,000 proteins whose concentrations span over 12 orders of magnitude as shown in Figure 1.

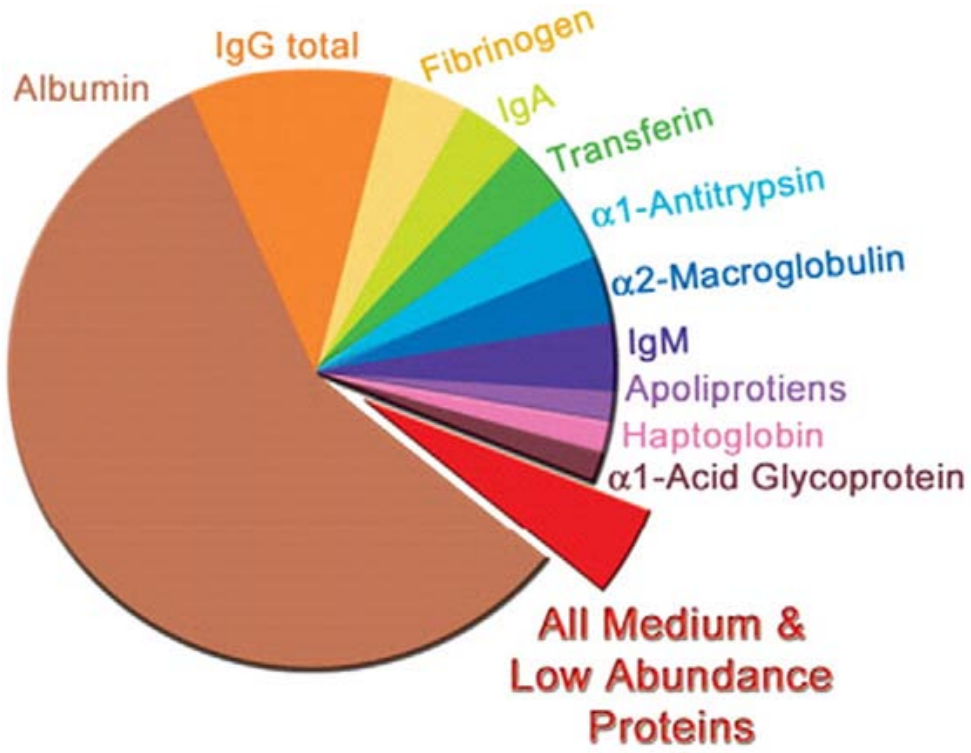

Figure 1: Overview of the major human plasma proteins (Kratz and Elsadek, 2012)

To be specific, the dynamic range of plasma from the most abundant albumin (40-50 mg/ml) to interleukin-6(<1ng/ml) differ by a factor of 10^{10} .The most commonly described opsonins are as follows

1.6.1. Fibrinogen

The biological activity of any protein adsorbed onto the nanoparticle surface is determined by its three dimensional conformation. Fibrinogen has a tendency to undergo conformational alteration upon adsorption to certain surfaces. This action can expose the cryptic epitopes of fibrinogen that can promote an interaction with Mac-1, the integrin receptor of fibrinogen. Mac-1 activation initiates the release of inflammatory cytokines. Subsequently, unfolding leads to inflammation and phagocytosis by Mac-1 positive macrophages and leukocytes. The

particle size does modulate the fibrinogen mediated Mac-1 activation as a size range around 5 nm provides proper contact for the unfolding of fibrinogen.

1.6.2. Albumin

Human serum albumin is a 67kDa protein which is the most abundant in blood with a concentration of 35-50g/L in human serum. Among the important functions, albumin maintains colloidal osmotic pressure, transports various fatty acids, liposoluble hormones and drugs and accumulates in malignant and inflamed tissue due to enhanced permeability and retention effect. The neonatal Fc receptors prevent the elimination of albumin via recognition and provide a half life of 19-22 days. Upon, nanoparticle administration rapid and non specific interactions with albumin proceed through ionic and hydrophobic interactions. Albumin is considered as a dysopsonin or passivating agent as its early deposition on the nanoparticle surface can prevent further opsonisation with other proteins. However, these contacts are transient and albumin is prone to displacement by other less abundant proteins with higher affinities. Hence, this Vroman effect limits the dysopsonising nature of the albumin.

1.6.3. Immunoglobulins

Immunoglobulins constitute another major component of the plasma protein corona. Immunoglobulins are pre programmed to bind to the Fc receptors on the surface of the patrolling cells of mononuclear phagocytic system. These proteins are the effector components of humoral immunity and mediate the capture of particles by the MPS. Hence their adsorption can accelerate the clearance of particles from the circulatory system.

1.6.4. Apolipoproteins

The abundant proteins of plasma, mainly albumin, fibrinogen and immunoglobulins would initially dominate the adsorption on the surface of the nanoparticles. However due to their weak binding affinity they get displaced by the proteins of lower abundance, higher affinity and slower kinetics such as apolipoproteins. Apolipoproteins, being part of high density lipoproteins are involved in the transport of lipids in the body. The transport of cholesterol to liver, adrenal glands, ovaries and testes are mediated through HDL receptors such as scavenger receptor B-1 or the cholesteryl ester transfer protein. Among the different apolipoproteins, apolipoprotein A-1 maximises the binding of HDLs. Nanoparticle surface adsorbed with apolipoproteins can mimic the circulating HDL complexes and hence dictate their fate and organ distribution accordingly. Apolipoprotein - E has been suggested to play a major role in the crossing of the blood brain barrier and is also specific to hepatocytes.

1.6.5. Proteins of the Complement

The complement system that comprises of almost 30 zymogens with comparatively high plasmatic concentration ensures their abundant interactions with the administered nanoparticles. Complement C3 is a large protein of the complement system with dimensions of (15.2 x 9 x 8.4) nm^3 and molecular weight of 180kDa. The adsorption of complement protein C3 can lead to the recognition, phagocytosis and elimination of nanoparticles by the macrophages. The conformational alteration of the complement protein after adsorption leads to the exposure of a reactive site and release of a signalling molecule that triggers the chain of biochemical events called the complement activation cascade. The activated

complement protein can undergo cleavage to produce fragments that are pro inflammatory or anaphylactic in nature.

1.7. Blood compatibility parameters: Implications on the constrains of intravenous drug delivery systems

The opsonisation of the nanoparticle surface by plasma proteins in combination with their physicochemical properties dictate the downstream cellular interaction, blood compatibility parameters and immune recognition. The major blood compatibility parameters include the complement and platelet activation, thrombosis and hemolysis that determine the circulatory half life of the nanocarrier after intravenous administration (Cavadas et al., 2011).

1.7.1 Complement Activation

The complement system constitutes a network of over 40 different soluble and membrane bound proteins that forms an important barrier to infection through pattern recognition of danger. The classical exogenous danger signals are the pathogen associated molecular pattern and the foreign surfaces of biomedical materials including the nanoparticle (Fadeel, 2012). In a simple outline, the complement system act by inducing the conversion of complement proteins from their soluble state to the surface bound state. This opsonisation of particle surface by complement proteins labels the surface as a target for several components of the immune system. After opsonisation, complement activation cascade generate biological response modifiers that potentiate chemotaxis and generation of pro inflammatory cytokines. Finally the cascade, in absence of inhibitory molecules, proceeds to the formation of membrane lytic complex that induce cell lysis. Hence, connects the humoral and cell mediated immunity by facilitating the material

recognition, uptake and rapid clearance by neutrophil granulocytes, monocytes, macrophages and dendritic cells of reticuloendothelial system that bear complement receptors.

Currently, there are three different modes of complement activation, mainly, classical, alternative and lectin mediated pathways, as shown in Figure 2.

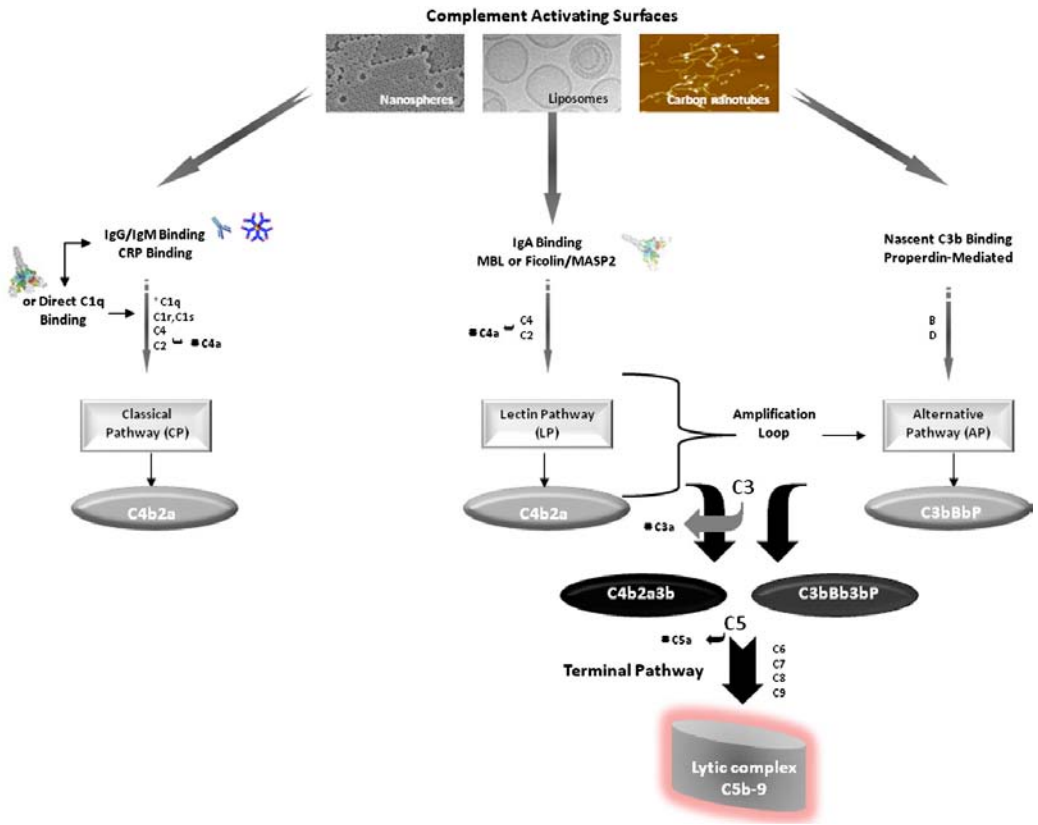

Figure 2: Complement Activation Pathways (Moghimi et al., 2011)

Although these three pathways make use of different moieties to detect a foreign particle (antibodies for classical pathway and mannose binding lectin and ficolin for lectin binding pathway), they merge at the point where the central complement protein C3 is cleaved to form the fragments C3a and C3b. The C3 division exposes an active thioester which forms a reactive acyl imidazole bond

with an immediate histidine residue that permits covalent attachment to target surfaces. The freed thiolated anion of the Cys residue of the thioester then acts as a base and catalyzes the transfer of acyl group to carboxyl groups present on the carbohydrate moieties of microorganisms. The covalent binding of C3 would promote the sequential activation of complement proteins C5 to C9 that assemble into the terminal C5b-9 membrane attack complex. The same principle applies for biomaterials via the alternative pathway. The surfaces that consist of negatively charged groups such as carboxyl, sulphate, sialic and heparin are in common non-activating as they contribute high affinity association between bound C3b and Factor H(Factor H down regulates complement activation cascade by inhibiting Factor I). Surfaces enriched with nucleophiles such as hydroxyl or amino groups are in general activating as they allow covalent binding of C3b that promote formation of the membrane lytic complex. However, for particulate systems both negative and positive charged surfaces are known to activate complement via classical and alternative pathway respectively. In addition, hydrophobic and irregular surfaces with large diameter and low radius of curvature are liable to complement activation.

Even in the absence of any activating moieties on the surface, certain materials like PLGA based nanoparticles are known to activate complement via hydrophobic interactions (Ekdahl et al., 2011). Hence, the nanoparticle mediated complement activation is a complex process inter regulated by physicochemical parameters like size, curvature, composition, morphology, functional groups and hydrophobicity/hydrophilicity. This highlights the importance of the precise mapping of the material structure mediated complement activation for the design of better drug carriers.

1.7.2. Platelet Activation and Thrombogenecity

Platelets are anuclear disc shaped cells that are derived from the megakaryocytes in the bone marrow. They have a diameter of 3-4 um at an average concentration of $200x10^6$ cells per ml. The main role of platelets in blood clotting is to preserve the integrity of vascular walls through interconnecting fibrin fibers to form a platelet plug. Platelets are activated in response to the contact of collagen on artificial surfaces like the injured endothelium, sub endothelium, thrombin or platelet activation factor, a cytokine produced by neutrophils. The activation of the coagulation cascade is initiated either by an injury exposing the tissue factor bearing cell to the blood flow(extrinsic pathway) or through contact activation on negatively charged particle surfaces. In either way it involves the interaction of agonists to specific receptors on the platelet plasma membrane (Gorbet and Sefton, 2004). Platelets upon activation generally elicit any or all of the physiological responses

- Secretion of biologically active compounds such as platelet factor-4, thrombospodin, ADP and serotonin.
- Release of p-selectin and its expression on the platelet membrane which mediates the adhesion of activated platelets to neutrophils, monocytes and subset of lymphocytes.
- Initiation of the platelet eicasanoid pathway that results in the synthesis and release of prostaglandins and thromboxane B2.
- Alteration in platelet membrane morphology that promotes platelet-platelet adhesion and aggregation.

- Exocytic budding of platelet microparticles that can co-aggregate with platelets after binding to fibrinogen and fibrin.

One dominant integrin receptor present on platelet surface termed GPIIB/IIIA invite particular attention to biomaterial induced coagulation. The opsonin fibrinogen present on the plasma protein corona can promote cross linking between the GPIIA/IIIB receptors on different platelets. In addition, the fibrinogen promotes crosslinking between platelets and leukocytes through the receptor Mac-1. The thrombotic complications associated with biomaterials are initiated with platelet activation (platelet release, PMP formation, p-selectin expression and aggregation) and platelet adhesion. The procoagulant nature of adherent platelets and PMPs accelerate the thrombus formation. Biomaterial induced platelet activation is manifested by high platelet turnover and formation of microemboli rather than mere adherence. The adherence or repulsion of platelets upon contact with a biomaterial surface is dependent on the array of receptors exposed on the plasma protein corona. The physicochemical characteristics of the nanoparticle as exemplified by the plasma protein corona decides the propensity of platelet activation and aggregation that results in vascular thrombosis. Nanoparticle induced platelet aggregation concomitantly leads to the phagocytosis and clearance of the particle containing platelets by macrophages.

Complement mediated platelet activation is possible through the C1Q induced GPIIb/IIIa, p –selectin expression and pro coagulant activity. Comprehensive evaluation of nanoparticle mediated platelet activation become crucial in the design of long circulating drug delivery systems.

1.7.3. Leukocyte Activation

The leukocyte population in circulation consist of neutrophils, monocytes, lymphocytes, basophils and eosinophils that are the major players of inflammatory response. Among the different cells, neutrophil comprises 40-60% of leukocyte population while monocytes represent only 5% of the total population. The usually short half life of neutrophils in blood can elevate upto threefold upon stimulation. The monocytes circulate in the blood for a short time period before their migration and maturation into tissue macrophages. Apart from pathogen invasion, neutrophil and monocytes get activated following the presence of complement and platelet activation products including cytokines. The leukocyte activation results in several physiological responses like

- Alteration in the membrane expression pattern on monocytes and neutrophils leukocytes such as up regulation of CD11b
- Expression of tissue factor and shedding of L-selectin
- Release of inflammatory mediators like cytokines, elastase, cathepsin G and lactoferrin
- Onset of oxidative burst and release of free radicals by neutrophils and monocytes
- Neutrophil and leukocyte adhesion to the endothelium.

As the neutrophils, monocytes and macrophages are unable to phagocytose the large dimensions of opsonised biomaterial surface, they undergo frustrated phagocytosis and release free radicals and proteolytic enzymes. The mechanism of leukocyte adhesion on artificial surfaces proceeds through fibrinogen and complement product iC3b (Anderson et al., 2008). The platelet's presence on the

surface is also responsible for leukocyte adhesion via the interaction between p-selectin and PSGL and/or GPIIb/IIIa and CD-11b. The pro coagulant nature of leukocytes and their adhesion to damaged endothelial cells or platelets further contribute to localised thrombogenesis.

1.7.4. Hemolysis

Considering the large blood fraction of red blood cells, the intravenously injected nanoparticles would primarily interact with erythrocytes prior to their encounter with the immune cells. Understanding of nanoparticle‘s haemolytic potential is considered to be an important initial parameter in assessing nanoparticle mediated blood compatibility (Dobrovolskaia et al., 2008a). Comparatively good correlation exists between in vitro hemolysis assays and in vivo toxicity studies. Nanoparticles, depending on the physicochemical characteristics can cause hemolysis or RBC aggregation. Besides the risk of anaemia, phagocytic cascade also get activated upon contact with the debris released from damaged RBCs. This would minimise the targeting efficiency that culminate in the rapid clearance of nanoparticles. Positive charged surface characteristics have proven history of hemolysis induction.

1.8. Clearance Mechanism of Nanoparticles from the blood stream

The clearance process developed as a natural protection mechanism against foreign invasion turns detrimental for the intravenal application of nanoparticles. The circulation time of nanoparticles after intravenous administration depends on the rate of clearance from the blood, spleen, liver & kidney (Wang et al., 2012b).

The rate of biological clearance is broadly divided in to three categories

- Disintegration of nanoparticles by protein adsorption
- Opsonisation mediated nanoparticle phagocytosis by reticuloendothelial system
- Filtration mediated removal by organs with fenestrated vasculature.

1.8.1. Disintegration of nanoparticles by protein adsorption

Protein adsorption can initiate the disintegration of nanoparticles, esp. polymeric micelles that can compromise their drug delivery applications. Protein adsorbed on to the micellar surface is able to penetrate and extract the drug that results in the destabilisation of nanoparticles. These unstable particles are quickly eliminated from the circulation.

1.8.2. Opsonisation mediated nanoparticle uptake by the reticuloendothelial cells

Immune cells circulating in the blood (leukocyte, monocytes, platelet and dendritic cells) and those residing in the organs (Kupffer cells in liver, macrophage and B cells in spleen and dendritic cells in lymph nodes) are engaged in the removal of nanoparticles mediated by the opsonised proteins (Lee et al., 2010).

1.8.3. The reticuloendothelial or mononuclear phagocytic system

The RES/MPS is a part of the immune system whose main function is to phagocytose microbes, immune complexes in blood and tissues and participates in inflammation. They comprise of a population of cells derived from the progenitor cells of the bone marrow that are destined to differentiate to form blood monocytes. After circulation in the blood they enter resident tissues to differentiate into tissue macrophages. The principal phagocytic cells are located in the liver

(Kupffer cells), spleen and bone marrow to actively participate in the phagocytosis of opsonised nanoparticle mediated drug delivery vehicles (Bertrand and Leroux, 2012). These macrophages have different receptors or glycoproteins on their surface for the recognition and interaction with myriad varieties of molecules on the external environment. Macrophage surfaces have receptors like FcϒR that are specific for opsonins like C3 and IgG. In addition, the scavenger receptors are known to phagocytose through an opsonin independent pathway via recognising repeated patterns that lead to the removal of sterically protected particles.

1.8.4. Phagocytosis

The cells of the reticuloendothelial system form the first line of defence of the body by their ability to phagocytose non self elements, infectious agents as well as exogenous particles like the drug delivery systems. Hence such specialised cells like macrophages and monocytes along with the dendritic cells and neutrophils are called the professional phagocytes. The cells like fibroblasts, endothelial and epithelial cells that display a lower extend of phagocytosis form the non professional phagocytes. The phagocytic entry of nanoparticles into cells can be defined in three distinct steps

- Recognition through opsonins in the circulatory system
- Adhesion of the opsonised particles to the macrophage receptors
- Ingestion of the particle

Following opsonisation, the receptor-ligand interactions promote the attachment of nanoparticle to macrophage surfaces. The major receptors include the complement C3 receptors, Fcϒ/IgG receptors, mannose/fructose receptors and scavenger

receptors. The receptor ligation initiates a signalling cascade executed by the Rho family GTPases. This leads to the formation of pseudopodia or cell surface extensions mediated through the actin assembly. Thus encloses the particle in a zipper manner and engulfs it (Panariti et al., 2012).

The resulting phagosome would undergo a series of fusion and fission events while ferrying the particle through the cytoplasm. In the process, the vacuolar contents would undergo maturation and fuse with the endosomes and lysosomes to become the phagolysosome. The vacuolar proton pump ATPase located in the membrane bestows the phagolysosome with an acidifed environment that gets aggravated by the presence of cathepsins and esterases. The rate and time gap of these events depends on the surface properties of the ingested particles.

Phagocytic cells upon danger sensing would also modulate the secretion of pro inflammatory cytokines like IL-1• and IL-18 through caspase-1 activation by forming a multi protein complex called inflammasome.

1.8.5. Non-Phagocytic Pathways

While phagocytosis is confined to specialised cells alone, the other endocytosis pathways, traditionally referred to as pinocytosis or cell drinking (as opposed to cell eating or phagocytosis), are virtually exhibited by all types of cell. These pathways can be broadly classified as clathrin mediated endocytosis, caveolae mediated endocytosis, macropinocytosis and other clathrin/caveolae independent pathways (Panariti et al., 2012).

1.9. Organ Filtrations

Certain organs and tissues are evolved with permeable vasculature in accordance to their physiological function. The endothelial cells of these organs present numerous gap junctions of various dimensions. They are typically termed as fenestrations and are critical determinants of nanoparticle's fate (Lee et al., 2010). An understanding of these fenestrations like splenic and hepatic sinuses is necessary to design strategies for enhancing the circulatory half life of nanoparticles in blood.

1.9.1. Kidneys

Kidneys are culpable for blood filtration and sustain the purity and constancy of body fluids. The distinctive clearance mechanism of kidney involves glomerular filtration, tubular secretion and urinary excretion and elimination of intravascular agents. The filtering unit in the glomerular capillary network include three different layers: fenestrated endothelium, glomerular basement membrane and the foot processes of glomerular epithelial cells (Bertrand and Leroux, 2012). The fenestrations of endothelium, in the size range of 60-80 nm form a flexible glycoprotein barrier for the passage of blood components. The solutes then pass through the glomerular basement membrane which is a 240-370nm hydrated, fibrous network. The collagen fibres form a mesh with anionic charge dispersal that could impede the fluid flux and the conduit of negatively charged solutes. The highly differentiated podocytes of Bowman's capsule form the filtration slits via numerous interdigitated foot processes that together contribute to the high selectivity of filtration process. Glomerular filtration restricts the passage of nanoparticles based

on the molecular size and charge and is termed as glomerular filtration threshold. Though the size of the renal filtration slits are around 45nm in rats, the highly stratified nature of glomerular capillary walls limits the threshold for the passage of heterogeneous and polydispersive nanoparticles to be in the range of 6-8nm. Surface charge is another important factor for glomerular filtration. The potential interactions between charged particles and serum proteins and the corresponding increase in hydrodynamic size along with presence of negative charges in the glomerular capillary wall together contribute to the charge effect. The electronic repulsion from the anionically charged membrane restricts the passage of anionic particles to the maximum, followed by neutral and cationically charged particles.

1.9.2. Liver

Hepatobiliary system engages in numerous metabolic, immunologic and endocrine functions and represents the major route of excretion for particles that escape out from renal clearance. Here, blood circulates through a permeable and discontinuous capillary network called the sinusoids. The sinusoids are 5-10µm blood vessels having a fenestrated epithelium without any basal membrane. These fenestrations of the size range 100-150nm provide a sieving function of the circulating blood. The functions of liver include catabolism and biliary excretion of blood borne particles as well as phagocytic removal of foreign substances. Kupffer cells and hepatocytes are together involved in liver clearance through phagocytosis, endocytosis and enzymatic breakdown of foreign particles. Particles of the scale 10-20nm fall in the size range of viruses and hence get immediately eliminated by the physiological mechanism of liver. Also during the detoxification process, Kupffer cells exclusively phagocytose on particles of the size

range 800 nm whereas hepatocytes mainly endocytose smaller particles of 50nm in size.

1.9.3. Spleen

Spleen is a large, highly irrigated lymphatic organ. The main function of the spleen is in the recycling of red blood cells and also in lymphocyte maturation. The micro anatomical structure of the spleen is specialised to filter the antigens, micro organisms and aged red blood cells from the blood. Spleen parenchyma consists of the red pulp which is formed by a network of reticular fibres where macrophages and senescent RBCs reside. The while pulp situated near the arteries are involved in the proliferation of both B and T type lymphocytes. . The endothelial cells are organised in the sinus wall to let the blood pass through slits of width 0.2-0.5μm in width before entering the sinus. The slit width limits the passage of large and stiff nanoparticles in a way similar to the removal of unhealthy red blood cells that lack certain degree of deformability. Ultimately, they are captured by splenic macrophages and lead to immunological complications. This exemplifies a physical filtration method based on the physicochemical properties of nanoparticles like the size, flexibility, shape and surface properties in addition to opsonin mediated recognition.

1.10. Long Circulation

For effective delivery of nanoparticles to target sites, it is critical to produce long circulating carriers (Moghimi et al., 2001). As most synthetic polymers are hydrophobic, the nanoparticles prepared are easily recognised by our

body as foreign and are rapidly filtered out via interaction with the RES system. Hence the concept of long circulating nanoparticles evolved through surface modification of intrinsically hydrophobic particles as illustrated in Figure 3.

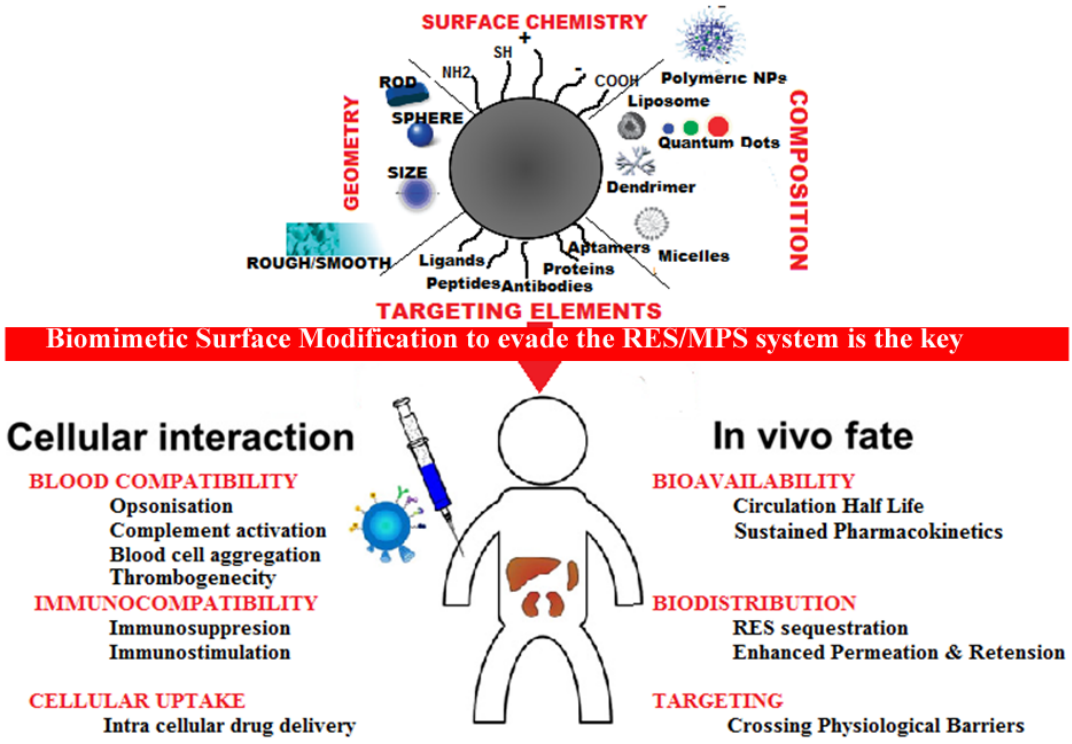

Figure 3: Optimised Bio-Nano Interface for Long Circulating Nanoparticles

This would render them invisible to the MPS and subsequently guide them to the desired target. A major breakthrough in the field came when the use of hydrophilic polymers to coat the bare nanoparticle surface produced an opposing effect to the uptake by the MPS. In the quest for perfect surfaces, a variety of techniques including physical modification, chemical modification and radiation has been tried (Xu et al., 2007).

1.11 Surface Modification Techniques

Covalent modification of Poly Lactic co Glycolic Acid (PLGA) matrix can be achieved by chemical modification through coupling agents

for conjugation. Carbodiimide derivatives are the most common reagents used for the conjugation of carboxyl groups and primary amine groups to from the amide linkages. In this process, the carboxyl group is activated with N- hydroxysuccinimide (NHS) in the presence of carbodiimide at room temperature. The NHS activated carboxyl group of PLGA yields an O-acylurea reactive ester intermediate which is highly reactive with amine groups but the solubility of carbodiimide should be taken into account. Under hydrophilic conditions, 1-ethyl-3-3 (Dimethylaminopropyl) carbodiimide hydrochloride is used under aqueous conditions while oil soluble dicyclohexyl carbodiimide is used for the conjugation reaction in the organic phase (Choi et al., 2003).

1.11.1 PEGylation

The past three decades witnessed a multitude of surface stabilisation approaches based on hydrophilic polymers or non ionic surfactants. In particular, PEG has emerged as a gold standard. The extended blood circulatory half life of PEG is mediated via steric hindrance. A flexible layer is formed on the surface in a brush or mushroom configuration depending on the density of adsorbed layer. Interference with cellular and endosomal uptake and the probability of immunological consequences via accelerated blood clearance has created the PEG dilemma that has instilled the search for alternative strategies. Polyoxazolines, poly amino acids, polyacrylamides, polybetaines, polyglycerols, polyvinylalcohols, and polysaccharides have been utilised for protecting nanoparticle surfaces against RES recognition and uptake (Amoozgar and Yeo, 2012).

1.12 Poly Lactic co Glycolic Acid (PLGA) Based Nanoparticles for Drug Delivery

Drug Delivery is the process of administering a pharmaceutical compound to achieve the desired therapeutic efficacy. Many efforts have been focussed on developing sustained release formulations where the drug is released over a period of time in a controlled manner. PLGA based nanoparticles represent a suitable model of drug delivery system for majority of administration routes owing to its biodegradability, drug biocompatibility, biodegradation kinetics, mechanical properties and ease of processing (Lu et al., 2009). The sub cellular and sub micron size of PLGA nanoparticles enable their penetration into tissues through the fenestrations present in the capillary walls. Several classes of drugs including anticancer agents, anti hypertensive agents, immunomodulators, hormones, nucleic acids and antibodies have been encapsulated inside PLGA nanoparticles (Danhier et al., 2012a).

1.13 Fabrication Techniques for Drug encapsulated PLGA Nanoparticles

Varieties of techniques are available for the preparation of nanoparticles like the solvent evaporation, phase separation or coacervation and spray drying (Makadia and Siegel, 2011). Structural organisation of the drug loaded nanoparticles is specific to the method of preparation. The nanoencapsulation method employed must fulfil the following requirements

- The stability and biological activity of the drug must be conserved.
- The yield of the nanoparticle with required size range and drug encapsulation efficiency must be high.

- The nanoparticle quality and drug release profile must be reproducible within specified limits.
- The nanoparticles must be free of aggregation or adherence.

1.14 Release Mechanism of Drugs from PLGA Nanoparticles

There are four possible mechanisms for the release of drug molecules form PLGA based matrix

- Diffusion through water filled pores
- Diffusion through the polymer
- Osmotic pumping
- Erosion

The biodegradation rate of PLGA polymers are governed by the molar ratio of lactic and glycolic acid in the polymer chain, molecular weight of the polymer, degree of crystallinity and glass transition temperature of the polymer. As many different variables influence the diffusion and erosion of the polymer, the release rate pattern is often unpredictable. However, biphasic curve for drug release from PLGA based nanoparticles are more common (Makadia and Siegel, 2011).

1.14.1 Biphasic Release

This include two different phases

1.14.1.1 Burst Release

Drug molecules present on the surface, in contact with the medium is released as a function of solubility along with water diffusion into the matrix.

1.14.1.2. Progressive Release

The second phase follows a more progressive release through the polymer matrix in a diffusion and erosion dependent manner.

During the drug release process, the drug is released from the hydrated polymer matrix to the aqueous phase. The process of hydration relaxes the polymer chain and enhances the diffusion of drug molecules. The rate of water intake of polymer matrix increases with the hydrophilicity of the polymer. Hence initial burst and quantity of drug released over a short time is higher for hydrophilic matrixes.

1.15 Rationale for Selection of Thiol, Glucose & Mucin based Modification of PLGA

The biocompatibility, biodegradability and tailor made physicochemical characteristics are the basic factors that have lead to the success story of PLGA family of thermoplastic polymers including its Food and Drug Administration approval for clinical use in humans. (Lu et al., 2009) (Makadia and Siegel, 2011). Though the PLGA based technology open new vistas in theranostics and tissue engineering applications, especially for cardio-vascular diseases and cancer, they do suffer from certain intrinsic drawbacks including the following (Sah et al., 2013).

- Relative hydrophobicity compared to the natural extracellular matrix
- Poor in vivo blood circulation time
- Rapid recognition and removal of PLGA by body s defence mechanism
- Negatively charged PLGA surface limiting the transport across biological barriers such as plasma membrane or tight junctions

- Passive diffusion into tumor via enhanced permeability and retention (EPR) effect doesn't meet the required clinical efficacy.

Taking into consideration that the mechanical and degradative characteristics of PLGA are apparently ideal, a promising approach seems to be the surface engineering of bare PLGA nanoparticles, post synthesis. This can help to provide the required surface characteristics to overcome these delivery challenges and improve the in vivo performance, without altering the properties of the bulk polymer, PLGA (Croll et al., 2004).

The concept of enhancing the hemocompatibility of a known FDA approved polymer, PLGA is significant from the viewpoint of the material s hydrophobicity. Well defined modifications of PLGA nanosystems could control the individual parameters involved in the chain of hemocompatibility sequence, in order to achieve an overall tolerance with the blood cells and the plasma. Several approaches to modify the PLGA nanoparticle surface has been attempted and published. However, their success is limited by the immunogenicity, compromised targetability and accelerated blood clearance mechanisms. This is often associated with the PEGylated nano-carriers which in turn compelled the search for better surface stabilizing alternatives. Nature has evolved many elegant immune evasive strategies that provide impetus for a more biomimetic approach towards material design. In nature, cells and pathogens are destined to resist non-specific biomolecule interaction while maintaining specific molecular recognition. Thus, in regard to the nitric oxide mediated non thrombogenecity of an endothelial cell, the compatibility of the glucose predominant cellular glycocalyx and the immune dodging mechanism of a mucylated pathogen inspired us to focus on three different molecules namely, thiol,

glucose, and mucin moieties to harmonize the interactions between the nanoparticle surface and the biological milieu. Further, as the selected moieties are biological in origin and are considerably smaller in size can help to optimise the non-fouling features of a comparatively hydrophobic PLGA surface while maintaining the cell specific recognition events.

1.16 The need for extensive hemocompatibility characterisation

In order to understand pathophysiological processes occurring at the blood-material interface, materials surface properties has to be correlated to the different hemocompatibility parameters. (Wang et al., 2004). The present modifications have been performed based on the long term goal of developing suitable intravenal therapeutics. Taking into consideration that these modifications have not been performed earlier on PLGA based nanoparticles, a detailed hemocompatibility analysis become mandatory. The work is justified on the basis of providing a systematic understanding of the influences of the surface features of PLGA based nanoparticles on the subtle parameters of hemocompatibility. Additionally, the enhanced hemocompatibility was integrated to the parameters required for drug delivery. Such an assessment of the hemocompatibility factors including protein adsorption, complement and platelet activation can provide reliable in vitro - in vivo extrapolation and thereby helping us to foresee the complications involved under clinical situations.

1.17. Hypothesis

We hypothesised that the modifications of the PLGA polymer based on thiol, glucose and mucin moieties as an efficient strategy to enhance the hemocompatibility of inherently hydrophobic PLGA nanoparticles. The enhanced hemocompatibility of modified PLGA nanoparticles could also contribute towards better pharmacokinetics after suitable drug encapsulation, under in vitro conditions.

1.18 Objective of the study

- PLGA polymer modification with ***Thiol***, ***Glucose*** & ***Mucin*** moieties and subsequent nanoparticle synthesis.
- Blood Compatibility evaluation of pristine and thiol, glucose & mucin modified PLGA nanoparticles.
- Chemotherapeutic drug (***Doxorubicin***, ***Curcumin*** & ***Betulinic acid***) encapsulation into pristine and modified (***Thiol***, ***Glucose*** & ***Mucin***) PLGA nanoparticles.
- Drug release kinetics and cytotoxic potential analysis of pristine and modified PLGA nanoparticles, under *in vitro* conditions.
- Selection of the most efficient drug-nanoparticle combination with respect to in vitro chemotherapeutic analysis of the differently modified PLGA nanoparticles.

The chapters discussed in the thesis are summarised below. The chapter 1, Introduction, provides an overview of the various topics related to polymer based nanoparticle mediated drug delivery. The chapter 2, literature review, illustrates the significance of PLGA, its properties and modification and significance of surface functionalised PLGA nanoparticles for drug delivery and their literature elsewhere. Chapter 3, materials and methods involves the preparation of modified PLGA nanoparticles, physico chemical and biological characterisation of synthesised nanoparticles, chemotherapeutic drug loading, release kinetics

and cytotoxic potential analysis. Chapter 4 is the result section followed by Chapter 5 which describes the discussions of the observed results. The chapter 6 would be dealing with the summary and conclusion of most important results and the thesis concludes by highlighting the major findings from the study.

CHAPTER 2
REVIEW OF LITERATURE

2 REVIEW OF LITERATURE

2.1 Poly Lactic co Glycolic Acid

Beginning in the 1970 s with biodegradable sutures, the copolymer, poly lactic co glycolic acid has a long history of use as biomaterials due to their excellent biocompatibility and biodegradability. PLGA are a family of FDA approved thermoplastic polymers that find application in various clinical and basic science research fields including drug delivery, diagnostics, cardiovascular diseases, vaccine, cancer and tissue engineering (Lu et al., 2009) (Makadia and Siegel, 2011).

2.2 Synthesis of PLGA

Polyester PLGA is a copolymer of poly lactic acid and poly glycolic acid where the enantiomeric forms of polymer lactic acid are in equal ratio. PLGA is a copolymer synthesised through random ring opening copolymerisation technique. The monomers or the cyclic dimers (1, 4-dioxane-2,5-dione) of glycolic and lactic acid form the basic units of polymerisation (Mundargi et al., 2008). The successive polymerisation of the monomer units of glycolic or lactic acid via ester linkages yields a linear, aliphatic and amorphous polyester product, as shown in Figure 4.

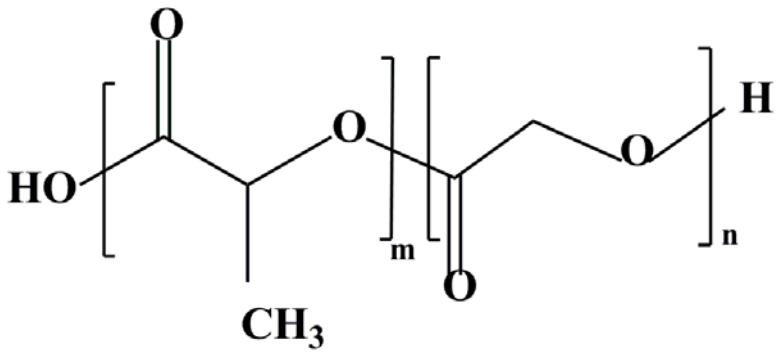

m: Number of units of lactic acid

n: Number of units of glycolic acid

Figure 4: Structure of poly lactic co glycolic acid (Lu et al., 2009)

Tin (II) 2-ethylhexanoate, tin (II) alkoxides or aluminum isopropoxide can catalyse the copolymerisation reaction. The ratio of monomers used identifies the different forms of PLGA, for e.g., 50:50 identifies a copolymer whose composition is 50% lactic acid and 50% glycolic acid(Lu et al., 2009).

2.3 Biological Properties of PLGA

2.3.1. Biodegradability

The mechanism of degradation of aliphatic polyester PLGA is through hydrolysis and subsequent cleavage of its backbone ester linkages (Shive and Anderson, 1997), (Okada and Toguchi, 1995). The hydrolysis results in the formation of its metabolite monomers, lactic acid and glycolic acid and undergoes metabolisation within the body via the Krebs cycle (Danhier et al., 2012a), as shown in Figure 5

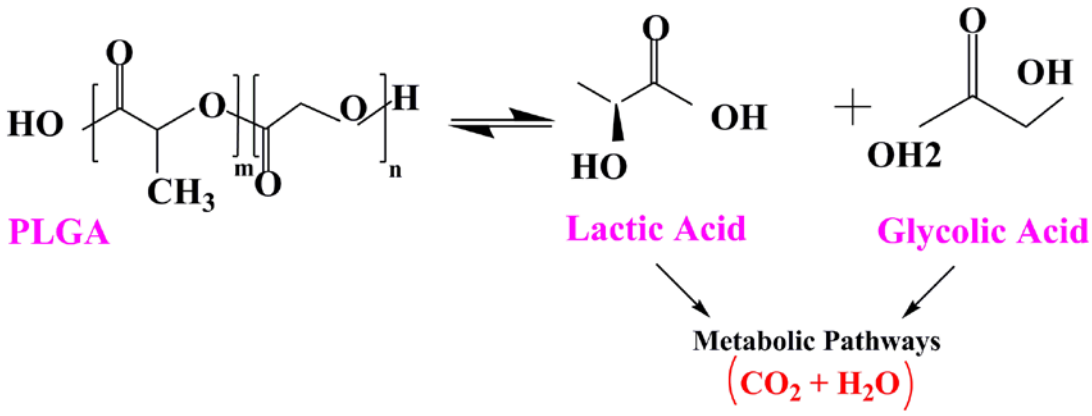

Figure 5: Hydrolysis of PLGA (Danhier et al., 2012a)

A triphasic mechanism for PLGA biodegradation has been proposed (Jain, 2000b)

- Random chain scission process – initially upon contact with water, the molecular weight of the copolymer decreases significantly as PLGA are hydrolytically unstable. However, soluble oligomer diffusion and weight loss are not observed.

- In the middle phase, osmotic pressure within the matrix increases as a result of the strong water affinity of the oligomers present inside the matrix. Subsequent crack propagation and micro cavity formation leads to diffusion of soluble oligomer and rapid mass loss.

- The final phase of erosion continues until the matrix is no longer mechanically stable and undergoes complete fragmentation and polymer solubilisation.

The factors that can influence the hydrolytic degradation behaviour of copolymer PLGA are indicated below (Shive and Anderson, 1997)

2.3.1.1 Water permeability and solubility (hydrophilicity/hydrophobicity)

The higher content of monomer, glycolic acid, makes the copolymer more hydrophilic and hence lead to faster degradation. An exception is the 50:50 PLGA, which exhibits the fastest degradation than those containing higher proportion of either of the two monomers.

2.3.1.2. Chemical composition

Altering the chemical composition by increasing the glycolide content in the copolymer can increase the biodegradation rate.

2.3.1.3 Mechanism of hydrolysis (non catalytic, autocatalytic and enzymatic)

Based upon the difference in the in vitro and in vivo degradation rate, Lewis et al have proposed the role of enzymes in PLGA breakdown (Alexis, 2005)

2.3.1.4. Additives (acidic, basic, monomers, solvents, drugs)

Acid compounds can calayse the cleavage of ester linkages and accelerate degradation while the basic compounds can neutralise carboxyl end groups and thereby decrease the biodegradation rate.

2.3.1.5. Morphology (crystalline/ amorphous)

Reduced crystallinity increases the rate of hydration and hydrolysis.

2.3.1.6 Device dimension (size, shape, surface to volume ratio)

Large sized devices undergo heterogeneous degradation where the rate of degradation in the core is greater than at the surface while particles less than 300 micrometer undergo homogenous degradation.

2.3.1.7. Porosity

Porosity enhances the rate of degradation by permitting the release of oligomers and enabling entry of phagocytic cells under in vivo conditions.

2.3.1.8. Glass transition temperature (Glassy/ rubbery)

Decrease in glass transition temperature, decreases the crystallinity and increases the rate of degradation.

2.3.1.9. Molecular weight and molecular weight distribution

Large or wide molecular weight distribution increases the rate of degradation by facilitating autocatalytic degradation.

2.4. Biocompatibility

An understanding of inflammatory and healing responses associated with colloidal drug delivery administration is required to evaluate the biocompatibility of delivery systems (Shive and Anderson, 1997). The sequence of

events following the administration of a colloidal drug delivery system is illustrated in Figure 6 and Table II

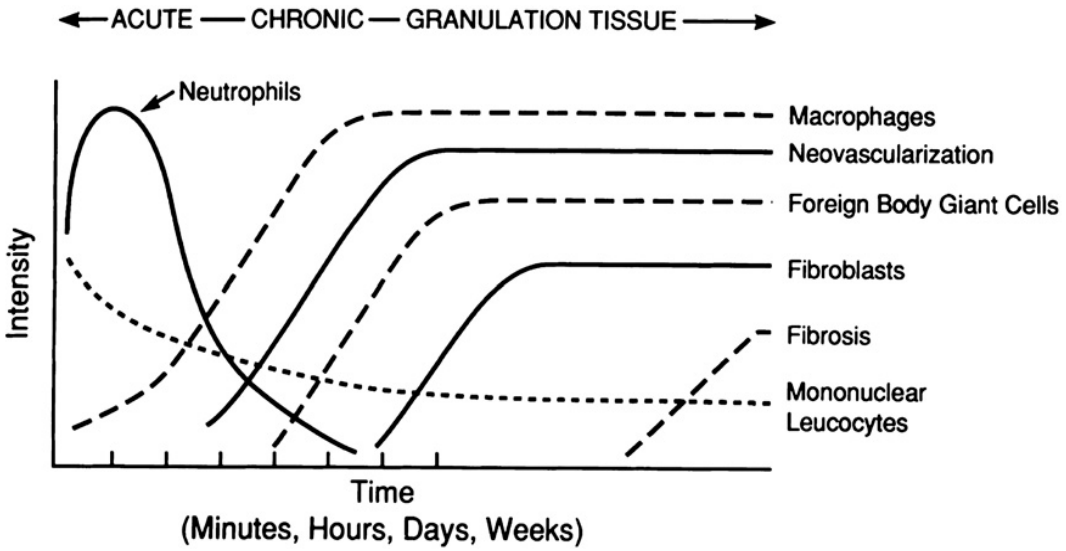

Figure 6: The temporal variation in the acute inflammatory response, chronic inflammatory response, granulation tissue development and foreign body reaction to implantable biodegradable microspheres (Shive and Anderson, 1997)

Table II: Sequence of local events following implantation: The tissue response continuum (Shive and Anderson, 1997)

Injury	Injection, Implantation
Acute inflammation	Polymorphonuclear Leukocytes
Chronic inflammation	Monocytes and Lymphocytes
Granulation tissue	Fibroblasts and New Blood Capillaries
Foreign Body Reaction	Macrophages and FBGCs at the Material-Tissue Interface
Fibrosis	Fibrous Capsule

Splenlehauer et al injected PLGA 75:25 microspheres in to the portal veins of rats for embolization within the liver. After 24h, the microspheres

were identified within the small vessels of liver without eliciting any inflammatory or haemorrhagic effects in the hepatic tissue. The microspheres remained intact even after 3 weeks following embolisation along with the presence of only few macrophages, lymphocytes and foreign body giant cells on the surface. The number and size of foreign body giant cells increased with the corresponding increase in the inflammatory responses at four week time interval. Alteration in the shape of PLGA microspheres is observed. At five weeks following embolisation, the activity of the giant cells was at the peak and the total integrity of the microspheres was lost. At six weeks, only remnants of 75:25 PLGA were observed and total resorption was achieved after 8 to 12 weeks following embolisation (Spenlehauer et al., 1989). PLGA exhibits minimal systemic cytotoxicity considering applications like drug delivery or biomaterial applications as the degradation products are easily metabolised in the body via the Krebs cycle. Athanasiou et al has conducted in vitro and in vivo studies that confirmed the satisfactory biocompatibility and absence of toxic potential of polylactic acid /poly glycolic acid copolymers (Athanasiou et al., 1996).

2.5. Biodistribution

Knowledge of biodistribution coupled with that of biodegradation is quintessential in understanding the pharmacokinetics as well as the design of drug delivery systems (Alexis et al., 2008). Major organs differ in the aspect of nanoparticle deposition and degradation over time. The route of administration significantly influences the biodistribution profile of nanoparticles, including the polymer PLGA. It is quite established from reported studies that orally

delivered nanoparticles reach the organs to a lower extend when compared to intravenal administration. For example, PLGA nanoparticles delivered orally exhibited 0.15% dose/g liver deposition while it increased to 1% dose/g liver through intravenal administration, under the same time frame (Simon and Sabliov, 2013). For PLGA based nanoparticles, irrespective of the size, liver is the site of highest deposition followed by spleen and lungs. Liver deposition is in accordance with the sequestration of nanoparticles by the MPS system. The highest particle concentration was observed after 4h in liver. In case of heart, low uptake of particles was seen during the first 24 h of administration. PLGA nanoparticles were detected within the brain at a maximum of 5% dose/g at all time points. Semete et al has studied the tissue distribution and retention following oral delivery of PLGA nanoparticles for 7 days (Semete et al., 2010). At the end of 7 days, PLGA particles remain detectable in the liver, heart, brain, kidneys, lungs and spleen. The highest and lowest percentage were localised in the liver (40.04%) and spleen followed by 25.97% in the kidneys and 12.86% in the brain. Owing to degradation and redistribution of soluble PLGA oligomers to different organs we find a time dependent decrease in the amount of nanoparticle deposition within each organ studied (Mohammad and Reineke, 2013). In other words, the safety of PLGA nanoparticles is apparent from this particle clearance kinetics within 24 h after administration.

2.6. Surface Modification of PLGA Nanoparticles

Several reports have demonstrated that nanoparticles once administered intravenously are prone to clearance by RES provided the surface is not protected from opsonisation (Moghimi et al., 2005). To be specific, there is a progressive interest in developing injectable drug polymeric carriers which are not identified as foreign particles. An ideal half life of over 6 h is minimal for the nanovehicle to exploit the pathophysiological peculiarities of the tumor environment. Hence, the surface modification of nanoparticles becomes indispensible in the context of extended circulatory half life (Dailey and Kissel, 2005).

2.6.1 Techniques to Modify Nanoparticle Surface

We can modify and functionalise the surface of nanostructures using different techniques that include physical, chemical and biological methods. Irrespective of the method adopted, surface modification provides enhanced solubility and stability of nanoparticles in aqueous media along with novel material functions and properties (Xu et al., 2007).

2.6.1.1 Physical Treatment

Leading strategies for physical surface modification of the nano surfaces include molecular coating (or adsorption), surface entrapment, plasma spraying, ozone ablation, or physical treatment with UV. This leads to functionalisation and activation of materials as different functional molecules, entities, varying charges and active chemical groups get introduced on the nano surfaces. The advantages include the mild reaction conditions that ensure the

complete retention of the bioactivity of the modifying biomolecules. Different non covalent mechanisms that come in to action during physical modification include hydrophobic, ionic and •-• interactions. Most of the proteins, enzymes and non-ionic polymers such as PEO-PPO copolymer and polysorbates get coated onto nanoparticle surface through hydrophobic interactions. Such modified nanosurfaces include PLGA and PLA nanoparticles. In case of hydrophilic polymers such as dextran, hydrophobic interactions are not sufficient enough to facilitate it's adsorption on to nanoparticles surfaces. However, following surface modification with a hydrophobic molecule such as phenoxy group, dextran turns amphilic and result in stable suspensions of polystyrene or PLA nanoparticles. Ionic interactions form the basis of a novel layer by layer electrostatic self assembly of polyelectrolyte nanoshell on individual carbon nanotubes while the surfactant SDS stabilisation of carbon nanotubes were mediated through •-• as well as hydrophobic interactions. The comparatively poor strength of the physical bond formed between the substrate and the modifiers during physical treatment limits its wide applicability. Further, the chances of detachment of these functional molecules are high when the nanoparticles are subjected to in vivo conditions.

2.6.1.2. Chemical Modification

Chemical reactions can covalently link the functional molecules on to the nanosurfaces. The stable covalent linkages can offer stronger interactions and activate the nanosurfaces to greater extent. Major limitations associated with chemical modification include the chances of denaturation of biomolecules, incompatibility and toxicity.

2.6.1.2.1 Surface oxidation

Oxidative acid treatment can be used to introduce carboxylic acid groups onto the surfaces of carbon nanotubes. This provides further possibility for immobilisation of functional molecules and ligands.

2.6.1.2.2 Carbodiimide and Glutaraldehyde Coupling Chemistry

The above two coupling linkers have found extensive application in chemical surface modification for conjugating diverse functional moieties such as proteins, enzymes, peptides, DNA and receptor ligands on to the nanosurfaces. These coupling reagents react covalently with the active chemical groups and sites, such as $–NH_{3,}$ -COOH, -SH present on the surfaces of nanoparticles.

2.6.1.2.3 Silane Chemistry

Silanization of silica and metal based nanoparticles forms another chemical modification technique that employs the conventional silanization agent trimethoxysilylpropyl-diethylene triamime (DETA).

2.6.1.2.4 Self Assembled Monolayer

The spontaneous self assembly of functional molecules on to the surface of nanoparticles through physical or chemical sorption lead to the formation of SAMs. For an instance, thiol functionalised poly (styrene co acrylic) nanoparticles could be self assemble on to a gold electrode.

2.6.1.3 Biological Modification

Enhanced biocompatibility and different functionalities can be imparted to the nanoparticle surface through biological modifications, either physically or chemically. The conjugation of nanoparticle surface with biospecific molecules can in turn provide additional sites for further immobilisation of ligands specific to these molecules. Biologically specific reactions such as antibody-antigen, receptor-ligand, avidin-biotin, DNA-DNA hybridization could be exploited for further immobilization of specific ligands. For example the surface modification with folic acid confers the nanoparticles with efficient internalisation capacity owing to the high affinity of the modifying moiety for folic acid receptors on the cancer cells.

2.6.2 The basis of Surface Modifications - Steric Shielding and Stealth Properties

The opsonin mediated interaction with nanoparticles in the bloodstream proceeds through Van der Waals, electrostatic, ionic and hydrophobic/hydrophilic forces. Hence, the critical factor for opsonisation becomes the surface features of the nanoparticles (Owens and Peppas, 2006). Generally hydrophobic and charged surfaces promote greater extend of opsonisation as compared to hydrophilic and neutral surfaces.

The last decade has seen the evolution of different theories that describe the pharmacokinetics of nanosized drug delivery systems. It is now accepted that long circulating nanocarriers, stealth systems, can be developed by surface coating with hydrophilic polymers that reduce the opsonisation process

(Moghimi and Szebeni, 2003). Reduction of opsonisation results in the prolongation of nanocarriers in the blood stream from few seconds to several hours. The term stealth is translated from the low observance technology applied to military tactics.

Peppas described the effect of surface modification in terms of elastic forces by taking the example of the widely used modifying moiety PEG (Salmaso and Caliceti, 2013). Accounting to the hydrophilic and flexible nature, PEG chains tend to exist in an extended conformation on particle surface. Opsonins on approaching the particle surface compress the extended PEG chains to a more compressed and energetically higher conformation. As a result, the magnitude of attractive forces between opsonins and particle get subdued and the repulsive forces might predominate the interactions.

2.6.3 Polymers used to modify nanocarrier surface

Hydrophilicity and flexibility top among the basic properties of the polymer that are used to modify the particle surface to confer steric stability. The range includes natural and semi synthetic polysaccharides to synthetic polymers have been used as surface modifiers. Dextran, polysialic acid, hyaluronic acid, chitosan and heparin are the most common natural polysaccharides. Synthetic polymers include polyvinyl pyrollidine, polyvinyl alcohol, polyacrylamide, polyethylene glycol and PEG based copolymers such as poloxamer, poloxamines and polysorbates.

2.6.3.1 PEGylation for Stealth Coating

Among the different non ionic hydrophilic polymers and surfactants, poly ethylene glycol has been the polymer of choice for current surface modification studies. In 1977, Abuchowskii et al reported that by covalently conjugating 2 kDa or 5kDa PEG to bovine liver catalase, a significant decrease in immunogenicity of the protein as well as enhanced blood residence time was observed. Since then an extensive use of PEG (5kDa) has been observed in the literature of nanoparticulate systems (Amoozgar and Yeo, 2012).

A flexible layer is formed on the surface of nanoparticles by the PEG molecule. The mechanism of steric hindrance exhibited by the PEG modified particles is based on the structured organisation of water molecules though hydrogen bonding to the ether oxygen molecules of PEG (Gref et al., 1995b). The tightly ordered water molecules repel against opsonisation by forming a hydrated film around the particles. Hence protects the surface from phagocytic cell interactions. This PEG surface layer can be compared to a mushroom or brush model. Mushroom like structure is predominant when the PEG surface density is relatively low (0.5-0.7 mol% PEG 5kDa) and hence maximises the surface coverage. Extension of PEG chains to reduce overlapping with other PEG molecules occur as the PEG density increases and thus results in the brush model. The optimal PEG content differs with each system studied. For example, in case of polylactic or poly glycolic acid nanoparticles, a 10 wt % PEG density was adequate to display their optimal particle dispersability and stealth effect. However Gref et al considered 5 % to be the optimal PEG density for maximal surface coverage. Whereas 5-7 mol%

PEG is optimal for liposomes for synthesising thermodynamically stable particles. The reports verifying the enhanced blood circulation after PEGylation are numerous. For example, Jokerst et al has provided an extensive review on the enhanced plasma concentration and lower accumulation of Pegylated PLGA nanoparticles in the liver when compared to non pegylated PLGA nanoparticles (Jokerst et al., 2011). Also, Cu et al has demonstrated the direct influence of PEG on the surface properties of PLGA nanoparticles that facilitated an easy diffusion in the human cervical mucus (Cu and Saltzman, 2009). Through freeze fracture transmission electron microscopy, the protein repulsion operated by PEG was also visualised (Peracchia et al., 1999).

2.6.3.2 Poloxamine & Poloxamer

Poloxamines (Tetronics) and poloxamers (Pluronics) belong to the family of amphilic block copolymers that are characterised by the presence of hydrophilic blocks of ethylene oxide and hydrophobic blocks of propylene oxide monomer units respectively. Poloxamers can also be categorised as a-b-a type triblock copolymers while poloxamines are tetrablock copolymers connected through ethylenediamine bridges (Salmaso and Caliceti, 2013).

2.6.3.3 Dextran

Dextran is a polysaccharide widely used for surface modification of nanoparticulate drug delivery systems. The steric effect of the long brushes of dextran is similar to PEG polymer in terms of reducing opsonisation. Hence, dextran has been found to enhance the stability and circulatory half life of liposomes. AMI227 particles(ultra small super paramagnetic iron oxide) of 4-5nm

coated with 20-30 hydrated brush like dextran molecules helped in extending the circulatory half life to 3-4 hrs .

2.6.3.4 Sialic Acid

Sialic acid belongs to the family of neuraminic acid and is bestowed with properties of phagocytic evasion and subsequent long circulation. As a component of eukaryotic cell surface, sialic acid plays a pivotal role in extending the lifetime of circulatory cells via inhibiting complement activation. The potential of polysialic acid and it derivatives in drug delivery for providing stealth properties has been characterised in liposomes by Surolia and Bachawat (Surolia and Bachhawat, 1977).

2.6.3.5. Zwitterionic Polymers

Liposome mediated complement activation can be reduced with the help of zwitter ionic phospholipid derivatives. Successively, synthetic zwitterionic molecules have been used for developing stealth carriers. These polymers reduce opsonisation via electrostatically induced hydration and bind water molecules more strongly than PEG. The stability, circulatory half life and pharmacokinetic profile of poly carboxybetaine coated liposomes are similar to the PEGylated counterparts.

2.6.3.6 Polyglycerols

Polyglycerol comprises of biocompatible and flexible hydrophilic aliphatic polyether polyols that exhibit antifouling character similar to PEG. The multivalent nature permits the simultaneous conjugation of targeting

agents, drugs and modifiers. The polyglycerol conferred enhanced blood circulatory half life to liposomes and decreased clearance by liver and spleen. The flexible aliphatic polyether structure, hydrophilic surface groups and the branched architecture contribute towards its protein resistant nature.

2.6.4 Surface requirements to set up long circulating nanocarriers

The ability of hydrophilic polymers to resist opsonisation has direct correlation to the polymer composition, polymer molecular weight, and density on the carrier surface, thickness of the coating, conformation, flexibility and architecture of the chains (Salmaso and Caliceti, 2013).

2.6.4.1 Architecture and molecular weight

The length of the polymeric strands on the modified nanoparticle surface must be greater than the range of van der Waals attractive forces between the plasma proteins in the bulk and phagocytic cells. A minimal of 2kDa molecular weight is considered to be the lower threshold to assure macrophage avoidance. Blood circulatory half life increases linearly with increase in polymer molecular weight. It has been demonstrated by Gref et al that the 5kDa PEG has the maximal capacity to reduce protein adsorption (Gref et al., 2000).

2.6.4.2 Polymer Density

The relevance of polymer density becomes evident with the fact that the high polymer density can compensate the low polymer molecular weight in conferring stealth characteristics. The investigation by Vittaz et al has demonstrated that a distance of 2.2 nm between two PEG chains (2kDa) that

corresponds to 0.2 PEG molecules/nm^2 and is the most efficient in terms of resisting complement activation (Vittaz et al., 1996). However, certain parameters including particle size and surface curvature have a role in deciding the polymer density threshold.

2.6.4.3 Surface polymer conformation

A polymer chain conformation in between the mushroom and brush configuration is found optimal in conferring stealth properties. This specific conformation ensures a constricted configuration with an optimal density for providing a homogenous surface coating. Presence of gaps between the polymeric strands could opsonise small protein molecules. Hence, Papisov et al highlighted the importance of brush density, brush rigidity, brush molecular length, substrate size and cooperative character of interaction on steric repulsion and obstruction (Papisov, 1998).

2.6.4.4 Polymeric Corona Thickness

Optimal polymeric layer thickness is critical in achieving stealth character. The thickness of the coating layer depends on the potential of opsonins and the particle size. Reports have demonstrated that the minimal effective hydrodynamic layer thickness is 5% of the particle diameter. Moghimi et al reported that 4 kDa PEG that provides around 5nm coating thickness can effectively resist protein adsorption and complement activation (Moghimi et al., 1993).

2.6.4.5. Polymer Flexibility

Polymer chain flexibility is also required for resisting opsonisation. Flexibility induces dynamicity in the PEG chain conformation that minimises the exposure of fixation sites for opsonins. The mobility of the flexible chains permits the polymer to undergo numerous conformational alterations that could expel the water molecules temporarily. This water cloud surrounding the nanoparticle protects the surface from opsonisation by conferring an interfacial free energy.

2.6.4.6. Amphiphilic polymer architecture

Polymer architecture is critical in determining opsonisation as it affects the conformation of the coating polymer on the nanoparticle surface. Studies were performed on liposomes modified with PEG-PE and PEG_2-PE to understand the effect of linear and branched PEG in conferring stealth characteristic to nanocarriers. The results highlighted the efficiency of PEG_2-PE in providing extended circulation in comparison to PEG-PE at low content. Increasing the ratio of PEG-PE provided more homogenous surface coverage. The PEG molecule is considered to form a single turned coil arrangement after attaching through both terminal groups to the nanoparticle surface (Salmaso and Caliceti, 2013). This endowed the particles with compact conformational structure to resist opsonisation. Another study by Rieger et al further compared the resistance to opsonisation by nanoparticles prepared from PEO grafted PCL copolymer and PEO-b-PCL di block copolymer reinforced the importance of polymer architecture in yielding stealth characteristics (Rieger et al., 2006) .

2.6.4.7 Controversial effect of polymer based surface modification

The above studies pinpoint that the particle opsonisation could be reduced by surface modification with hydrophilic flexible polymers and this phenomenon has been described by mathematical elaborations. However the literature cites several controversial results also. Some commercially successful stealth nanocarriers like Doxil remain in the circulation for a long time in spite of extensive opsonisation. This focuses on the complexity of stealth behaviour or long circulation and it cannot be simplified in terms of opsonin repulsion alone.

2.7. Limitations in current surface modification strategies.

2.7.1 The PEG Dilemma

2.7.1.1 Interference with cellular uptake and endosomal escape of nanoparticles

Recent studies have emphasised on the drawbacks of PEGylation even with its surface protective nature. For drug delivery applications the nanoparticle must meet several criteria including

- Transport in the extracellular medium
- Attachment to the cell membrane via receptors
- Internalisation into the cells
- Escape from intra cellular vesicles and drug release to the cytosol
- Transport to target organelles.

The major problem is that the surface aqueous moiety formed after PEGylation that prolongs the residence time dramatically hinders cell-particle interactions. As a result, cellular uptake becomes minimal. Furthermore, the greater surface stability achieved through PEGylation can result in poor endosomal escape of liposomes via membrane fusion. Thus we conclude that though PEGylation favourably controls the biodistribution and tumor accumulation of nanoparticles, it significantly compromises on the uptake and intracellular trafficking of nanocarriers (Hatakeyama et al., 2013a). For example, PEGylated liposomal doxorubicin displayed reduced tumor accumulation than non pegylated liposomes that intensify the concept of PEG interference with cell-liposome interactions. Another investigation by Hatakeyama et al concluded that PEGylated multifunctional envelope type nanodevice (MEND) resulted in a lower gene expression than unmodified MEND (Hatakeyama et al., 2011). Moreover, Mishra et al demonstrated that PEGylation of non viral gene vectors (branched polyethlyeneimine) or beta cyclodextrin containing polymer led to considerable decrease in gene expression (Mishra et al., 2004). The fluorescence resonance energy transfer based investigation on the intracellular fate of PEGylated liposomes by Remaut et al further reinforced the concept of PEG Dilemma (Remaut et al., 2012).

In addition, immune responses to PEGylated nanomedicine have also been reported. Ishida et al reported about the rapid clearance of PEGylated liposomes from blood upon repeated administrations (Ishida et al., 2006). The production of PEG specific IgM, after the initial sensitization of PEGylated particles was responsible for this accelerated blood clearance of the second dose of PEG

modified particles. Also, the non degradable nature of PEG molecules can cause toxicity with accumulation inside the lysosomes.

2.7.2 Drawbacks of other polymer based modifications

Some reports have failed to demonstrate increased circulation half time following intravenous injection of poloxamine or poloxamer coated nanoparticles of poly-phosphazene, PLGA and polyglycerol to mice and rats when compared to uncoated particles. This exceptional behaviour could arise from the combined effect of the desorption of the modifier from the nanocarrier surface as well as the opsonin adsorption to the exposed hydrophobic portions of poloxamer or poloxamines (Salmaso and Caliceti, 2013).

Similarly, certain reports demonstrate the production of antidextran antibody that contributes to the macrophage recognition of iron oxide nanoparticles. In addition, orosomucoid failed to yield adequate stealth nature to polyisobutylcyanoacrylate particles. The reason could be the low density of sialic acid molecules on the particle surface that could lead the inefficient coating or conformation of the clustered glycans.

In case of zwitterion based modification, the excellent stability and resistance to opsonisation offered by such polymers could translate to exceptionally lower cellular uptake.

The above mentioned PEG Dilemma and the related limitations of current surface modification approaches have propelled the need to develop alternate

surface functionalisation strategies on PLGA nanoparticles for drug delivery applications.

2.8 Biomimetic Modification of PLGA based Nanoparticles

Nature has evolved many elegant immune evasive strategies that provide impetus for a more biomimetic approach toward material design. In nature, cells and pathogens are destined to resist non-specific biomolecule interaction while maintaining specific molecular recognition. Thus, in regard to the nitric oxide mediated non thrombogenecity of an endothelial cell, the perfect compatibility of the glucose predominant cellular glycocalyx and the immune dodging mechanism of a mucylated pathogen inspired us to focus on three different molecules namely, thiol, glucose, and mucin moieties to harmonize the interactions between the nanoparticle surface and the biological milieu (Duan and Lewis, 2002a), (Veerapandian et al., 2009) and (Chen et al., 2004). Figure 7 provides a glimpse of the modification criteria.

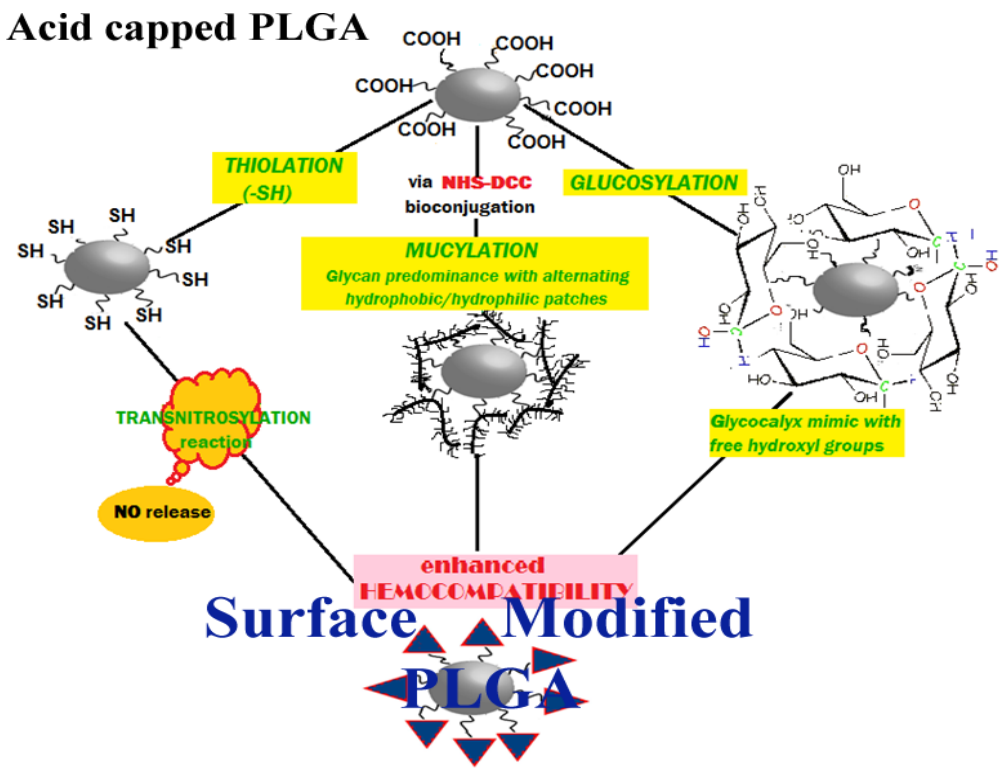

Figure 7: Strategies for Modification of PLGA Nanoparticles

2.8.1 Thiolation

The perfect thromboresistance of the human endothelium has been partly associated with the slow but continuous release of a messenger molecule named nitric oxide (Frost et al., 2005b). Nitric oxide has been widely recognised as an inhibitor of platelet adhesion, aggregation and activation as well as for its ability to relax smooth muscle cells. Hence the localised release of nitric oxide at the particle/blood interface at or above the physiological flux, to some extent, could be able to mimic the non thrombogenecity exhibited by the endothelial cell surface. The S-nitroso adducts with thiol groups, primarily in the form of S-nitrosoalbumin, S-nitroso cysteine or S-nitrosoglutathione, circulate in the blood as a potential source for generating nitric oxide in situ at the particle/blood interface. Studies have shown that nitrosylated albumin readily transfer nitric oxide, both in vitro and in vivo, to

low molecular weight thiols such as L-cysteine, either free or immobilised on a surface. The resulting instability of nitrosylated L-Cysteine would accelerate the release of nitric oxide from CySNO through transnitrosylation reaction and hence promote the hemocompatibility of cysteine modified PLGA nanoparticles (Singh et al., 1996).

2.8.2 Glucosylation

Glyconanobiology offer much potential for nanoparticle surface functionalization with monosaccharides like glucosamine. The multiple hydroxyl groups present on the glucose conjugated nanoparticle surface would partially mimic the hydrophilic glycocalyx that shield against non specific plasma protein adsorption while maintaining specific cellular interactions. We reasoned that this small monosaccharide would bypass the limitations of existing surface modifiers by acting as a passivating agent that seldom causes any steric repulsion at the targeting site (Moros et al., 2012).

2.8.3 Mucylation

Mucins are a central class of large and heavily glycosylated proteins present in the mucus of the epithelium, with roles in modulating cell–cell interactions, immune response and cell signalling (Svensson and Arnebrant, 2010). Mucins are characterized by extended regions of densely clustered serine and threonine residues bearing O-linked glycans that initiate with a linked N-acetyl galactosyl amine. Owing to their characteristic pattern of glycosylation, the polypeptide backbone extends above the cell surface forming a protective barrier against cell-protein–pathogen interaction in a glycan specific manner (Chaturvedi et al., 2008). The distinguished interfacial activity of mucin owe to their unique tandem

repeat structure of heavily glycosylated hydrophilic domains intermitted by hydrophobic protein domains rendering a natural surfactant action like the pluronics (Shi et al., 2000). Their biological origin, first line of defence against pathogen in all moist mammalian epithelia and antifouling features mediate favourable host reactions, compatibility and controlled cellular interplay. Hence, suggest possible roles for mucin as biocompatible coatings for synthetic materials. These functions when extended in the context of nanoparticle modification leads to the masking of biomaterial surface epitopes and thereby conferring greater longetivity to circulating nanoparticles by dodging the immune surveillance (Rabuka et al., 2007).

2.9. Surface Modification of PLGA Nanoparticles with Respect to Various Applications

The surface of PLGA is often modified with various moieties with different end group functionalities. Currently, amine, aldehyde, carboxyl, maleimide, succinimidyl ester and sulfhydryl functionalised PLGA derivatives are available (Sah et al., 2013)

2.9.1 Bisphosphonate functional PLGA Nanoparticles

Bisphosphonates are generally used to treat bone metastases as it cause osteoclast apoptosis. The tendency of bisphosphonates to accumulate in bones due to their strong affinity to calcium has been utilised to synthesise bisphosphonate-PLGA conjugates that can be used as nanoparticle forming matrixes. Pignatello et al has conjugated nitrogen containing bisphosphonate, alendronate to PLGA and the synthesised nanoparticles that exhibited better adsorption onto

hydroxyapaptite in comparison to bare PLGA nanoparticles. In addition to better bone targetability, these modified nanoparticles had minimal cytotoxic effects on endothelial cells or trabecular osteoblasts. The cytotoxicity of bisphosphonates to tumor cells and macrophages had imparted the modified PLGA nanoparticles with the potential for cancer immunotherapy.

2.9.2 Lectin Functional PLGA Nanoparticles

Lectins are conjugated to PLGA based nanoparticles to promote the cellular uptake process through clathrin and caveolae mediated pathways as they show specific binding affinity to glycosylated membrane components. For instance, wheat germ agglutinin, assist in enhancing interactions with tumors and mucus membranes via N-acetyl D- glucosamine and sialic acid containing glycoproteins. Lectin functionalisation also bestows the drug carriers with the potential for brain targeting.

2.9.3 Mannan decorated PLGA nanoparticles

C- type lectin receptors such as mannose receptors are examples of dendritic cell endocytic receptors which is also expressed in macrophages. Surface modification with mannan groups proceeds via physical adsorption or through NHS-DCC conjugation chemistry. Mannan decorated PLGA nanoparticles have been widely used as vaccine carriers to dendritic cells.

2.9.4 Sialic Acid functional PLGA nanoparticles

Sialic acid has been used to penetrate the blood brain barrier or to target the brain in view of its abundance within the brain parenchyma. The

importance of sialic acid was evident in the findings of Tosi et al where the PLGA nanoparticles modified with sialic acid and BBB penetrating peptide displayed enhanced pharmacological efficacy over free drug and other nanoparticulate systems. Tosi et al has described this phenomenon on the basis of interactions between bifunctional PLGA nanoparticles and sialic acid receptors in the brain (Tosi et al., 2010).

2.9.5 Biotin functional PLGA Nanoparticles

Cancer cells over express many different tumor specific receptors such as biotin, which has been used to deliver cytotoxic agents. Recently, Patil et al has discussed the relevance of concurrent delivery of chemosensitizers and chemotherapeutics via biotin functional PLGA nanoparticles for overcoming multidrug resistance (Patil et al., 2009).

2.9.6. Folate functional PLGA Nanoparticulate

Folate receptor serve as a useful biomarker for tumor targeted drug delivery as they are over expressed 100-300 times the rate of normal cells. Considering this fact, Yoo and Park used a folate receptor for targeting biodegradable doxorubicin micelles, self assembled from a diblock copolymer of poly lactic co glycolic acid and poly ethylene glycol (Yoo and Park, 2004). This study recorded the enhanced cytotoxic potential of folate functional micelles to the human squamous carcinoma cell line of oral cavity in comparison to the control. The major contribution behind the enhanced therapeutic efficacy occurred through the efficient endocytosis of micelles through the folate receptor. Sunoqrot et al has

encapsulated folate polyamidoamine dendrimer conjugates inside PEGylated PLGA nanoparticles in order to minimize their pre mature elimination while interacting with cellular receptors (Sunoqrot et al., 2012).

2.9.7 Transferrin functional PLGA nanoparticles

Transferrin is another tumor specific receptor for surface functionalising polymeric, lipid and liposomes for realising efficient receptor mediated cellular uptake. Literature cites several examples of transferring conjugated PLGA nanoparticles for efficient targeting to tumors, especially gliomas (Chang et al., 2012).

2.9.8 Peptide functional PLGA nanoparticulates

Integrin family comprises of the major anchoring molecules in multicellular organisms that mediate contact with neighbouring cells and surrounding ECM through their role as cell adhesion receptors. Pierschbacher and Rouslahti has identified the tripeptide sequence, RGD, as the minimal essential cell adhesion peptide sequence that can promote cell adhesion following surface functionalisation (Hersel et al., 2003). Accordingly, Toi et al has conjugated cRGD peptide to maleimide conjugated PLGA nanoparticles to promote accumulation and retention of nanoparticles inside the tumors tissues. Alternatively, cell penetrating peptides such as transactivating transcriptional activators do exhibit high translocational activity and promote cellular uptake of large molecules and nanoparticles. Hence, several TAT peptides have been conjugated to PLGA nanoparticles to achieve targeted delivery to tumors and for crossing the blood brain barrier. For instance, Yu et al has

functionalised the PEGylated PLGA nanoparticles encapsulating paclitaxel with K237 peptide for enhancing the drug activity (Yu et al., 2010). Similarly, intracellular cell adhesion molecules are also used for PLGA surface functionalisation to achieve selective targeting to various tissues including tumors.

2.9.9 Antibody directed PLGA immunonanoparticles

Surface functionalisation of PLGA nanoparticles with monoclonal antibodies directed against over expressed or lineage restricted tumor specific antigen is performed to improve the targeting efficiency. However the therapeutic efficacy of such modified nanoparticles depends heavily on the attachment process of the antibody molecule. For example, Kocbek et al has presented a comparative study of monoclonal antibody conjugation via physical adsorption and EDC chemistry in relation to tumor targeting (Kocbek et al., 2007). The study demonstrated the reduced cellular uptake proficiency of nanoparticles functionalised via EDC chemistry owing to the compromised structural integrity of the monoclonal antibody following EDC conjugation. In addition, these PLGA based immunonanoparticles were also used to penetrate blood brain barrier and induce dendritic cell maturation.

2.9.10 Nucleotide functional PLGA nanoparticles

Among the major nucleotide based therapies, the unique specificity and sequence specific three dimensional structure of aptamers has made them versatile cancer targets, including extra cellular ligands and cell surface proteins. Following the approval of Macugen, the first clinically approved synthetic

PEGylated oligonucleotide, several different DNA aptamers have been used to functionalise PLGA nanoparticles (Ng et al., 2006). For instance Guo et al has evaluated the efficacy of AS1411 nucleolin interaction for effective drug delivery to gliomas (Guo et al., 2011). Additionally, RNA aptamers such as A10 2'fluoropyrimiidne has demonstrated specific binding affinity to the extra cellular domain of a prostate specific membrane antigen.

2.9.11 Magnetic Based PLGA nanoparticles

Paramagnetic gadolinium chelates and super para magnetic iron oxide nanoparticles are the major contrast agents used for biocompatible polymer based bimodal imaging as an initial step in nanomedicine. Doiron et al , Lim et al and Wang et al has demonstrated the suitability of PLGA in encapsulating more than one imaging agents, from exogenous dyes to metals for assisting drug delivery application (Sah et al., 2013).

2.10 Methodology for PLGA nanoparticle preparation

Methods available for PLGA nanoparticle synthesis are broadly classified into two types- bottom up and top down techniques. The bottom up techniques such as emulsion or micro emulsion polymerisation, interfacial polymerisation and precipitation polymerisation utilise a monomer as a starting point. The top down techniques proceed from the pre formed polymer as in case of emulsion evaporation, emulsion diffusion, solvent displacement and salting out.

The most commonly used technique for PLGA nanoparticle preparation is the single or double emulsion solvent evaporation technique. Single

emulsion process involves oil in water emulsification while the double emulsion process includes water in oil in water method. Briefly, the oil in water process, the polymer is first dissolved in a water immiscible, volatile organic solvent followed by addition of the drug as a solution or dispersion. The polymer-solvent-drug dispersion is emulsified in a larger volume of water in presence of an emulsifier (PVA, polysorbates) to yield oil in water emulsion. The nanosized droplets are induced by subjecting the emulsion to sonication or homogenisation. This is followed by solvent removal by either evaporation or extraction process to harden the oil droplets. The solid nanospheres obtained are washed and collected by centrifugation, filtration or sieving followed by lyophilisation to give the final free flowing injectable nanosphere product (Astete and Sabliov, 2006)

The water in oil in water method is appropriate to encapsulate water soluble drugs while the oil in water emulsification is ideal for water insoluble drugs such as steroids (Jain, 2000a). The physical characteristics (size, size distribution, morphology and zeta potential) of PLGA nanoparticles can be modulated by controlling the parameters specific to the synthesis technique employed.

2.11 History of PLGA based nanoparticles in controlled drug delivery

The ability to provide a sustained drug release by virtue of tailor made physicochemical properties of the biodegradable polymer, PLGA, has found applications in the delivery of several therapeutics such as drugs, proteins, peptides, plasmids and DNA (Danhier et al., 2012b).

2.11. 1 Encapsulation of small hydrophobic drugs

PLGA nanoparticles encapsulated with hydrophobic drugs are most commonly synthesised by solvent evaporation or nanoprecipitation technique. Drug release kinetics of PLGA nanoparticles are determined by surface modification, method of preparation, particle size, molecular weight of the encapsulated drug, ratio of lactide to glycolide moieties. Literature describes PLGA nanoparticles as efficient carriers of various hydrophobic drugs such as taxol (Mu and Feng, 2003), paclitaxel (Fonseca et al., 2002), nitrocamptothecin (Derakhshandeh et al., 2007), cisplatin (Avgoustakis et al., 2002), estradiol (Mittal et al., 2007), haloperidol (Budhian et al., 2007) etc.

2.11.2 Encapsulation of Proteins

The encapsulation of therapeutic proteins into the PLGA matrix provides enhanced bioavailability by protecting against enzymatic and hydrolytic degradation at in vivo conditions. Studies were performed to find out the influences of process parameters on the efficiency of protein encapsulation in PLGA nanoparticles (Shubhra et al., 2013). The presence of acidic degradation products such as lactic and glycolic acid as well as carboxylic end groups could induce aggregation or alter or block the release of encapsulated proteins. In order to increase the protein stability, various stabilisers like pluronic F68, trehalose, sodium bicarbonate, among others, have been utilised (Danhier et al., 2012b)

2.11.3 Encapsulation of nucleic acids

As an alternative to viral delivery, PLGA based nanoparticles have been developed to enhance the transfection efficiency of the usually fragile molecules. Nucleic acid encapsulated PLGA nanoparticles are formulated by water in oil solvent evaporation (Davda and Labhasetwar, 2002) or modified nanoprecipitation (Niu et al., 2009). In order to enhance the solubility of nucleic acid in organic solvent, pre-complexing the nucleic acid with a cationic moiety has been tested (Tahara et al., 2008b). Encapsulation efficiency of nucleic acids was found to improve upon addition of cationic polymers such as polyethyleneimine (Patil et al., 2010) or chitosan (Tahara et al., 2008a).

2.11.4 Vaccination with PLGA Nanoparticles

PLGA is one of the most widely studied polymers for the delivery of subunit vaccines. The long term release characteristic of PLGA enabled them to replace the multiple immune boosting administrations required to generate protective immunity. As a controlled delivery system, PLGA polymer can potentially encapsulate antigens as proteins, peptides (Clawson et al., 2010), lipopeptides (Diwan et al., 2004), cell lysates (Prasad et al., 2011), viruses (Thomas et al., 2011) or plasmids (Tian and Yu, 2011) to desired locations at pre determined rates and intervals (Zhao and Feng, 2010). The dose requirement to elicit adequate T cell response has been lowered with the use of PLGA nanoparticles at similar efficacy (Diwan et al., 2004)

2.11.5 Regenerative medicine with PLGA based nanoparticles

PLGA nanoparticles are promising in the field of regenerative medicine by providing a sustained and spatially and temporally controlled delivery of bioactive molecules required to induce cell migration, proliferation or differentiation. Glial cell line derived neurotrophic factor was encapsulated in PLGA drug delivery system for the stereotaxic implantation in animal models in the treatment Parkinson's disease (Garbayo et al., 2011). Due to the growing interest in the angiogenesis in tissue engineering, proangiogenic growth factors such as VEGF (Panyam and Labhasetwar, 2003), platelet derived growth factor and fibroblast derived growth factors loaded PLGA nanoparticles have been formulated and optimized. Studies conducted on PLGA nanoparticle encapsulating VEGF by Golub et al in a mouse femoral artery ischemia model were successful in promoting vascular growth (Golub et al., 2010).

2.11.6 Cardiovascular disease treatment with PLGA nanoparticles

The rapid innovations and advancements of PLGA based nanotechnology have significantly improved diagnostic and treatment intervention for cardiovascular occlusive diseases. The biodegradable, mechanical and elastic properties of PLGA polymer have prompted the development of synthetic grafts (Sarkar et al., 2006). Further, PLGA nanoparticle coated stents can effectively deliver drugs, genes or proteins to the vessel wall at controlled kinetics. Klugertz et al has reported the first successful transfection in vivo in the rat aortic smooth muscle cells using DNA loaded PLGA nanoparticle coated stents (Klugherz et al., 2000).

2.11.7 Cerebral Disease treatment with PLGA nanoparticles

PLGA based nanoparticles provide an efficient and non invasive approach for the drug delivery to central nervous system. Reddy et al has investigated the neuroprotective efficacy of superoxide dismutase in cultured human neurons challenged with hydrogen peroxide induced oxidative stress after encapsulation in PLGA nanoparticles (Reddy et al., 2008). PLGA nanoparticles demonstrated better neuro protection from oxidative stress when compared to pegylated superoxide dismutase or superoxide dismutase alone (Reddy et al., 2008). Targeted delivery to specific receptors of brain capillary endothelium was achieved by coating the surface of PLGA nanoparticles with specific brain endothelial ligands. A novel biodegradable brain drug delivery system was developed by conjugating lactoferrin to PEG-PLGA nanoparticles. Following intravenous injection, lactoferrin coated nanoparticles were found in the substantia nigra, cortex and striatum region that confirms the transport across blood brain barrier (Hu et al., 2009).

2.11.8 Inflammatory disease treatment with PLGA nanoparticles

The ability of PLGA nanoparticles to enhance drug localisation in target site along with sustained release find application as drug carriers for the treatment of inflammatory diseases, such as arthritis and bowel disease, in the animal models (Gref et al., 1994). Encapsulation of anti inflammatory drugs such as glucocorticoids reduces systemic side effects on long term treatment (Higaki et al., 2005). The selective uptake of PLGA nanoparticles in inflamed areas after RES sequestration together with the possibility of coating or conjugating the nanoparticles surface with inflamed specific targeting moieties promote the

therapeutic efficacy of drugs as an intravenous treatment for inflammatory diseases (Ulbrich and Lamprecht, 2009)

2.11.9 Infectious Disease treatment with PLGA nanoparticles

Several reports have investigated the development of antibiotic loaded PLGA nanoparticles as an alternative treatment to bacterial infections. Sustained release of antibiotics from PLGA nanoparticles could maintain the plasma concentrations at therapeutic levels and thus improve the treatment efficacy. Further, as PLGA nanoparticles facilitate intracellular delivery of antibiotics, they are more effective against intracellular pathogen inclusion complexes that are basically refractory to antibiotic therapy (Toti et al., 2011). In general, PLGA nanoparticles enhance the effectiveness of antibiotics at both intracellular and localised regions by reducing microbial burden. Encapsulation of antibiotics with poor solubility and cell penetration capacity inside PLGA nanoparticles enabled better pharmacokinetic parameters (Gupta et al., 2010).

2.12 CANCER therapy using PLGA nanoparticles

Cancer is one of the ten leading causes of death in India and accounts for more deaths worldwide than AIDS, malaria and tuberculosis combined. Chemotherapy for cancers are hindered by the systemic toxicity and limited tolerated dose of anticancer agents. PLGA based nanoparticles are under intense investigation for enhancing the therapeutic efficacy of anti cancer agents (Frank et al., 2014).

2.12.1 Important concepts in nanoparticle mediated Drug Delivery for Cancer

The basic concepts that are important in nanoparticle mediated drug delivery include the enhanced permeability and retention effect, mononuclear phagocyte mediated nanoparticle clearance and the optimal physicochemical characteristics of nanoparticles for cancer therapy (Wang et al., 2012a).

2.12.1.1 Enhanced Permeability and Retention Effect

The abnormality of tumour vasculatures is exemplified through aberrant branching and leaky walls. The origin of the leaky vasculature is the direct consequence of the rapid proliferation of endothelial cells and the decreased number of pericytes which resulted in the formation of large number pores in the tumor blood vessels. These pores of several hundred nanometres in diameter can provide a higher vascular permeability and hydraulic conductivity in tumors and permit the entry of large macromolecules such as nanoparticles. Importantly, the rapidly proliferating tumor vessels can result in the compression of surrounding lymphatic vessels and this effect become more pronounced at the centre of the tumor. Hence the impaired lymphatics constitute a prominent feature of the solid tumors. As a result, the extravasated nanoparticles, following the enhanced permeability are retained in the tumor for extended time periods. The impaired lymphatic system in succession with the enhanced permeability of tumor blood vessels could constitute the EPR effect. Hence, contribute to the greater concentration of nanoparticles within the tumour tissue, in comparison to plasma (Li et al., 2012).

2.12.1.2 Nanoparticle Clearance by Mononuclear Phagocyte System

In order to fully exploit the EPR effect, the formulated nanoparticles must fulfil the basic criteria of long circulation. The major obstacle is posed by the mononuclear phagocytic system, previously called as the reticuloendothelial system. The MPS, a part of the immune system comprises of the bone marrow progenitors, blood monocytes, and tissue macrophages, kupffer cells of the liver and macrophages of the spleen. The formulation of immune evasive or stealth nanocarriers is critical in the prevention of the premature elimination of nanocarriers from circulation.

2.12.1.3 Optimal Nanoparticle Characteristics for Cancer Treatment

Delineating the characteristics of the nano drug carriers that are perfectly suited for oncology applications can be a landmark in the history of drug delivery systems. It is quite well known that size, shape and surface charge affect the nanoparticle biodistribution and intracellular trafficking in tumours. Although no clear consensus exists for optimal characteristics, generally, neutral or negatively charged particles of size ~ 100nm are preferred for tumor targeting and clinical applications (Petros and DeSimone, 2010).

2.12.2 General Biological Barriers for Cancer Therapy

The success of chemotherapy demands the subvertion of various biological barriers from systemic to organ to cellular level. The initial barriers and the corresponding design parameters of the carrier depend on the mode of administration. Overcoming the multiple organ level clearance mechanisms,

prevalent among liver and spleen becomes necessary for reaching the intended destination of the nanocarriers. Several strategies such as the induced saturation of the phagocytic capacity of carriers through injecting decoy carriers preceding the delivery of active ingredient, reducing the rate of opsonisation by rendering greater hydrophilicity to the particle surface, conjugating specific proteins or markers of self on the nanoparticle surface to avoid complement and immune mediated activation can be employed to escape from macrophage sequestration. At the cellular level, an engineered nanoparticle must confront with several barriers starting with the plasma membrane that allows diffusion of macromolecules larger ~1 kDa. Following endocytosis, the nanoparticles require to escape the endolysosomes and finally penetrate the nuclear membrane for achieving its therapeutic index (Petros and DeSimone, 2010).

2.12.3 Mechanisms of Drug Resistance

One of the main reasons for the rise in mortality rate of malignancy is the recurrence of chemoresistant cancer. The multi drug resistance or the resistance of cancer to related or unrelated classes of chemotherapeutic drugs can be innate or acquired with a complex biological interplay of different factors. It includes inhibition of apoptosis, induction of DNA repair mechanisms, alterations of drug target structure, modification in cell membrane composition leading to reduced drug uptake and increased activity of drug efflux pumps such as ABC transporters (Markman et al., 2013).

2.12.3.1 Efflux pump mediated MDR

The primary means of drug efflux is mediated through ATB binding Cassette super family. Located on the plasma membrane of cells and vesicles they protect the cell from various intrusions including foreign substances and toxic molecules. Among the 48 known ABC transporters, the first discovered mdr1 gene codes for the high molecular weight p-glycoprotein. The up regulation of these multidrug resistant proteins can effectively decrease the drug accumulation within the tumor cells.

2.12.3.2 Efflux pump independent MDR

Decreased drug influx, activation of DNA repair, metabolic modification and detoxification, mutations in apoptosis associated proteins and tumor suppressors such as p53 are the additional mechanisms of MDR. The over expression of anti apoptotic pro survival regulator Bcl-2 and nuclear factor kappa that induce genes that suppress apoptotic responses can increase the survival of tumor cells.

2.12.4. Challenges to successful Antineoplastic therapy

Primary concern is based on the formulatory and delivery challenges associated with poor aqueous solubility of drugs. In addition, the pathophysiology of tumor microenvironment reduces drug bioavailability. Further, the serum proteins when adsorbed to drug molecules can reduce the antineoplastic activity by inhibiting their absorption and cellular internalisation. Body mechanisms like renal clearance and physiological instability can further decrease the drug

concentration at the target site. The dose dependent adverse effects of chemotherapeutic pose the greatest challenge in the therapeutic efficacy.

2.12.5 Nanotechnology based Approaches to Cancer Therapy

The encapsulation of the drug within a nanosystem overcomes the majority of formulatory and delivery challenges under in vivo conditions, specifically with lipophilic drugs. The encapsulation efficiently protects from metabolic degradation and physiological inactivation. As the nanosystem are able to bypass the reticuloendothelial system owing to their small size and surface features, the circulation half life and pharmacokinetic profile of drug enhances dramatically. EPR phenomenon displayed by tumor cells realises the possibility of passive targeting and accumulation. The possibility of active and passive targeting specifically increases the concentration of drug within the tumor tissue along with reducing non specific distribution. Finally, the nanosystem undergo direct uptake in to the tumor cells via endocytic pathways and hence bypass the efflux pump mediated drug resistance (Brigger et al., 2002).

2.12.5.1 Passive targeting and Enhanced Permeability and Retention Effect

Passive targeting exploits the unique anatomical and pathological characteristics of tumor vasculature and also take advantage of the sub cellular size of nanoparticles. This leads to extravasation and accumulation of nanoparticles in the interstitial spaces and thereby contributing to an enhanced permeability. Moreover, the lymphatic drainage is slow or ineffective in tumor leading to an enhanced retention. These two phenomena constitute the enhanced

permeability and retention effect that is considered as the gold standard in designing new chemotherapeutic drug delivery systems. EPR effect was first described by Maeda and colleagues (Maeda et al., 2000).

2.12.5.2 Active Targeting

The nanosystem with the large surface area to volume ratio is particularly amenable to attaching various target moieties. In active targeting, targeting ligands specific to receptors over expressed by tumor cells or specific to tumor vasculature are grafted at the nanoparticle surface (Danhier et al., 2012b). Such systems capitalise on the formation of a ligand-receptor complex. Monoclonal antibodies such as anti-transferrin receptor, anti-folate receptor, anti-glycoprotein receptor, nucleic acid aptamers (Farokhzad et al., 2006), tumor homing peptides with RGD sequence motif have been investigated to target cancer cells. Smart polymers or stimuli responsive polymers can contribute to the targeting nature by responding to the physiological changes that characterise the tumor microenvironment such as the lower pH.

2.12.6 Examples of currently developed PLGA based nanoparticles as chemotherapeutic drug delivery systems

Various anticancer drugs such as Paclitaxel, 9-Nitrocamptothecin, Cisplatin, Xanthones, Rosebengal, Triptorelin, Dexamethasone have been encapsulated in PLGA nanoparticles and have been evaluated in vitro and in vivo to treat various cancers. The Table III gives an overview of PLGA based nanoparticles as anticancer therapeutics.

Table III: PLGA based nanoparticulate as anticancer therapeutics (Kumari et al., 2010)

Drug Loaded in PLGA Nanoparticles	Main Targets	In Vitro Application	In Vivo Application	Encapsulation Efficiency
Paclitaxel	Microtubules	Efficiency of paclitaxel mediated nanoparticulate delivery was investigated on human small cell lung carcinoma (NCI-H69 SCLC), human adenocarcinoma (HT- 29), human laryngeal cancer (Hep-2), breast carcinoma (MCF-7) and carcinoma cervicis (HeLa) cell lines.	In vivo efficacy of paclitaxel-loaded nanoparticles was tested on transplantable liver tumor in male NMRI mice and in glioblastoma tumor models	>90%
Cisplatin	DNA Adducts	Cisplatin in PLGA nanoparticles demonstrated greater therapeutic efficacy on human prostate cancer LNCaP cells	Pharmacodynamics of cisplatin-loaded PLGA or PLGA-mPEG nanoparticles upon administration to tumor-bearing mice/Balb C mice was investigated by different groups	90%
Doxorubicin	Topo II	Multifunctional PLGA nanoparticles were used	In vivo pharmacokinetics of DOX loaded NPs was evaluated in	80%
Curcumin	Cytoplasmic proteins	Nanoparticle encapsulation improves oral bioavailability of curcumin and was effective against metastatic ovarian , breast cancer and prostate cancer cells	In vivo bioavailability of curcumin-loaded PLGA nanoparticles was performed in Balb/c mice. Another independent study proved the marked anticancer efficacy of	>72%

			curcumin microparticles in nude mice bearing MDA-MB-231 xenografts	
Dexamethasone	Cytoplasmic receptors	Efficiently suppress the proliferation of vascular smooth muscle cells by drug loaded NP	Nanoparticle encapsulation improves oral bioavailability of curcumin and was effective against metastatic ovarian , breast cancer and prostate cancer cells	6%
9-Nitrocamptothecin	Topo-I	PLGA nanoparticles provide release upto 160h and maintained the biological cavity of drug by shielding the lactone ring		30%

2.12.6.1 Doxorubicin

Doxorubicin, belonging to the family of anthracyclines, is a highly potent antineoplastic agent that is approved for treatment against a wide spectrum of tumors. It is commonly known under the trade name of Adriamycin, this antibiotic blocks DNA synthesis and transcription by intercalating between the nucleotides. It also inhibits topoisomerase II and generates damaging radicals from its metabolism. The intravenous administration of doxorubicin is performed at the dose of 60-90mg/m^2 at 21 days interval. However, the long term clinical usage of doxorubicin is compromised by acute cardiotoxicity and multidrug resistance. This has lead to alternative drug delivery systems for doxorubicin by entrapping it in submicron sized carriers such as liposomes and nanoparticles. This decreases

doxorubicin induced cardiomyopathy by modifying the biodistribution and increasing the delivery to tissues harbouring tumors. The difficulty in controlling the drug release rate and the quick immune recognition of several commercially available liposomal preparations of doxorubicin such as Doxil and Daunoxome and the subsequent removal by reticuloendothelial system has challenged the optimisation of dose regimens. Hence, the FDA approved PLGA nanoparticles with similar ability to reduce toxicity and retain biological activity are widely investigated (Betancourt et al., 2007).

Tewes et al has investigated on controlling the polarity of doxorubicin by adjusting the pH in order to enhance the encapsulation efficiency inside PLGA nanoparticles. The results indicated that the encapsulation of doxorubicin in PLGA nanoparticles prepared by single emulsion enhanced the drug encapsulation efficiency by 1.4 times along with substantial reduction in burst effect (Tewes et al., 2007b).

Betancourt et al has utilised oil in water nanoprecipitation technique with bovine serum albumin as the stabiliser for the encapsulation of doxorubicin into acid end capped PLGA. This formulation could overcome the dose limiting toxicities by controlling the release of drug in a pH dependent manner and was effective in delivering high payloads of drug in an active form to MDA-MB-231 breast cancer cells (Betancourt et al., 2007).

Park et al utilised a unique surface modification technique to synthesize PEGylated PLGA nanoparticles encapsulating doxorubicin. The investigators successfully reduced the decrease in cardiotoxicity associated with free

doxorubicin following encapsulation inside PLGA nanoparticles. The cytotoxic potential of nanoparticle encapsulated doxorubicin was greater due to efficient intracellular uptake and release. Also PEGylation increased the circulatory half life of PLGA nanoparticles (Park et al., 2009).

Cui et al synthesised transferrin conjugated magnetic silica nanoparticles encapsulating doxorubicin and paclitaxel for the effective treatment of malignant glioma. The efficiency of this inorganic-organic composite with a targeting ligand for the delivery of the dual drug system could be enhanced using a magnetic field (Cui et al., 2013).

Chittasupho et al has studied the possibility of targeting PLGA nanoparticles encapsulated doxorubicin to a molecular marker, ICAM-1, over expressed in inflammatory diseases and cancer. Cyclo-(1,12)-PenITDGEATDSGC (cLABL) display specific binding to ICAM-1 and hence was used to modify the surface of PLGA nanoparticles to enable them to target lung epithelial cells for controlled doxorubicin delivery (Chittasupho et al., 2009).

Yadav et al compared the doxorubicin encapsulation into a novel hyaluronic acid polyethyleneglycol PLGA copolymer based nanoparticles versus monomethoxypolyethylene glycol nanoparticles in terms of sustained release. In this model, HA-PEG-PLGA nanoparticles exhibited longer tumor retention times along with higher delivery of doxorubicin (Yadav et al., 2007).

2.12.6.2 Curcumin

Curcumin is a low molecular weight, natural polyphenolic compound which is extracted from the rhizome of the herb *curcuma longa* (turmeric). It is a lipophilic fluorescent molecule with the chemical structure (1, 7-bis (4- hydroxy-3-methoxyphenyl)-1, 6-heptadiene-3, 5-Dione). The presence of phenolic groups and conjugated double bonds render the compound considerable hydrophobicity. The pharmacological activities exhibited by curcumin range from neoplastic, neurological, cardiovascular, pulmonary, metabolic and psychological diseases. The interference in multiple signalling pathways includes cell cyclins, apoptosis (activation of caspases and down regulation of anti apoptotic gene products, proliferation (HER-2, EGFR & AP-1), survival (P13K/Akt pathway), invasion (MMP-9, adhesion molecules), angiogenesis (VEGF), metastasis (CXCR-4) and inflammation (NF- k• , TNF, IL-6, IL-1, COX-2). Curcumin is well known for its dose dependent chemo preventive and chemotherapeutic effects in various carcinogenic models and preclinical trials, without causing cytotoxic effects in normal cells. In fact, dose as high as 8g/day to healthy organs demonstrated no toxicity in clinical trials. However, the lipophilic characteristic of curcumin, render the molecule poor aqueous solubility, low systemic bioavailability and poor pharmacokinetics that limits the in vivo therapeutic efficacy. Various formulation techniques of curcumin have been developed with the aim of increasing the retention time in the body. The incorporation of curcumin into liposomes, phospholipid vesicles, copolymeric micelles, cyclodextrin and polymer based nanoparticles are among the forefront. Among the different approaches, the use of nanoparticles

prepared from polyester like PLGA are gaining much attention because of its biodegradability, bioavailability and better storage (Anand et al., 2007).

Mukherjee et al has encapsulated curcumin in PLGA nanospheres and evaluated the in vitro release profile, cellular uptake and cytotoxic potential in prostate cancer cell lines. The PLGA nanospheres demonstrated high encapsulation efficiency, efficient uptake and activity of curcumin. Hence it highlighted the potential of PLGA nanospheres in chemotherapy as the nanospheres were capable of sustained release and activity maintenance of the encapsulated curcumin (Mukerjee and Vishwanatha, 2009).

Yallappu et al has attempted to encapsulate curcumin in PLGA nanoparticles via nanoprecipitation. The presence of polyvinyl alcohol and poly lysine stabiliser helped to impart better stability and sustained release of the curcumin. Further this study has denoted the enhanced therapeutic potential of the nano formulation in metastatic cancer cells in comparison to free curcumin (Yallapu et al., 2010).

Sahoo et al has proposed to enhance the bioavailability of curcumin by encapsulating in glycerol mono oleate based nanoparticles in the presence of pluronic F-127. The authors had attributed the enhanced systemic availability to the better cellular internalisation and sustained release of entrapped curcumin from the nanoformulations (Mohanty and Sahoo, 2010).

Anand et at has utilised a polymer based nanoparticle approach to improve the bioavailability of the potential anticancer agent, curcumin.

They have reported a 97.5% encapsulation efficiency using the biodegradable PLGA nanoparticles in the presence of the stabiliser PEG-5000. The authors have reported a higher cellular uptake, dose dependent inhibitory effect, suppression of NF-Kb, TNF induced expression of cyclin D1 and significant enhancement of vivo bioavailability with nano encapsulated curcumin (Anand et al., 2010).

Khalil et al has analysed the potential of PLGA and PEG modified PLGA based nanoparticles in providing better pharmacokinetics along with increased bioavailability when compared to free curcumin. They have concluded that the nano encapsulated curcumin exhibits much higher bioavailability when compared to free curcumin. Further, the C_{max} of curcumin encapsulated in modified PLGA was 4.5 times higher than unmodified nano encapsulated curcumin and 55.4 fold higher than free curcumin (Khalil et al., 2013).

2.12.6.3. Betulinic Acid

Betulinic acid (3•-hydroxy 20(19)-lupaen-28-oic acid) is a natural compound widely distributed in the plant kingdom. The compound is mainly derived from betulin, a lupane type penatcyclic triterpene, which is mainly confined to species of betuliacea, rhamnaceae, myrtceae etc. Betulinic acid and its reduced form betulin are significant for their pharmacological properties including anti bacterial, anti malarial, anti inflammatory, inhibition of human immunodeficiency virus and induction of apoptosis in melanoma cells. Literature has reported the in vivo efficacy of betulinic acid in inhibiting the proliferation of ovarian and melanoma induced xenografts in mice. The betulinic acid is considered to be an inhibitor of topoisomerase-2 and promotes antiproliferative action against a wide

range of human cell lines. The mechanism of action is thought to proceed through activation of mitochondrial membrane permeabilisation that leads to the release of cytochrome c and smac proteins. Finally the modulation of the expression of several growth related proteins and the activation of caspases can trigger the induction of apoptosis. The most promising potential of this drug is the minimal cytotoxicity against healthy cells (Suresh et al., 2012).

In order to bypass the limitations in delivery and bioavailability of the hydrophobic drug betulinic acid, nanoencapsulation inside liposomes and polymeric nanoparticles were attempted.

Mullauer et al has treated nude mice xenografted with human colon and lung cancer tumors, using liposomal formulations encapsulated with betulinic acid. The authors have reported enhanced survival of the mice with around 50% reduction in tumor growth in comparison to the control group (Mullauer et al., 2011).

Das et al has encapsulated betulinic acid in PLGA nanoparticles after stabilisation with F-68. The results suggested enhanced drug bioavailability of betulinic acid after nano encapsulation against induced lung cancer in mice models and upon interaction with A549 cells at in vitro conditions (Das et al., 2012).

2.13. Landmarks in polymer based nanoparticulate therapeutics- From discovery to the clinic

The first synthesis of a nanoparticle therapeutic – drug-polymer conjugate could be traced back to 1950 s when Jatzkewitz prepared a polyvinylpyrrolidone-mescaline conjugate that consisted of a short peptide spacer between the drug and the polymer. Another landmark event in the field of drug delivery occurred in 1960 s with the discovery of liposomes (Petros and DeSimone, 2010). These two events manifested the advent of the field of nanocarriers and together, these two classes of nanocarriers constitute the most marketed and extensively investigated nanoparticle therapeutics till date. An imaginary timeline of the clinical developments in nanomedicine is provided in Figure 8.

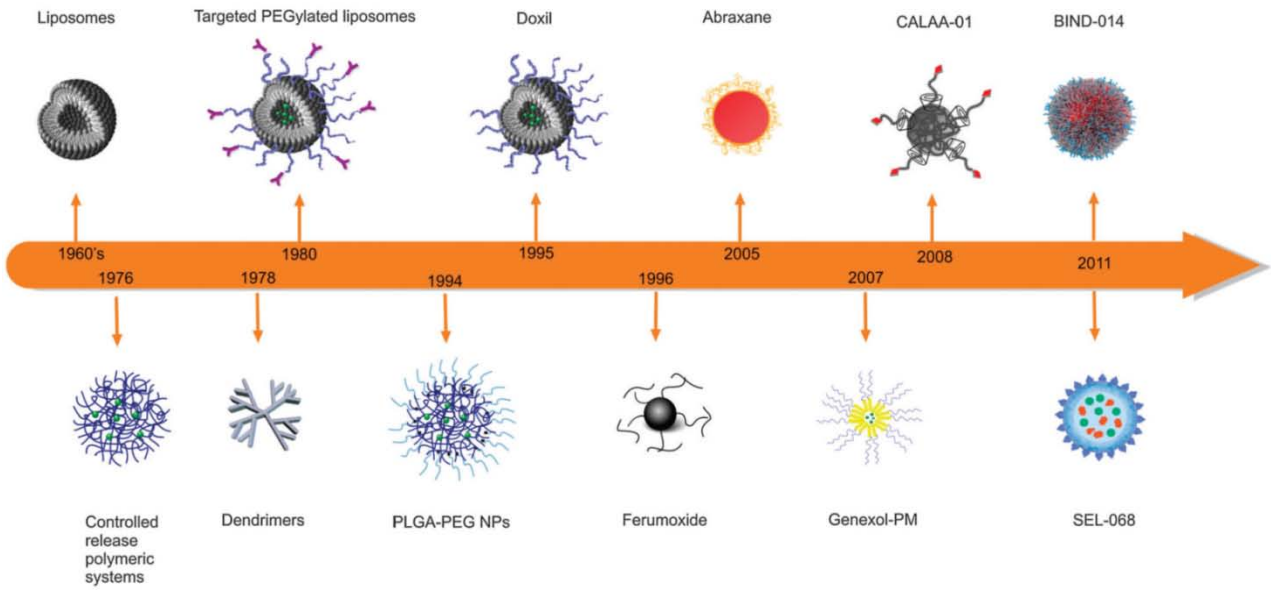

Figure 8: Timeline of Clinical Stage of Nanomedicine (Kamaly et al., 2012).

The concept of targeted drug conjugates was brought forward by Ringsdorf, in the 1970s, and proposed the basic principles of current

nanotherapeutics. Albumin based nanoparticles was reported in 1972 and was the precursor to the first protein based nanoparticle, Abraxane to receive regulatory approval in 2005. Abraxane is an albumin bound paclitaxel treated for metastatic breast cancer. Following this, polymer based nanoparticles was introduced in 1976. In 1980s, Maeda and co-workers discovered the phenomenon enhanced permeability and retention effect, while investigating polymer-drug conjugate polystyrene co maleic acid conjugated to the cytotoxic drug, neocarzinostatin. Nanoparticle therapeutics was first discovered in the 1980s. Successively, Sandimmune, a mixture of cyclosporine and cremophor (polyoxyethylated castor oil) was marketed by Novartis following approval by FDA in 1983. Cremophor is also the major constituent of the cytotoxic anticancer drug paclitaxel, also known as Taxol. The first controlled release polymer composition or drug depot, Zoladex, consist of an implantable form of goserelin acetate, a synthetic analogue of luteinizing hormone releasing hormone. This product was approved by FDA for the treatment of certain types of prostate and breast cancer in 1989. Similarly, a biodegradable depot form of another cytotoxic drug, carmustine, was approved by the FDA for the treatment of brain cancer in 1996.

Here, liposomes, micelles, proteins etc belong to the first generation of clinically approved nanoparticle drug delivery technologies and were successful in improving the safety and efficacy of the drug carried. However it lacked controlled release and active targeting properties. Doxil, Abraxane and Genexol –PM belong to the first generation of nanotherapeutics directed against cancer. Doxil was the first FDA approved liposomal nanomedicine marketed in 1995

for AIDS related Kaposi's syndrome. FDA approval of Abraxane, NP albumin bound platform of paclitaxel, marked the beginning of second class of therapeutic nanoparticles and eliminated the need for toxic excipients such as cremophor-EL. Genexol-PM utilised the polymeric micelle technology for loading paclitaxel and exhibited enhanced maximum tolerated dose of drug, following the elimination of cremophor. Hence it is clear that each clinically approved nanoparticle platform has enhanced the drug safety and efficacy in spite of having unique challenges. Unless the nanoparticle platform change the pharmacokinetics, biodistribution and tissue exposure kinetics of the drug molecule in a favourable manner, it becomes difficult to improve the therapeutic efficacy of the loaded drug. Hence the successful development of such nanoparticle platform is equivalent to the discovery of novel drugs (Kamaly et al., 2012).

CHAPTER 3
MATERIALS AND METHODS

3 MATERIALS AND METHODS

3.1 Synthesis of modified PLGA based polymers

3.1.1 Materials

PLGA 50:50 (Resomer RG 502 H(12-24 kDa), I.V. 0.16–0.21) was obtained from Boehringer Ingelheim, Ingelheim am Rhein, Germany, Dicyclohexyl carbodiimide (DCC), N-hydroxy succinimide (NHS), L-cysteine and Mucin from porcine stomach Type II were from Sigma Aldrich, Missouri, United States. Glucosamine hydrochloride was from SRL, Maharashtra, India. Organic solvents such as Dimethyl formamide was from Merck Specialities Private Limited, Karnataka, India. All other chemicals were of analytical grade and used as received.

3.1.2. Synthesis of Thiol modified PLGA

Carboxyl groups in PLGA were conjugated to the amino group of cysteine with the help of NHS in presence of DCC (McCarron et al., 2008). Initially, PLGA (0.5 g) was dissolved in 10 mL anhydrous dimethyl formamide (DMF) and NHS (0.05 g) was added to the polymer solution. The reaction was allowed to proceed for 1 h at room temperature, thereafter DCC (0.05 g) was added to the stirring solution. Stirring was continued for another 2 h. Subsequently, the solution under stirring was reacted with 0.5 mL cysteine solution (0.02 g dissolved in 0.5 mL distilled water). The reaction was allowed to proceed for another 3 h on ice bath and modified polymer was precipitated by pouring into100 mL of distilled water. The precipitated polymer was filtered to separate the dicyclohexyl urea and

dried under reduced pressure, stored at -20° C in order to avoid humidity induced autocatalytic degradation. The reaction scheme is provided in Figure 9.

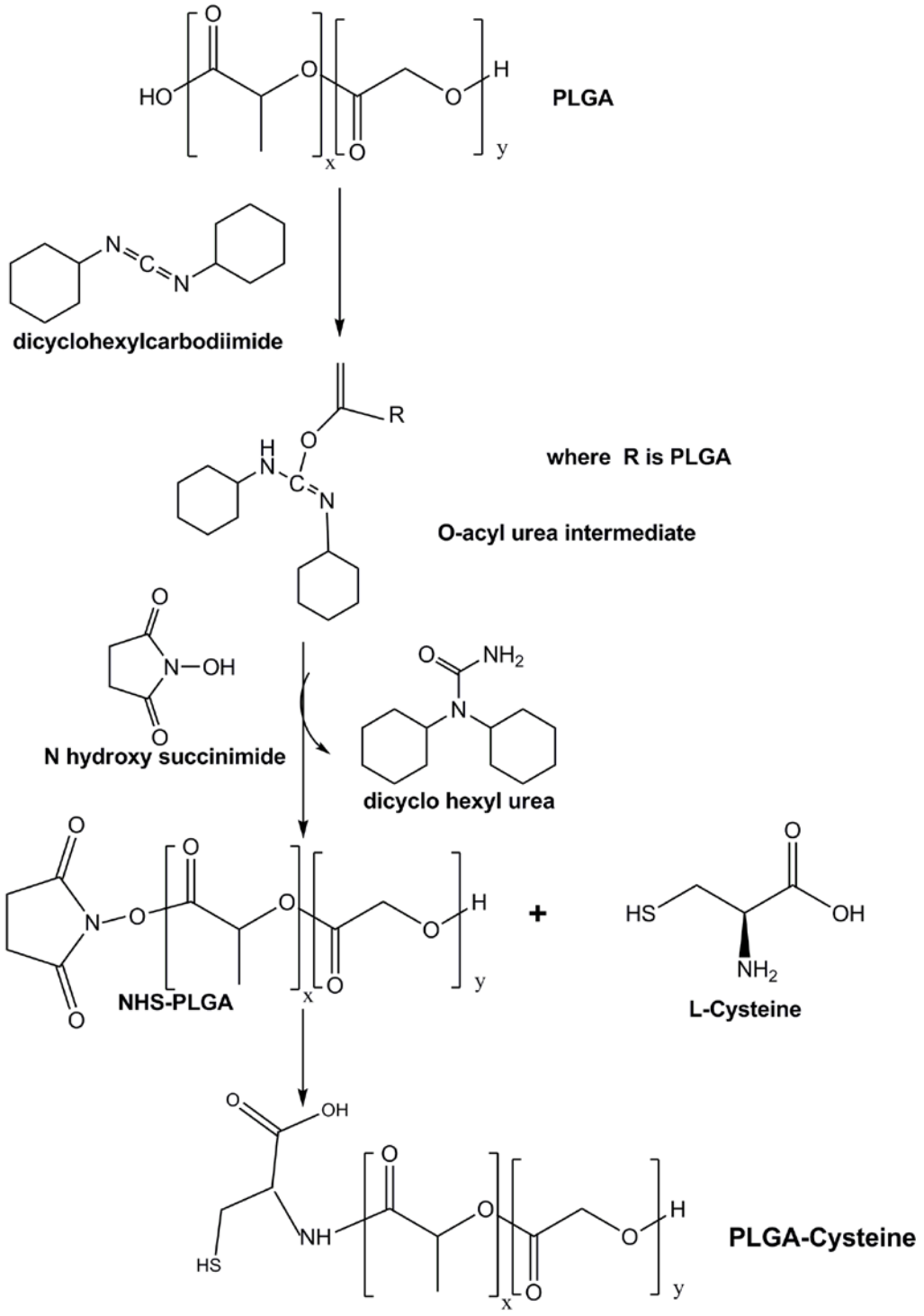

Figure 9: Reaction mechanism for the conjugation of L-Cysteine to PLGA via NHS-DCC chemistry.

3.1.3 Synthesis of Glucose modified PLGA

Carboxyl groups in PLGA were activated with NHS in the presence of DCC prior to its conjugation with the amino groups of glucosamine (McCarron et al., 2008). Briefly, PLGA (0.5 g) was dissolved in 10 ml anhydrous dimethyl formamide and NHS (0.05 g) was added to the polymer solution. On completion of first hour, DCC was added and stirring continued for another 2 h. Subsequently, the solution under stirring was reacted with 0.5 ml glucosamine solution (0.02 g dissolved in 0.5 ml distilled water). The reaction progressed for another 3 h on ice bath and modified polymer was precipitated by pouring into 100 ml of distilled water. The precipitated polymer was filtered to separate the dicyclohexyl urea and dried under reduced pressure and stored at -20° C in order to avoid humidity associated autocatalytic degradation. The reaction scheme is provided in Figure 10.

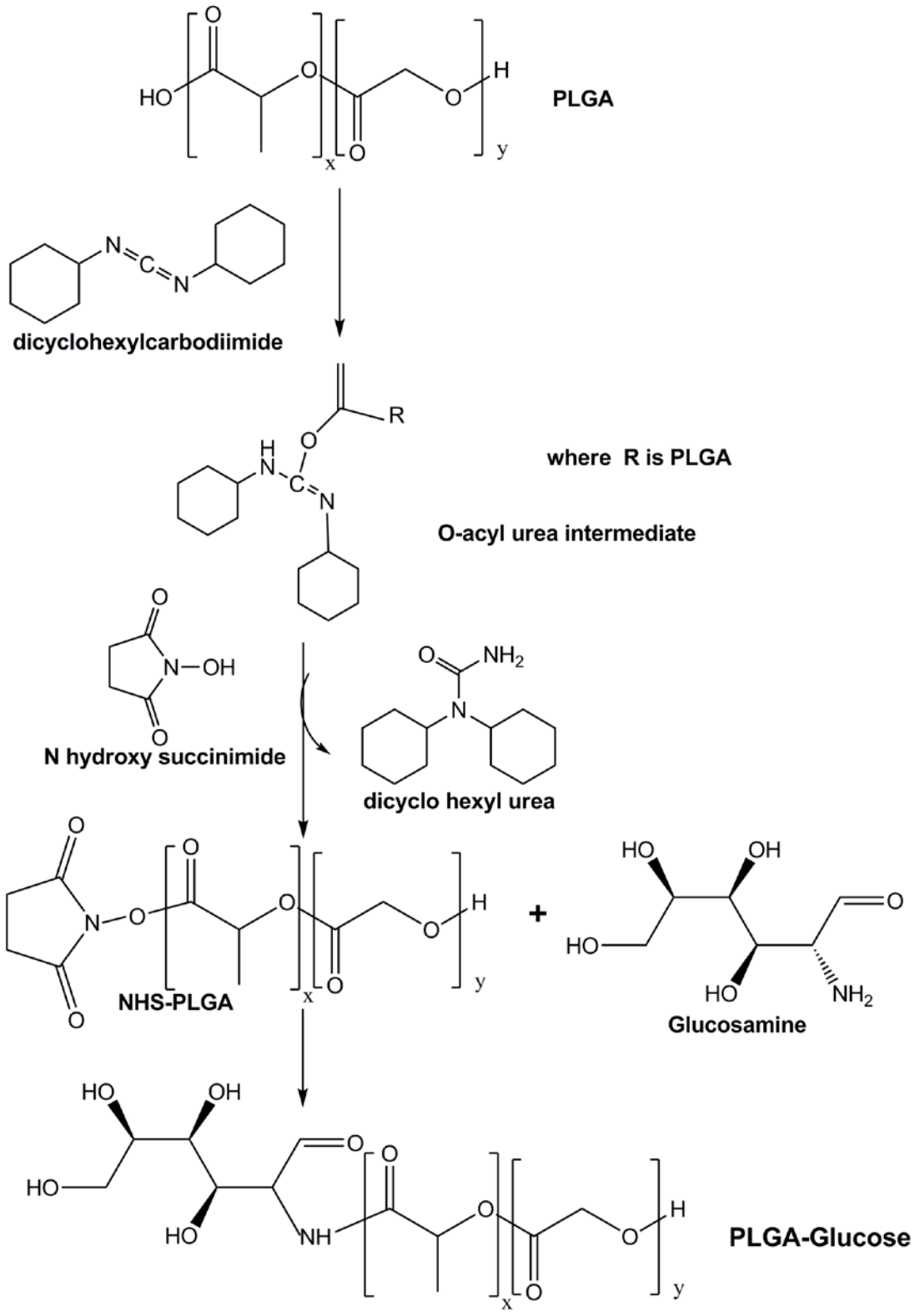

Figure 10: Reaction mechanism for the conjugation of Glucosamine to PLGA via NHS-DCC chemistry.

3.1.4 Synthesis of Mucin modified PLGA

Mucin modified PLGA was synthesized through coupling reaction by forming amide linkage between porcine mucin and the polymer (McCarron et al., 2008). Briefly, carboxyl groups in PLGA were activated by carbodiimide method with NHS in the presence of DCC prior to its conjugation with the amino groups of mucin. PLGA (0.5 g) was dissolved in 10 ml of anhydrous dimethyl formamide and NHS (0.05 g) was added to the polymer solution. On completion of first hour, DCC was added in equimolar quantity and stirring continued for another 2 h. Subsequently, the solution under stirring was reacted with 500 µl of mucin solution (5 mg/ml). The reaction progressed for another 3 h on ice bath and the modified polymer was precipitated by pouring into 100 ml of distilled water. The precipitated mucin modified PLGA polymer was filtered to separate the dicyclohexyl urea and dried under reduced pressure, stored at -20 ˚C in order to avoid humidity induced autocatalytic degradation. The reaction mechanism is provided in Figure 11.

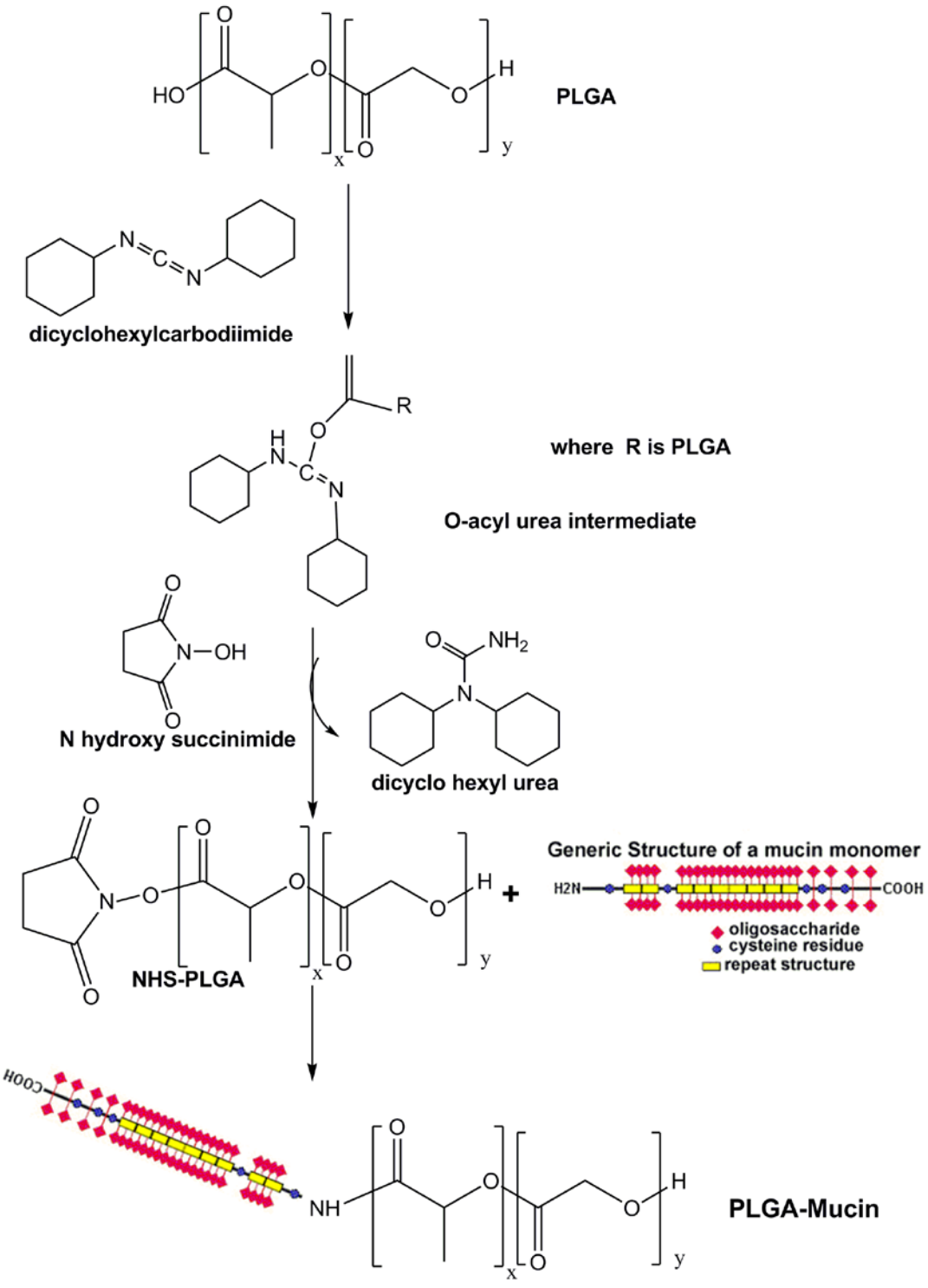

Figure 11: Reaction mechanism for the conjugation of mucin monomer to PLGA via NHS-DCC chemistry.

3.2 Characterization of PLGA and modified PLGA based polymer

3.2.1 Differential Scanning Calorimetry

Variations in the glass transition temperature of PLGA and thiol, glucose and mucin modified PLGA polymers were evaluated by using a DSC Thermal Analyser (DSC Q20, USA). Thermograms covered a range of 0– 300° C with heating and cooling rates of10° C/min under a nitrogen stream.

3.2.2 Fourier Transform Infrared (FTIR) Spectroscopy

To confirm the modification on polymer surfaces, FTIR spectra of PLGA and thiol, glucose and mucin modified PLGA polymers were obtained with Nicolet Impact 410 FTIR spectrophotometer. Polymers were mixed with KBr and pellets were made to record the IR spectra (600cm^{-1}–4000 cm^{-1}).

3.2.3 Nuclear Magnetic Resonance

^{1}H NMR spectra of PLGA and thiol, glucose and mucin modified PLGA polymers were measured in deuterated DMSO using a 300 MHz spectrometer (Bruker Avance DPX 300).

3.2.4 Contact Angle Measurement

Contact angle of unmodified and differently modified PLGA polymer coated glass coverslips, characterising surface wettability were measured with Goniometer Kernco using a previously established procedure (Croll et al., 2004). Contact angles of water were measured at room temperature within 10 s of application of the drops of water, taken at six different locations on the polymer coated coverslip.

3.3 Synthesis of Nanoparticles

3.3.1 Materials

Pluronic F-68 was from Sigma Aldrich, Missouri, United States. Rhodamine B was from SD Fine Chemicals, Maharashtra, India. Solvents, such as ethyl acetate were from Merck Specialities Private Limited, Karnataka, India.

3.3.2 Synthesis of PLGA and modified PLGA based nanoparticles

Nanoparticles were prepared by a typical solvent evaporation method (Vauthier and Bouchemal, 2009). PLGA and the thiol, glucose and mucin modified polymers (0.05 g) dissolved in 10 mL ethyl acetate was emulsified with the primary aqueous phase consisting of 10 mL of 0.2% pluronic F-68 in distilled water. The emulsion was sonicated for 1 min at 30 W (MISONIX 3000) and poured immediately into 100 ml aqueous solution containing 0.2% pluronic F-68 under magnetic stirring. The particle formation was left to continue until the solvent evaporated and the nanoparticles were obtained as a pellet by centrifugation at 9500 rpm for 15 min. Further purification with distilled water was given thrice by centrifuging at 9500 rpm for 10 min to remove the surfactant. The nanoparticles obtained were lyophilized (Freeze Zone 4.5, Labconco) and stored at -20° C in order to avoid humidity induced autocatalytic degradation.

3.3.3 Synthesis of fluorescent labelled nanoparticles

Fluorescent dye, rhodamine B loaded polymeric nanoparticles were prepared using a similar procedure applied for the preparation of PLGA and modified PLGA nanoparticles; expect for the addition of rhodamine B in acetone

solution to the ethyl acetate mediated polymer dispersion. Considering the prevention of fluorescence quenching and autocatalytic degradation of polymer PLGA, the dye encapsulated nanoparticles were stored under dark conditions and at -20° C respectively.

3.4 Characterisation of Nanoparticles

3.4.1 Materials

Histopaque-1077, 3-(4,5-dimethylthiazol-2-yl)-2,5-diphenyl tetrazolium bromide (MTT), Branched polyethyleneimine 25 kDa (PEI), Fluorescein isothiocyanate (FITC), Sodium dodecyl sulphate, Tris(hydroxyaminomethane) were from Sigma Aldrich, Missouri, United States. Acrylamide, Bisacrylamide, Ammonium per sulphate were from SRL. Coomassie Brilliant Blue-R-250 was from AMRESCO, Solon, United States. Solvents such as methanol, ethanol, acetic acid and dimethyl sulfoxide were from Merck Specialities Private Limited, Karnataka, India. Human PF-4 ELISA kits were from Asserachrom, Paris, France and Ray Biotech Inc., Georgia, United States. Terminal complement complex (TCC) ELISA kit was from USCN Life Science, Wuhan, China. C6 and L929 cell lines were obtained from National Centre for Cell Science (NCCS), Pune, India and American Type Culture Collection, Virginia, United States, respectively.

3.4.2 Dynamic Light Scattering

The volume based average particle size and distribution was determined by Dynamic Light scattering (DLS) using Nanosizer (Malvern instruments, UK). Nanoparticles were dispersed in distilled water and experiments were performed at a temperature of 25.0 ± 0.1°C in triplicate.

3.4.3 Atomic Force Microscopy

The surface topography of PLGA and modified PLGA nanoparticles was analysed by atomic force microscopy (WITEC Confocal Raman Microscope system with AFM extension, Germany). The AFM sample preparation included the addition of a drop of the diluted nanoparticle suspension in water over a coverslip and subsequent drying in vacuum desiccator.

3.4.4 Transmission Electron Microscopy

Transmission electron microscopy (TEM) was used to determine the size, shape and dispersion of PLGA and modified PLGA nanoparticles using a Hitachi H-7650 microscope at an accelerating voltage of 100 kV. The specimens were prepared by drop-coating the sample dispersion onto a carbon-coated 300 mesh copper grid, which was placed on filter paper to absorb any excess solvent present. Uranyl acetate (2% w/v) was used as the contrast enhancer.

3.5 Blood Compatibility Analysis

3.5.1 Protein adsorption studies

3.5.1.1 Adsorption studies from human plasma

Human venous blood from healthy volunteered donors was collected in tubes containing 3.8 % sodium citrate at a ratio of 9:1 (blood: anticoagulant). Supernatant plasma was separated following centrifugation of anticoagulated whole blood at 700 rpm for 10 min. PLGA and modified PLGA nanoparticles (5 mg) were incubated with plasma samples (250 µl) for 1 h at 37°C, in a rotary shaker at 35 rpm. Centrifugation at 7000 rpm was carried out for 15 minutes

to separate the particles from the incubation medium followed by a single wash with 1 ml of distilled water. Desorption of the adsorbed plasma proteins from the nanoparticle surface was achieved with 2 h incubation in 50 µl of Laemmelli buffer, pH 6.8 (62.5 mM Tris HCl containing 25% glycerol, 10% SDS), at room temperature. The eluted samples following centrifugation were then analyzed by SDS–PAGE on 7% resolving gel at 100 V for 90 min using Mini-PROTEAN electrophoresis system (Bio-Rad, CA) followed by coomassie blue staining and documentation using an image analyzer (LAS 4000, Fuji). A densitometric scan analysis of the documented image was performed with the help of multigauge software.

3.5.1.2 Labelling of single plasma proteins with fluorescein isothiocyante (FITC)

A solution of 2mg/ml of bovine serum albumin and fibrinogen was prepared in 0.1 M sodium carbonate buffer at pH 9. Owing to the insolubility of gamma globulin in sodium bicarbonate buffer, it was initially solubilised in saline and made up with bicarbonate buffer. To each 1ml of protein solution, 50µl of FITC in DMSO (1mg/ml) was added. The reaction was continued for 8 h under dark conditions to avoid the photochemical quenching of FITC. Additionally, the reaction was carried out at 4°C in order to avoid the room temperature induced plasma protein degradation. The reaction was terminated by the addition of 50µl of 50 mM ammonium chloride solution and the incubation continued for 2 more hours. The unbound FITC was eliminated by dialysing against PBS at 4°C.

3.5.1.3 Adsorption studies from fluorescein isothiocyante labelled single plasma proteins

Protein adsorption from single protein solution was performed according to a reported procedure {Gaucher., 2009}. PLGA and modified PLGA nanoparticles (1 mg) were incubated with 1mg/ml of FITC labelled protein solution (albumin, fibrinogen and globulin) separately in PBS at 37°C for 1 h. After the incubation period, samples were centrifuged to separate 50 µl of the supernatant and the fluorescence intensity was analysed using a fluorescent plate reader TECCAN Infinite M200 at excitation wavelength of 495nm and emission wavelength of 525nm. Protein adsorption on the nanoparticles was quantified by comparing the fluorescence intensity between the supernatant samples and the FITC labelled control protein solution of concentration 1 mg/ml.

Results were expressed as the percentage of protein adsorbed onto the nanoparticle surface using the formula.

$$Percentage\ of\ protein\ adsorbed\ on\ the\ nanoparticles = Fluorescence\ intensity\ of\ \frac{test}{\text{control}}\ 100$$

3.5.2 Complement Activation Analysis

3.5.2.1 Complement Protein C3 Nephelometry

The specific activation of C3 complement component by the modified and unmodified PLGA nanoparticle surfaces in human plasma was assessed by comparative measurements of C3 cleavage by nephelometry. Nanoparticles (100 µg) were incubated for 1 h at 37° C with human plasma diluted with 1:1 PBS solution (containing 0.15 mM Ca^{2+} and 0.5 mM Mg^{2+}) under gentle

agitation. Plasma samples were analysed immediately within 30 minutes of collection. Normal saline and PEI solution served as negative and positive controls, respectively. The concentration of C3 was quantified by comparison from a calibrator of known C3 concentration ranging from 0.33 to 2.6 g/L and analysis was performed as per the protocol provided by the kit manufacturer (Orion Diagnostica, Finland). Specifically, 10 µl of the plasma samples were mixed with 40 µl of antihuman C3 antibody (raised in goat) at pH 7.5. Absorbance was read at 340 nm filter before and exactly 2 min after antibody complexation with Varian 50 Conc. UV−Visible spectrophotometer.

3.5.2.2 Terminal Complement Complex (TCC) Elisa

For a comprehensive evaluation of complement activation, the downstream complexation of complement split product, SC5b-9/TCC was calibrated using ELISA. Precisely 100 µg of modified and bare PLGA nanoparticles were incubated with undiluted serum for 30 min at 37° C. On completion of incubation, supernatant plasma diluted to 1/2000 times with PBS was added to microtiter plate precoated with a monoclonal antibody specific to SC5b-9. C5b-9 was detected using the colour change in biotinylated anti C5b-9 polyclonal antibody and HRP conjugated avidin upon addition of TMB substrate. PEI activated plasma and serially diluted solution of purified TCC served as the positive control and calibration standards respectively. Absorbance was measured at 450 nm with a microplate reader TECCAN Infinite M200.

3.5.3 Platelet Activation Analysis

3.5.3.1 Platelet Factor-4 Quantification

Venous blood from healthy donors was collected in centrifuge tubes containing 3.8% sodium citrate at a blood citrate ratio of 9:1. Platelet rich plasma (PRP) from human blood was obtained by centrifugation at 1200 rpm for 15 min. Modified and cysteine modified PLGA nanoparticles were added to PRP to a final concentration of 300 µg/ml. The samples were incubated for 15 min at 37°C followed by Platelet Factor 4 (PF 4) assay by ELISA (Asserachrom, France). Plasma supernatant (2ml) following 1:21 times dilution with phosphate buffer was added onto microplate wells precoated with specific rabbit antihuman PF4 antibodies. The bound PF4 from samples were detected by rabbit antihuman PF4- peroxidase immunoconjugate giving a colour change upon TMB substrate addition, whose intensity was measured by taking absorbance at 450 nm using TECCAN Infinite M200. The concentration of PF4 in samples was compared with quality control samples provided by the kit manufacturer in the working range between 2 and 120 IU/ml.

In case of glucose and mucin modified PLGA nanoparticles, the PF-4 assay followed the protocol provided by Ray Biotech Inc. The concentration of PF-4 in the samples was compared with quality control standards provided by the kit manufacturer at the working range of 15,000–20.58 pg/ml respectively.

3.5.4 Blood Cell Studies

3.5.4.1 Red Blood Cell, White Blood Cell & Platelet Aggregation Analysis

Freshly collected citrated blood was centrifuged at 700 rpm for 10 min to separate the RBC layer followed by washing and dilution with PBS (1:4) as required for the aggregation studies. For the separation of WBC and platelets, blood was layered over an equal amount of Histopaque-1077 in clean glass tubes. Centrifugation was carried out at 750 rpm for 30 min to obtain the upper yellow PRP and middle WBC rich buffy coat. Modified and unmodified nanoparticles (1 mg) were incubated with 100 µl of RBC, WBC and platelet suspensions at 37° C for 30 min, separately. The differential blood fractions incubated with normal saline were used as the control. After incubation the respective cell morphology were examined by transmitted bright field light microscopy using LEICA DMIRB. A hemolysis assay was performed on the above mentioned nanoparticles along with normal saline and Triton x 100 as negative and positive controls respectively. The measurement of the absorbance was carried out at 541 nm with a UV–visible spectrophotometer (Varian).

3.6. Cell Culture Studies

Cell culture studies were performed using C6 and L929 cells, an adherent glioma and normal fibroblast cell line respectively derived from rat and mouse. All experiments were carried out in the cell culture medium that included DMEM/Ham's F12: MEM (1:1) and MEM together supplemented with 10% FBS for C6 and L929 cells respectively. Both cell lines were incubated at 37° C using a humid 5% CO_2 incubator.

3.6.1 Cytotoxicity Studies

3.6.1.1. MTT 3-(4, 5-Dimethylthiazol-2-yl)-2, 5-Diphenyltetrazolium Bromide) Analysis

Viability and proliferation of cells following an exposure of modified and unmodified PLGA nanoparticles were analysed by the 3-(4, 5-dimethylthiazol-2-yl)-2, 5-diphenyltetrazolium bromide (MTT) assay. Briefly, C6 cells were seeded in 24 well tissue culture plates at a concentration of 2×10^5 cells. The monolayer was incubated with modified and unmodified PLGA nanoparticles of concentration 1 mg for a period of 24 h. Further incubation was followed in the presence of 100 µl MTT (0.5 mg/ml) for another 3 h. The formazan crystals formed were dissolved in 250 µl DMSO and absorbance at 570 nm was read using a microwell plate reader (Finstruments microplate reader, USA). The internal controls were served by cells treated with the medium and 1% triton- X-100.

3.6.1.2 Flow Cytometric Analysis

To minimize the interference of false negative results with plate based assays, flow cytometry was performed to evaluate the cytotoxic effect of modified and unmodified PLGA nanoparticles on normal cell lines following the LIVE/DEAD viability/cytotoxicity (Molecular Probes) assessment on L929 cells. Briefly, L929 cells (3×10^4) were added onto four well plates followed by exposure to 100µl of 1 mg/ml concentrated modified and unmodified PLGA nanoparticles for 48 h. On completion of the required incubation, cells were detached by trypsin and pooled together with the medium containing serum. The percentage of viable cells versus non-treated cells was quantified using BD FACSAria cell sorter (BD

Biosciences) as per manufacturer's instructions. Atleast 10,000 cells were evaluated in each experiment using the BD FACS Diva™ software for data acquisition and analysis.

3.6.3 Cellular Uptake Studies

Initially, C6 cells were sub cultured from the stock culture and seeded onto 4 well plates. The cells were incubated with 100µg of rhodamine B encapsulated modified and unmodified PLGA nanoparticles for 3 and 24 h at 37°C in DMEM/Ham's F12: MEM (1:1) medium containing 10% FBS. Cells were washed with phosphate-buffered saline to remove nonadherent or noninternalized, free particles that remained in the supernatant followed by fixing with 4% paraformaldehyde for 10 minutes. Detailed evaluation of nanoparticle uptake was followed by confocal laser scanning microscope, Zeiss LSM 510 Meta, Germany. Rhodamine B encapsulated nanoparticles were excited using Helium Neon laser of 543 nm and detected through emission LP 560 filter and the images analyzed using LSM 510 software image analyser (version 5).

3.7 Drug Delivery Applications

3.7.1 Synthesis of Drug Encapsulated Nanoparticles

3.7.1.1 Materials

Curcumin and Betulinic Acid were from Sigma Aldrich. Doxorubicin was from Parenteral Drugs Limited, Maharashtra, India. LIVE DEAD Viability/Cytotoxicity Assay kit was from Molecular Probes, Oregon, United States.

3.7.1.2 Synthesis of Doxorubicin Encapsulated Nanoparticles

Nanoparticles were prepared by a typical solvent evaporation method. PLGA or modified PLGA polymers (0.1 g) and Doxorubicin (0.01g) added to the 10 mL of ethyl acetate was emulsified with the primary aqueous phase consisting of 10 mL (0.2%) pluronic F-68 in PBS. The emulsion was sonicated for 1 min at 30 W (MISONIX 3000) and poured immediately into 100 mL PBS solution of 0.2% pluronic F-68 under magnetic stirring. The reaction was left to continue until the solvent evaporated and nanoparticles were pelleted following centrifugation at 9500 rpm for 15 min. Further purification with distilled water was given thrice by centrifuging at 9500 rpm for 10 min to remove the surfactant. The nanoparticles obtained were lyophilized (Freeze Zone 4.5, Labconco) and stored under dark conditions to avoid the photo bleaching of encapsulated drug and at a temperature of -20° C to avoid the room temperature induced degradation of nanoparticles.

3.7.1.3 Synthesis of Curcumin Encapsulated Nanoparticles

Curcumin loaded nanoparticles were prepared using a similar procedure applied for the preparation of PLGA and modified PLGA nanoparticles, expect for the addition of Curcumin in to the polymer dispersed in ethyl acetate. Encapsulated nanoparticles were stored under similar conditions as mentioned above.

3.7.1.4 Synthesis of Betulinic acid Encapsulated Nanoparticles

Similarly, Betulinic acid loaded nanoparticles were prepared using the aforementioned procedure applied for the preparation of PLGA and modified PLGA nanoparticles, expect for the addition of Betulinic acid in to the

polymer dispersed in ethyl acetate. Encapsulated nanoparticles were stored at -20° C under dark conditions to avoid room temperature induced degradation and photo bleaching of drug molecules.

3.7.2 Characterisation of Drug Encapsulated Nanoparticles

3.7.2.1. Dynamic Light Scattering

Average particle size and size distribution of the drug loaded nanoparticles were determined by Dynamic light scattering (DLS) using Nanosizer (Malvern instruments, UK). Drug loaded nanoparticles were dispersed in distilled water and experiments were performed at a temperature of 25.0 ± 0.1°C in triplicate.

3.7.2.2. Differential Scanning Calorimetry

Variations in the glass transition temperature of drug encapsulated PLGA and thiol, glucose and mucin modified PLGA nanoparticles were evaluated by using a DSC Thermal Analyser (DSC Q20, USA). Thermograms covered a range of 0– 250°C with heating and cooling rates of 10 °C/ min.

3.7.2.3 Fourier Transform Infrared Spectroscopy

To determine the presence of drug inside PLGA based nanoparticles, Fourier Transform Infrared (FTIR) spectra of drug loaded PLGA and thiol, glucose and mucin modified PLGA polymers were obtained with Nicolet Impact 410 FTIR spectrophotometer. Drug loaded polymeric nanoparticles were mixed with KBr and pellets were made to record the IR spectra (600–4000 cm^{-1}).

3.7.2.4 UV Spectrometry

UV spectra of released drugs at 25°C were obtained using a Jasco J-810 spectropolarimeter using a 1-cm path-length quartz cell at the concentration of 1 mg/ml. Analysis conditions include 0.5 nm bandwidth, 10-mdeg sensitivity, 0.2-nm resolution, 2-s response, 10 nm/min scanning speed and 190–600 nm measuring range. Each spectrum is the average of at least three runs, being the buffer baseline subtracted from the average spectra.

3.7.2.5 Encapsulation Efficiency of Doxorubicin loaded PLGA and modified PLGA nanoparticles

The resulting drug loaded PLGA and modified PLGA nanoparticles were evaluated in terms of drug encapsulation efficiency (EE, established as ratio between encapsulated over initial drug amount). For the EE determination, a known amount of freeze dried doxorubicin- loaded nanoparticles (5mg) was completely dissolved in dimethyl sulfoxide (DMSO) and then the drug fluorescence at •ex/•em at 480/580 nm was taken using a fluorescent plate reader (TECCAN M200). The doxorubicin encapsulation efficiency was calculated based on the standard curve of doxorubicin in DMSO using the formula.

$$Entrapment\ Efficiency = Doxorubicin\frac{Encapsulated}{Total}\ 100$$

3.7.2.6 Encapsulation Efficiency of Curcumin loaded PLGA and modified PLGA nanoparticles

Similarly, for the EE determination of curcumin loaded PLGA and modified PLGA nanoparticles, a known amount of freeze dried curcumin-loaded nanoparticles (5mg) was completely dissolved in dimethyl sulfoxide (DMSO)

and then the drug absorbance was measured at 420 nm using a plate reader TECCAN M200. The curcumin loading content and the entrapment efficiency were calculated based on the standard curve of curcumin in DMSO using the formula.

$$Entrapment\ Efficiency = Curcumin\ \frac{Encapsulated}{Total}\ 100$$

3.7.2.7 Determination of Encapsulation Efficiency of Betulinic acid loaded PLGA and modified PLGA nanoparticles.

Encapsulation efficiency of betulinic acid loaded PLGA and modified PLGA nanoparticles were calculated by quantifying the amount of betulinic acid recovered from the very first wash supernatants ($M_{\text{Bet supernatant}}$) and assuming that the rest of the drug used during preparation ($M_{\text{Bet total}}$) had been encapsulated. Initially, 10mg of the drug and 100mg of polymer was used for drug encapsulated nanoparticle preparation. Following the completion of betulinic acid encapsulated nanoparticle preparation, a fixed volume of the preparation was centrifuged to pellet the drug encapsulated nanoparticles. Subsequently, the supernatant was subjected to absorbance measurement at 210nm using UV-Vis spectrophotometer (Varian-50-Conc).

The following equation was used to calculate the encapsulation efficiency of Betulinic acid

$$Entrapment\ Efficiency\ of\ Betulinic\ Acid = \frac{M\ Bet\ total - M\ Bet\ supernatant}{M\ Bet\ total}\ 100$$

3.7.2.8 In Vitro Drug Release Kinetics of Doxorubicin

Drug release studies were performed in 10mM PBS (pH 7.4). A known mass (20mg) of Doxorubicin loaded PLGA nanoparticles were suspended in 3ml of buffer and maintained in an incubator shaker at 37˚C. At specific time intervals of 1, 2, 3, 4 & 5 days, the samples were centrifuged for 10 minutes and an aliquote of the supernatant was removed, collected for analysis and replaced with fresh buffer. Fluorescence of the supernatant at •ex/•em 480/580 nm was measured using the TECCAN M200 plate reader for determining the amount of doxorubicin released, as per standard curve in the same buffer.

3.7.2.9 In Vitro Drug Release Kinetics of Curcumin

Similarly, a known mass (20mg) of Curcumin loaded PLGA nanoparticles were suspended in 3ml of buffer and maintained in an incubator shaker at 37˚C. At specific time intervals of 1, 2, 3, 4 & 5 days, the samples were centrifuged for 10 minutes and an aliquot of the supernatant was removed, collected for analysis and replaced with fresh buffer. Curcumin release profile from PLGA and modified PLGA nanoparticles were quantified by recording the absorption of released drug in PBS at 420 nm using the TECCAN M200 plate reader.

3.8. Therapeutic Efficacy of Drug Loaded Nanoparticles at In Vitro Conditions

3.8.1 Internalisation studies of drug loaded nanoparticles

The internalisation of doxorubicin and curcumin loaded nanoparticles by C6 cells were studied using cellular imaging by confocal

microscopy. The uptake of thiol, glucose and mucin modified PLGA nanoparticles along with the unmodified PLGA nanoparticles were examined after encapsulating doxorubicin and curcumin respectively. The inherent fluorescence of encapsulated doxorubicin and curcumin was utilised for tracking the drug loaded nanoparticles and hence for analysing the uptake by confocal microscopy. In case of Doxorubicin, the nanoparticle concentrations varied from 67.8 µg, 69.6µg, 223.8µg & 87.6µg for PLGA, PLGA-Thiol, PLGA-Glucose & PLGA-Mucin concentrations respectively for an equivalent concentration of 12.5µM of the free drug in a volume of 300ul. Similarly, the nanoparticle concentration varied from 201.3µg, 221.4µg, 272.7µg & 189.3µg for PLGA, PLGA-Thiol, PLGA-Glucose and PLGA-Mucin based matrixes respectively for an equivalent concentration of 76µM of free drug, Curcumin in a volume of 300µl culture medium. Following 3 h incubation of drug encapsulated nanoparticles, the culture medium with the particles were removed and the cells were washed with PBS buffer and fixed with 1% paraformaldehyde for viewing under confocal microscope (Nikon AIR).

3.8.2. Cytotoxicity

The therapeutic efficacy of drug loaded PLGA and modified PLGA nanoparticles were evaluated in C6 cell lines by MTT assay, first described by Mossmann (Mosmann, 1983). Cells were seeded on 96 well plates at a cell density of 1×10^3 cells per well and incubated under normal growth conditions. After 24 h of incubation, cell culture media was replaced with the free drug and the drug encapsulated in PLGA and modified PLGA nanoparticles respectively dispersed in 200µl of PBS. The concentration of drugs studied was in the range of 3.6µM, 5.5µM,

9µM & 13µM respectively for Doxorubicin and 20µM, 40µM, 60µM, 80µM, respectively for Curcumin and Betulinic Acid respectively. The free drug concentrations were equalised to the total drug encapsulated in the nanoparticles. The incubation continued for 24 h in culture medium before cell viability was assessed with MTT assay.

3.8.3 Live Dead Assay

The LIVE DEAD viability/cytotoxicity Assay Kit was used for the simultaneous monitoring of live and dead cells following drug loaded particle interaction with C6 cells. Briefly, C6 cells were seeded on to four well plates and incubated with Doxorubicin, Curcumin and Betulinic Acid loaded PLGA and modified PLGA nanoparticles at a fixed concentration for 30 h. The nanoparticle concentrations varied from 226µg, 232µg, 746µg and 291µg for PLGA, PLGA-Thiol, PLGA-Glucose & PLGA-Mucin matrixes respectively for an equivalent concentration of 12.5µM of the free drug, Doxorubicin in a volume of 1ml culture medium. In case of Curcumin, the nanoparticle concentration varied from 671µg, 738µg, 909µg and 631µg for PLGA, PLGA-Thiol, PLGA-Glucose and PLGA-Mucin concentrations respectively for an equivalent concentration of 76µM of free drug, Curcumin in a volume of 1ml of culture medium. Similarly, for the concentration of 41µM of Betulinic Acid in a volume of 1ml of culture medium, it was required to add an equivalent concentration of 462µg, 504µg, 629µg and 434µg of PLGA, PLGA-Thiol, PLGA-Glucose and PLGA-Mucin nanoparticles, respectively. Working solution of live/dead staining was prepared by diluting ethidium bromide stock (2mM) in 10mL distilled PBS (tissue culture grade) along

with 4µm of calcein AM. A volume of 200µl of the working solution was added to the four well plates followed by 30 minutes incubation at room temperature. The stained cells were washed with PBS buffer to remove unbound particles and the images were observed under fluorescent microscopy (Leica DMIRB, Germany).

3.8.4 Quantification of Cell Death by Flow Cytometry

Briefly, C6 cells were cultured on to four well plates for 24 h prior to incubation with Doxorubicin, Curcumin and Betulinic Acid encapsulated PLGA and modified PLGA nanoparticles respectively. A comparison of cytotoxicity was made against the respective free drugs at similar concentrations. The concentration of nanoparticles and drugs were kept similar to Live DEAD Assay. The incubation time was set for 30 h followed by propidium iodide staining. Stock solution of propidium iodide in DMSO (1mg/ml) was diluted 1:4 times in PBS buffer. A volume of 200µl of the working solution was added to the four well plates followed by 10 min incubation. On completion of the required incubation, cells were trypsinised and pooled with the medium containing serum. The percentage of dead cells was determined by the BD FACSAria cell sorter (BD Biosciences). Atleast 10,000 cells were evaluated in each experiment using the BD FACS Diva™ software for data acquisition and analysis.

3.9. Statistics

Statistical analysis was conducted using Student's T-test. All the results are expressed as mean ± standard deviation. The statistical differences between two groups were judged to be significant at $p < 0.05$.

CHAPTER 4
RESULTS

4 RESULTS

4.1 Synthesis of Thiol, Glucose and Mucin modified PLGA Polymers

Carboxyl terminated PLGA was used for the end group attachment of L-cysteine, glucosamine and mucin using standard NHS-DCC chemistry. The successful synthesis of modified PLGA polymers was confirmed by the following physicochemical characterization techniques.

4.2 Characterisation of Modified PLGA Polymer

4.2.1 Differential Scanning Calorimetry

The DSC curve of pure and modified PLGA polymer as shown in Figure 12 exhibits an endothermic peak at 50°C without any distinct melting point. An additional peak appeared at 200°C after modification.

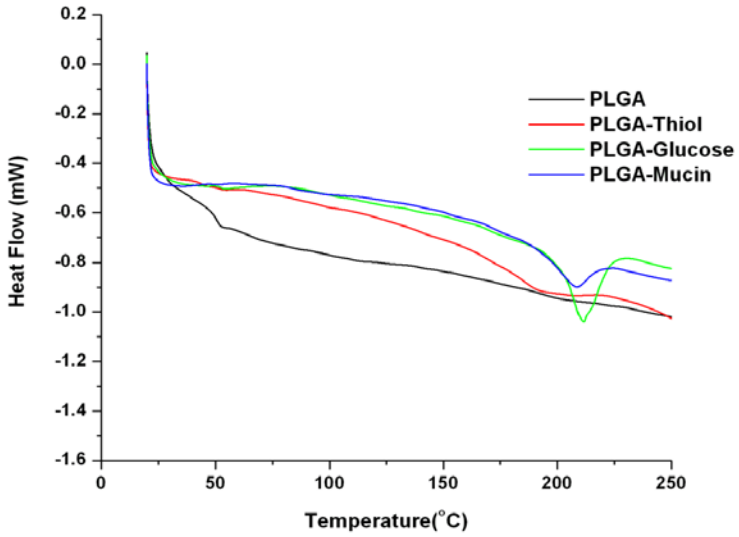

Figure 12: DSC curve of PLGA, PLGA-Thiol, PLGA-Glucose & PLGA-Mucin based polymers.

4.2.2 Fourier Transform Infrared Spectroscopy

The FTIR spectrum analysis provided in Figure 13 revealed a stable polymer structure before and after modification. All the three modifications maintained homogeneity with the structure of expected PLGA polymer. The IR spectra helped to probe and confirm the presence of modifying moiety on PLGA polymer. PLGA showed characteristic peak at 1746 cm^{-1} as shown in Figure 13A.

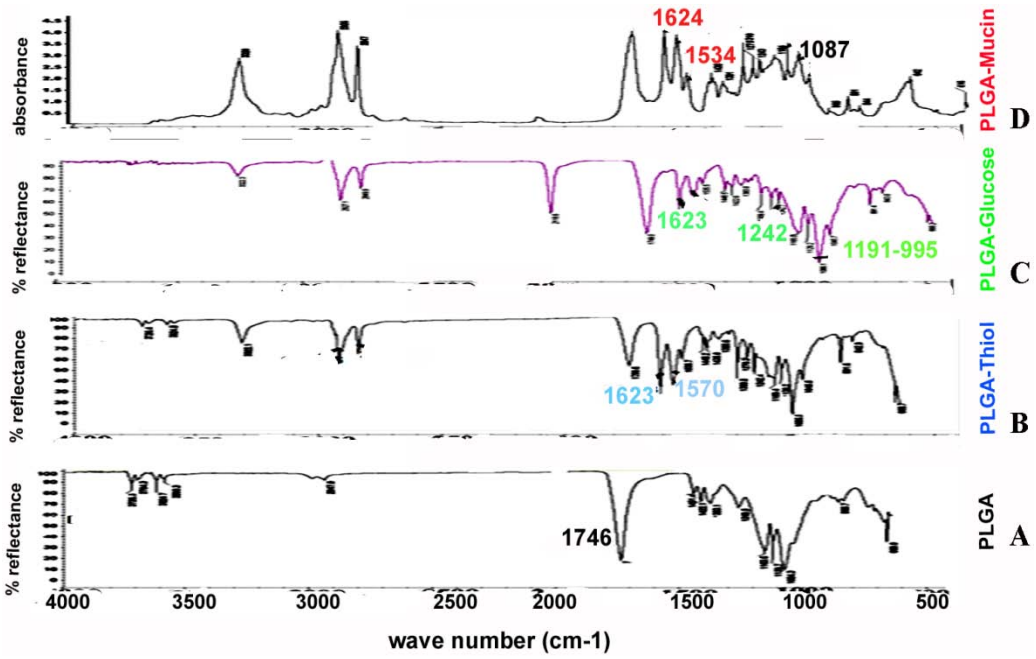

Figure 13: FTIR spectrum of modified and unmodified PLGA polymers

Following thiol based modification, additional peaks appeared at 1623cm^{-1} and 1570 cm^{-1} respectively, as provided in Figure 13B. In case of glucosylation, Figure 13C denotes new peaks at 1242 cm^{-1}, 1623 cm^{-1} and also between 1191 cm^{-1} to 995cm^{-1} respectively. With mucin based modification, new bands were formed at 1534 cm^{-1}, 1047cm^{-1}, 1087cm^{-1} and 1132 cm^{-1} respectively as provided in Figure 13 D.

4.2.3 Nuclear Magnetic Resonance

NMR spectra of PLGA and the three modified PLGA polymers have maintained homogeneity with the structure of expected parent PLGA polymer as depicted in Figure 14.

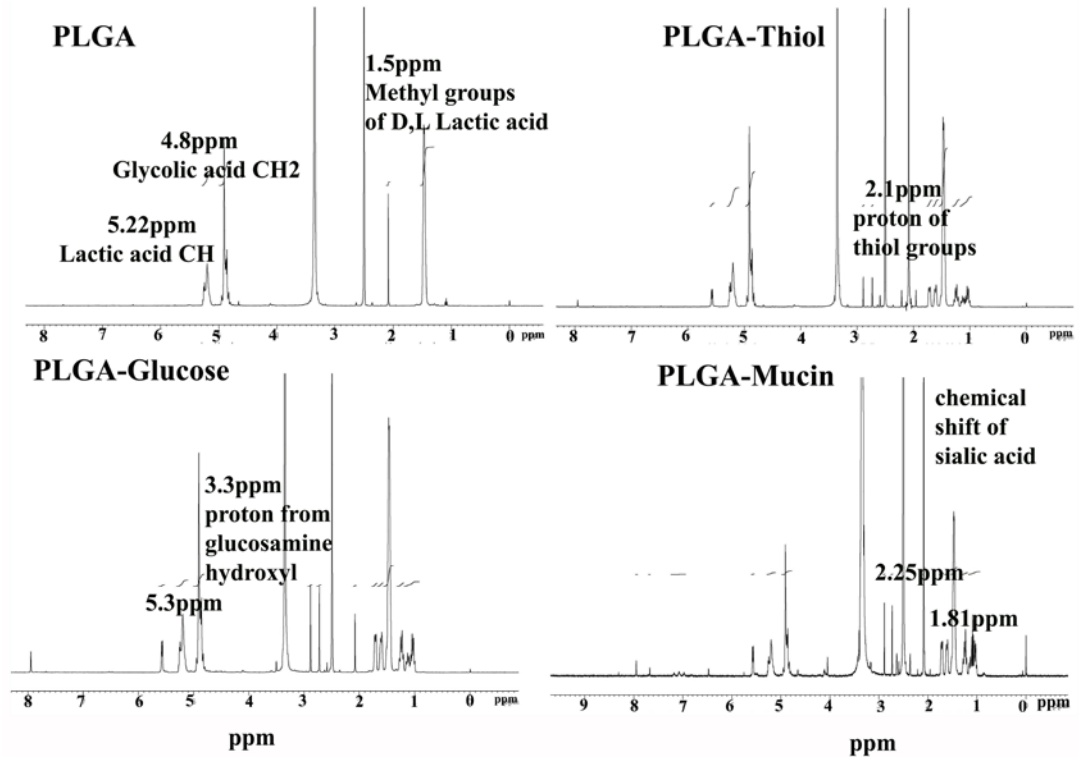

Figure 14: NMR spectra of PLGA, PLGA-Thiol, PLGA -Glucose &PLGA-Mucin

The major ^{1}H NMR signals for PLGA appeared at 1.5ppm, 4.8ppm and 5.2 ppm. Following PLGA modification, a peak that corresponds to amide bond has appeared at 8ppm for PLGA-Thiol, PLGA-Glucose and PLGA-Mucin modified polymers. The thiol based modification of PLGA was followed by additional signals at 2.1 ppm, while in case of glucosylation, additional signals appeared at 3.3ppm and 5.3ppm. Following mucin based modification, new NMR signals appeared at 1.81ppm and 2.25ppm.

4.2.4 Contact Angle Measurement

Contact angle is directly proportional to the hydrophobicity of a surface. The variations in contact angle following modifications are given in Table IV. The static contact angle of PLGA is 71° and it declines to 41°, 42° and 59°, respectively following the thiol, glucose and mucin modifications.

Table IV: Contact Angle Measurements of PLGA & Modified Polymers

Sample	Contact Angle
PLGA	71°±3
PLGA-Thiol	42°±5°
PLGA-Glucose	41°±6°
PLGA-Mucin	59°±5°

4.3 Synthesis of Nanoparticles

4.3.1 Synthesis of PLGA and modified PLGA based nanoparticles

Solvent evaporation technique was utilised for the synthesis of pristine and surface functionalized PLGA nanoparticles as per standard method with slight modifications.

4.3.2 Synthesis of Fluorescent Labelled Nanoparticles

Similarly, Rhodamine B loaded fluorescent PLGA and modified PLGA nanoparticles were also synthesised using solvent evaporation technique. 10µl

of 1mg/ml rhodamine in acetone was added to the organic phase of PLGA or modified PLGA.

4.4. Characterisation of Nanoparticles

4.4.1 Dynamic Light Scattering

The mean diameter and dispersity index against the volume distribution of the prepared PLGA and modified PLGA nanoparticles were measured by dynamic light scattering and the results are presented in the Table V.

Table V: Size & dispersity Index of PLGA & Modified PLGA Nanoparticles

SAMPLE	Volume Distribution	
	Size (nm)	Dispersity Index
PLGA	**114±10**	**0.09**
PLGA-Thiol	**97±6**	**0.14**
PLGA-Glucose	**198±15**	**0.24**
PLGA-Mucin	**165±5**	**0.18**

4.4.2 Atomic Force Microscopy

The detailed surface morphology of PLGA and modified PLGA nanoparticles through AFM observation is shown in Figure 15. PLGA nanoparticles upon modification exhibit spherical shape with uniform size range without any noticeable pinholes and cracks. The modified nanoparticles were small and discrete without adhesion or cohesion.

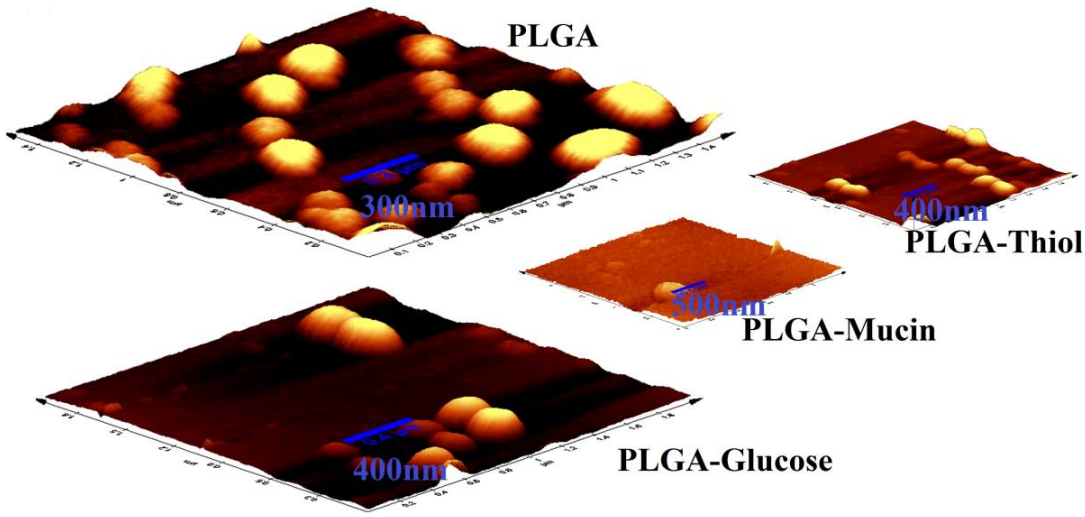

Figure 15: AFM images of PLGA, PLGA-Thiol, PLGA-Glucose and PLGA-Mucin

4.4.3 Transmission Electron Microscopy

Transmission electron microscopic (TEM) images provided in Figure 16 displayed the size of the PLGA and modified PLGA nanoparticles to be around 200 nm. Moreover, the TEM data also verifies that PLGA and modified PLGA nanoparticles are mono-dispersed and spherical in shape.

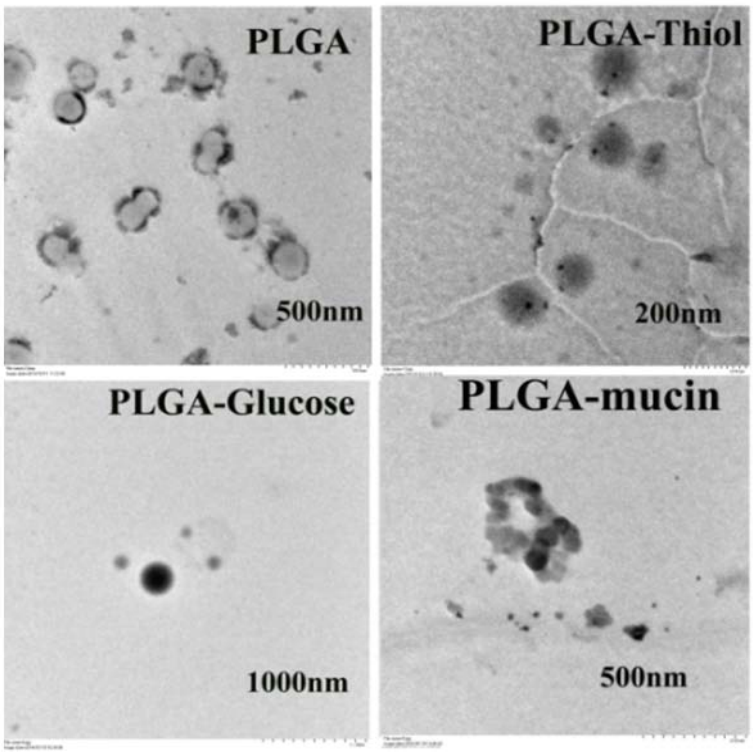

Figure 16: TEM images of PLGA, PLGA-Thiol, PLGA-Glucose& PLGA-Mucin

4.5. Blood Compatibility Analysis

4.5.1 Protein Adsorption Studies

4.5.1.1 Adsorption Studies from Human Plasma

The polyacrylamide gel profile of plasma proteins desorbed from modified and unmodified PLGA nanoparticles following incubation is depicted in Figure 17A.

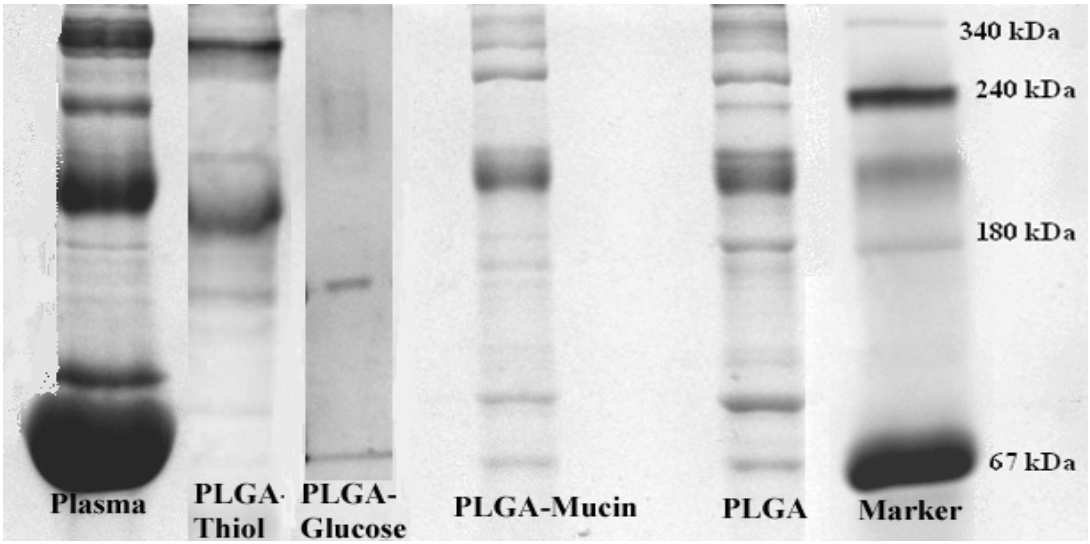

Figure 17A: Polyacrylamide gel electrophoresis pattern of plasma proteins desorbed from PLGA, PLGA-Thiol, PLGA-Glucose and PLGA-Mucin based nanoparticles following 1 h incubation in plasma.

Plasma protein adsorption patterns were similar at specific molecular weight regions observed for both nanoparticles. Adsorption comparison was performed mainly for the major three plasma proteins, albumin (67 kDa), fibrinogen (340 kDa) and γ-globulin (240 kDa). The PAGE profile suggest that all three major proteins, predominantly globulin, adsorbed at a lower amount on modified PLGA nanoparticles in comparison to the unmodified one. This observation was further verified by a semi quantitative analysis of the major protein bands using the densitometric scans of the gel image given in Figure 17B.

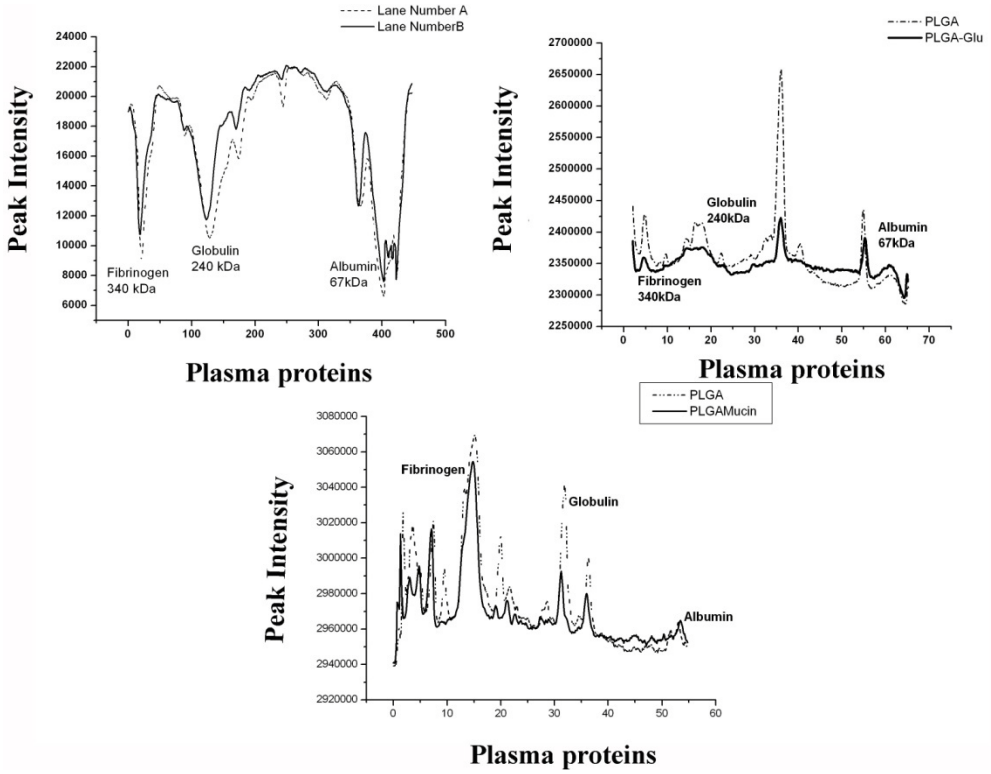

Figure 17B: Densitometric scan analysis of the desorbed protein bands

4.5.1.2 Adsorption Studies from FITC Labelled Single Plasma Proteins

In addition to PAGE studies, single protein adsorption experiments were performed to confirm the plasma protein adsorption pattern. It was observed from Figure 18 that all the three major plasma proteins namely albumin, fibrinogen and globulin adsorbed at a higher amount on unmodified PLGA nanoparticle surface in comparison to modified particles, at the nanoparticle concentration studied here. Specifically, the modifications reduced fibrinogen and globulin adsorption in comparison to the adsorption of the dysopsonin, albumin.

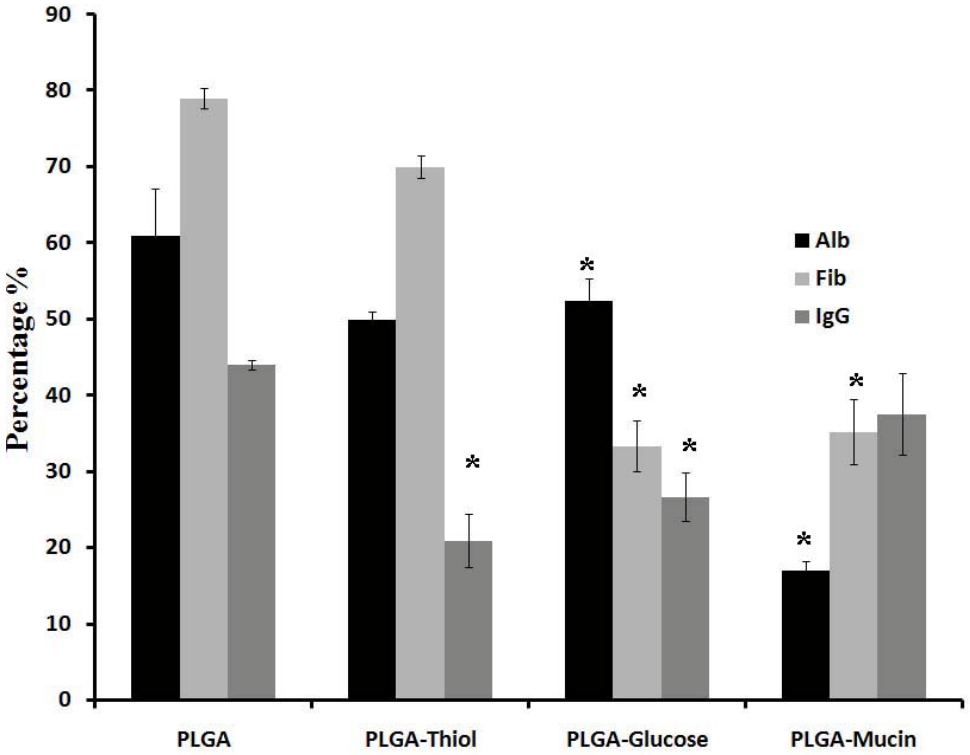

Figure 18: Single Protein Adsorption Pattern of PLGA, PLGA-Thiol, PLGA-Glucose and PLGA-Mucin based nanoparticles following 1h incubation in FITC labelled albumin (1mg/ml), fibrinogen (1mg/ml) and globulin (1mg/ml) solutions. * Statistically significant difference from corresponding PLGA group, $p<0.05$.

4.5.2 Complement Activation Analysis

4.5.2.1 Complement Protein C3 Nephelometry

The turbidimetric estimation of C3, was performed to evaluate the degree of complement activation induced by the PLGA and modified PLGA nanoparticles after incubation in plasma for 1 h. The concentration of complement protein C3 in plasma (negative control) was estimated to be 1.38g/l and the maximum activation obtained after 100 µg of PEI incubation (positive control) reduced the C3 concentration to 0.08 g/l. The concentration of C3 protein after interaction with 1mg of PLGA and thiol, glucose and mucin modified PLGA

nanoparticles were 0.62g/l, 1.2g/l, 1.01g/l & 0.85 g/l respectively as provided in Figure 19.

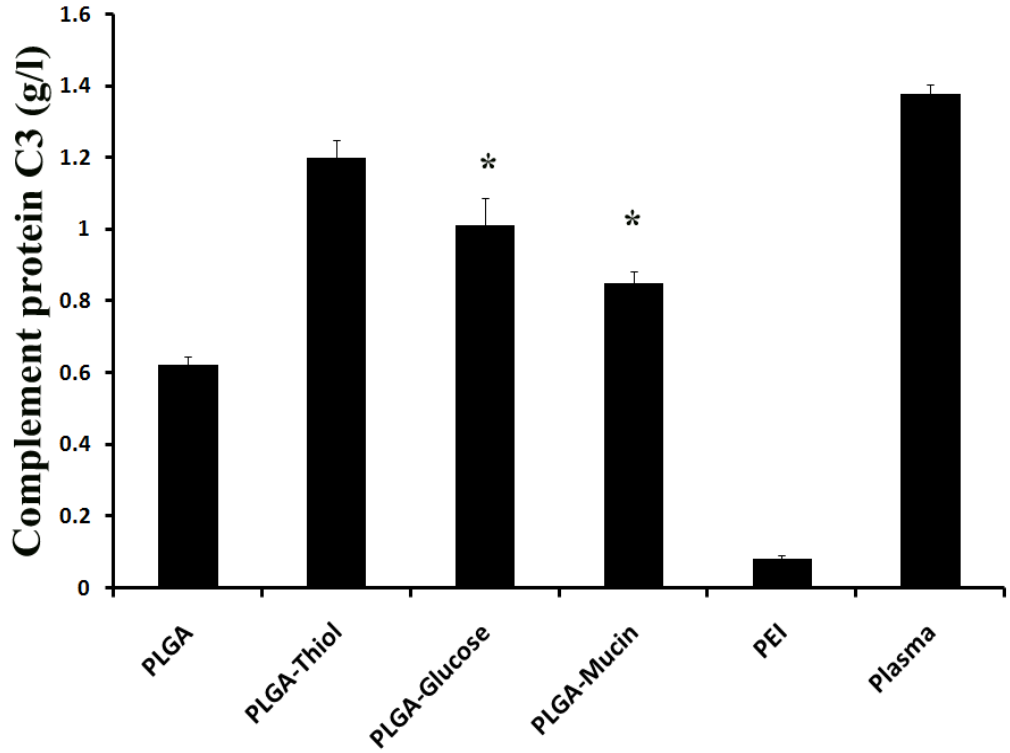

Figure 19: Complement activation studies of PLGA, PLGA-Thiol, PLGA-Glucose and PLGA-Mucin based nanoparticles in human plasma evaluated by Nephelometric method (n=3).
*** Statistically significant difference from the corresponding PLGA group, p<0.05.**

4.5.2.2 Terminal Complement Complex Elisa

For an extended understanding about the complement activation status in plasma, complement activation product SC5b-9 was evaluated upon contact with the nanoparticles.

The upper and lower limits of complement activation denotes that the positive and negative controls enacted by PEI and PBS figured up to a concentration of 774 and 154 pg/ml of TCC, respectively. PLGA nanoparticles (100 µg) in plasma induced the production of TCC to 241.4pg/ml, which decreased to

165pg/ml, 201pg/ml & 193pg/ml upon thiol, glucose and mucin based PLGA modifications, respectively, at equal nanoparticle concentrations as indicated in Figure 20.

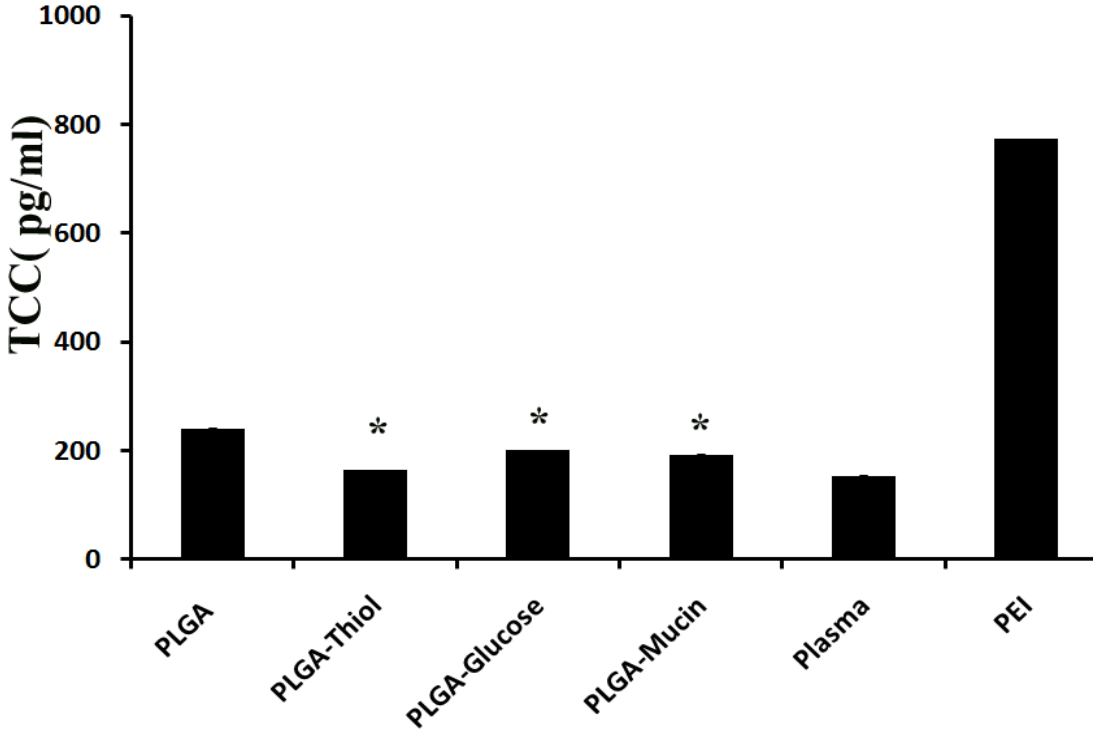

Figure 20: Complement activation studies of PLGA, PLGA-Thiol, PLGA-Glucose and PLGA-Mucin nanoparticles in human plasma evaluated by TCC Elisa (n=3). * Statistically significant difference from corresponding PLGA group, p<0.05.

4.5.3 Platelet Activation Analysis

4.5.3.1 PF-4 Quantification

PLGA and modified PLGA nanoparticles were exposed to PRP and the quantification of PF-4 was performed with the help of two different PF-4 Elisa kits. The PLGA nanoparticle exposure activated the platelets from minimal plasma levels as per the release of PF-4 at 13.7±1.55 pg/ml. In response to the thiol, glucose and mucin based modifications of the PLGA nanoparticles, the activation of

PF-4 reduced to a concentration of 11.49±0.1, 6.63±1.22 pg/ml and 6.76±1.22 pg/ml, respectively as provided in Figure 21.

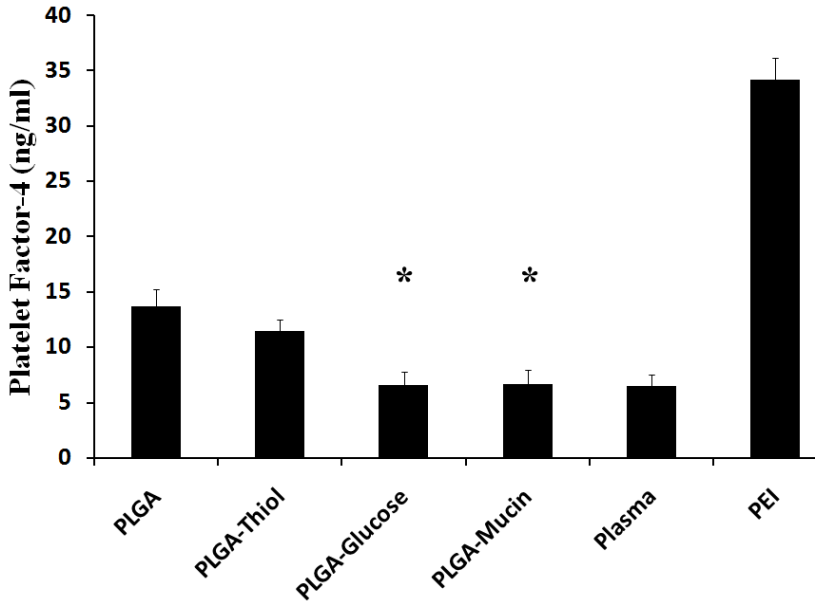

Figure 21: Platelet activation studies of PLGA, PLGA-Thiol, PLGA-Glucose and PLGA-Mucin nanoparticles in human plasma evaluated by PF-4 quantification (n=3). * Statistically significant difference from corresponding PLGA group, p<0.05.

4.5.4 Blood Cell Studies

4.5.4.1 Blood Cell Aggregation Studies

All three blood cell fractions (RBC, WBC, platelets) exhibited favourable compatibility to both PLGA and modified PLGA nanoparticles. These nanoparticles demonstrated minimal level of aggregation tendency after 30 min of in vitro incubation conditions and were almost comparable to the control (saline) in terms of blood cell membrane integrity as observed in Figure 22 A, 22B and 22C respectively, under a light microscope.

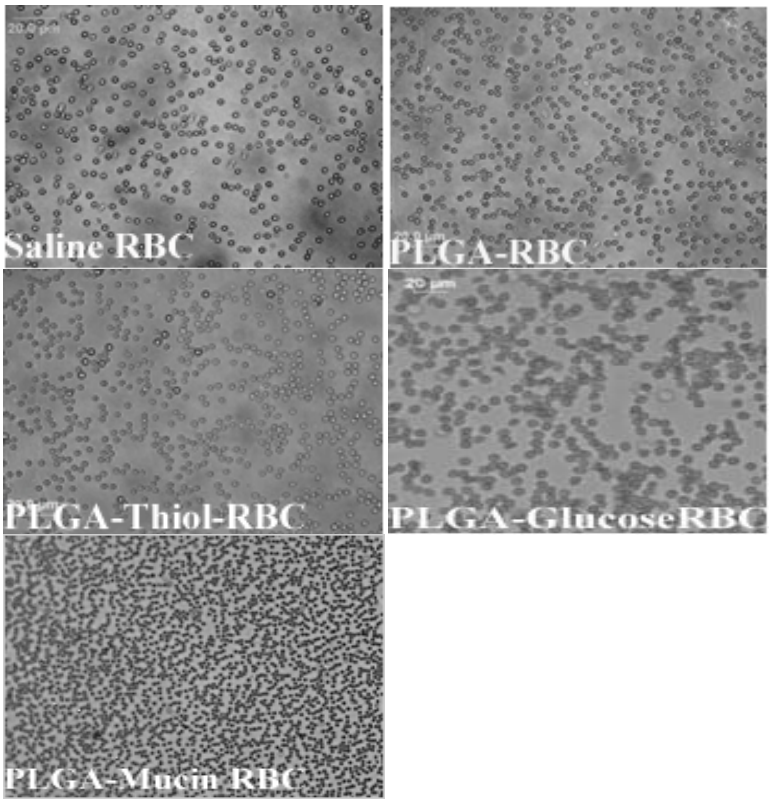

Figure 22A: Microscopic view of RBC after incubation with saline, PLGA NPs, PLGA-Thiol NPs, PLGA-Glucose NPs and PLGA-Mucin NPs.

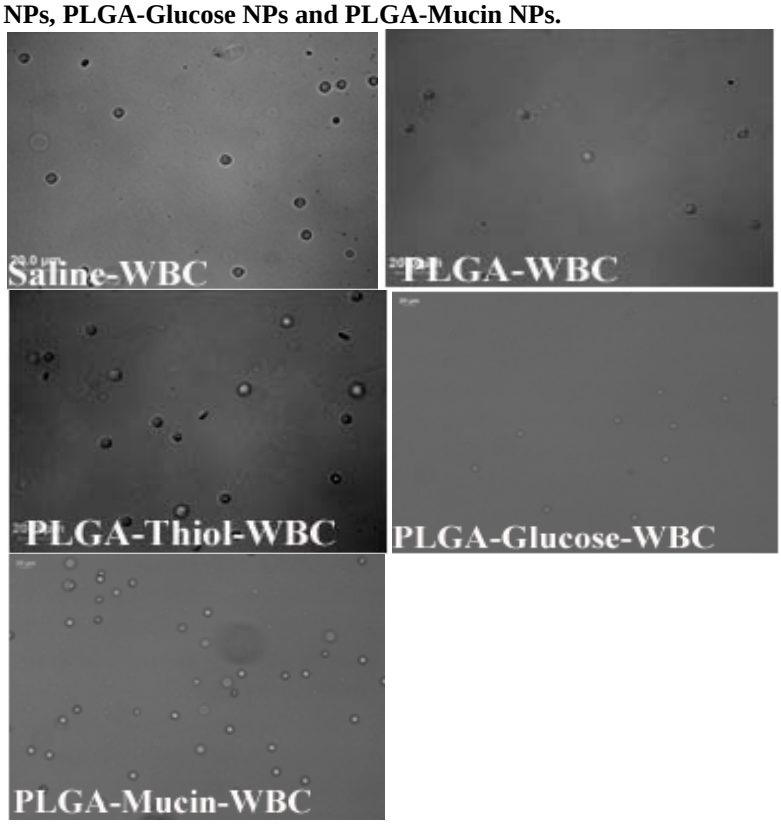

Figure 22B: Microscopic view of WBC after incubation with saline, PLGA NPs, PLGA-Thiol NPs, PLGA-Glucose NPs and PLGA-Mucin NPs.

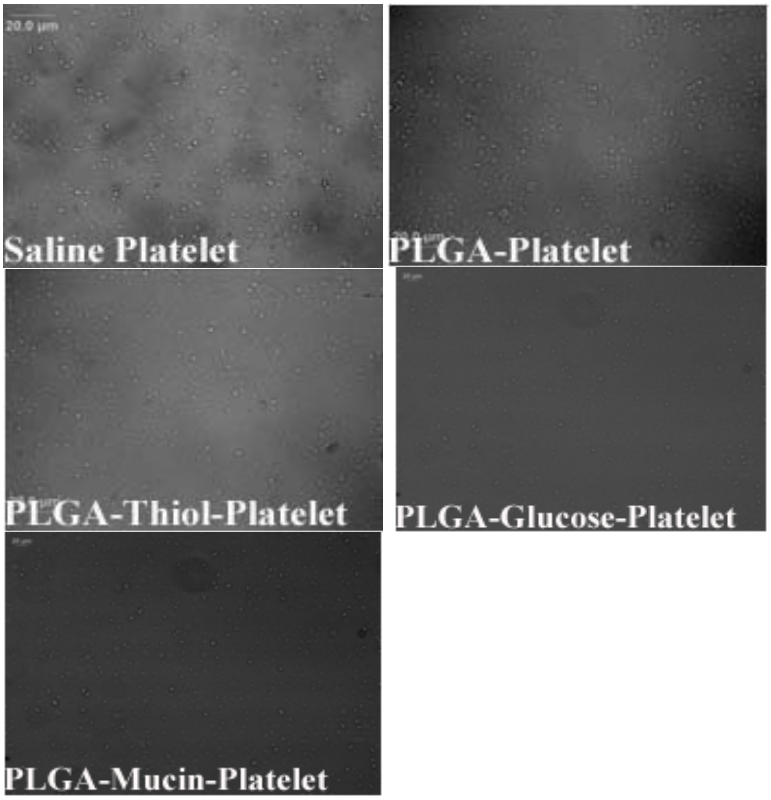

Figure 22C: Microscopic view of platelets after incubation with saline, PLGA NPs, PLGA-Thiol NPs, PLGA-Glucose NPs and PLGA-Mucin NPs.

4.5.4.2. Hemolysis

Figure 23 summarizes the percent hemolysis of PLGA and modified PLGA nanoparticles along with the controls. All values were far below the permissible hemolysis index of 1% when compared with the positive control (Triton-x100) that induced 100% hemolysis.

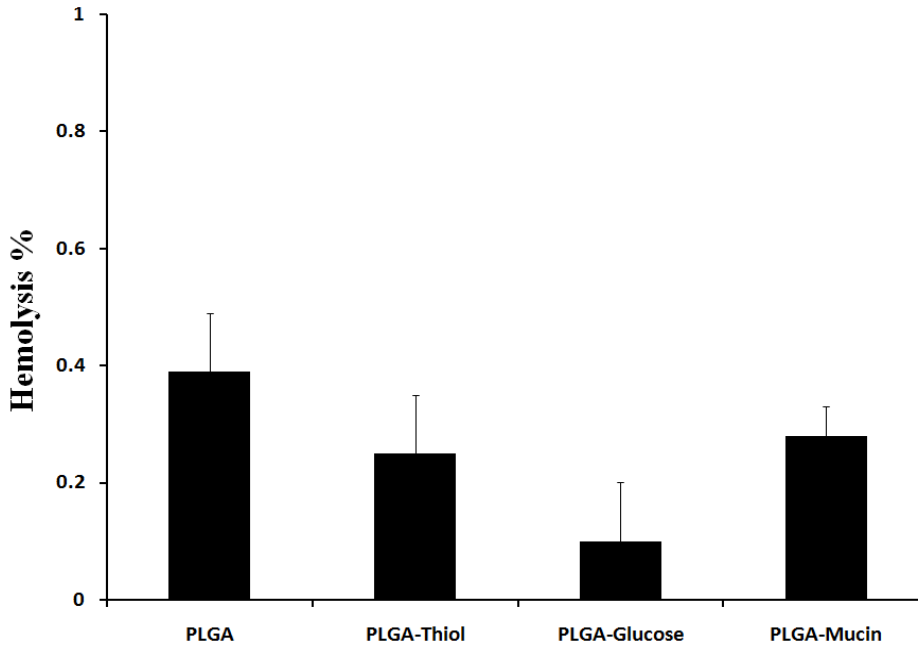

Figure 23: Hemolytic potential of PLGA and modified nanoparticles as per the hemolysis%

4.5.5 Cell Culture Studies

4.5.5.1 Cytotoxicity Assessment

4.5.5.1.1 MTT (3-(4, 5-Dimethylthiazol-yl)-2, 5-Diphenyltetrazolium) Analysis

The toxic potential of PLGA and the modified PLGA nanoparticles on the mitochondrial dehydrogenase activity of C6 cells was measured by the MTT assay, as shown in Figure 24.

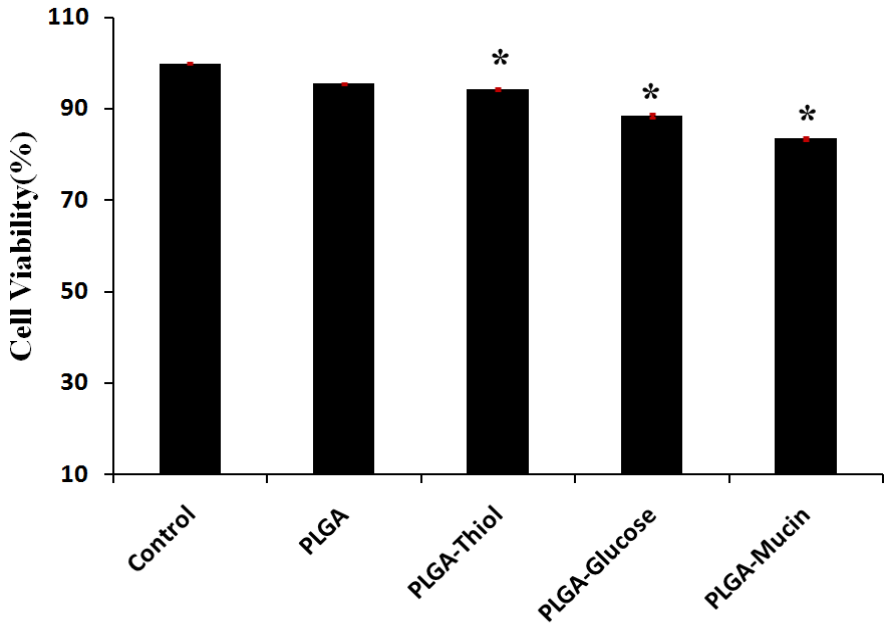

Figure 24: Cytotoxicity assessment of PLGA, PLGA-Thiol, PLGA-Glucose and PLGA-Mucin nanoparticles by MTT assay in C6 cell line. * Statistically significant difference from corresponding PLGA group, p<0.05.

As expected, both the particles are non-toxic and compatible in the concentration range of 1 mg/ml as per the quantification of the conversion of tetrazolium salt into formazan crystals. Cells remain viable (more than 90%) for 24 h after exposure to PLGA and modified PLGA nanoparticles when compared to the negative control system. Positive control was exposed to Triton-X-100 (1%) and it resulted in complete permeabilisation of C6 cell membranes leading to 100% cell death

4.5.5.1.2. Flow Cytometric Analysis

As a supplement to the traditional MTT assay, an assessment of the cytotoxic potential of nanoparticles on normal cells was performed by direct cell counting via flow cytometry. PLGA and modified PLGA nanoparticles (1 mg/ml) were incubated on a non-tumorogenic cell line, L929 for 48 h. Figure 25 displays the flow cytometric analysis of the number of live cells after exposure with the nanoparticles in relation to the control, unstained cells.

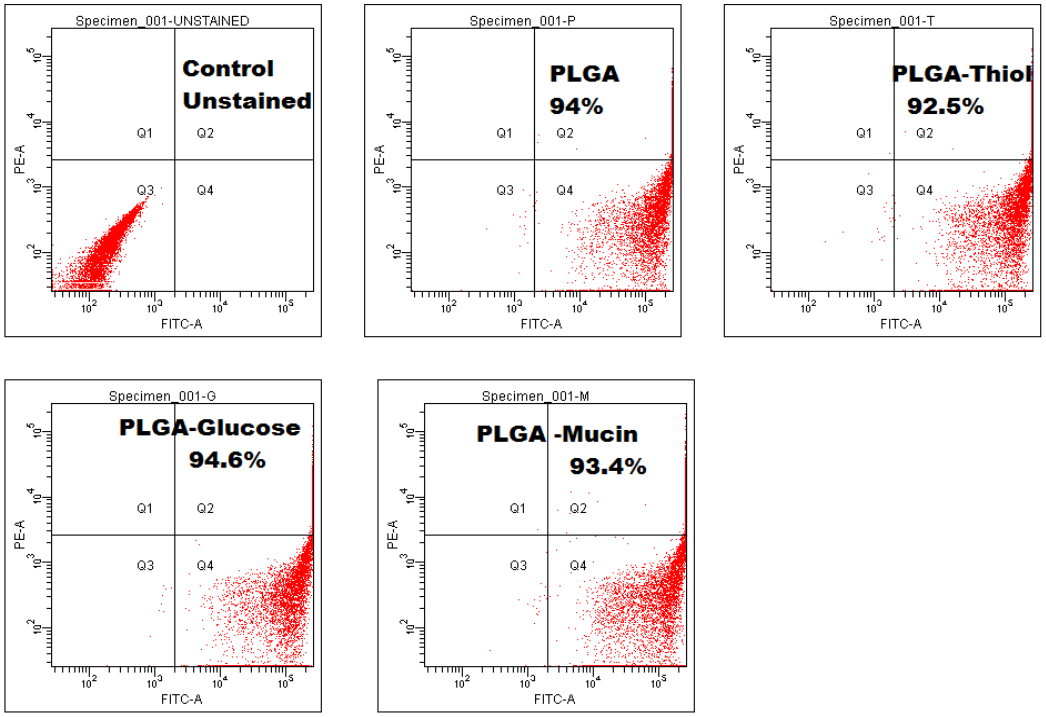

Figure 25: Viability assessment of PLGA, PLGA-Thiol, PLGA-Glucose and PLGA-Mucin nanoparticles by Flow cytometry in L929 cell line

Flow cytometry confirmed the cytocompatibility of surface functionalized PLGA nanoparticles with a percentage viability of 94%, 92.5%, 94.6%, and 93.4% following unmodified, thiol, glucose and mucin modified PLGA nanoparticle exposure, respectively.

4.5.5.2 Cellular Uptake Studies

Cellular internalisation and cytoplasmic access of nanoparticles were investigated from uptake studies using confocal microscopy. A comparative evaluation of the intracellular distribution of PLGA and modified PLGA nanoparticles after 3h and 24h are provided in Figure 26A and Figure 26B respectively.

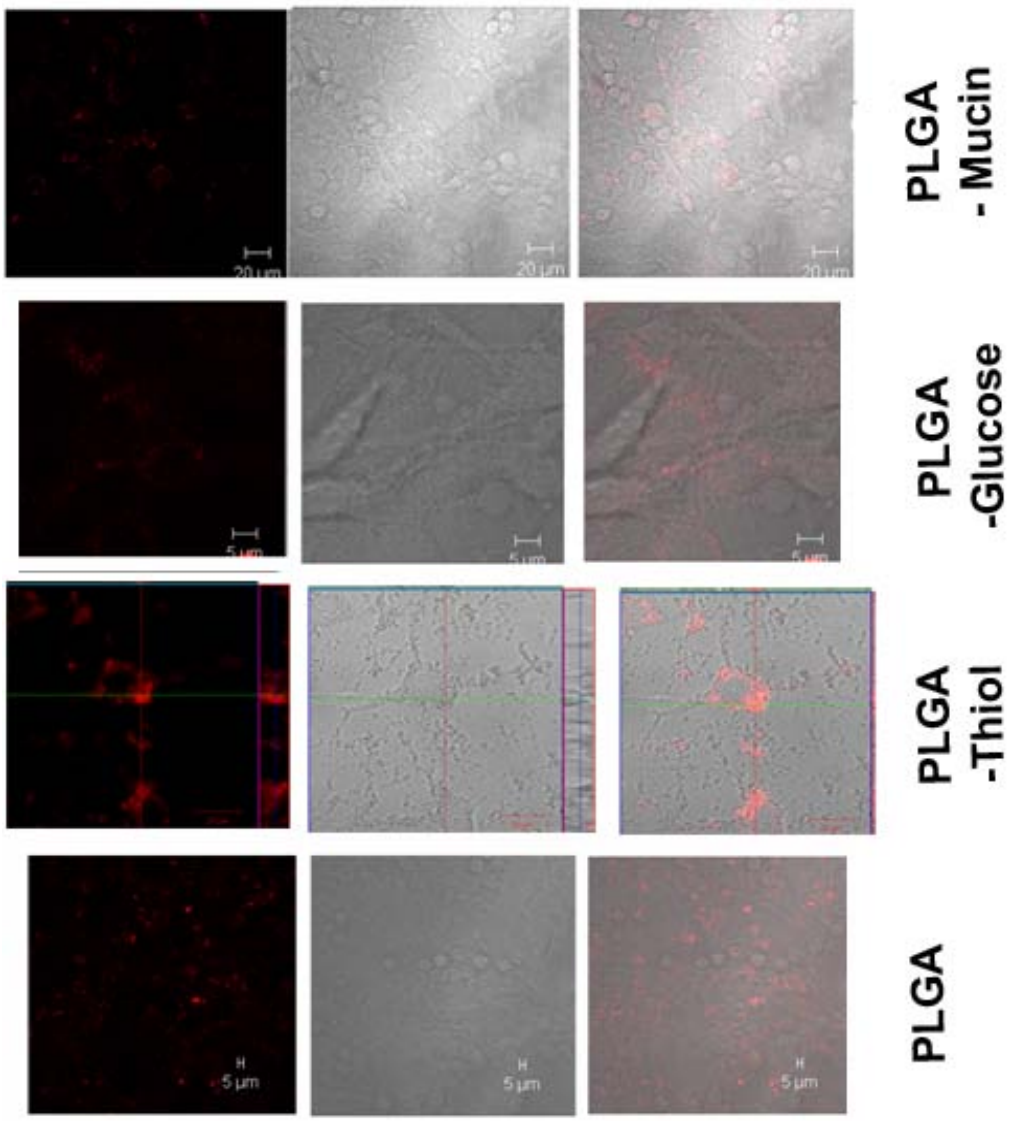

Figure 26A: Uptake analysis of PLGA, PLGA-Thiol, PLGA-Glucose and PLGA-Mucin nanoparticles after 3 hour incubation in C6 cell lines by confocal microscopy. The concentration of all the modified PLGA based nanoparticles is in the range of 100µg per 300µl medium.

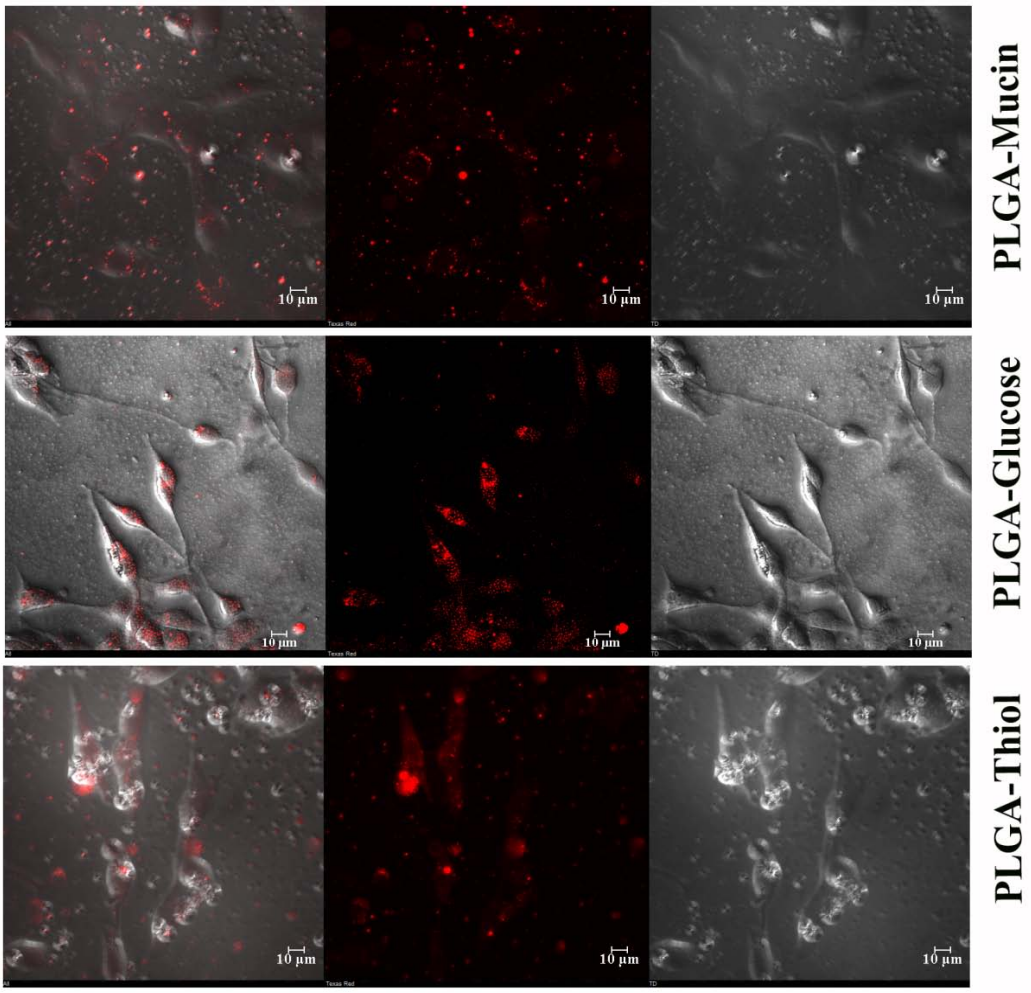

Figure 26B: Uptake analysis of PLGA-Thiol, PLGA-Glucose and PLGA-Mucin nanoparticles after 24 hour incubation in C6 cell lines by confocal microscopy. The concentration of all the modified PLGA based nanoparticles is in the range of 100µg per 300µl medium.

Reliable evidence for the internalization of functional PLGA nanoparticles was provided in Figure 26 C and indicates the depth code analysis form of Z-stacking by confocal imaging after 3h.

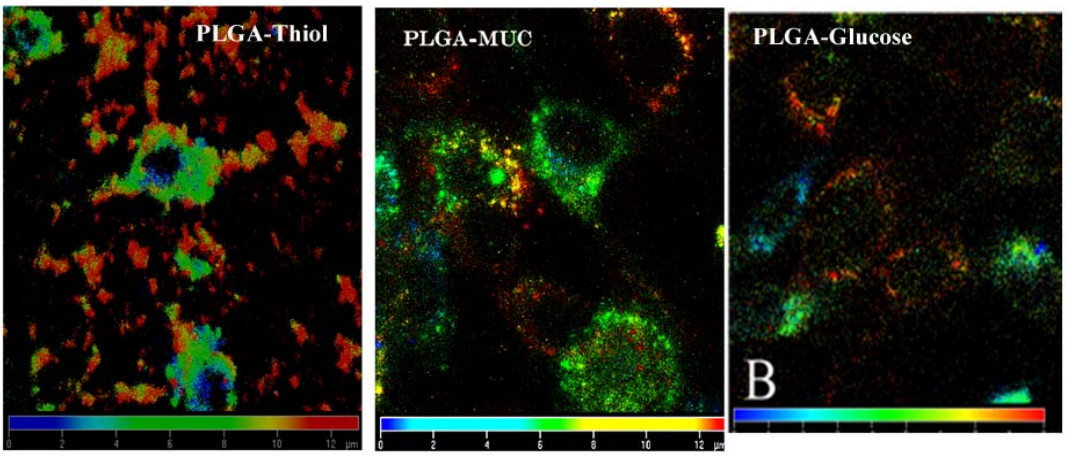

Figure 26 C: Depth code analysis of PLGA-Thiol, PLGA-Glucose and PLGA-Mucin nanoparticle in C6 cell lines.

This observation has helped to differentiate the nanoparticles attached to the outer cellular membrane from the particles retained inside the cytoplasm. Hence confirmed the internalisation of PLGA and differently modified PLGA nanoparticles.

4.6. Drug Delivery Applications

4.6.1 Synthesis of Doxorubicin, Curcumin and Betulinic Acid Encapsulated Nanoparticles

Doxorubicin, curcumin and betulinic acid loaded PLGA and modified PLGA nanoparticles were successfully prepared by solvent evaporation technique with drug: polymer ratio as 1:10.

4.6.2 Characterisation of Drug Encapsulated Nanoparticles

4.6.2.1 Dynamic Light Scattering

Table VI summarises the size and dispersity index against volume distribution of blank and drug loaded PLGA and modified PLGA nanoparticles

Table VI: Size and Dispersity Index of drug loaded PLGA and differently modified PLGA nanoparticles

Sample	Volume Distribution	
	Size	Dispersity Index
P-Dox	82±10	0.13
P-T-Dox	297±15	0.24
P-G-Dox	128±8	0.3
P-M-Dox	126±13	0.2
P-Cur	203±8	0.07
P-T-Cur	211±13	0.12
P-G-Cur	251±20	0.32
P-M-Cur	268±15	0.31
P-Bet	250±10	0.3
P-T-Bet	265±15	0.34
P-G-Bet	284±5	0.24
P-M-Bet	158±6	0.23

Drug loading had an effect on increasing the size of the nanoparticles; nevertheless, all the synthesised nanoparticles were in the size range below 300nm.

4.6.2.2 Differential Scanning Calorimetry

The physical state of the drugs, doxorubicin, curcumin and betulinic acid, following encapsulation inside the PLGA and modified PLGA nanoparticles were characterised by the analysis of DSC curves. The pure drugs, doxorubicin, curcumin and betulinic acid displayed their characteristic endothermic peak at 168°C, 172°C and 300°C respectively that disappeared following encapsulation inside the nanoparticles. However, as the polymer PLGA undergo decomposition at the melting temperature of betulinic acid at 300°C, the characterisation of the thermal events of betulinic acid encapsulated PLGA nanoparticles were difficult to predict. Otherwise, the three different drug encapsulated PLGA and modified PLGA nanoparticles exhibited similar endothermic events, such as the relaxation peak at 50°C following the glass transition as provided in the Figure 27.

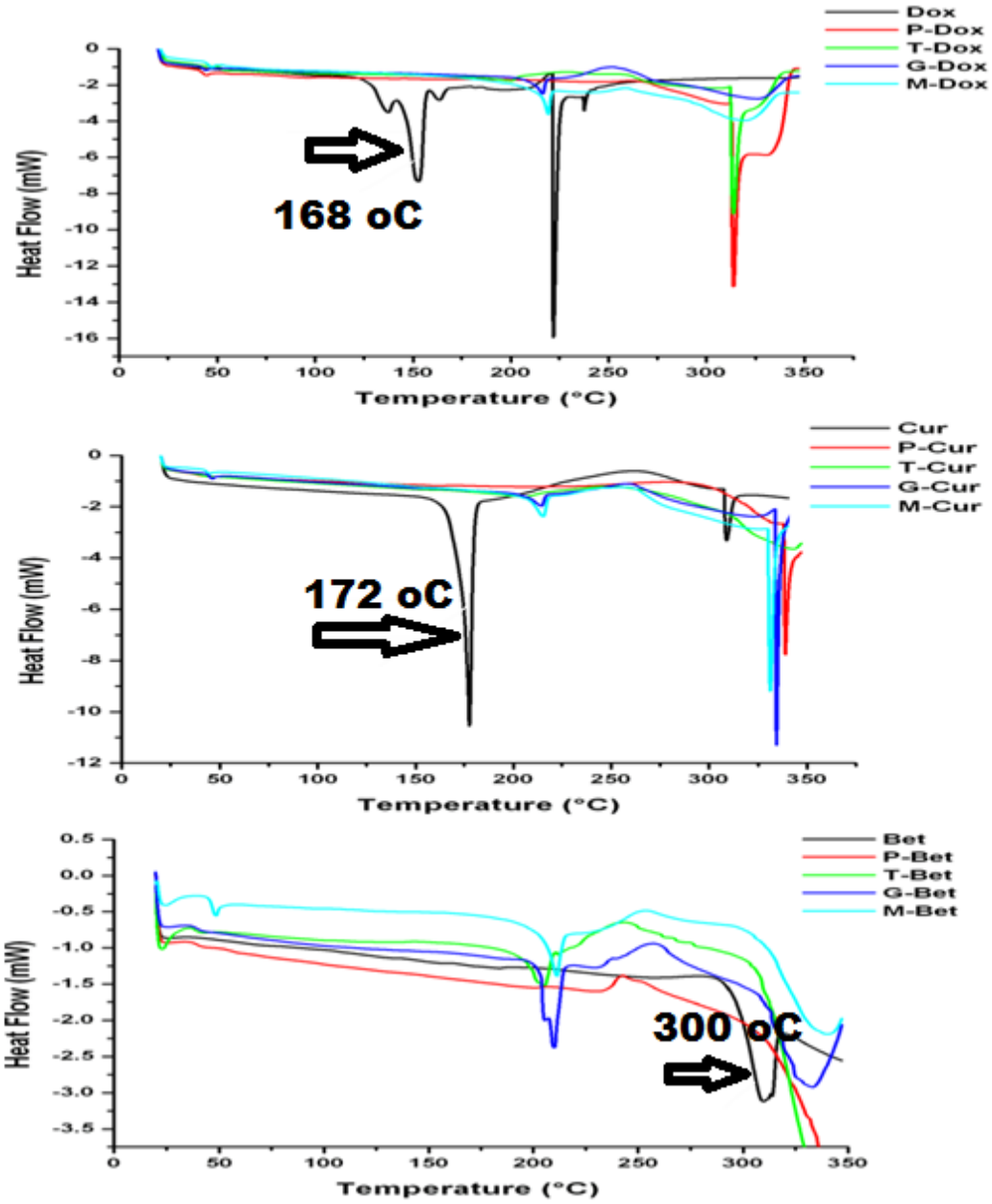

Figure 27: DSC analysis of Doxorubicin, Curcumin and Betulinic Acid loaded PLGA and modified PLGA nanoparticles

4.6.2.3 Fourier Transform Infrared Spectroscopy

Additional characterisation technique like FTIR was required to specifically confirm the presence of nanoparticles within the encapsulated nanoparticles.

The FTIR spectra of doxorubicin, curcumin and betulinic acid in the pure and encapsulated form within PLGA and modified PLGA nanoparticles were performed. In case of doxorubicin, bands appeared at 1580cm^{-1}, 3300cm^{-1}-3600cm^{-1} before and after encapsulation as given in Figure 28 A.

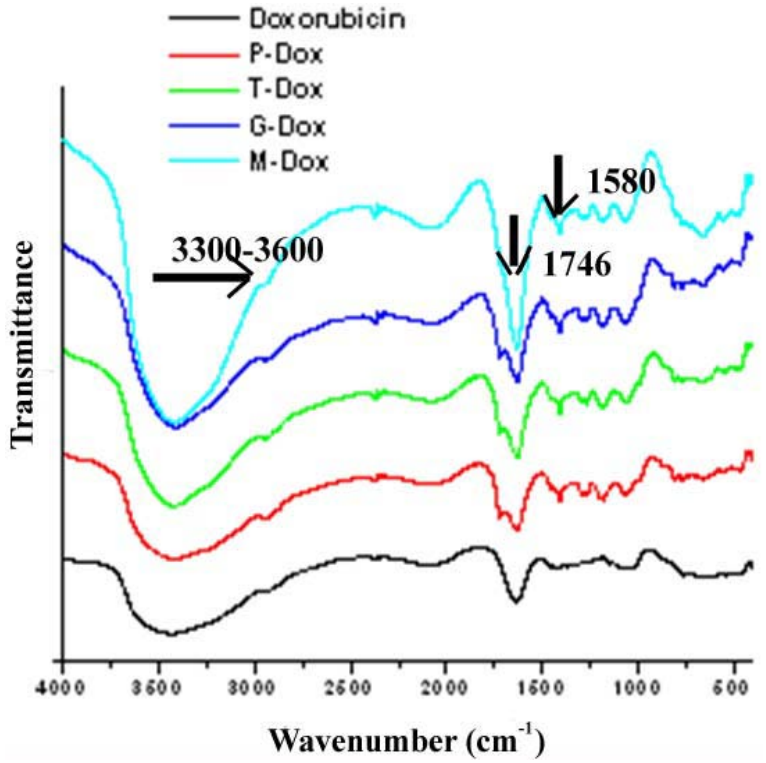

Figure 28 A: FTIR spectra of Doxorubicin loaded PLGA and modified PLGA nanoparticles

Spectral analysis showed characteristic bands due to different functional groups such as C=C double bonds and aromatic C=C double bonds at 1510cm^{-1} and 1627cm^{-1}

respectively for curcumin and its loaded polymeric nanoparticulate formulations. Additionally, the characteristic band of curcumin at 3524cm^{-1} is absent, exclusively for PLGA loaded curcumin nanoparticles alone, as provided in Figure 28B.

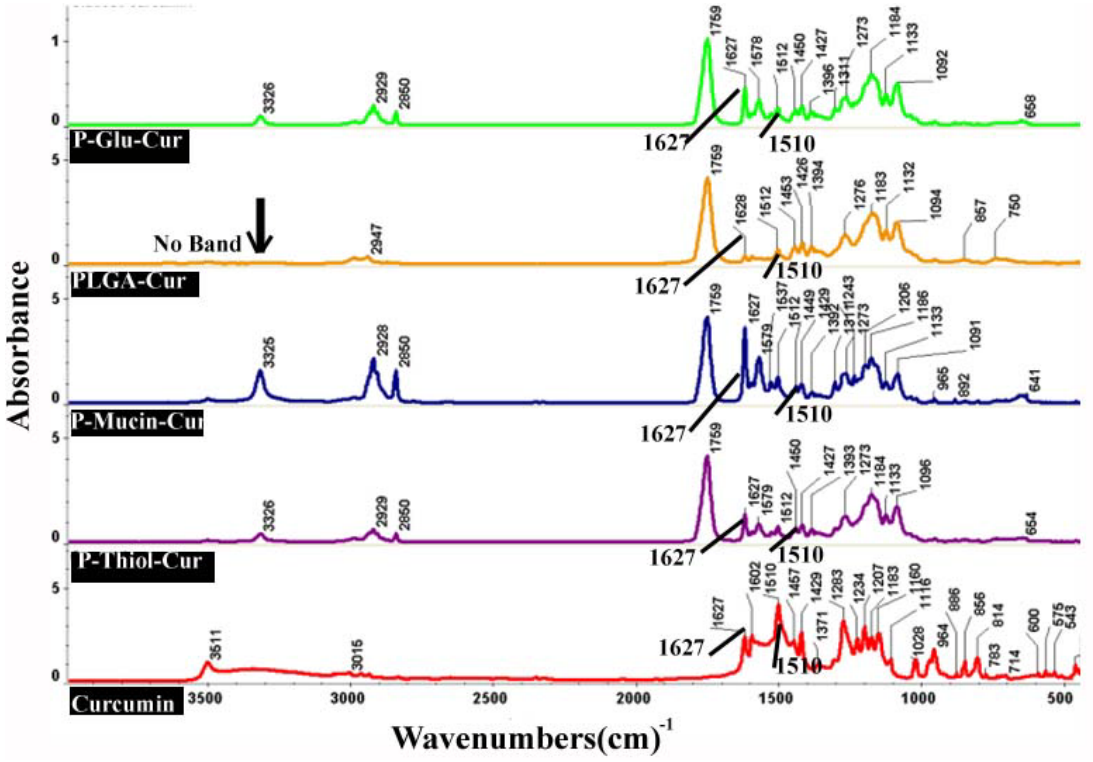

Figure 28B: FTIR spectra of Curcumin loaded PLGA and modified PLGA nanoparticles

The FTIR spectrum of betulinic acid loaded nanoparticles also displayed the dominant IR absorption bands at 1642cm^{-1}, 1043cm^{-1} and 885cm^{-}, similar to the pure drug as shown in Figure 28C.

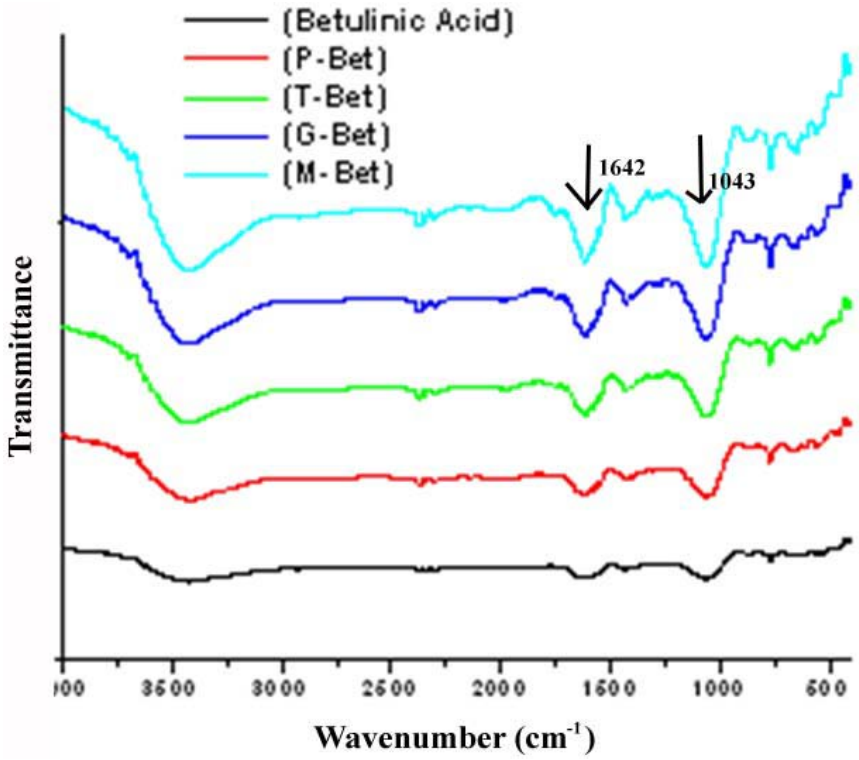

Figure 28 C: FTIR spectra of Betulinic Acid loaded PLGA and modified PLGA nanoparticles

4.6.2.4 UV Spectrometry

The chemical stability of the entrapped drugs, doxorubicin, curcumin and betulinic acid were analysed by comparing the UV-Visible absorbance spectra of pure drug and the drug released into the release medium, PBS. The doxorubicin based UV spectra of pure drug and the released drug from the modified and unmodified PLGA nanoparticles had recorded the absorption maxima at wavelength 485nm and 250nm as given in Figure 29A.

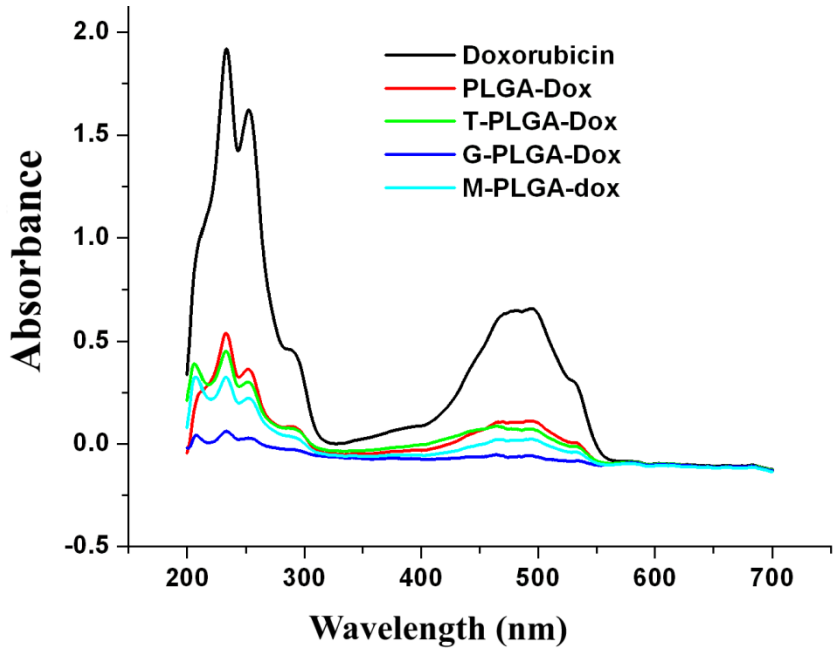

Figure 29 A: UV-Visible absorption spectra of Doxorubicin and the drug released from PLGA and modified PLGA nanoparticles

The Figure 29B also displays the UV spectrum of free and released curcumin that shows an absorbance peak at the wavelength, 415nm.

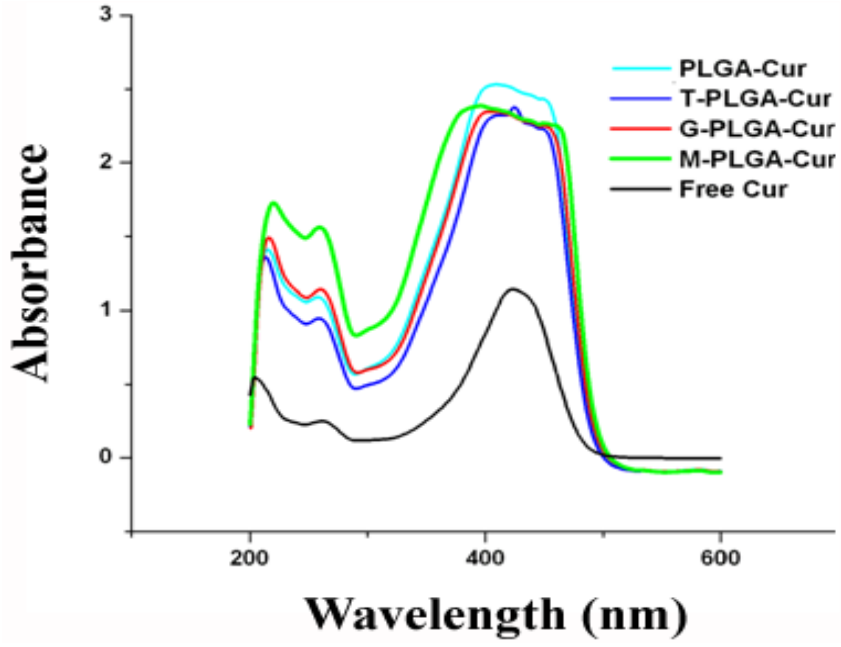

Figure 29 B: UV-Visible absorption spectra of Curcumin and the drug released from PLGA and modified PLGA nanoparticles.

In case of betulinic acid, the absorbance maximum is at 210nm for the pure and released forms, as shown in Fig 29 C.

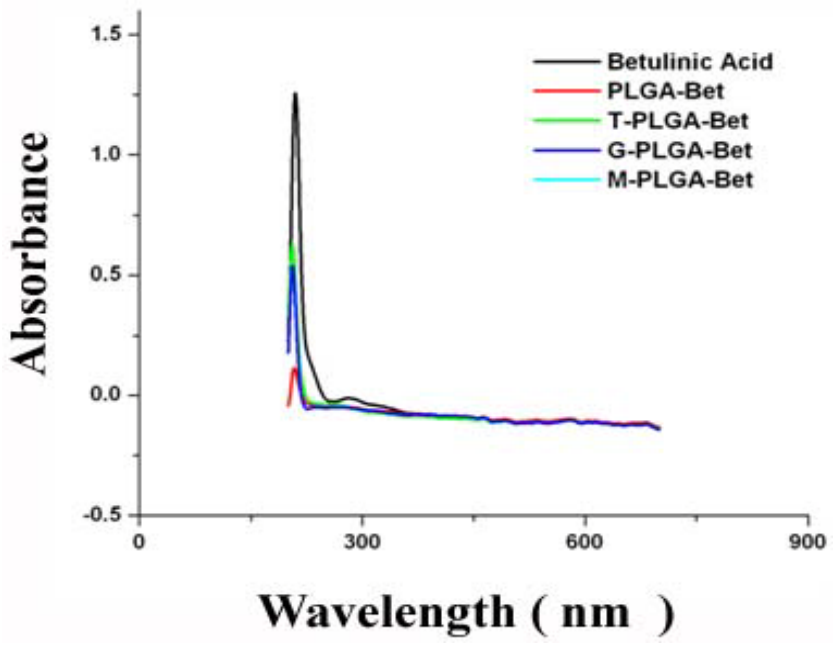

Figure 29 C: UV-Visible absorption spectra of Betulinic Acid and the drug released from PLGA and modified PLGA nanoparticles

4.6.2.5 Determination of the Encapsulation Efficiency

In order to quantify the amount of doxorubicin and curcumin encapsulated inside PLGA and modified PLGA nanoparticles, a known amount of loaded polymeric nanoparticles were dissolved in DMSO followed by fluorescent reading at • $_{ex}$/• $_{em}$=480nm/580nm for doxorubicin , absorbance at 420 nm and 210nm for curcumin and betulinic acid respectively. The results of encapsulation efficiency are provided in Table VII.

Table VII: Encapsulation Efficiency of drug encapsulated PLGA and modified PLGA nanoparticles

SAMPLE	ENCAPSULATION EFFICIENCY (%)
PLGA-Doxorubicin	29.6±2.3
PLGA-Thiol-Doxorubicin	29.06±2.6
PLGA-Glucose-Doxorubicin	9.25±3.9
PLGA-Mucin-Doxorubicin	23.12±3.1
PLGA-Curcumin	40.39± 12.9
PLGA-Thiol-Curcumin	36.93±3.8
PLGA-Glucose-Curcumin	29.72±3.1
PLGA-Mucin-Curcumin	43.98±1.5
PLGA-Betulinic Acid	83.09±15.8
PLGA-Thiol-Betulinic Acid	61.71±17
PLGA-Glucose-Betulinic Acid	52.40±21
PLGA-Mucin-Betulinic Acid	70.57±1.6

PLGA nanoparticles prepared by single emulsion technique with free doxorubicin exhibited an encapsulation efficiency of 29.6%. The encapsulation efficiency did not exceed this value for all the formulations studied, while it decreased to 9.25% and 23% following glucose and mucin based modifications. However, thiol based PLGA

modification helped in maintaining the encapsulation efficiency of doxorubicin at 29.06%.

In case of curcumin, PLGA nanoparticles demonstrated an encapsulation efficiency of 40%. Glucosylated PLGA nanoparticles had the lowest encapsulation of 29.3% and mucylated PLGA nanoparticles had the highest encapsulation of 43% followed by thiolated PLGA with 36% encapsulation efficiency for the drug, curcumin.

Interaction between the PLGA polymer and the hydrophobic drug betulinic acid produced an encapsulation efficiency of 83% for unmodified PLGA nanoparticles. Glucosylated PLGA nanoparticles exhibited the least encapsulation efficiency of 52%. This was followed by thiolated PLGA and mucylated PLGA nanoparticles in the increasing order of encapsulation efficiency with 61% and 70% respectively.

4.6.2.6 In Vitro Drug Release Kinetics

In order to evaluate the potential of employing modified and unmodified PLGA nanoparticles as carriers of the drugs, doxorubicin and curcumin, cumulative in vitro release behaviour of the respective drug loaded nanoparticles were studied for 5 days at 37°C in PBS.

In the present study, the cumulative release of doxorubicin corresponding to 10% was observed for PLGA nanoparticles prepared by single emulsion technique. Modifications based on glucose and mucin accelerated this burst effect to 18% and 14% respectively. Thiol based modification maintained the burst

release similar to unmodified PLGA nanoparticles. Following the burst release, thiolated, glucosylated, mucylated and unmodified PLGA nanoparticles did not provide much release for the time period of our study, 5 days, as provided in Figure 30A.

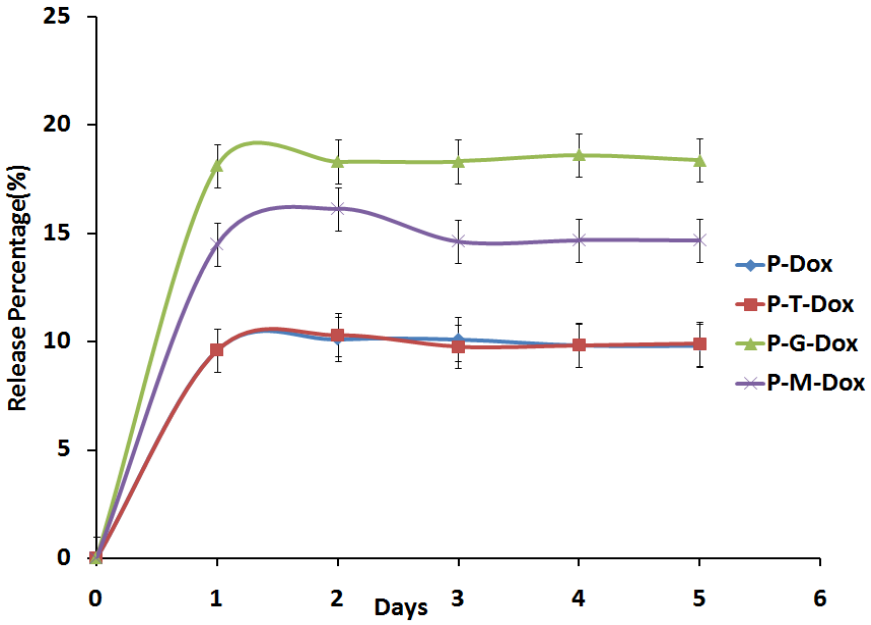

Figure 30 A: Release profile of doxorubicin from PLGA and modified PLGA nanoparticles. A uniform nanoparticle concentration of 20mg/ml in 3ml PBS was maintained.

A biphasic release pattern of curcumin was observed from PLGA and modified PLGA nanoparticles. Here, unmodified PLGA nanoparticles were found to produce a cumulative release of 15% of drug content. Hydrophilic modifications of the polymer with thiol, glucose and mucin moieties resulted in a higher release pattern with a cumulative percentage of 26%, 22% and 14% respectively as provided in Figure 30B.

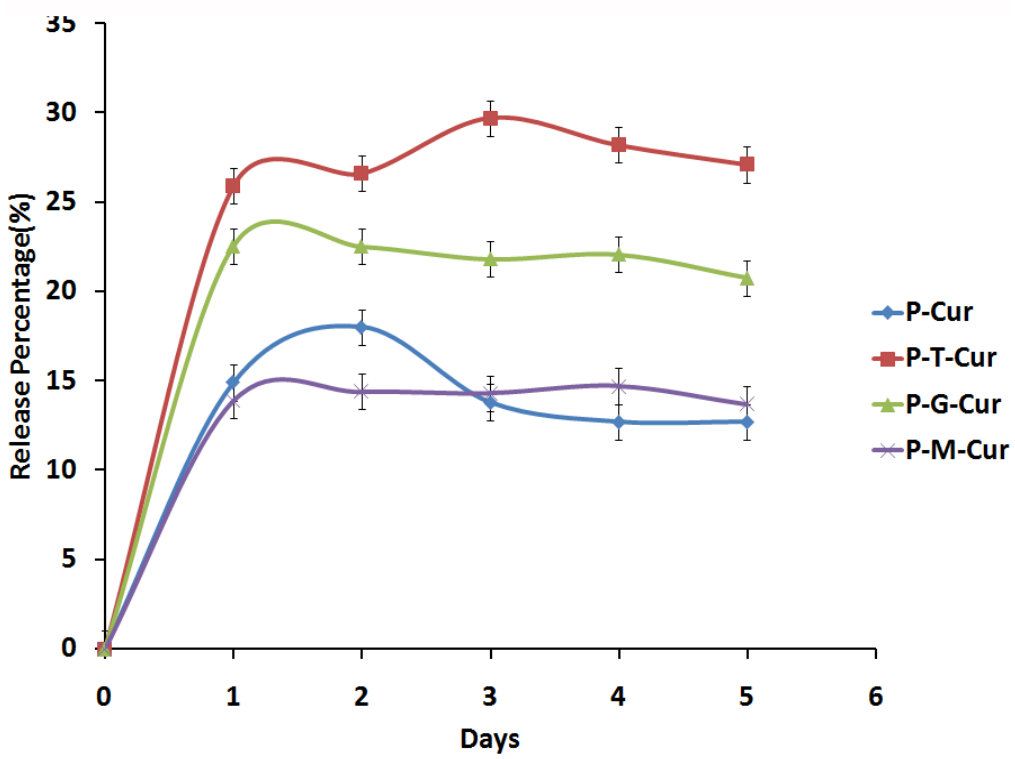

Figure 30 B: Release profile of curcumin from PLGA and modified PLGA nanoparticles. A uniform nanoparticle concentration of 20mg/ml in 3ml PBS was maintained.

4.6.3 Therapeutic Efficacy of Drug Loaded Nanoparticles at IN Vitro Conditions

4.6.3.1 Internalisation studies of drug loaded nanoparticles

The ability of doxorubicin and curcumin loaded PLGA and modified PLGA nanoparticles to be endocytosed by C6 cells were observed by confocal laser scanning microscopy. The photochemical properties of the drugs, doxorubicin and curcumin, were used to study the intracellular uptake of nanoparticles. The modified and unmodified PLGA nanoparticles exhibited significant uptake of drug loaded nanoparticles, in both the nuclei and cytoplasm as per the intensity of fluorescence signals from doxorubicin and curcumin.

To be specific, the intensity of doxorubicin fluorescence was highest with unmodified PLGA nanoparticles in regard to the higher encapsulation of the drug. Also, the glucosylated and mucylated PLGA nanoparticles emitted better fluorescence in comparison to thiolated PLGA nanoparticles, as given in

Figure 31 A.

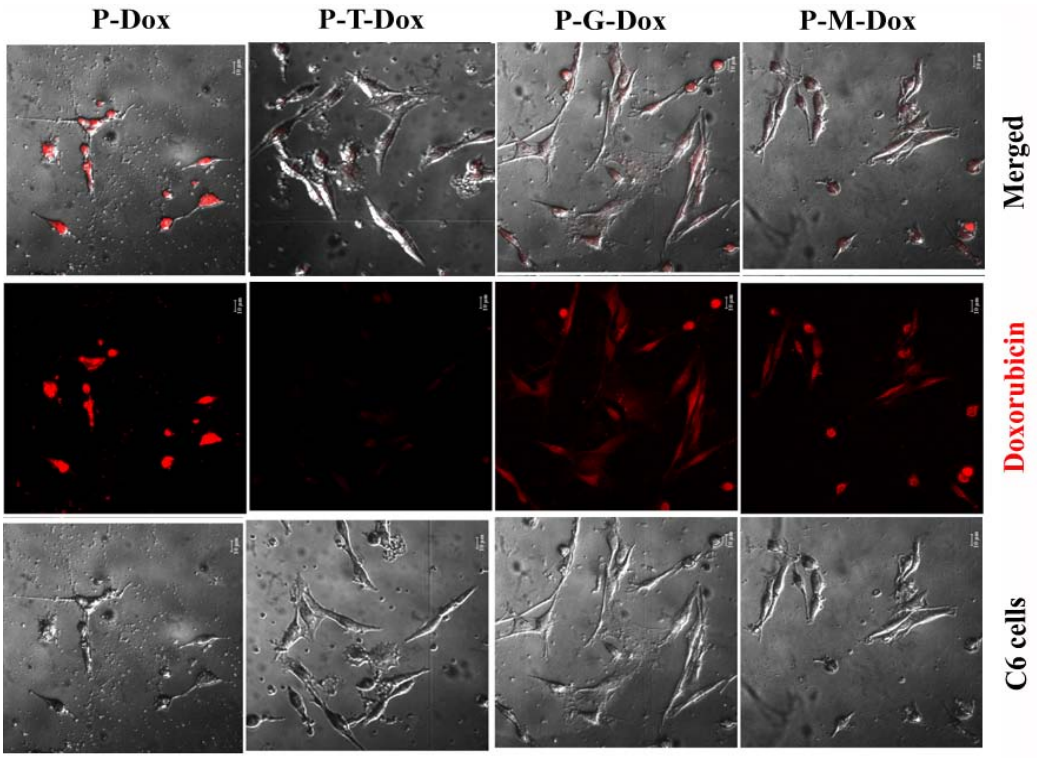

Figure 31 A: Uptake analysis of doxorubicin loaded PLGA and modified PLGA nanoparticles in C6 cell lines, following 3 h incubation. The nanoparticle concentration includes 67.8 µg, 69.6µg, 223.8µg & 87.6µg for P-Dox, P-T-Dox, P-G-Dox and P-M-Dox respectively.

In case of curcumin, the mucylated PLGA nanoparticles presented the maximum fluorescence intensity corresponding to the highest encapsulation efficiency. Thiolated PLGA nanoparticles also produced significant fluorescence when compared to unmodified PLGA nanoparticles. The florescent intensity was least in case of glucosylated PLGA nanoparticles as provided in

Figure 31 B.

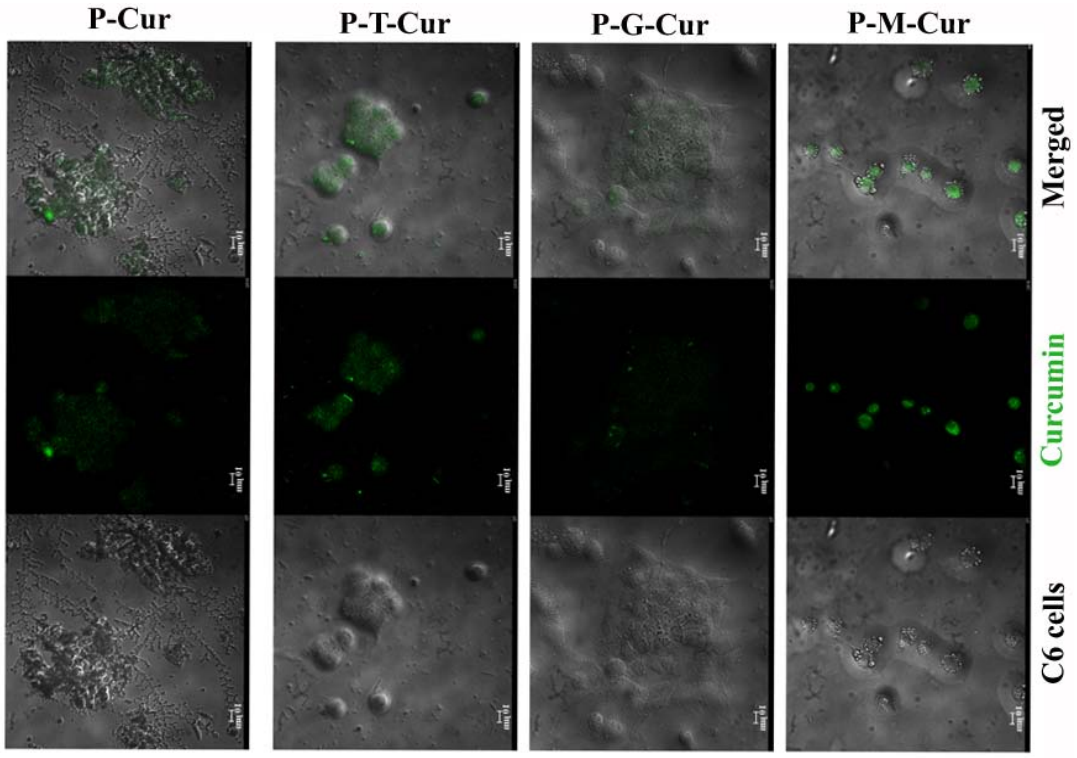

Figure 31 B: Uptake analysis of curcumin loaded PLGA and modified PLGA nanoparticles in C6 cell lines, following 3 h incubation. The nanoparticle concentration includes 201.3µg, 221.4µg, 272.7µg & 189.3µg for P-Dox, P-T-Dox, P-G-Dox and P-M-Dox respectively.

Hence the intensity of fluorescence of both the doxorubicin and curcumin loaded nanoparticles followed the pattern of drug encapsulation efficiency.

4.6.3.2 Cytotoxicity

The in vitro anticancer efficacy of free drugs and corresponding drug loaded nanoparticles containing different ranges of concentration of free drug was evaluated by MTT assay in C6 cell lines. The cellular cytotoxicity of doxorubicin, curcumin and betulinic acid was plotted on a linear scale as percentage toxicity versus drug concentration. The doxorubicin concentrations of

3.6µM, 5.5µM, 9µM and 13µM resulted in 26%, 30%, 40.1% and 43.5% cytotoxicity, respectively, with free drug. The PLGA nanoparticle encapsulation increased the cytotoxicity to 21%, 24%, 46.4% and 51.3% respectively for the above mentioned drug concentrations. Similarly, the modification had further enhanced the cytotoxicity to 27%, 34%, 55.6% and 65.6% respectively in case of drug encapsulated thiol modified PLGA nanoparticles. Also the mucin modification had rendered 38%, 40%, 66.8%, 68.1% cytotoxicity for the drug encapsulated PLGA nanoparticles respectively. Moreover the glucose based modification had produced the maximum cell death of doxorubicin encapsulated PLGA nanoparticles with 41%, 50%, 65.7% and 74.5% respectively for the above mentioned drug concentrations as understood from Figure 32 A.

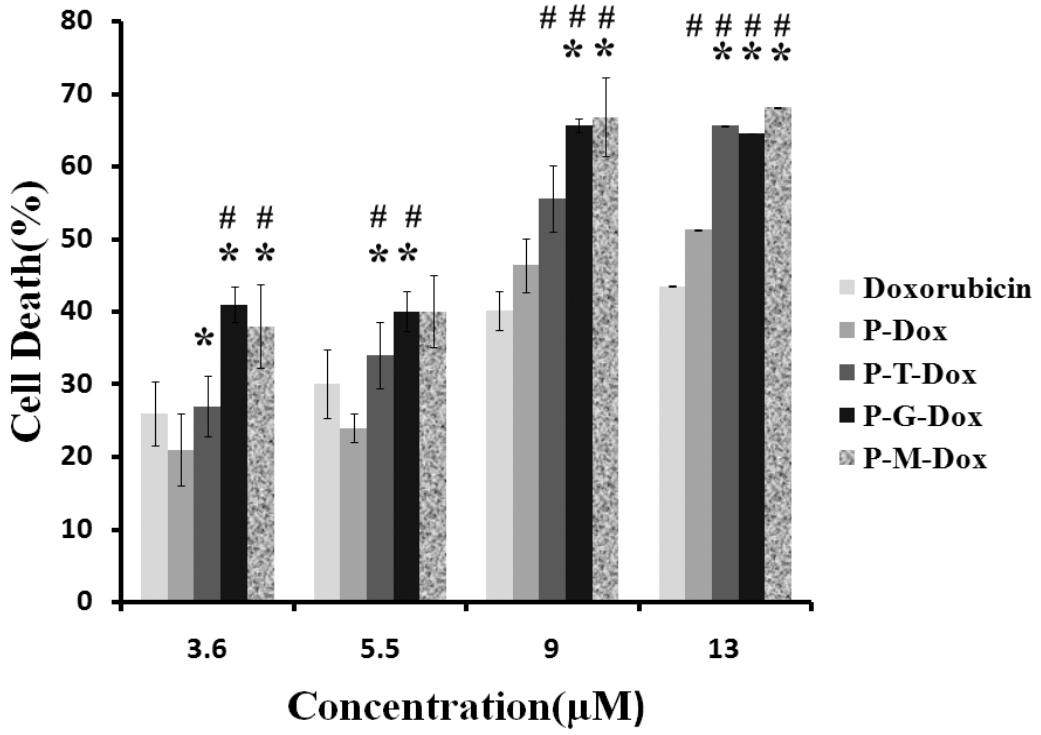

Figure 32 A: Cytotoxic profile of doxorubicin loaded PLGA and modified PLGA nanoparticles at specific drug concentrations, in C6 cell lines. *Statistically significant difference from corresponding PLGA group, p<0.05. # Statistically significant difference from corresponding free drug (Doxorubicin), p<0.05.

The curcumin concentrations of 20µM, 40µM, 60µM and 80µM produced 10%, 31.4%, 45% and 50% respective cytotoxicity for the free drug. The PLGA nanoparticle encapsulation increased the cytotoxicity to 22%, 46.1%, 62% and 65% respectively for the above mentioned drug concentrations. Similarly, the modification had further enhanced the cytotoxicity to 41%, 46%, 50% and 60% respectively in case of drug encapsulated glucose modified PLGA nanoparticles. Also the mucin based modification had rendered 32%, 41.6%, 57%, 65% cytotoxicity for the drug encapsulated PLGA nanoparticles respectively. Moreover, thiol modification produced the maximum cell death of curcumin encapsulated PLGA nanoparticles with 42%, 51%, 58.7% and 67% respectively for the above mentioned drug concentrations as shown in Figure 32 B.

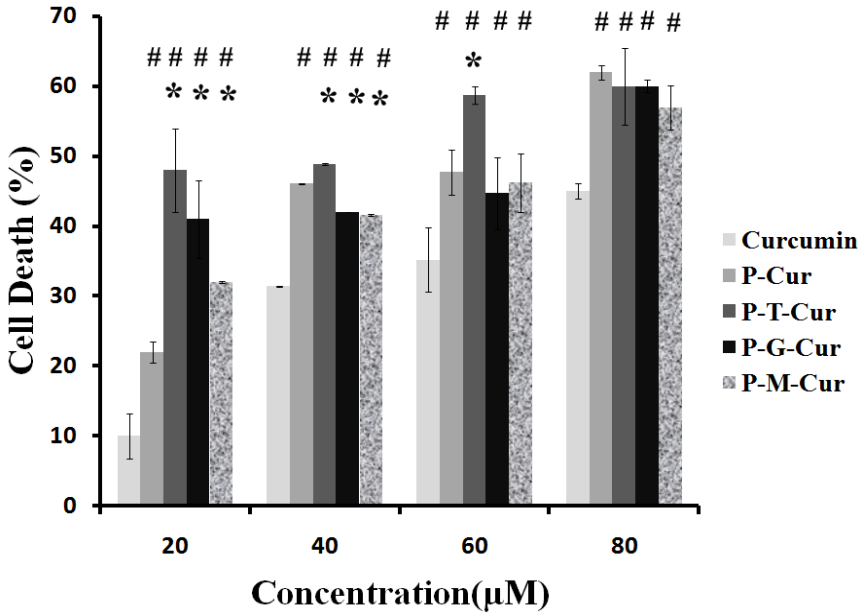

Figure 32 B: Cytotoxic profile of curcumin loaded PLGA and modified PLGA nanoparticles at specific drug concentrations, in C6 cell lines. * Statistically significant difference from corresponding unmodified PLGA group, p<0.05. # Statistically significant difference from the corresponding free drug (Curcumin), p<0.05.

The betulinic acid concentrations of 20µM, 40µM, 60µM and 80µM produced 2%, 28.9%, 44% and 46% respective cytotoxicity for the free drug. The PLGA nanoparticle encapsulation increased the cytotoxicity to 15%, 25.2%, 34.4% and 52% respectively for the above mentioned drug concentrations. Similarly, the modifications further enhanced the cytotoxicity to 14%, 38.7%, 42.4% and 58% respectively in case of drug encapsulated thiol modified PLGA nanoparticles. Glucose based modification had provided considerable cell death percentage of betulinic encapsulated PLGA nanoparticles with 13%, 38.2%, 45.8% and 55% respectively for the above mentioned drug concentrations. Also the mucin modification rendered 14%, 33.7%, 38% and 50% cytotoxicity for the drug encapsulated PLGA nanoparticles respectively, as provided in Figure 32 C.

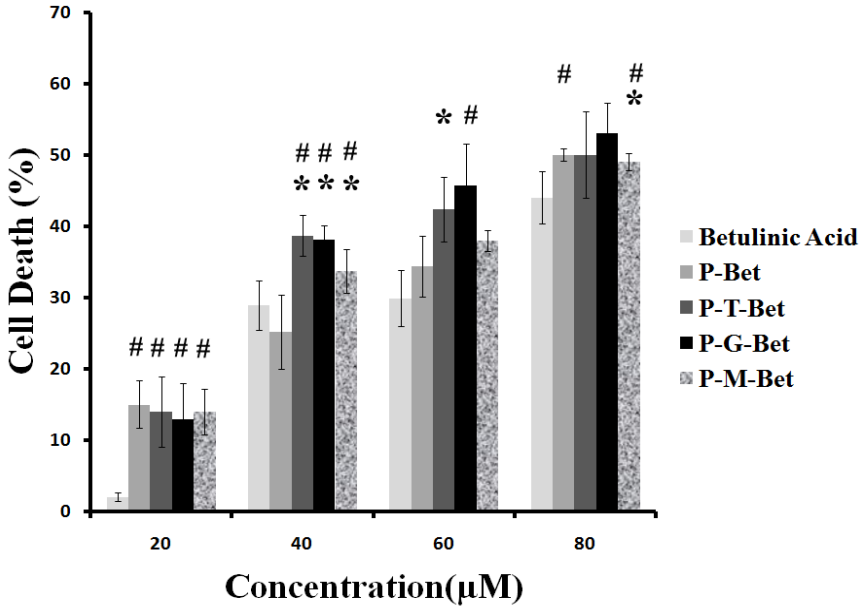

Figure 32 C: Cytotoxic profile of Betulinic Acid loaded PLGA and modified PLGA nanoparticles at specific drug concentrations, in C6 cell lines. * Statistically significant difference from corresponding unmodified PLGA group, p<0.05. # Statistically significant difference from the corresponding free drug (Betulinic Acid), p<0.05

4.6.3.3 Live Dead Assay

Further insight to the qualitative analysis of live and dead cells following the drug loaded nanoparticle interaction with the C6 cells demanded a LIVE/DEAD assay. Green cells denote live cells and red cells refer to dead cells. Control cells were not incubated with the nanoparticles. The significant increase in the dead cell population for the drug loaded samples when compared to free drugs, Doxorubicin, Curcumin and Betulinic Acid was visually evident from the LIVE DEAD images provided in Figure 33 A , 33 B and 33C respectively.

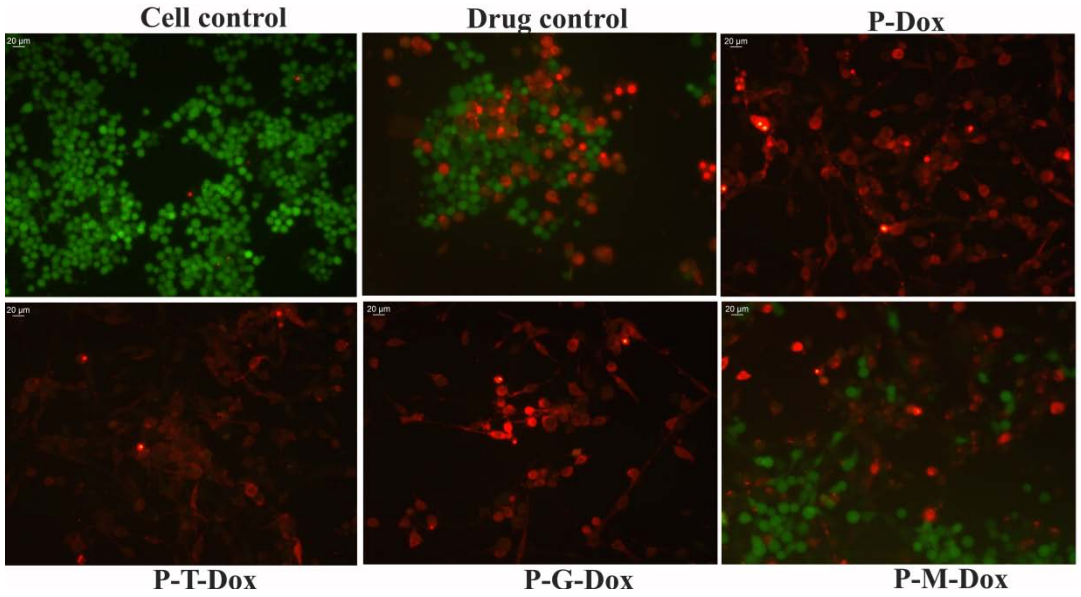

Figure 33 A: Live Dead Assay of Doxorubicin loaded PLGA and modified PLGA nanoparticles in C6 cell lines. The nanoparticle concentrations were in the range of 226µg, 232µg, 746µg and 291µg for P-Cur, P-T-Cur, P-G-Cur and P-M-Cur respectively for an equivalent concentration of 12.5µM of free doxorubicin. A 30h incubation period was followed.

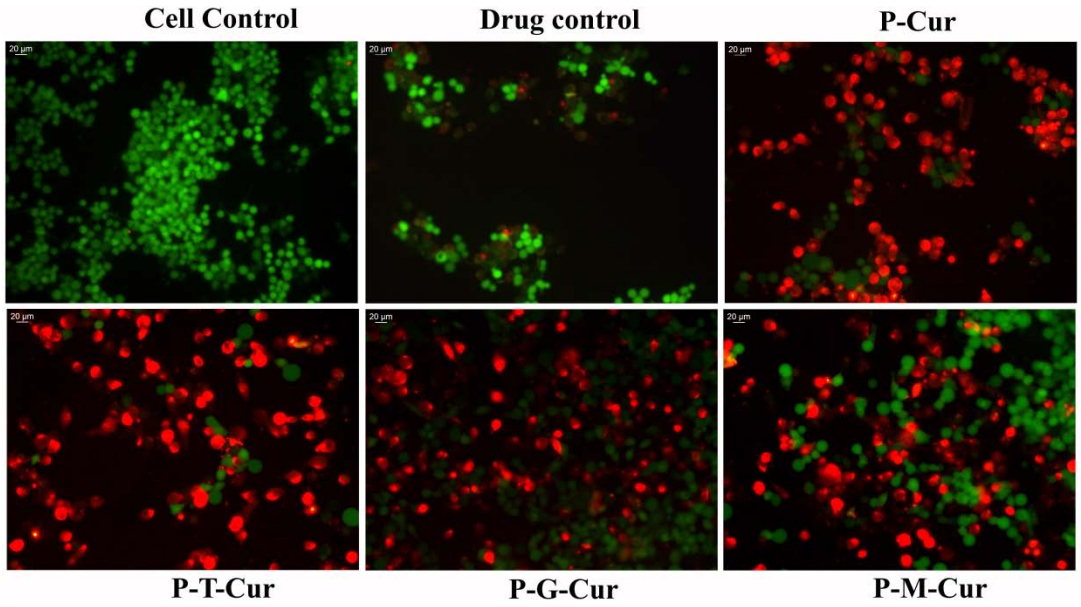

Figure 33 B: Live Dead Assay of Curucmin loaded PLGA and modified PLGA nanoparticles in C6 cell lines. The nanoparticle concentrations were in the range of 671µg, 738µg, 909µg and 631µg for P-Cur, P-T-Cur, P-G-Cur and P-M-Cur respectively for an equivalent concentration of 76µM of free curcumin. A 30h incubation period was followed.

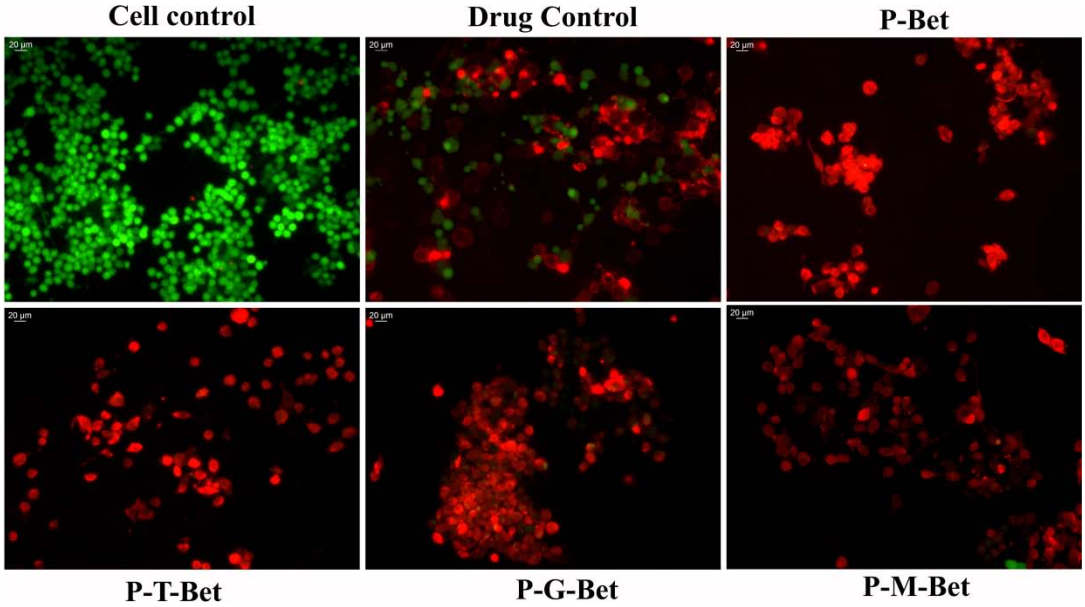

Figure 33 C: Live Dead Assay of Betulinic Acid loaded PLGA and modified PLGA nanoparticles in C6 cell lines. The nanoparticle concentrations were in the range of 462µg, 504µg, 629µg and 434µg for P-Cur, P-T-Cur, P-G-Cur and P-M-Cur respectively for an equivalent concentration of 41µM of free betulinic acid. A 30h incubation period was followed.

The specific drug concentration encapsulated within the modified and unmodified PLGA nanoparticles varied from 12.5 µM for doxorubicin to 76µM for curcumin and 41µM for betulinic acid respectively. Selection of the particular concentration of the drugs was based on the known cytotoxic value that could retain a monolayer of C6 cells within the 30 h incubation period. Lower or higher drug concentration resulted in inadequate or excessive cell death and was not suitable for imaging purpose. These results were in accordance with the MTT assay and suggest that PLGA nanoparticle encapsulation, with and without modification, have enhanced the toxic potential of the free drugs.

4.6.3.4 Quantification of Cell Death by Flow Cytometry

Flow cytometric results provided in Figure 34 A confirmed the percent cell death of free doxorubicin to be 45.1% alone that increased to the maximum with 98.9% following the glucosylated PLGA nanoparticle encapsulation.

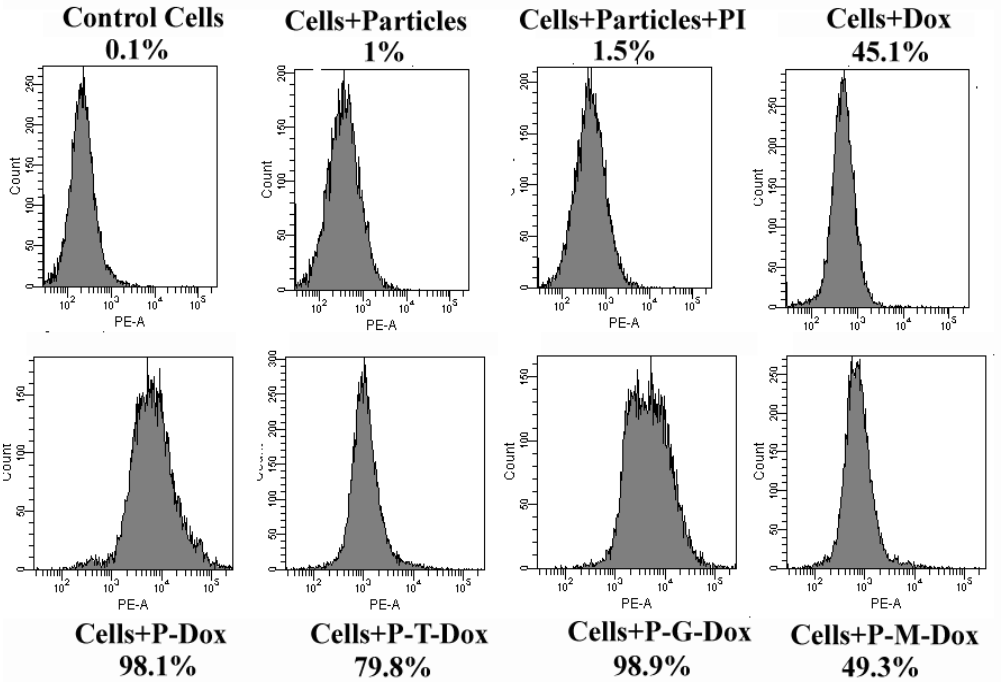

Figure 34 A: Cytotoxic potential of doxorubicin loaded PLGA and modified PLGA nanoparticles in C6 cell lines through flow cytometry. The nanoparticle concentrations were in the range of 226µg, 232µg, 746µg and 291µg for P-Cur, P-T-Cur, P-G-Cur and P-M-Cur respectively for an equivalent concentration of 12.5µM of free doxorubicin. A 30h incubation period was followed.

This was almost equal to the cell death exhibited by unmodified PLGA nanoparticles that registered a percentage of 98.1%. However, the rest of modifications produced comparatively lower toxic potential with a percentage of 79.8 % and 49.3% of cell death upon interaction with thiol and mucin modified PLGA nanoparticles respectively.

Figure 34 B demonstrate that when the free curcumin presented with a cell death of 21.7%, the unmodified, thiol, glucose and mucin modified PLGA nanoparticles induced 55.9%, 81.4%, 71.5% and 40.03% of cell death respectively.

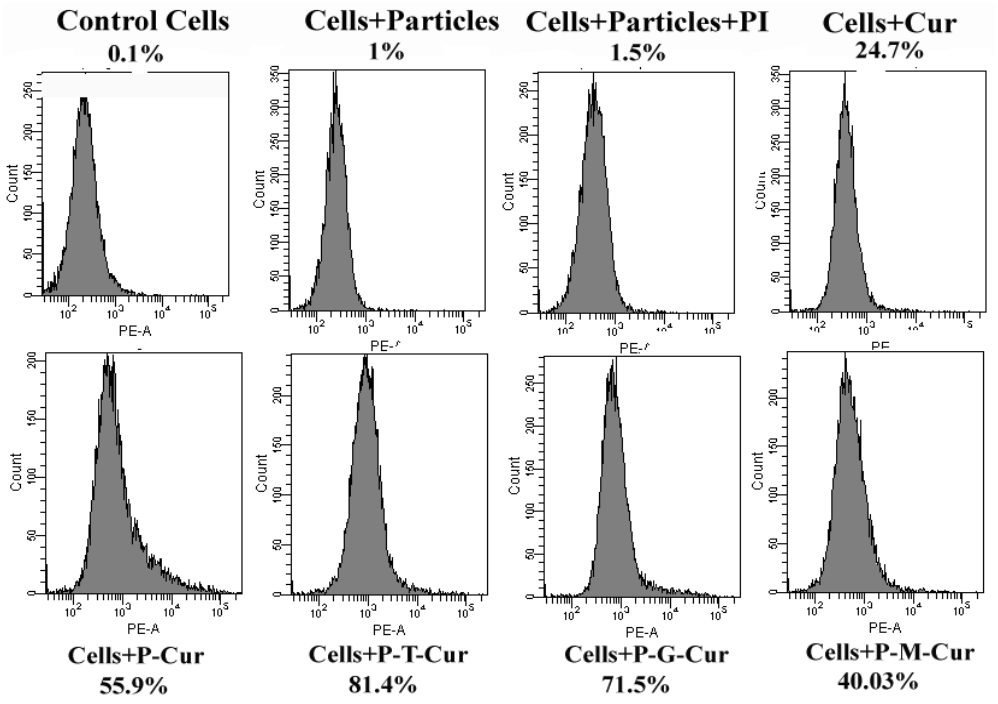

Figure 34 B: Cytotoxic potential of curcumin loaded PLGA and modified PLGA nanoparticles in C6 cell lines through flow cytometry. The nanoparticle concentrations were in the range of 671µg, 738µg, 909µg and 631µg for P-Cur, P-T-Cur, P-G-Cur and P-M-Cur respectively for an equivalent concentration of 76µM of free curcumin. A 30h incubation period was followed.

The free form of the drug, Betulinic acid induced a cell death of 21.7% as determined by flow cytometry. In comparison, unmodified PLGA nanoparticles marginally increased the cytotoxicity to 29.6% following encapsulation of Betulinic acid. Modification further enhanced the toxic potential of Betulinic acid to 46.6% with thiolation, 49.5% with glucosylation and 48.2% with mucylation respectively. The results provided in Figure 34 C summarise the quantitative evaluation of cytotoxic potential of free and encapsulated forms of betulinic acid.

All the conditions were similar as that of live dead assay including the concentration of individual drugs.

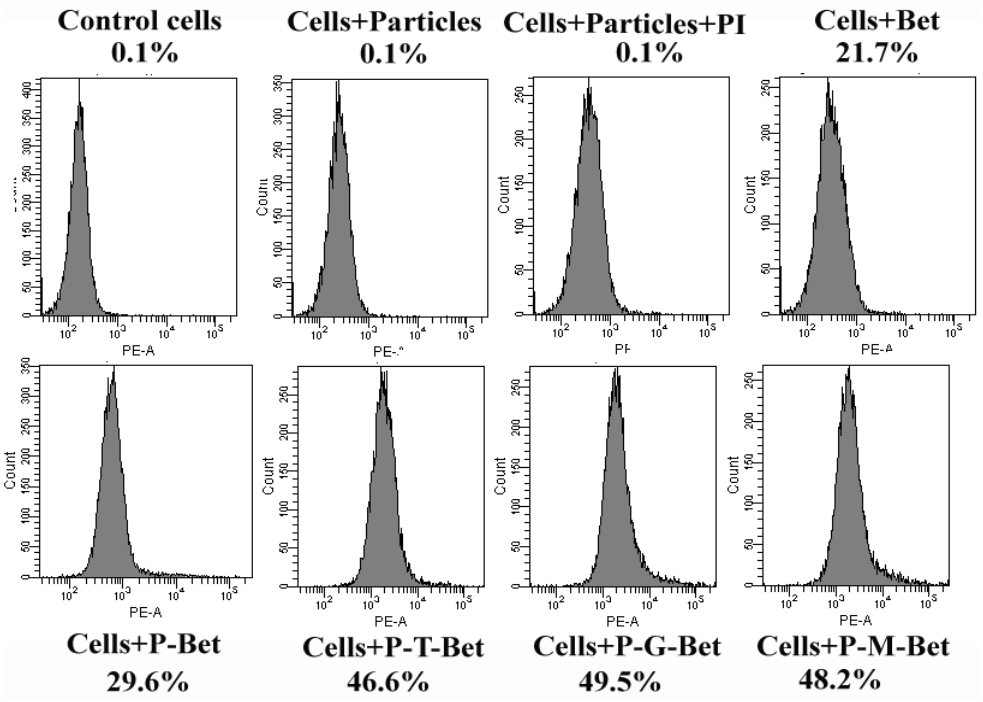

Figure 34 C: Cytotoxic potential of Betulinic Acid loaded PLGA and modified PLGA nanoparticles in C6 cell lines through flow cytometry. The nanoparticle concentrations were in the range of 462µg, 504µg, 629µg and 434µg for P-Cur, P-T-Cur, P-G-Cur and P-M-Cur respectively for an equivalent concentration of 41µM of free betulinic acid. A 30h incubation period was followed.

CHAPTER 5
DISCUSSION

CHAPTER 5 DISCUSSION

5.1 Synthesis of Thiol, Glucose and Mucin modified PLGA Polymers

Modification of hydrophobic polymers with hydrophilic moieties is an attractive strategy for designing long circulating drug carriers in the blood circulation. Oliveira et al has highlighted the importance of carbodiimide based conjugation chemistry for modifying the surface of aliphatic polyesters (Oliveira et al., 2013). In this sense, 1- ethyl-3-(3-dimethylaminopropyl) carbodiimide hydrochloride (EDC) and N, N'-dicyclohexylcarbodiimide (DCC) are widely used to form a covalent attachment via amide bond formation between one carboxylic acid and one amino group. As an example, Bondioli et al has activated the carboxylic groups of PLGA by means of an ester with NHS in the presence of DCC for decorating the nanoparticle surface with sialic acid, a key component of mucin molecule (Bondioli et al., 2010). Nobe et al has highlighted the advantages of using L-cysteine over cystamine moieties while introducing thiol functions on the PLA nanoparticle surface via carbodiimide chemistry (Nobs et al., 2003).

Yoon et al has introduced the disaccharide form of glucose, i.e, galactose on the surface of PLGA films through similar conjugation chemistry (Yoon et al., 2002). Similarly, Cheng et al has synthesised amphiphilic block copolymers of PLGA-PEG followed by conjugation to an amine terminated aptamer through the reaction with EDC-NHS (Chen et al., 2005) .

In concert with the above literature, the current investigation was initiated by surface modifying PLGA polymer with L-cysteine, glucosamine and mucin moieties respectively via carbodiimide conjugation chemistry (Thasneem et al., 2011), (Thasneem et al., 2013b) and (Thasneem et al., 2013a). To avoid an aqueous environment, PLGA was dissolved in an organic solvent such as DMF, prior to the conjugation reaction. The hydrophobic carbodiimide reagent, DCC, reacted with the carboxyl groups in PLGA to produce an amine reactive-O-acyl urea intermediate. In order to bypass the side reactions, NHS was added to transform the intermediate to its NHS ester derivative. This promoted the rapid reaction of the primary amine group present in L-cysteine, glucose amine and mucin with the PLGA -NHS ester derivative. The liberation of the NHS was accompanied with the formation of PLGA-thiol, PLGA-glucose and PLGA-mucin conjugate respectively, that was linked through an amide bond (Choi et al., 2003).

5.2 Characterisation of Modified PLGA Polymer

The modification was confirmed by DSC, FTIR, NMR and contact angle measurements.

5.2.1 Differential Scanning Calorimetry

DSC, as a thermal analysis technique was utilised to examine the physical property changes of PLGA following modifications when monitored against a range of temperature. The polyester PLGA with 50:50 lactide and glycolide content exhibited a glass transition below 50° C, without any distinct melting point and degraded at 270° C, as provided in Figure 12. The absence of melting point is expected as the copolymer PLGA with less than 85% glycolide content are

amorphous in nature. (Fouad et al., 2013). The DSC analysis is significant from the view point of drug delivery as any alteration to the glass transition temperature can lead to varied release pattern.

As sugars do not have a sharp melting point, the melting endotherm of glucose modified PLGA is quite broad. Hurtta et al has reported the melting range of glucose to be between 160°C -192°C (Hurtta et al., 2004). This correlates well with the additional enthalpy peak of glucose modified PLGA polymer. Analogous to the reported literature by Davies et al, mucin modified PLGA exhibits a broad endotherm without any distinct glass transition (Davies and Viney, 1998).

Hence following modifications, there is no obvious glass transition for PLGA polymer, a characteristic of the thermal degradation of thiol, glucose and mucin moieties respectively. Thus ensures that any further changes observed in the drug release pattern of the modified PLGA based nanoparticles are not due to bulk polymer changes. Additionally as the glass transition temperature of PLGA is a function of the molecular weight, modification results in no distinct molecular weight changes in the basic polymer. The additional enthalpy peak at 200°C relate to the thermodynamic variability of PLGA polymer following the respective modifications.

5.2.2. Fourier Transform Infrared Spectroscopy

The molecular fingerprint of PLGA polymer obtained by FTIR spectra display bands at 3500 cm^{-1} and 3459cm^{-1} corresponding to lactide and glycolide units, as provided in Figure 13. The confirmatory evidence for

modification of the PLGA polymer was provided by the characteristic peak shift of carboxylic groups of PLGA at 1746cm^{-1} to 1623 cm^{-1} upon amide bond formation following the respective thiol, glucose and mucin modifications and is analogous to the reported literature (Stevanovi• et al., 2008).

Komorov et al has established that the stretching vibrations of the thiol group (-SH) produce an absorption band around 2500 -2600cm^{-1} in the IR spectrum of L-Cysteine. However this specific peak for thiol group is not visible following modification of PLGA. One reason behind its disappearance could be the weak nature of the SH peak. In fact FTIR taken in the absorbance mode could have given more information regarding this SH peak. (Komarov et al., 2013).

Similarly, in case of glucosylated PLGA, the band at 1242 cm^{-1} and broad intensity stretching at 1637 cm^{-1} correspond to strong absorption of C-O group of glucosamine and carbonyl group of secondary amide linkage. This was in accordance with the reported literature by Mazare et al who characterised the C-O bond stretching of pyranosic D-glucose ring at about 1250cm^{-1} (Maz•re et al.)

The hydrophobic protein segment of mucin present in mucylated PLGA display strong IR absorbance at 1640cm^{-1}-1650 cm^{-1} and 1540 cm^{-1}-1550 cm^{-1} due to the amide I and amide II absorbance bands, respectively while the bands between 1100cm^{-1}–1200 cm^{-1} arises from the composite modes of vibration of the sugar ring. The bands at 1534 cm^{-1} corresponds to the C=O stretching vibration of sialic acid present on mucin backbone. The glycopeptide nature of mucin modification gets reflected by the bands at 1047 cm^{-1}, 1087 cm^{-1} and 1132 cm^{-1} respectively. The mucin characterisation was in accordance with the

reported literature by Johnson et al and Travo et al respectively (Travo et al., 2010), (Johnson et al., 2009).

5.2.3 Nuclear Magnetic Resonance

NMR spectroscopy was used to identify the characteristic functional groups of PLGA and modified PLGA nanoparticles. The basic chemical structure of PLGA polymer displayed overlapping doublets at 1.5ppm in the ^{1}H NMR spectra that correspond to the D and L-lactic acid repeat units, as provided in Figure 14. Further the lactic acid •CH and glycolic acid $=CH_2$ results in the multiplets at 5.2ppm and 4.8ppm respectively. The high complexity of the peaks could arise from the different D-lactic and L-lactic acid sequences in the polymer backbone (Li et al., 2001). Following carbodiimide based modification of PLGA polymer, the signal corresponding to the amide bond had appeared at 8ppm.

Rosen et al and Aryal et al has assigned the spectral peaks of L-cysteine at • 3.3 and • 2.4ppm to the protons attached to • and • carbons respectively (Rosen and Gu, 2011), (Aryal et al., 2006). In addition, Aryal et al has also mentioned the shifting of • carbon peak of cysteine to •2.6ppm with quantitative splitting following the conjugation to gold nanoparticles. Liu et al has determined that the anomeric protons of glucosamine appeared in the range of 5.3-4.5ppm (Liu et al., 2011). 1H NMR spectra of mucin by Patel et al has associated the sp^2 carbon spectra at 5.5ppm and of possible ketone functionality at signals around 2.8ppm-3 ppm (Patel et al., 2003).

Detailed analysis of the modified PLGA using ^{1}H NMR analogous to the above literature has confirmed the successful incorporation of the modifier in to the copolymer, as was evident from the thiol proton resonance around

2.6 ppm, glucosamine hydroxyl proton resonance around 5.3ppm-4.5ppm and mucin responsive protons in the region of spectrum at 5.5 ppm 2.8ppm-3.0ppm respectively.

5.2.4 Contact Angle Measurement

Surface wettability (i.e, hydrophilic or hydrophobic) has been traditionally determined by water contact angles (•) according to the definition of hydrophobic surfaces as having a water contact angle (•) greater than 65°. Prior to the modification of PLGA polymer, contact angle was measured to confirm the difference in the hydrophobicity following thiolation, glucosylation and mucylation, as provided in Table IV. However, the probability of water intrusion into the voids present on the polymer film formed on the coverslips cannot be avoided. Hence, these results are not to be considered as an absolute value, but rather a measure of relative wettability, that can just help to compare the degree of hydrophilisation on the parent polymer PLGA following the modification with different moieties.

The water contact angle confirmed that the PLGA is more hydrophobic before the modification. According to He et al, the water contact angle of PLGA was significantly reduced following the introduction of hydrophilic groups (He et al., 2013). This led us to assume that the contact angle decreases in proportion to surface hydrophilicity. Consequently, glucose based modification with the lowest contact angle has rendered the polymer with maximum hydrophilicity followed by thiolation and mucylation respectively. Herrweth et al has highlighted the importance of the interaction of water molecules with a surface in determining the extent of plasma protein adsorption and blood compatibility (Herrwerth et al., 2003). It is possible that

the significantly reduced interfacial free energy of a highly hydrophilic surface coating may orient the water molecules more favourably around the structure to form a 'cloud' of hydrated layer as indicated by the reduced contact angle.

5.3 Synthesis of Nanoparticles

5.3.1 Synthesis of PLGA and modified PLGA based nanoparticles

In this study, PLGA with a 50:50 poly-lactide and poly-glycolide composition (Resomer RG 502 H) was chosen for nanoparticle synthesis owing to its established biodegradability and the relative ease of forming colloidal nanoparticle suspensions. Among the different methods for nanoparticle preparation, a modified solvent evaporation technique was preferred. During solvent evaporation technique, majority of the modifying moieties project towards the aqueous phase and the long polymer chains get buried under inside the nanoparticle core. This is based on the hydrophilic-hydrophobic interactions happening in an aqueous environment. This concept strengthens the claim of surface modification and the formulated PLGA nanoparticles are most suggestive to be surface modified.

The choice of the organic phase solvent and the stabiliser has to be proper as it a determining factor of the particle size formed. In this method, the organic phase consisting of PLGA or modified PLGA polymer in ethyl acetate provided the oil phase and the 0.2% pluronic aqueous solution serves as the water phase in the oil in water emulsion. Physical sonication induces the reduction in size of nano droplets in this emulsion. The introduction of water into the emulsion destabilises the thermodynamic equilibrium between the organic solvent phase containing PLGA and the aqueous phase containing stabiliser causing the organic phase to diffuse to the

external aqueous phase. Pluronic F-68, the non toxic surfactant in the external continuous phase, provided suitable stability to the emulsion droplets formed by preventing the macroscopic phase separation. The mechanism of nanoparticle formation is based on the evaporation of organic solvent from the emulsion droplets followed by precipitation of polymer as nanoparticles in the presence of stabiliser at the organic –aqueous liquid interface. Desgouilles et al has investigated about the nanoparticle formation by solvent evaporation technique at the molecular and supra molecular level (Desgouilles et al., 2003). Accordingly, in case of poly esters, a single or few emulsion droplets produced a single nanoparticle. Usually the solvent evaporation continued overnight to ensure the complete evaporation of organic solvent, ethyl acetate. In reference to the formulation of nanoparticles by Fields et al centrifugation was performed at 9500 rpm instead of 12,000 rpm to avoid particle aggregation (Fields et al., 2012).

Specifically, the equilibrium conformation of the polymer chains in the solvent following sonication and the organic phase viscosity or in simple words, the polymer/solvent pair is the determining factor on the final nanoparticle architecture.

5.3.2 Synthesis of Fluorescent Labelled Nanoparticles

In the present work PLGA nanoparticle loaded with rhodamine were prepared via solvent evaporation technique as tools for the investigation of nanoparticle- cell interaction and uptake as PLGA and the modified polymers were inherently nonfluorescent in nature. A minimal loading of rhodamine was only required for the nanoparticles used in this study because of the high

quantum yield and photostability of the dye, rhodamine. Earlier studies by Betancourt et al have confirmed the identical physicochemical properties of rhodamine loaded and plain PLGA nanoparticles, in particular to size, morphology and surface chemistry (Betancourt et al., 2009). Moreover, release studies revealed that RHO nanoparticles were optimal for imaging studies because the agent is released at a very slow rate in a pH-dependent manner as a result of its hydrophobicity and favourable interactions with the polymer. This ensures the utility of the rhodamine encapsulated particles for *in vitro* studies by allowing the precise tracking of nanoparticles instead of the released dye.

5.4 Characterisation of Nanoparticles

Accurate characterisation of synthesised nanoparticles becomes essential for correlating a particular physicochemical property of a nanoparticle to specific biological response.

5.4.1 Dynamic Light Scattering

Among the multitude of physicochemical and physiological factors that control the lifespan and clearance of intravenously injected nano particulates, size plays a prominent role. Nanoparticle size can influence the composition and thickness of protein corona and may modulate cellular interactions. The optimum size of nanoparticle can vary depending on the cell type and particle surface properties. Generally, the critical size of nanoparticle for efficient cellular uptake and circulation half time has been optimized around 100-200nm (Hillaireau and Couvreur, 2009), (Liu et al., 2012a). Dynamic Light Scattering is a simple and

quick technique for measuring nanoparticle size in suspension or biological media. Nanoparticles in suspension produce scattering intensity fluctuations due to Brownian motion. This is the basis of DLS which correlates the diffusion coefficient to the particle size via the Stokes Einstein equation. The size and dispersity index against volume distribution was presented in the Table V as it provides the complete information regarding the size variations of all the particles present in the sampling medium. The hydrodynamic diameter measured represents the dimension of the core plus shell of the nanoparticle including the layer of surface bound solvent. In the present study, all the synthesised PLGA nanoparticles exhibited a particle diameter ranging from 100-150nm and narrow dispersity index, suitable to obtain an effective intracellular uptake. Song et al has attributed the small size of PLGA nanoparticles formed during solvent diffusion technique to the partially water miscible nature of ethyl acetate that lowers the interfacial tension between aqueous and organic phases (Song et al., 2006). The three different modifications have not induced drastic variations in the PLGA based nanoparticles size. This is surprising as the long brush model structure of mucin moiety that can tower above the nanoparticle is very suggestive of increasing the hydrodynamic size. The maintenance of PLGA nanoparticle size after mucin modification can be explained in terms of the interactions among the mucin polymer chains. Mucin (8–14 M Da) consist of a core apoprotein in which polyanionic glycosylated blocks containing sialic and sulfate ester terminals alternate periodically with the hydrophobic cysteine-rich blocks that resembles the typical architecture of synthetic amphiphilic brush multiblock copolymers. This gives mucin a broad potential for surfactancy, folding and remaining in a condensed phase. Hence compacts and constrains the mucin chains

within a drastically limited volume as reported by Verdugo et al (Verdugo, 2012). The mean droplet size of the emulsion formed during solvent evaporation technique is another major factor that determines the size of nanoparticles formed. According to Shi et al, the surfactancy of mucin plays an important role in yielding the smallest possible particle size by reducing the surface tension at the oil and water interphase so that stabilizes the formed nanoemulsion and prevents particle aggregation (Shi et al., 1999). Hence, the block co-polymeric and condensed structure of mucin polymeric chains together plays an important role in minimizing the size of PLGA nanoparticles.

5.4.2 Atomic Force Microscopy & Transmission Electron Microscopy

The surface morphology and size of synthesised PLGA and modified PLGA nanoparticles were also characterised by AFM & electron microscopy as they provide accurate size measurements than those obtained via DLS. In Figure 15, glucose modified PLGA nanoparticles become an exception as the size provided in TEM data doesn't correlate with the DLS measurement provided in Table V. This can be explained in terms of the broader dispersity index of glucose modified particles which is most suggestive of the presence of multiple sized nanoparticle populations in the sampling medium. Surface morphology of the prepared nanoparticles becomes crucial in the context of different cellular functions including phagocytosis and viability. Spherical particles are considered to be long circulating in comparison to rod shapes. Also, the lower membrane wrapping time required for spherical nanoparticles enhance its uptake and targetability (Verma and Stellacci, 2010). Generally, solvent evaporation technique produces spherical nanoparticles under different solvent systems as observed by Song et al using AFM

images (Song et al., 2006). It was also observed that partially water soluble solvents like ethyl acetate provided nanoparticles in the size range of ˜100nm.

AFM gave clear two or three dimensional morphological images of PLGA and modified PLGA nanoparticles at high resolution on a nanometre scale that revealed spherical structure that correlated well with the DLS data. The TEM images obtained displayed discrete spherical outline and monodisperse size distribution. Interestingly mucin modified PLGA nanoparticles were particularly smaller in TEM when compared to its DLS data. Huang et al has reasoned out that as the nanoparticles exist in a dehydrated state in TEM measurements, the size could be comparatively smaller to the hydrated size analysis of DLS (Huang et al., 2014). However, the adhesive nature of mucin could result in the spreading nature of mucin modified PLGA nanoparticles on the cover slips and hence a slight increase in size is observed in case of AFM studies.

5.5 Blood Compatibility Analysis

The compatibility of nanoparticles in blood stream becomes important as the blood constituents are capable of rendering the nanomedicine inactive following immunological interactions. The significance of modification of nanoparticles becomes most predominant in the blood stream as RES rapidly cleared particles that lacked surface modification (Gref et al., 1995a). Hence the preclinical evaluation of the hemocompatibility of nanoparticles must include studies of plasma protein adsorption, complement activation, platelet activation, and hemolysis and blood cell interactions (Dobrovolskaia et al., 2008b).

5.5.1 Plasma Protein Adsorption Studies

Once nanoparticle come in contact with blood, a primary nano bio interface get established with the non specific plasma protein adsorption by the so called protein-corona effect. Adsorption of plasma proteins is a multi step process driven by the free energy generated at the liquid-solid interface and is not mechanistically well defined. Probably, a combination of van der Waals attraction, electrostatic interactions along with hydrogen bonding defines the dynamics of adsorption. Plasma proteins upon adsorption on surfaces undergo conformational alterations and can further promote hydrophobic interactions. The composition and conformation of this plasma protein corona that exposes inflammatory epitopes following the conformational alterations of adsorbed proteins can be the decisive factor driving either the biocompatible or bio adverse response of an organism to nanoparticle exposure. In general, non specific protein adsorption from biological milieu must be minimised.

Besseling has emphasised on a molecular level understanding of the surface properties that prevent opsonisation. He has suggested the influence of chemical properties of a surface in the state of hydration and the resulting dominance of attractive or repulsive forces following the surface interactions (Besseling, 1997). Grunze and de Gennes had separately discussed the importance of the conformational flexibility of surface bound groups in mediating their resistance to opsonisation or plasma protein adsorption (Ostuni et al., 2001) Considering this mediation of synergy between nanotherapeutics and plasma proteins, we have prioritised on the modification of PLGA nanoparticles with thiol, glucose and mucin moieties

In order to maintain the stability of nanoparticles in systemic circulation or in any flow conditions, it becomes necessary to introduce repulsive interactions capable of overcoming the attractive van der waals forces. It is a known fact that neutral or negatively charged surfaces in absence of hydrogen bond donors can minimise the plasma protein adsorption (Holmlin et al., 2001). The polar nature of amino acid cysteine that possesses a negatively charged SH group can promote repulsive interactions when approached by the negatively charged plasma proteins. Importantly, the thiol side chain of Cysteine serves as a nucleophile or a hydrogen bond acceptor and hence imparts the PLGA nanoparticles with the molecular level characteristics required to resist non specific plasma protein adsorption (Lee et al., 2006), as depicted in Figure 17.

The carbohydrate modified surfaces have a unique way of repelling protein adsorption. The presence of multiple hydroxyl groups of glucosamine deter non specific plasma protein adsorption without contributing to the increase in hydrodynamic size. Lindblad et al has highlighted the protein repelling properties of hydroxyl groups owing to its charge neutrality and hydrophilic nature (Lindblad et al., 1997). Grunze et al has also specified that the uncharged carbohydrates can orient upto three layers of water (Ostuni et al., 2001). Hence repulsion dominates when glucose modified PLGA nanoparticles approach each other or the various proteins present in plasma.

Kesimer et al has explained that the glycosylated portions of the mucin are protruded in to the aqueous medium and forms highly hydrophilic, hydrated monolayers around the PLGA nanoparticle surface with around 95% of adsorbed mass being water

(Kesimer et al., 2010). Such favourable interactions with water can limit the access of major opsonins like fibrinogen, globulin, complement proteins and mononuclear phagocytic cells towards the mucin modified PLGA nanoparticle surface.

Hence the reduced opsonisation following modification directly implies the escape of PLGA nanoparticles from the reticuloendothelial sequestration which is triggered by the receptor mediated recognition of the adsorbed plasma proteins.

5.5.2 Single Protein Adsorption Studies

The primary goal of modification of PLGA nanoparticles is to control the amount and composition of plasma protein adsorption as well as to minimise the conformational alteration of individual proteins, as provided in Figure 18.

Albumin is a well known anti inflammatory or passivating protein whose adsorption can promote the blood compatibility of surfaces. While fibrinogen adsorption has a major role in weakening the blood compatibility as it enhances the surface induced thrombosis. Following 1 h of adsorption, fibrinogen changes its secondary structure (amide 1 band) and exposes multiple receptor induced binding sites. A specific receptor for the fibrinogen molecule, the glycoprotein complex II B-IIIA (GP-IIB-IIIA) is present on the platelet membrane. Fibrinogen and globulin proteins are known activators of platelets through the formation of globulin/ fibrinogen-GP IIB-IIIA complexes. In addition, the immunoglobulins are extreme complement activators (Dufort et al., 2012).

On a closer inspection of the adsorption pattern on these nanoparticles via single protein adsorption studies, we find that the PLGA system demonstrated reduced adsorption of major plasma proteins ,specifically fibrinogen, and γ-globulins following modification.

Loscalzo et al has specified the ability of low molecular weight thiols such as cysteine in reducing fibrinogen adsorption along with the inhibition of thrombin catalysed fibrin polymerisation via transnitrosylation reaction (Loscalzo, 1992). Computer simulation experiments of Thevenot et al has discussed the ability of water molecules in successfully competing with fibrinogen over adsorption to hydroxyl modified surfaces (Thevenot et al., 2008). Also, an optimum concentration of hydroxyl groups can promote the passive albumin binding over fibrinogen, as explained by Martin et al (Martins et al., 2003). Studies by Sandberg et al has discussed the significance of mucin s loop and tail surface conformation in preventing fibrinogen and globulin adsorption cum denaturation on biomaterials surfaces (Sandberg et al., 2009b). These reports strengthen the reduced adsorption pattern of fibrinogen and globulin following thiol, glucose and mucin based modification of PLGA nanoparticles.

Another observation is that the glucose modified nanoparticles that displayed minimal protein adsorption from plasma was not effective enough to prevent adsorption form single protein solutions. This can be explained in terms of Vroman effect which can result in varied protein adsorption patterns with plasma and single protein solutions. Based on this effect, the rapidly adsorbing fibrinogen, immunoglobulin and albumin are replaced in second step by apolipoproteins and coagulation factors. Single protein adsorption study lack this exchange of proteins

Hence there is lower adsorption of fibrinogen and immunoglobulin in plasma incubated samples when compared to single protein incubated samples.

5.5.3 Complement Activation Analysis

5.5.3.1 Complement Protein C3 Nephelometry

The protein adsorption has effects beyond opsonisation as it initiates the blood clotting cascade leading to fibrin formation and anaphylaxis because of complement activation. Particular attention should be paid to complement system, as it activation products prime the nanoparticle surface for interaction with a plethora of macrophage complement receptors as well as platelets and erythrocytes. Drug delivery system capable of inducing a strong activation of complement are quite easily recognized by the MPS, while one with lower complement activation may have a prolonged circulation in the blood stream. The complement system, which is a part of the innate immune system, is largely devoted for the recognition and clearance of foreign materials. Presence of any foreign surface in contact with blood can initiate the complement activation via the alternative pathway. Activation could be triggered by the conformational alterations occurring in adsorbed immunoglobulins, C1 or C4 that results in the deposition of C3 and subsequent cleavage to C3a and C3b fragments. In vitro evaluation of complement activation induced by particles is a convenient technique to predict the in vivo fate after intravenous administration. As an indication of complement activation, quantifying the extent of cleavage of complement protein C3, the central component of complement system becomes important (Andersson et al., 2005).

Basically, the half lives of C3 and TCC in plasma are in the range of few hours and are readily detectable. Comparatively, TCC is more stable under invitro conditions. In order to obtain more clarity in the analysis of complement activation, the present work has quantified both the C3 and TCC complexes. Also, plasma was collected in EDTA containing vacutainers to avoid minimal complement activation during blood withdrawal followed by introduction of calcium and magnesium based divalent ions for ensuring proper complement functioning.

The collected plasma was immediately quantified without any delay or storage within 30 minutes to avoid the probability of any in vitro degradation of the complement components.

Surface properties/charge plays a major role in the complement activation mechanism induced by the polymeric nanoparticles. Likewise, the presence of negatively charged carboxyl groups of PLGA can promote the complement mediated compatibility of nanoparticle surface to some extend via promoting high affinity association between bound C3b and factor H. This results in the inactivation of C3b by Factor I and the termination of the complement cascade propagation (Gorbet and Sefton, 2004). However, recent studies by Ceonzo et al had suggested that the hydrolysis of biocompatible polymers like poly glycolic acid activated the classical and alternative pathways of complement activation following degradation (Ceonzo et al., 2006). Moreover, the inherent hydrophobicity of PLGA surface invite activated complement factor deposition that necessitates effective modification strategies for minimizing complement activation.

The complement activation studies as shown in Figure 19 specified that the PLGA modified with cysteine successfully reduced the activation cascade under in vitro experimental conditions as per the concentration of C3 measured by nephelometry. This is in accordance with the findings of Liping et al that specified the significance of L-Cysteine coated surfaces in mediating minimal complement activation and inflammatory responses (Tang et al., 1998).

Monosaccharides like glucosamine predominate over the conventional hydrophilic and inert surface coatings in terms of blocking the complement activation without compromising the nanoparticle mediated targetability. The molecular mechanism behind the reduction of the activation of complement receptor Type 3 by the glucosamine can be plotted back to the effective suppression of the phosphorylation of p38 MAPK, (a serine/threonine kinase belonging to the family of MAPKs) (Hua et al., 2002). Hair et al has further manifested the role of hyperglycaemic conditions in preventing the activation of complement C3 to functionally active forms (Hair et al., 2012). Bernacca et al has also established the significance of glucosamine in reducing the biomaterial mediated complement C3 activation over other modifications such as heparin, taurine and PEO (Bernacca et al., 1998).

The glycoprotein layer of mucin, rich in sialic acid is said to suppress antigenicity and act as an immune barrier for cells. Sialic acid mediated masking of inflammatory epitopes which inhibit complement activation is a common strategy adopted by pathogens to reduce immunogenicity. Earlier reports have identified sialic acid as a crucial structure of glycocalyx that prevents C1Q binding and hinder the C1 activation along with the C3 cleavage (Linnartz et al., 2012).

Translation of these reported literatures emphasise on the effectiveness in blocking the complement activation of PLGA nanoparticles, via separate mechanisms, by the three different modifications based on thiol, glucose and mucin moieties.

5.5.3.2 Terminal Complement Complex Elisa

Complement activation proceeds to the lysis of foreign microorganisms through the formation of a membrane attack complex, also known as SC5b-9. Even though the pivotal component of the complement cascade is reflected by the C3, masking of the C3 cleavage products in the complement sample can happen at times, and this recommends the evaluation of SC5b-9 along with C3a and C3b.

The detection of SC5b-9 which represents the soluble, non lytic terminal complement complex also helps in checking the extent of activation of terminal pathway to completion following the cleavage of complement protein C3. Mollness et al had suggested that TCC is one of the most sensitive marker of complement activation (Mollnes et al., 1999).

In the Figure 20, the reduction in complement activation following thiol, glucose and mucin modification as observed with turbidimetry was in accordance with the reduction of TCC. The C3 nephelometry and terminal complement complex ELISA emphasize on this protective role of modification that nullifies any complement activation induced by the hydrophobicity and terminal carboxyl groups of PLGA nanoparticles. However, this inherent polymeric

hydrophobicity can further have a negative influence on the platelet compatibility of PLGA nanoparticles.

5.5.4 Platelet Activation Analysis

Thrombosis is the inevitable interaction between platelets and plasma proteins that complicate the use of all blood contacting surfaces. As no artificial surface is completely inert towards blood, realisation of a perfectly thromboresistant blood compatible surface has yet to happen. The functional aspects of thrombosis have been described by platelet adhesion, activation and aggregation that culminate in a coagulation cascade leading to fibrin polymerisation. As part of hemocompatibility evaluation, the interactions of nanoparticles with blood platelets are of particular importance as platelet induced particle aggregation is the initiating step to thromboembolic complications.

Human platelets display a discoid shape in their resting state with an average diameter of 1-2µm and possess a net negative charge at physiological pH in plasma or saline. Platelet adhesion occurs in a coordinated manner characterised by tethering, rolling, activation and stable adhesion. Being the most adhesive among the plasma proteins, fibrinogen, reinforce stable platelet adhesion and subsequent thrombus formation through the interaction with the activated form of integrin GPIIb/IIIa located on platelet plasma membranes. Finally, thrombin converts the fibrinogen to fibrin for providing a stable lattice for the developing thrombus. Hence, the major culprit behind the formation of thrombotic fibrin network is fibrinogen (Kiefer and Becker, 2009).

As hydrophobic surfaces accelerate platelet adhesion via fibrinogen adsorption, PLGA surfaces are capable of triggering the thrombotic response. Buay Koh et al has reasoned this in regard to lower heat of adsorption of hydrophobic domains of plasma proteins such as fibrinogen on the hydrophobic PLGA surfaces by promoting the rate of unfolding, denaturation and internal protein entropy. Modification can effectively control the adhesion of inflammatory cells like platelets on PLGA nanoparticle surface as emphasised by Koh et al (Koh et al., 2008).

Nitric oxide has been widely recognized as a potent vasodilator and inhibitor of platelet adhesion and activation. Thiolated surfaces can promote the release of nitric oxide via transnitrosylation reaction. The NO releasing polymers have been developed and proven to exhibit enhanced blood compatibility. Frost et al has extensively reviewed the current status of nitric oxide releasing materials to develop polymers with superior biocompatibility (Frost et al., 2005a). Duan et al has exploited the transnitrosylation reaction for improving the hemocompatibility of polymers following the surface modification with L-Cysteine (Duan and Lewis, 2002a). This catalysed the release of nitric oxide from S-nitroso proteins present in the plasma and inhibited platelet adhesion and aggregation on polymer surfaces. Even very low levels of NO (<1 nM) can be effective in maintaining a non-thrombogenic surface (Duan and Lewis, 2002b). Moreover the micromolar concentration of S-nitroso proteins present in plasma eliminate all concerns about genotoxicty or cytotoxicity and establishes the non thrombogenecity of thiol modified PLGA nanoparticles.

The multiple hydroxyl group functionality present in glucosamine represents a neutral, hydrophilic surface. Lestelius et al has discussed the significance of hydroxyl group functionality in promoting platelet compatibility by lowering plasma protein adsorption (Lestelius et al., 1994). This is in accordance to the general property of hydrophilic surfaces that provide high blood compatibility by mediating low interfacial free energy that decreases the non specific protein and cellular adhesion. Hua et al has identified glucosamine, a naturally occurring amino monosaccharide, as a novel and safe anti platelet agent for preventing thrombotic disorders (Hua et al., 2004). Studies have revealed that glucosamine is able to moderately suppress platelet aggregation, release of granule contents (ATP and PF-4), TXA2 production and calcium mobilization via the inhibition of ADP binding to the purinergic receptors. Bernacca et al has highlighted the maintenance of platelet compatibility following the surface modification of polymers with glucose as it mediates a well organised surface structure of plasma proteins following adsorption (Bernacca et al., 1998). Correlating the studies of Bernacca et al lead us to propose that the glucose based surface modification prevented the denaturation of proteins at the particle-blood interface and protected the PLGA nanoparticles from activation of thrombogenic factors.

Sandberg et al has suggested that mucin coatings are highly surface passivating and can be used to suppress the adhesion of neutrophils on biomaterial surfaces (Sandberg et al., 2009a). Neutrophils in addition to platelets are mediators of acute inflammatory response. The microdomain structured mucin molecule with its alternating hydrophilic oligosaccharides and hydrophobic protein segments confer the nanoparticle surface with excellent interfacial surfactant activity.

Hence reduce the probability of any platelet aggregation or activation at the mucin modified PLGA nanoparticle surface.

5.5.4.1 Platelet Factor-4 Quantification

The response of platelets to external stimuli such as nanoparticle exposure are initiated with a change in shape, followed by stickiness and aggregation and finally culminate in the release of granules such as platelet factor-4. ELISA technique was utilised for platelet factor-4 quantification. Normal plasma concentration of PF-4 is around 4-28 ng/ml that can elevate upto 30 times upon activation during diseased conditions (Simi et al., 1987), as provided in Figure 21. The concentration of PF-4 following exposure to modified and unmodified PLGA based nanoparticles were all within the normal range of PF-4 in plasma. Hence, the results authentified the hemocompatibility of thiol, glucose and mucin modified PLGA nanoparticles analogous to the unmodified PLGA nanoparticles. This was quite evident from the absence of elevation in platelet activation marker, PF-4 following the modification of PLGA nanoparticles.

5.6 Blood Cell Adhesion Studies

Blood is a complex biological fluid that consists of RBC, monocytes, platelets and proteins in the liquid portion called plasma. Of the different cell types, RBCs, WBCs and platelets are the most studied in terms of hemocompatibility, as provided in Figure 22A, 22B and 22C. Safety evaluation of nanoparticles begins with RBC interactions, a key player of systemic homeostasis.

They are the first cells to interact with the nanoparticles following intravenous inoculation. Agglutination, knizocyte formation, internalisation and rupture of membranes are possible with nanoparticle-blood cell interactions. Electrostatic interactions are responsible for the hemagglutination and agglomeration of RBCs that occur between the negatively charged RBC membranes and positively charged particles such as gold or titanium based nanoparticles and polycations. Excluding the toxic membrane disruptive effect with certain nanoparticles such as silica, nanoparticles normally interacts with the red blood cell membrane glycocalyx components such as Duffy antigen/chemokine receptor (Kutwin et al., 2014). This interaction can lead to either the sequestration of nanoparticles or in its unaltered transport and lengthy circulation, depending on its surface characteristics. Kim et al has established the hemocompatibility of PLGA nanoparticles by studying the interaction with human blood constituents (Kim et al., 2005). PLGA nanoparticles maintained the bioconcavity of RBCs without inducing any corrugation or damage to cell membrane.

Since white blood cells form a critical component for the phagocytosis of administered nanoparticles or the foreign body response to implanted biomaterials, analysing the leukocyte interactions are of prime importance. Neutrophil Extracellular Traps (NET) is another interesting mode of eliminating foreign particles carried out by polymorphonuclear phagocytes of white blood cell population. Cenni et al has demonstrated the leukocyte compatibility of PLGA nanoparticles as no significant reduction or aggregation in the total WBC or a specific subpopulation (neutrophils, eosinophils, lymphocytes, and monocytes) was observed (Cenni et al., 2008).

Platelets are key players of haemostasis and thrombosis. Platelet adhesion and aggregation at the particle-blood interface can lead to embolism. Li et al has demonstrated the platelet compatibility of PLGA nanoparticles as they do not induce platelet activation and aggregation (Li et al., 2009)

Owing to this inherent compatibility of PLGA polymer, RBC, WBC and platelet cell incubation studies with PLGA and modified PLGA nanoparticles gave equally intact and similar cell surface morphology as the control cells. The nanoparticles neither altered the blood cell shape nor induced any pseudopodia formation. Surface wettability has a direct correlation with cellular interactions. The reduced contact angle of PLGA following modification can further lower the interactions with RBC, WBC and platelets. Hence, thiol, glucose and mucin based modifications tend to promote the cellular compatibility of PLGA nanoparticles.

5.7 Hemolysis

Understanding the haemolytic potential is recognized as an important initial step in assessing the biocompatibility of nanoparticles. Several studies have identified hemolysis to be a toxic effect since there exist a good correlation between the results of in vitro hemolysis assay and in vivo toxicity studies. According to the ASTM International protocol E2524-08, if the hemolysis index for a test-nanomaterial falls below 2%, the material is considered non-hemolytic; hemolysis values between 2 and 5% are considered as moderately hemolytic and those above 5% interpret the test material as haemolytic in nature

(Dobrovolskaia and McNeil, 2013). In our hemolysis experiment, as provided in Figure 23, all the nanoparticles were qualified as non haemolytic in nature. This was in correlation to the studies of Yallappu et al who has specified that drug loaded PLGA nanoparticles demonstrated no signs of hemolysis at any concentration tested (Yallapu et al., 2010).

5.8 Cell culture studies

5.8.1 Cytotoxicity Studies

Toxic concerns specific to nanoscale materials in biological systems present unique challenges for deploying these materials in vivo. Cytotoxicity of nanoparticles includes physical, physiological and molecular aspects. Toxicity exerted by nanoparticles emphasise on the specific surface area that exposes more reactive groups. Such exposed electron donors or acceptors on the surface increase the chances of nanomaterial interaction with molecular oxygen resulting in the production of reactive oxygen species such as superoxide anion or hydrogen peroxide. This catalyses an electron transfer mechanism and oxidation of key proteins in the cellular pathways, which could possibly culminate in toxic effects. Also following the internalisation through plasma membrane, nanoparticle can affect the intracellular biochemical pathways in different ways and cause cytotoxicity (Lewinski et al., 2008).

The cytotoxic evaluation by multiple parameters that included flow cytometric analysis together with MTT assay endorsed the minimal cytotoxicity of PLGA and modified PLGA nanoparticles, as shown in Figure 24. Following modification, the variations in cell viability is minimal that has lead to minute significant Semete et al

has detailed about the cytotoxicity of PLGA based nanoparticles in cell culture and following oral administration in Balb/c mice (Semete et al., 2010). Neither the surface area of PLGA nanoparticles nor the chemical composition contributes towards toxicity. The hydrolysis following the polyester biodegradation also doesn't interfere with cell function as the metabolic by products, lactic acid and glycolic acid, formed at a slow rate are metabolised and removed via citric acid cycle.

According to Walczyk et al , the contact point of nanoparticle in the cell membrane, specific to the surface architecture of the cell line used would decide how a cell ''sees'' the nanoparticle or precisely, the protein coated particle surface (Walczyk et al., 2010). Here, in concert with Mahmoudi et al, ''cell vision'' must also be recognised as a crucial factor complementary to particle-protein corona and it should be considered for the safe design of nanoparticles used for biomedical applications (Mahmoudi et al., 2011). Cell vision supports the concept that the responses elicited by nanoparticles to different cell lines are different. This occurs due to the influence of cell vision in the rate and extent of uptake of foreign particles and their intracellular disposition. The influence of modification in the cytotoxicity and uptake level of PLGA nanoparticles can also vary depending on the asymmetric cell division and proliferation of the cell line used. In this study we have performed cytotoxicity on two different cell lines, a tumorigenic C6 and normal L929 cell lines which together confirmed the compatibility of both modified and unmodified PLGA nanoparticles. However, under the influence of cell vision, we understand that the viability level from two separate cell lines cannot be generalized as a whole for the hundred different cell lines of varied origin present in our human body.

The significance of p value of the unmodified PLGA based nanoparticle in comparison to the unmodified nanoparticles following statistical analysis lead us to further validate the non-cytotoxicity of PLGA based nanoparticles through flow cytometry.

5.8.2 MTT and Flow Cytometric Analysis

Despite the frequent lack of consistency between in vitro model and in vivo observations, cell based assays still seek validation as a screening bridge before the in vivo deployment of nanoparticles. The nanoparticle mediated toxicity can be evaluated by either functional assays which assess the influence of nanoparticles on cellular processes or viability assays that probe whether nanoparticle cause death in a cell or system of cells. Majority of cytotoxic assays are based on measuring the nanoparticle mediated cell death via colorimetric assays. One such method, MTT viability assay measures the mitochondrial activity using tetrazolium salts as mitochondrial dehydrogenase of live cells cleave the tetrazolium ring to produce the dark blue formazan product.

Preliminary screening of nanoparticles for cytotoxic effects was performed by MTT assay, followed by the multiparametric flow cytometry, the contemporary advanced technology for quantitative single cell analysis, as provided in Figure 25. Flow cytometry realizes the rapid assessment of individual cell viability by distinguishing the different physiological states of cell into the four distinct quadrants when used in combination with fluorescent dyes like calcein and ethidium homodimer. Unstained, control live cells (without any nanoparticle exposure) were

detected in quadrant 3, while live (calcein positive) cells were detected in quadrant 4. The FACS results confirm the biocompatibility of modified PLGA nanoparticles as they did not affect the cell viability in the 48 h cytotoxic test in L929 cells. These studies plainly certified the safety of thiol, glucose and mucin based modified PLGA nanoparticles for drug delivery in a way similar to its FDA approved PLGA counterpart.

5.8.3 Uptake Studies

Successful delivery of therapeutics to targeted cells becomes possible only through favourable interactions with the plasma membrane allowing rapid passage inside the cytosol. According to Walczyk et al. analyzing what the biological cell 'sees' when interacting with a nanoparticle dispersed in a biological fluid like blood become crucial for the design of safe, engineered nanoparticles intended for biomedical applications (Walczyk et al., 2010). For instance, the rate and extent of endocytosis is specific to cell types with macrophages ingesting 3% of its plasma membrane by pinocytosis while fibroblasts ingest at a lower rate of 1% per minute. The processes of nanoparticles penetrating the physiological barriers like cell membrane directly relate to their cellular uptake which in turn depends on the physiochemical characteristic of the nano-bio interface. Hence, a preliminary study to analyse the rate and extend of uptake by PLGA based nanoparticles over a minimum time course of 0-24 h is necessary to understand the appropriate dose and incubation time to the cell type of choice, C6 glioma, as provided in Figure 26A and 26B. Previous work by Desai et al had demonstrated that the uptake of PLGA nanoparticles is time, size and concentration dependent (Desai et al., 1997).

Qaddoumi et al has specified highest uptake of PLGA based nanoparticles of size 100nm in comparison to microparticles (Qaddoumi et al., 2004).

Analogous to Cartiera et al, rhodamine encapsulation in modified and unmodified PLGA nanoparticles were used to explore the uptake process using confocal microscopy (Cartiera et al., 2009). Confocal laser scanning microscopy realises the unique optical sectioning capability which permits three dimensional reconstructions of fluorescent images. Confocal imaging provided different micro sections of C6 cells at defined planes in the Z direction that displayed increasing fluorescence intensity towards the centre following incubation with modified PLGA nanoparticles. Uptake was confirmed by acquiring and evaluating 1µm thick image sections of the C6 cell monolayer following stacking and analysis. Evaluating the cross sectional slices perpendicular to the plane of the C6 monolayer midpoint (Z axis) revealed the presence of modified PLGA nanoparticles in different planes throughout the thickness of C6 monolayer. The pinpoint localization of plain and surface functionalized PLGA nanoparticles along a depth wise manner inside the total volume of C6 cells confirms the successful uptake. Hence, the optical sectioning of C6 cells in the focal plane by the Z stacking tools revealed evidence of modified nanoparticles internalisation rather than their mere adsorption to cell surface. In accordance with the studies of Qaddoumi et al, the uptake of modified and unmodified PLGA nanoparticles were observed to be in a diffused manner inside the C6 cell cytoplasm (Qaddoumi et al., 2004).

Following 24h incubation, the amount of modified PLGA nanoparticles that fill the cytoplasm of C6 cells seem to increase in comparison to 3h. This was in concert with the studies of Xiong et al who has highlighted the

importance of longer incubation time for increasing the uptake of PLGA nanoparticles (Xiong et al., 2011). However, evidence of saturation of PLGA nanoparticle uptake with time is possible depending on the cell type as PLGA nanoparticles follow intracellular localisation through a receptor mediated endocytic pathway.

To date, PEG is the most widely applied passivating agent as it provides steric stabilization and prevent serum protein adsorption that extends the particle circulation half life. However, the shielding effect of the long chains of PEG molecule that bestows it with fine hemocompatibility can turn detrimental for targeted cell therapeutic purposes, as it suppresses interaction with the cell membrane along with hindering the intracellular traffic of the nanoparticles (Hatakeyama et al., 2013b). Several studies have reported on the enhanced cellular association and internalisation presented by thiol reactive moieties present on nanoparticles or polymers. It has been reported that during the virus infection process, cell-surface thiols promote the membrane fusion between some viral envelopes and the host-cell membrane. However, the actual mechanism of thiol-mediated cellular uptake remains obscure. Thiolated biomolecules are assumed to interact with exofacial thiols, followed by standard endocytic pathways to penetrate the plasma membrane (Li and Takeoka, 2014).

Literature cites several examples of carbohydrate functionalised nanoparticle interaction with the molecules on cell membrane. For instance, Marradi et al has highlighted in the role of carbohydrate functionalisation in overcoming biological barriers such as plasma membrane and blood brain barrier (Marradi et al., 2013). Being a prominent feature of the apical glycocalyx of all

epithelia, glucose moieties traffic within the cells like native cell surface molecules. In this regard, pharmacologically active and naturally occurring amino sugar, glucosamine was used to functionalise PLGA nanoparticles. Further studies by Monsigny et al and Duverger et al had summarized on the nuclear localizing signal imparted by glucose functionalisation (Duverger et al., 1995, Monsigny et al., 1999) . These results reinforce the use of simple carbohydrates such as glucose, as an alternative to PEG molecules for PLGA surface functionalisation when cellular uptake is required.

By virtue of their negative charge and extended configuration, mucin-like glycoproteins may act as a repulsive barrier around reticuloendothelial cells; however when an opposing cell has specific receptors for the mucin, adhesion dominates repulsion. Furthermore, the presence of plurality of different types of carbohydrates on the protein backbone of mucin provides the potential for high levels of specificity when targeting specific cell types. Studies by Savla et al had identified mucin functionalisation as an effective alternative to conventional targeting agents such as peptides and antibodies (Savla et al., 2011). In concert with the results of Savla et al, mucin modification could increase the penetration of PLGA nanoparticles through cell membranes as evident from the present confocal images.

Likewise, the fluorescence and confocal laser scanning microscopy, as a qualitative visualization technique, confirmed the cellular internalization of both modified and unmodified PLGA nanoparticles. CLSM clearly differentiated the internalization of modified PLGA nanoparticles from the particles adsorbed onto the outer cell membrane with the help of Z stack tools. The high resolution of the confocal technique aids the researchers in understanding the cellular

biodistribution and particle tracking which becomes important for establishing the safety and efficacy of delivery mechanisms.

Apart from the standard 3h time period for uptake process, an additional 24h has also been performed as the PLGA based nanoparticles attain the uptake saturation under extended time periods. The thiol, glucose and mucin based PLGA modification gains over the steric stabilisation offered by the PEGylated nanoparticles. Also unlike cationic polymers, the enhanced uptake is not compromised by non specific protein adsorption mediated rapid clearance from the plasma compartment. Additionally, the punctuate fluorescence signals provided by thiol and mucin modified PLGA nanoparticles suggest a receptor mediated uptake while the more diffused fluorescence signals of glucose modified PLGA nanoparticles predict towards a passive kind of uptake mechanism (Li et al., 2014), (Gromnicova et al., 2013), (Rabuka et al., 2008). Hence, we propose that thiol, glucose and mucin based modifications should be considered in future design of synthetic biomolecules for enhancing the hemocompatibility along with providing optimized cellular delivery.

5.9 Drug Delivery Applications

5.9.1 Synthesis of Doxorubicin, Curcumin and Betulinic Acid Encapsulated Nanoparticles

Since the inception of the encapsulation of bioactive substances, laid down about 70 years ago, manufacturing strategies of particularly BCS Class IV drugs that exhibit a low solubility and low permeability forms an

important aspect in pharmaceutics. The establishment of poly lactic acid and later its copolymer, poly lactic co glycolic acid, as biodegradable and biocompatible polymers for drug delivery has gradually occurred following the initial focus on the protection of vitamins from oxidation. Beck, Tice and co-workers were the pioneers in encapsulating the hydrophobic drugs such as steroids and studying their efficiency in vivo (Beck et al., 1985) & (Wischke and Schwendeman, 2008).

The suitability of a nanoparticle preparation method for effective encapsulation of chemotherapeutic agents depends on several parameters such as the right choice of polymer composition, stabilizer, solvent, drug solubility and technique. The classic emulsification solvent evaporation technique (ESE) was elaborated by several pioneers such as Bodmeier and Mc Ginity and slight modifications are available for encapsulation of various substances from simple pharmaceutical products to proteins and DNA. Subsequently, a modified emulsification-solvent evaporation technique was chosen for encapsulating the chemotherapeutic drugs, doxorubicin, curcumin and betulinic acid inside the PLGA and modified PLGA nanoparticulate system. This was done with the goal of enhancing the drug bioavailability without compromising its bioactivity.

It is a well known fact that the double emulsion method, proceeds through a two-step process; the emulsification of a polymer solution containing either polar or non polar therapeutics, followed by the polymer droplets containing the drug molecules, hardening in to particles in presence of a suitable surfactant, through solvent evaporation and polymer precipitation. Uniform and complete emulsification of the organic and aqueous phases is critical for the formation of nanoparticles, as indicated by the homogenous, milky white or coloured

opaque solution (based on the colour of drug). The solvent evaporation from the emulsion is followed by the distribution of drug molecules between the polymeric droplets and the surrounding emulsifier phase. The surfactant, pluronic F-68, was chosen in our study, owing to its low toxicity and immunogenicity profile. The energy input provided by the ultrasonication for an optimised time interval successfully reduced the size of emulsion globules to the nanoscale.

Volatile organic solvents are used to dissolve the matrix polymer and drug employed during the microencapsulation of therapeutics. The most common solvent used for encapsulation of hydrophobic drugs in solvent evaporation technique is methylene chloride owing to its high volatility, low boiling point and high immiscibility with water. However, being a less toxic substitute of methylene chloride, ethyl acetate was the solvent of choice in this study. The partial miscibility of ethyl acetate in water can result in its sudden and huge extraction from the dispersed phase. This leads to precipitation of PLGA polymer into fibre like agglomerates. In order to avoid this, the dispersed phase of PLGA was dissolved in a small quantity of aqueous solution prior to its emulsification in large quantity of water (Wischke and Schwendeman, 2008).

Rosca et al has investigated the mechanism of particle formation in single and double emulsions under controlled solvent evaporation conditions (Rosca et al., 2004). This study exemplified the direct consequence of the mechanism of particle formation in the nanoparticulate layer formed. As the solvent, ethyl acetate slowly evaporates; the PLGA precipitates at the water droplet interface and forms a continuous crust around the emulsion droplet that contains the drug molecules. Gradually, the PLGA particles undergo shrinkage in volume as the

solvent evaporates resulting in the continuous fragmentation of polymer crust around the emulsion droplet. Finally, the nanoparticles encapsulating drug molecules are formed as the solvent is transported under diffusion from the initial droplet through the aqueous phase and is evaporated through the emulsion-air interphase. The combined effect of solvent elimination accompanied by volume shrinkage decides the morphology of nanoparticles in addition to drug encapsulation and release behaviour.

Extensive research within the last two decades had implied that curcumin and betulinic acid can prevent carcinogen induced tumorigenesis and inhibit the growth of implanted human tumors. Recently, curcumin has been investigated as a magic drug due to its anticancer effect. Similarly betulinic acid is a promising new lead compound for use against human cancer. Although Phase I clinical trials have demonstrated the safety of curcumin and betulinic acid at high doses, the poor bioavailability and sub optimal pharmacokinetics largely hampered its anticancer activity. Various techniques have been utilised to improve the delivery of curcumin and betulinic acid including incorporation into liposomes or phospholipid vehicles. Recent years have witnessed many dosage forms of curcumin based on nanoparticles of poly (butylcyanocrylate), poly lactic co glycolic acid, chitosan, albumin and Eudragit.

The emulsion solvent evaporation technique has a successful history of hydrophobic drug encapsulated PLGA particle synthesis including chlorpromazine, diazepam, the anticancer agents aclarubicin, lomustine and paclitaxel. Accordingly, the single emulsion technique was applied for the encapsulation of these hydrophobic cargos, curcumin and betulinic acid, within

PLGA nanoparticle for their controlled release in pharmaceutical applications. The term “hydrophobic drugs” describes heterogeneous groups of molecules that are poorly soluble in water but are typically, but certainly not always, soluble in various organic solvents. The solvent of choice, ethyl acetate provided improved dissolution of curcumin. Being lipophilic, curcumin and betulinic acid partitions to the hydrophobic core of PLGA polymer and forms a stable colloidal dispersion. This was based on the reports of Tsai et al which demonstrated that the bioavailability of curcumin significantly increased upon encapsulation inside low or high molecular weight PLGA nanoparticles (Tsai et al., 2011). Additional in vivo studies in rats by Sheikh et al has discussed the significance of PLGA nanoparticles, in enhancing the bioavailability of curcumin to twenty six fold times when compared with oral curcumin suspension and to at least nine fold times when compared to curcumin administered in conjunction with piperine as an absorption enhancer (Shaikh et al., 2009). This was due to the sustained release and a longer residence time in vivo provided by the carrier, PLGA nanoparticles. Furthermore, similar PLGA nanoparticles, synthesised by Anand et al using F-68 as the solubiliser, were found to possess increased half life and enhanced serum levels in comparison to free curcumin upon intravenous administration (Anand et al., 2007).

Parallely, Csuk et al has studied the possibility of realising the in vivo administration of betulinic acid by encapsulating inside commercially available liposomal formulations (Csuk et al., 2011). Das et al has suggested that the PLGA based nanoencapsulated form of betulinic acid increases the bioavailability and hence possess a better chemo-preventive action against lung cancer in vivo and on A549 cells in vitro (Das et al., 2012).

The above cited literature, confirms that nanoencapsulation technique significantly increase the aqueous dissolution of otherwise hydrophobic curcumin and betulinic acid and accordingly enhance the drug bioavailability and stability by protecting them from the outside environment. Hence, improves their clinical applicability in cancer therapy.

While the lipophilic drugs are easily encapsulated by this technique, the scenario is quite different for hydrophilic drugs. The encapsulation suffers as the hydrophilic drugs, such as doxorubicin, rapidly partition to the external aqueous phase. Tewes et al has compared the encapsulation of doxorubicin inside PLGA nanoparticles synthesised by single oil in water and double water in oil in water emulsification method based on the drug polarity (Tewes et al., 2007a). The results successfully established the increased efficacy of single emulsion technique. Further, Park et al has demonstrated the importance of a modified single emulsion technique in maximising the efficacy of Doxorubicin loaded PEGylated PLGA nanoparticles along with minimising the dose limited cardiotoxicity (Yoo et al., 2000). Based on these literatures, a modification of the single emulsion technique was adopted to realize the improved delivery of drugs with compromised organic solvent solubility. Doxorubicin, an anthracycline drug against broad spectrum of tumors, is generally used in the form of hydrochloride that offers good solubility in aqueous solutions. However, it drastically reduces the solubility in organic solvents suitable for PLGA nanoparticle preparation, such as ethyl acetate used in our study. However, Cohen Sela et al has utilised the partially water soluble organic solvent, ethyl acetate in a double emulsion solvent diffusion technique to encapsulate a hydrophilic low molecular weight drug, alendronate within PLGA nanoparticles

(Cohen-Sela et al., 2009). For this reason, the method of single emulsion (W-O-W) using ethyl acetate as the organic solvent and PBS as the outer aqueous phase as performed by Wohlfart et al was chosen for loading doxorubicin hydrochloride in the PLGA and modified PLGA nanoparticles (Wohlfart et al., 2011). Here the drug is first solubilised in the inner aqueous medium. Importantly, the hydrophilic drug exhibited lower solubility in the external aqueous phase, PBS as the doxorubicin hydrochloride is converted into a less soluble doxorubicin phosphate. This lower solubility facilitated the drug distribution into the organic polymer phase and thus enhanced the efficacy of hydrophilic drug encapsulation within PLGA based modified and unmodified nano drug formulations.

5.9.2 Characterisation of Drug Encapsulated Nanoparticles

The in vivo fate of a drug after administration is directly dependent on the physicochemical properties of the drug and on its chemical structure. This necessitates the physicochemical characterization of drug loaded nanoparticle system.

5.9.2.1 Dynamic Light Scattering

The particles size is an important parameter in drug delivery system as it determines the pharmacokinetic indices such as the time of circulation, absorption and distribution. Unequal particle size or large polydispersity index can cause irregular pharmacokinetic parameters leading to therapeutic inefficiency of a drug formulation. The drug loaded PLGA and modified PLGA nanoparticles prepared by single emulsion method had a consistent size range below 250-300nm with a low dispersity index suggesting narrow size distribution, as determined by

dynamic light scattering method provided in Table VI. Kumar et al has highlighted the significance of the solvent, ethyl acetate in producing smaller PLGA nanoparticles (Ravi Kumar et al., 2004). Mukherjee et al has discussed the influence of process variables such as surfactant concentration and sonication time on the particle size variations. Accordingly, the sonication time was optimised at two minutes for yielding the smallest sized drug loaded PLGA based nanoparticles.(Mukerjee and Vishwanatha, 2009)

Although, polyvinyl alcohol, forms the most common emulsifier used in the formulation of uniform sized PLGA nanoparticles with small size, it has been recently demonstrated by Sahoo et al that the PVA forms an interconnected network with the PLGA polymer at the interface (Sahoo et al., 2002). Hence, in the current study, PVA was conveniently replaced with Pluronics as the former would compromise the good redispersability and cellular uptake of PLGA nanoparticles. Though it was reported by Yadav et al that an increase in the concentration of surfactant, Pluronic F-68 can lead to even smaller particle size, it was actually not followed as it becomes difficult with the washing procedure to remove the traces of surfactant adsorbed on to the particle surface (Yadav et al., 2007). Also, Reddy et al mentions about the optimum concentration of surfactant above which no decrease in particle size was observed due to the attainment of saturation point (Reddy and Murthy, 2005).

The slight increase in size following the addition of the drugs in the PLGA based formulations could be due to the presence of surface adsorbed drug molecules. The expansion of the PLGA based polymeric matrix could be

another reason for the observed increase in size of PLGA and modified PLGA nanoparticle system following the respective drug encapsulation. The surfactant nature of mucin modification resulted in the lowest size among the three different modified, drug encapsulated PLGA nanoparticles. Comparing the three drugs, betulinic acid displayed the smallest size after encapsulation inside PLGA and modified PLGA nanoparticles. The reason behind this could be the better encapsulation of betulinic acid leading to negligible presence of drug on the particle surface.

Further, the low dispersity index can aid in the stability of the formulated nanoparticles. In addition, the nano size of drug loaded carriers tends to promote passive targeting to tumor tissues via enhanced permeability and retention; as well as increase the chances of cellular uptake and intracellular trafficking (Mohanty and Sahoo, 2010). Further investigation by Smola et al and He at al has separately provided confirmatory evidence for the ability of nanocarriers below 200nm to cross the biological barriers like vascular endothelium and pulmonary alveoli, leading to efficient distribution within tumors (Smola et al., 2008). Moreover, Peppas et al has cautioned that the nanoparticles larger than 300nm would be at greater risk of being captured by the splenic macrophages (Owens III and Peppas, 2006). Hence, all the drug loaded PLGA based nanoformulations with a size below 250nm could have enhanced circulation half lives by evading the reticuloendothelial system.

5.9.2.2 Differential Scanning Calorimetry

The glass transition temperature of the polymers along with the physical state of the drug inside the nanoparticles has an influential role in drug release characteristics. In this view, the DSC analyses of pure drugs, doxorubicin, curcumin and betulinic acid before and after encapsulation inside the differently modified PLGA nanoparticles were performed as depicted in Figure 27. Musumeci et al has described that different combinations of drug-polymer interactions such as an amorphous drug in an amorphous or crystalline polymer and crystalline drug in either an amorphous or cyrstalline polymer can possibly coexist in the polymeric nanocarrier (Musumeci et al., 2006). Importantly, Yallappu et al has suggested that the transition of the cyrstalline drug to amorphous phase is a commonly observed phenomenon while encapsulating into PLGA nanoparticles (Yallapu et al., 2010). However, Panyam et al has observed an exception to the above general observation with the nanoparticles prepared from low molecular weight PLGA (12,000 Da) as 10% of the total drug encapsulated was present in crystalline form (Panyam et al., 2004). Larger size of such nanoparticles could be a reason for favouring entrapment of drug crystals.

The drugs, curcumin, betulinic acid and doxorubicin provided sharp peaks at 172˚C, 306˚C and 168˚C, respectively that corresponded to their individual melting points and hence indicates the crystalline nature of pure drugs. These melting points disappeared following the respective drug encapsulation within PLGA and modified PLGA nanoparticles. In concert with the respective studies of Mukerjee et al, Sanna et al and Soica et al, the absence of the sharp endothermic

peak of the pure drugs, curcumin, doxorubicin and betulinic acid, respectively following the nanoencapsulation refers to the absence of any crystalline drug material in the loaded polymeric PLGA nanoparticles (Mukerjee and Vishwanatha, 2009), (Sanna et al., 2011) & (Soica et al., 2014). These results indicate that the intermolecular interactions between the drug molecules and the PLGA/modified PLGA polymeric chains inhibited the crystallization of respective drugs during the nanoencapsulation process. Hence, it seems that these drugs are highly distributed throughout the polymeric chains of the differently modified PLGA nanoparticles either in an amorphous or disordered molecular dispersion or solid solution state. The pure PLGA polymer is thermally stable up to 250˚ C. All the different drug loaded nanoparticles possessed the same thermal decomposition value including the glass transition temperature as the control polymeric PLGA nanoparticles. This was in accordance to the reports of Xie et al who described that the nanoencapsulation process does not affect the basic polymeric structure (Xie and Wang, 2007). Thus, the DSC analysis helped in establishing the chemical integrity of all the three drugs, doxorubicin, curcumin and betulinic acid following their interaction with the modified and unmodified PLGA polymer. Further, it confirmed that the encapsulation process retained the properties of the respective drugs within the differently modified PLGA nanoparticles.

5.9.2.3 Fourier Transform Infrared Spectroscopy

FTIR analysis was used to distinguish any chemical changes or the formation of any chemical bonds that occurred in the PLGA polymer due to the incorporation of drugs during the synthesis reaction, as provided in Figure 28.

This was taken into consideration for confirming the presence of drugs within PLGA based nanoparticulate formulations.

The characteristic broad peak at 3300cm^{-1}-3600 cm^{-1}, corresponds to the NH and CH stretching of pure doxorubicin (Figure 28A). Chouhan et al has attributed the peaks at1000-1260cm^{-1} and 675-900 cm^{-1} in response to C-O stretching of alcohol and out of plane O-H bending of doxorubicin (Chouhan and Bajpai, 2009). The aromatic N-H bending vibrations and the C=O stretching results in the signature peaks at 1580 cm^{-1} and 1746 cm^{-1} that is observed both in the native doxorubicin and doxorubicin loaded nanoparticles. Hence, the resemblance of spectra between pure drug and loaded nanoparticles confirms the successful encapsulation of doxorubicin inside pristine and modified PLGA nanoparticles (Khemani et al.).

Similarly, the signature peaks at 1510 cm^{-1} and 1627 cm^{-1} observed in the native curcumin and curcumin loaded modified and unmodified PLGA nanoparticles readily confirms the successful drug encapsulation (Figure 28B). These peaks represent the stretching vibrations of C=C double bonds and aromatic C=C double bonds, respectively of the curcumin molecule. As this peak at 1627cm^{-1} has not displayed any shifting following encapsulation and was in concert with the studies of Pan et al and Mohanty et al, it was concluded that the curcumin molecules are present in a dispersed state inside the nanoparticles (Pan Ch et al., 2006)& (Mohanty and Sahoo, 2010). It is noteworthy that the characteristic peak of curcumin at 3524cm^{-1} has disappeared following encapsulation inside PLGA nanoparticles. In contrast, the encapsulated curcumin within the three surfaces modified PLGA nanoparticles retained this peak. In concert with Xie et al, the

formation of intermolecular hydrogen bonds between the O-H band of curcumin and C=O groups of PLGA has resulted in this feature (Xie et al., 2011). Accordingly, following modification of PLGA, the C=O groups were not freely available to form hydrogen bonds with the encapsulated curcumin. Hence ensured the presence of hydroxyl band of encapsulated curcumin at 3524cm^{-1} within thiol, glucose and mucin modified PLGA nanoparticles.

In the FTIR spectrum of betulinic acid encapsulated nanoparticles (Figure 28C), the broad and prominent band at 3314 cm^{-1} corresponds to the stretching vibrations of O–H bond, the peak at 1697cm^{-1} represents the stretching vibrations of the carbonyl group C = O and the band at 1043cm^{-1} refers to C–OH stretching vibrations of the drug molecule. Aisha et al has attributed the bands at 135cm^{-1} and 1232cm^{-1} to the C-OH deformation vibrations (Aisha et al., 2013). Hence the resemblance of spectra proves the successful nanoencapsulation of the drug, betulinic acid. In short, the peaks found in the respective individual drug forms are present both in the pristine and modified PLGA nanoparticulate formulations and hence indicate that all the three drugs are present in their native form without any chemical interaction with the polymer in the drug loaded nanoparticles, except in case of curcumin encapsulated PLGA nanoparticles.

5.9.2.4 UV Spectrometry

An ideal nanoparticulate formulation for drug delivery must ensure that the synthesis process has not altered the chemical structure of the drug that provides the pharmacological properties. UV absorbance spectral analysis

demonstrated the stability of drugs at physiological pH following the nanoencapsulation within differently modified PLGA nanoparticles.

According to Kumar et al, free doxorubicin presented a typical optical absorbance centered at 480-490nm (Kumar et al., 2012). Similarly, Yang et al has specified that free doxorubicin absorbs strongly at 233,253,291 and 480nm (Yang et al., 2008). In regard to these reports it is quite evident that the encapsulated doxorubicin inside PLGA and modified PLGA nanoparticles retains the typical molecular doxorubicin fluorescence characteristic feature, as shown in Figure 29A.

Gangwar et al has specified the absorption peak of curcumin at 415nm to be the signature of basic diaryl heptanoid chromophore group of curcumin, as provided in Figure 29B (Gangwar et al., 2013). It is quite evident that curcumin retains it heptanoid chromophore group following encapsulation inside PLGA and differently modified PLGA nanoparticles. However, in case of curcumin released form mucylated PLGA nanoparticles, the comparatively noticeable broadening of the basic diaryl heptanoid chromophore group could indicate some attractive drug-polymer interactions which were further evident in the release studies.

In concert with the studies of Taralkar et al, the betulinic acid has produced a UV absorbance peak at 210nm that was also present following the encapsulation and release from PLGA and modified PLGA nanoparticles, as shown in Figure 29C (S V, 2012).

Hence the similarity in the UV spectra of free and encapsulated drugs suggests the physical stability of the drug inside the PLGA and

modified PLGA nanoparticles. To be specific the chemical structure of all the drugs remains same during nanoparticle loading and release process.

5.9.2.5 Determination of the Encapsulation Efficiency

The encapsulation of therapeutic compounds into biocompatible and biodegradable nanoparticles represents an attractive tool for chemotherapy. Curcumin and betulinic acid mediate its chemotherapeutic effects in the micromolar concentration range. In order to sustain this concentration over an extended period of time and to minimise the dose of nanoparticle administration, it became necessary to formulate nanoparticles with high encapsulation efficiency. Hence, an ideal drug carrier is expected to have high encapsulation efficiency. The literature describes two different techniques for incorporating therapeutics within the polymer, PLGA. Drugs could be incorporated simultaneously while synthesising PLGA nanoparticles, as observed in the current study or it could be absorbed/adsorbed, following incubation with a concentrated drug solution. Most attempts at enhancing the encapsulation efficiency stems from the basic principle of preventing drug loss into the continuous phase, during nanoparticle synthesis. This is enabled by accelerating the precipitation of the polymer on the surface of dispersed phase (Bodmeier and McGinity, 1988). Consequently, a delay in the precipitation of the dispersed polymer phase can cause more drug molecules to diffuse out to the continuous aqueous phase and thereby decrease the encapsulation efficiency.

According to Panyam et al, encapsulation efficiency of the particulate systems formulated by solvent evaporation technique would depend on the partitioning of the drug between the polymeric phase and the continuous aqueous

phase and its subsequent separation from the continuous phase and deposition on the nanoparticle surface (Panyam et al., 2004). The distribution of drug in the polymeric phase would in turn depend on the solid state solubility of the drug and the capacity of the polymeric matrix to entrap the drug in the dispersed state. Higher the solid state solubility of the drug within the polymeric matrix, higher would be the drug loading.

Shahani et al has investigated on the influence of various processing parameters on encapsulation efficiency and reported that the increase in glycolide content and molecular weight of PLGA or the increase in organic to aqueous volume ratio caused the polymer to precipitate quickly and resulted in higher encapsulation efficiency (Shahani and Panyam, 2011). However their preliminary studies reported that the increase in particle size in micrometer range and the increase in drug to polymer ratio had negligible effect on the encapsulation percentage. Mehta et al has signified the solubilities of polymers in the organic solvents to be a determining factor in the solidification rate and subsequent encapsulation efficiency (Mehta et al., 1996).

Drug loss or diffusion of drugs into the continuous phase usually occurred during the initial ten minutes of emulsification, while the dispersed phase remained in a transitional semi solid state. This drug diffusion was governed by the solubility of the drug in the continuous aqueous phase to the dispersed polymeric phase. Hydrophilic drugs manifest spontaneous diffusion to the continuous aqueous phase. Hence, the modified and unmodified PLGA nanoparticles demonstrated consistently lower encapsulation efficiency for the hydrophilic drug,

doxorubicin, in comparison to the hydrophobic drugs, curcumin and betulinic acid. Subsequently, the emulsified drug containing polymer dispersion was quickly transferred to the outer aqueous phase in order to prevent the decrease in encapsulation efficiency by reducing the time the polymer remained in the emulsification phase.

The encapsulation efficiency demonstrated by the PLGA nanoparticles for the drugs, doxorubicin, curcumin and betulinic acid, as provided in the Table VII, were in accordance to the reported literature by Yoo et al, Tsai et al and Das et al respectively (Yoo et al., 2000), (Tsai et al., 2011) and (Das et al., 2012). All the PLGA based formulations followed the general trend of decreased encapsulation efficiency with increased hydrophilicity of the matrix polymer. This trend is acceptable for hydrophobic drugs such as curcumin and betulinic acid as the surface hydrophilisation of PLGA matrix would compromise the hydrophobic interactions between the drug molecules and the hydrophobic PLGA core. Subsequently reduces the encapsulation efficiency of curcumin and betulinic acid within modified PLGA nanoparticles. However, in case of hydrophilic drugs such as doxorubicin, the above statement place itself in a contradictory position to the established reports of Johansen et al that specified higher encapsulation efficiency for hydrophilic drugs within hydrophilic PLGA matrixes (Johansen et al., 1998). Johansen et al cited that the carboxylic end groups conferred the PLGA with adequate hydrophilic character, sufficient enough to accelerate its precipitation and solidification rate in the solvent and resulted in the higher encapsulation efficiency.

In case of doxorubicin, the efforts to maximise the encapsulation efficiency were only partially successful as the hydrophilic drug escaped to the aqueous media during the emulsification process. This was in concert to the reports by Barichello et al that correlated the higher hydrophilicity of a drug to lower encapsulation efficiency within PLGA nanoparticles (Barichello et al., 1999). It appears that there exists a strong electrostatic attraction between the positively charged amino groups of doxorubicin and the negatively charged carboxyl groups of PLGA. Modification of carboxyl groups of PLGA with the glucose and mucin moieties literally nullifies this attraction as the carboxyl groups are now unavailable for interaction with doxorubicin. This could justify the observed decrease in encapsulation efficiency of doxorubicin following hydrophilisation of PLGA surface with glucose and mucin moieties. A similar reduction in the encapsulation efficiency of PLA nanoparticles following surface hydrophilisation with PEG was observed by Tobio et al (Tobio et al., 1998). The precise mechanism for the decrease in the encapsulation efficiency was unclear and Tobio et al has attributed this to the steric interference of drug/polymer interactions by the PEG moieties. Thus, the two different modifications of the PLGA, namely, glucosylation and mucylation have reduced the number of free carboxyl groups on the PLGA matrix when compared to the unmodified polymer. Hence there is a marked decrease in the encapsulation efficiency of modified PLGA in concert with reduced electrostatic interactions. Glucosylated PLGA, possessing the highest number of hydroxyl groups, displayed the least encapsulation efficiency. However, thiolated PLGA could maintain the encapsulation efficiency of doxorubicin in spite of the decrease in free carboxylic groups. Here, the prominence of ionic interactions between the anionic thiolated

PLGA and the cationic doxorubicin were successful enough to overcome the weak hydrophilic interactions of drug with the aqueous media and hence resulted in the enhanced affinity of doxorubicin for thiol matrix. Additionally, the presence of carboxyl groups in the cysteine molecule could neatly substitute for the loss of carboxyl group in the PLGA backbone, on a one to one basis. Hence, irrespective to the enhanced hydrophilicity, thiolation could maintain similar electrostatic attraction between doxorubicin and the modified matrix, as in the case of unmodified PLGA nanoparticles. Thus, justify the almost similar encapsulation efficiency between PLGA and thiol modified PLGA matrix for the drug, doxorubicin.

The numerous negatively charged sugars like sialic acid present in the mucin moiety could maintain the electrostatic interactions with the doxorubicin even in the absence of the free carboxylic groups on PLGA polymer. This conferred the mucin modified PLGA nanoparticles with adequate encapsulation efficiency for the drug, doxorubicin.

In case of curcumin and betulinic acid encapsulation, the presence of multiple hydroxyl groups in the glucose modified surface of PLGA polymer could reduce the strong hydrophobic interactions between the PLGA core and curcumin and accordingly minimise the encapsulation efficiency. The modification based on thiol moieties has helped to slightly increase the encapsulation efficiency of the hydrophobic drugs in comparison to glucosylated PLGA on the basis of keto-enol tautomerisation of curcumin as reported by Gupta et al. Accordingly, the tautomerisation enable curcumin to function as a Michael acceptor to nucleophilic interactions and bind covalently to nucleophiles, such as cysteine

(Gupta et al., 2011). The highest encapsulation efficiency for curcumin was provided by the mucylated PLGA and that could be attributed to the exertion of hydrogen bonding as well •-• interactions between the phenolic moieties of curcumin and mucin. This mechanism was explained in the reports of Chuah et al (Chuah et al., 2013). However in case of betulinic acid, unmodified PLGA nanoparticles had surpassed the three modified matrix versions in providing the maximum encapsulation efficiency owing to the highest hydrophobic potential. Otherwise, the encapsulation efficiency of betulinic acid was similar to curcumin with respect to the different modifications of PLGA polymeric matrix.

5.9.2.6 In Vitro Drug Release Kinetics

In nanoparticle mediated drug delivery, drug encapsulation efficiency and release rates are crucial parameters required for the optimisation of the bioavailability of the loaded drug. Specifically, the controlled release of encapsulated drugs from the polymeric matrices is critical in meeting the therapeutic goal.

Once the polymer PLGA comes in contact with the aqueous media, water penetration and hydrolytic cleavage of ester bonds commences irrespective of the polymer, PLGA s insolubility in water. This is followed by the polymer degradation and simultaneous drug diffusion. Fredenberg et al has specified that various parameters including chemical degradation of the polymer by autocatalytic ester hydrolysis, polymer erosion, evolution of pore structure as a result of mass erosion, the aqueous pore structure and the diffusive transport of the drug through the polymer matrix collectively contribute to the kinetics of drug release from PLGA based drug carriers (Fredenberg et al., 2011). Involvement of such

variables and the resulting complexity of the physical and chemical mass transport mechanism of the polymer PLGA, often results in an unpredictable release rate pattern (Siepmann and Siepmann, 2008). Hence it becomes difficult to generalise the results obtained with specific drug delivery systems. Nevertheless, diffusion, erosion, osmotic mediated events or combination of these mechanisms are the principal factors that control the release rate from the PLGA based drug delivery devices. In accordance to Pitt et al, diffusion through the polymeric matrix could be the major principle underlying the release of small molecular weight drugs such as curcumin and doxorubicin (Shah et al., 1992).

In reference to the reports of Seo et al, hydrophilic and hydrophobic drug release from the PLGA and modified PLGA nanoparticles occur in a biphasic manner, with an initial burst phase followed by diffusion controlled slower drug release phase owing to the gradual degradation of the polymer (Zentner et al., 2001). A systematic study by Lu et al and Park et al has demonstrated that the absolute value of degradation rate increases with the glycolic acid proportion of the copolymer, PLGA (Lu and Park, 1995). Their results had assigned hydrophilicity of the polymer as the critical parameter that accelerates the degradation and release rate, presumably due to faster water uptake and subsequent pore formation in the matrix. In this regard, the modification of PLGA polymer with hydrophilic thiol, glucose and mucin moieties would promote a more rapid drug diffusion facilitated by the faster degradation of the PLGA matrix. The significance of rapid drug release become obvious from the studies of Yoo et al where the PLGA nanoparticles conjugated with doxorubicin were less efficient in comparison to free drug in spite of sufficient

particle internalisation. The inadequate release of the drug within the stipulated time period was the reason behind the poor performance of nano-drug conjugates (Yoo et al., 2000).

Physicochemical properties of the encapsulated drug can be another significant factor controlling the release rate, specifically through the drug molecules present on the particle surface. Siegal et al had concluded that the drug release rate and degradation of the polymer, PLGA, vary as a function of the drug type (Siegel et al., 2006). However, further studies are required to correlate the release rate parameters to the drug chemistry or hydrophilicity. Nevertheless, Stevanovic et al has attributed freely water soluble drugs to facilitate water penetration and creation of a highly porous polymer network following the hydrophilic drug leaching (Stevanovic and Uskokovic, 2009). In contrast, lipophilic drugs can retard the polymer degradation and release rate by hindering water diffusion in to the drug encapsulated matrix.

It was quite evident that modification influenced the release rate as the release profile of drugs from the modified PLGA nanoparticles differed substantially from the unmodified polymeric matrix. The release pattern of the drugs, doxorubicin and curcumin from the differently modified PLGA matrix is based on the drug and matrix's combined hydrophobic/hydrophilic aspects, as provided in Figure 30A and 30B. Any deviation from this predicted pattern occurred under the influence of additional non covalent interactions between drug and the surface modifying moieties present on the polymer matrix.

As earlier explained, electrostatic interactions exist between the weakly basic doxorubicin and the carboxylic acid groups of acid capped PLGA. Modification would probably nullify such interactions and hence produce a higher release profile in comparison to unmodified PLGA matrix. As expected, among the different modified PLGA nanoparticles, the initial release of hydrophilic drug, doxorubicin, was fastest through the superficial layers of glucosylated PLGA nanoparticles, in correspondence to the maximum surface hydrophilicity. However with thiolated PLGA nanoparticles, the burst effect was reduced, irrespective of hydrophilicity and almost similar to that of unmodified PLGA nanoparticles. This probably might be due to the restoration of electrostatic interactions through the carboxylic acid groups of cysteine molecule present in the thiolated PLGA matrix and the Dox.HCl, a positively charged amphiphilic drug with a protonable amino group in the sugar moiety. These electrostatic interactions could restrict the otherwise fast release of doxorubicin from the hydrophilised thiolated PLGA matrix. Following the initial burst, the drug release followed a minimal release corresponding to the slow diffusion of drug molecules from inner polymeric matrix. This release profile was similar to the pattern obtained by Tewes et al while performing a comparative study of the doxorubicin encapsulated PLGA nanoparticles prepared by single and double emulsion techniques (Tewes et al., 2007a).

The release profile of curcumin was followed as a model profile for the general hydrophobic drug release pattern from PLGA based modified and unmodified

nanoparticles. Hence curcumin release profile was speculated to be an indicator for the release pattern of the other hydrophobic drug, betulinic acid also.

The slow release profile of the drug curcumin from the PLGA matrix could be attributed to the delayed hydration of the hydrophobic PLGA nanoparticle surface adsorbed with hydrophobic drug molecules. It can also result from the insolubility of hydrophobic curcumin towards the external aqueous release phase as explained by Khalil et al (Khalil et al., 2013). PBS maintained at pH 7.4 was employed as the release medium in order to simulate physiological conditions. Xie et al has mentioned about the intermolecular hydrogen bond interactions of the polymer, PLGA with curcumin. These interactions resulted in the restricted release of curcumin from unmodified PLGA nanoparticles and consequently reduce the drug availability and efficacy (Xie et al., 2011). Alternatively, modification with thiol, glucose and mucin moieties can block the hydrogen bond formation between PLGA matrix and curcumin. Also as the modifying moieties enhance the hydrophilicity of PLGA surface, it can promote the water permeation and drug diffusion through the polymer matrix. To be specific, thiolation and glucosylation can accelerate the wettability of PLGA polymer surface and inner matrix as well as nullify the drug-polymer interactions and hence contribute to the increase in drug release. The reason behind the elevated release of curcumin from the thiolated PLGA matrix when compared to the more hydrophilic glucosylated PLGA nanoparticles could be due to the higher drug encapsulation within the thiolated matrix. This was in reference to the reports of Sah et al and O'Hagan et al that correlated higher drug encapsulation to higher initial release profile (Sah et al., 1994), (O'Hagan et al., 1994). Surprisingly,

irrespective to the hydrophilicity of mucylated PLGA matrix, the mucin modification with the highest encapsulation efficiency provided the lowest release profile that was comparable to unmodified PLGA nanoparticles. Studies by various groups have confirmed the existence of hydrogen bonding and •-• interactions between the phenolic moieties of curcumin and mucin. Hence, we propose that the curcumin interactions with mucylated PLGA matrix could have an inhibitory effect on its release profile, in spite of the higher encapsulation efficiency (Chuah et al., 2013). Earlier, this drug –polymer attraction was evident in the UV spectrometric profile.

The results of in vitro release kinetics of the hydrophilic drug, doxorubicin and the hydrophobic drug curcumin from the modified and unmodified PLGA nanoparticles indicate that the majority of the drug, almost greater than 50% was retained inside the nanoparticles during the five day time period of the study. Justification for the efficacy of the formulations could be provided in accordance to the reports of Tewes et al that specified the release of the remaining drug molecules occurred following several weeks, contributed by the expected hydrolysis cum degradation of the polymer, PLGA (Tewes et al., 2007a). Hence all the modified PLGA formulations may lead to sustained release on an extended time scale.

In short, the in vitro release kinetics provided a fundamental understanding of the possible interactions between the drug –polymer matrix and the external environment in addition to the implications on the porosity of the nanoparticles on a molecular level and their influence on the mechanism and rate of drug release. In future, such information would facilitate in the predictive design and development of sustained delivery in in-vivo biological systems.

5.9.3 Therapeutic Efficacy of Drug Loaded Nanoparticles at In Vitro Conditions

5.9.3.1 Internalisation studies of drug loaded nanoparticles

The therapeutic effect of drug loaded nanoparticles depends upon the specificity, internalisation and retention of nanoparticles inside the target cells. Insufficient cellular uptake of a therapeutic, or therapeutic-loaded nanoparticles, leads to suboptimal intracellular therapeutic concentration, less effective chemotherapy and the potential for drug resistance. The administration of free drugs frequently fails to maintain the effective drug concentration within the cell on account of active extrusion of drug molecules from the cytoplasm to the outside of plasma membrane via Pgp, a 170kDa membrane associated glycoprotein. In accordance to Endicott et al and Gottesmann et al over expression of p-glycoprotein is one of the principle mechanisms that contribute to the multi drug resistant phenotype (Endicott and Ling, 1989). Overcoming this resistance by increasing the drug dose becomes impractical due to the dose limiting cytotoxic effects mediated by chemotherapeutics. Particulate drug delivery systems such as polymeric nanocarriers potentially improve the therapeutic ratio of cancer therapy without causing normal tissue side effects. The bottom line is that P-glycoprotein mediated recognisation and efflux of drugs happen while they are in the plasma membrane and not when the drug is located in the cytoplasm after endocytosis. The possibility of encapsulating a large payload of drugs within polymeric nanoparticles potentially prevents its exposure cum interaction with the cell membrane associated efflux transporters. The minimal amount of drug released from the nanocarriers doesn't activate the expression of p-glycoproteins, unlike in the case of free drug delivery, where an exodus of drug

molecules comes in contact with the plasma membrane. This is expected to enhance the accumulation and retention of drugs within multidrug resistant cancer cells and lead to the favourable modulation of the pharmacokinetic profile and biodistribution in comparison to free drugs in solution. Further it sustains the drug effect by promoting the slow, intracellular release of drug molecules from the nanoparticles localised within the cells. This was also explained by Semet et al and Desai et al in regard to the nano size range of particles facilitating the enhanced intracellular uptake of therapeutics to specific cellular location, a mechanism not very efficient with conventional formulations (Desai et al., 1996). In case of polymeric nanoparticles based on PLGA, an inherent capacity to overcome the multidrug resistance as explained by Sahoo and Labeshwar et al, favours their exploitation as chemotherapeutic drug carrier (Sahoo and Labhasetwar, 2005). Lie et al has also mentioned that the PLGA nanoparticle internalisation by the cells is mediated through endocytosis that transports drugs into cells more efficiently in comparison to passive diffusion of free drugs. In short, the nanoencapsulation of chemotherapeutic drugs within PLGA nanoparticles could improve the overall chemotherapeutic efficacy by moderating the mediation of multidrug resistance, to some extent.

Acharya et al has mentioned that PLGA nanoparticles enter the cells through internalisation and subsequently release the drug inside the cells. The interfacial phenomenon occurring between the nanocarrier and the cell surface mediate the potential of cellular uptake and possible intracellular transport mechanisms (Acharya and Sahoo, 2011). In concert with Conner et al, the simple physical proximity of the nanoparticles to the plasma membrane can cause the uptake or in a more specific mechanism through interactions with the receptors on the cell

surface (Acharya and Sahoo, 2011). The latter can result in different internalisation pathways. The basic mechanism which is common to all internalisation pathways includes the invagination of the cell membrane to engulf the nanoparticles present in the extracellular fluid. Subsequently, it is enclosed within an intracellular vesicle termed endosome and the process is termed as endocytosis. This early endosome decides the fate of the internalised nanoparticle by sorting them for either degradation or translocation into other organelles such as lysosomes or still for recycling towards the extracellular space. As the major proportion of internalized nanoparticles are trapped within endolysosomal compartment, the protection of the therapeutics from degradation in the acidic environment of lysosomes and exocytosis become critical in the context of nanocarrier mediated drug delivery. A highly relevant work by Panyam et al has ensured the successful delivery of the payload by PLGA based nanoparticles as it undergo rapid endolysosomal escape in addition to efficient internalisation (Panyam et al., 2002). Panyam et al has explained about the selective surface charge reversal of the PLGA based nanoparticles in the acidic endolysosomes. Instead of opening the endolysosomal vesicle, PLGA based nanoparticles induce a localised destabilisation of the endolysosomal membrane at the point of contact followed by the extrusion of the nanoparticles through the membrane. Following their escape, nanoparticles are retained intracellularly in the cytoplasm and slowly release the drugs leading to sustained therapeutic effect. This escape of nanocarrier from the endosomal vesicle is necessary for drugs which exercise its pharmacological action in the cytoplasm. Doxorubicin intercalates with the nuclear DNA and disrupts the action of Topoisomerase II following diffusion into the nucleus from the cytoplasmic compartment. Curcumin mediates its

chemotherapeutic effect through epigenetic modifications such as DNA methylation histone acetylation and activation of transcription factors that necessitate the translocation to nucleus through the cytoplasm. According to the aforementioned uptake experiments of differently modified PLGA nanoparticles, it is anticipated that the modification of PLGA nanoparticles could result in greater cytoplasmic localisation and enhance the therapeutic efficacy of drugs which require cytoplasmic delivery for chemotherapeutic action, such as doxorubicin and curcumin.

Doxorubicin and curcumin functioned as a fluorescence probe facilitating the visualisation of the invitro cancer targeting of the formulated nanoparticles through the uptake experiments, as provided in Figure 31A and 31B. Confocal microscopy demonstrated the rapid internalisation of drugs, doxorubicin and curcumin, facilitated within 3 h of incubation with C6 cells following their delivery by PLGA based modified and unmodified nanoparticles. The confocal images ensured reasonable cellular internalisation of PLGA and modified PLGA nanoparticles as evident from the adequate distribution of drug fluorescence within the whole volume of the cell. This was in accordance to the previously established uptake proficiency of all the three modifications of PLGA. However, the possibility of variations in uptake proficiency following drug encapsulation cannot be overruled as the mere presence of drug molecules on the nanoparticle surface provides ample opportunities for the breakage and renewal of several different non covalent interactions between drug molecule, nanoparticle surface and cellular membrane. Additionally, the increase in nanoparticle size following drug encapsulation can also affect the uptake proficiency. On a closer inspection of the uptake images, a correlation could be achieved between the fluorescence intensity and the drug

encapsulation efficiency of formulated nanoparticles. As expected, magnitude of fluorescence intensity was maximised within cells treated with unmodified PLGA nanoparticles containing doxorubicin and mucin modified PLGA nanoparticles containing curcumin, in accordance to their highest encapsulation efficiency. A deviation from the expected pattern could be observed with thiolated PLGA nanoparticles encapsulating doxorubicin. The reduced doxorubicin fluorescence observed with thiolated PLGA nanoparticles, in spite of highest encapsulation efficiency among the different modifications, could only be due to the lower amount of thiolated PLGA nanoparticles taken up by the cells. As explained by Li et al the exact mechanism behind thiol mediated uptake is unclear and is thought to proceed through interactions with exofacial thiols, followed by standard endocytic pathways (Li and Takeoka, 2014). As the thiol moieties present on the modified PLGA nanoparticle surface are already engaged in electrostatic interactions with the doxorubicin molecules, further interactions of thiol modified nanoparticles with the exofacial thiols are compromised and hence reduce the cellular uptake. Also, the surface charge variations following the drug adsorption can also lead to altered uptake phenomenon. All other formulations demonstrated reasonable drug fluorescence intensity which seems to imply the adequate intracellular distribution and retention of the drug required for the therapeutic efficacy.

5.9.3.2 Cytotoxicity

The cytotoxic action of the majority of chemotherapeutic drugs proceeds through inhibition of DNA synthesis and interference in the process of cell division and metabolism of rapidly dividing cells such as tumor neoplasm.

However this mechanism of chemotherapeutics, places the healthy, proliferating cells of bone marrow, skin and intestinal mucosa at greater risk of tissue damage.

For instance, Doxorubicin, known under the brand name of Adriamycin is the most potent anti cancer drug ever developed. It produces toxicity by acting on the nucleic acids of diving cells. More specifically, prevents the replication and transcription in rapidly growing cancer cells by inhibiting DNA and RNA synthesis following intercalation between the base pairs in DNA strands. The structural features of the doxorubicin enable rapid intercalation of the anthroquinone planar ring in to the double stranded DNA in addition to the electrostatic interactions between the positively charged mannose amine of drug moiety and the negatively charged phosphate diester groups of DNA. Secondly, doxorubicin prevents the relaxation of supercoiled DNA by inhibiting the enzyme Topoisomerase-II which forms an additional mechanism of blocking DNA transcription and replication. Most importantly, the oxidative induced damaging effect on DNA, proteins and cell membrane lipids via forming iron mediated free radicals forms the major reason behind doxorubicin mediated toxicity and side effects. Standard care treatment by conventional doxorubicin includes systemic administration in the range of 10-50mg/m^2 (Barenholz, 2012).

An emerging alternative in chemotherapy is the use of phytochemicals, such as curcumin and betulinic acid, favoured for its clinically established safety profile that tolerates large dosage regimen. The characteristic feature of curcumin and betulinic acid cytotoxicity is the temporal and dose dependent inhibition of cell proliferation by the induction of cell death through various pathways. Molecular mechanisms of

curcumin induced cytotoxicity constitute a complex phenomenon including the generation of reactive oxygen species, down regulation of BcL-XL and IAP, the release of cytochrome c and inhibition of Akt (Woo et al., 2003). More specifically at a cellular level, the nutraceutic curcumin result in the cell cycle arrest by reducing the S phase of mitosis via inducing a G2/M block. Direct mitochondrial alterations, formation of reactive oxygen species, cell cycle arrest, modulation of BCL-2 and BAX levels, topoisomerases I• and II• have been suggested for the cell death mechanism exhibited by Betulinic acid (Fulda and Debatin, 2000).

Whether it is the anthracycline antibiotic, Doxorubicin or the comparatively safe phytochemicals, curcumin and betulinic acid, the long term clinical usages of these drugs are severely compromised due to multiple reasons. In case of anthracyclines, if the acute cardiomyopathy and related toxicities jeopardise the drug administration, the formulatory challenges, poor aqueous solubility, tissue penetration and absorption are the blocking factors associated with hydrophobic phytochemicals. Additionally, multidrug resistance associated rapid systemic clearance pose a common challenge compromising the chemotherapeutic efficacy of all the three drugs, simultaneously. As a consequence, the drugs could maintain the intracellular concentration only transiently while administered as a free solution and subsequently shortens its therapeutic effect. In addition, free drugs, following passive diffusion, predominantly accumulate in lysosomes on account of the pH gradient mediated intracellular compartmentalisation as highlighted by Duvvuri et al (Duvvuri and Krise, 2005). Subsequently, the free drug molecules undergo degradation and exhibit compromised cytotoxic potential.

Encapsulating the chemotherapeutics within a suitable carrier seems promising in terms of increasing the therapeutic efficacy by minimising exposure to the non pathological sites of the body and by overcoming multidrug resistance. Despite the clinical potential of particulate drug delivery systems, therapeutic efficacy of microparticles is limited to local administration and implantation and liposomal formulations exhibit untimely drug release. Also, the drug-polymer conjugates suffer from undesirable modifications in in-vivo activity. Alternatively, the use of solubilising excipients such as cremophor, DMSO, cyclodextrin etc for the delivery of hydrophobic drugs demand large quantities of the complexation agent, leading to additional formulation based toxicity. All these factors collectively contributed to the choice of polymeric nanoparticles as delivery vehicles owing to the possibility of circulation through narrow capillaries, stabilisation of drugs prone to systemic degradation, passive targeting and retention as a result of EPR effect and enhanced intracellular delivery via increased uptake. Enhanced permeability and retention effect was first described by Matsumura and Maeda et al and facilitate the selective extravasation and accumulation of macromolecules, including drug carriers in the size range of 10-500nm through the highly permeable tumor blood vessels with compromised lymphatic drainage (Matsumura and Maeda, 1986).

Based on the reported literature of chemotherapeutic applications of polymeric nanocarriers, PLGA based nanoparticles seem to enhance the cytotoxicity of free drugs, at in vitro and in-vivo conditions. The endocytosis mediated uptake mechanism and the slow drug release profile of PLGA based nanoparticles together

contribute to the bypass of drug resistance seen within cancer cells and thereby enhance the pharmacokinetic and pharmacodynamic profile of therapeutics. This feature was presented in the reports of Panyam et al that discussed about the improved intracellular delivery of PLGA nanoparticles following endosomal escape facilitating slow and sustained delivery of drugs within the cytosol (Panyam et al., 2002). Most importantly, this mechanism provides therapeutic efficacy comparable to those obtained with higher extracellular concentration of free drugs and simultaneously overcome the free drug associated cell resistance and dose limiting toxicities. For instance, Lie et has highlighted about the enhanced antiproliferative potential of functionalised and non functionalised drug encapsulated PLGA nanoparticles compared to free drugs at higher concentration (Lei et al., 2011).

The basic step towards understanding the chemotherapeutic efficacy of drug loaded nanoparticles involves cell culture studies. Measuring the cell proliferation as an index of cell viability via MTT assay provided the rapid assessment of drug/drug loaded nanoparticle sensitivity towards the specific cell line studied. Here, lower cell viability corresponded to a better antitumor therapeutic effect. Unlike clonogenic assays, MTT assay cannot determine the cytostatic effect of chemotherapeutic drugs. Nevertheless, a favourable correlation could be obtained between the in vitro chemo sensitivity on rat C6 glioma cell line via MTT assay and the clinical response in human glioma as in the reports of Hand et al (Hand et al., 1998). Further, Hwang et al has mentioned high sensitivity (91%) and specificity (78%) for this viability assay (Hwang et al., 1993). Hence justifies the feasibility of methyl tetrazolium MTT assay in the evaluation of the chemotherapeutic efficacy of

doxorubicin, curcumin and betulinic acid loaded modified and unmodified PLGA nanoparticles against C6 rat glioma cell lines.

The selection of the drug concentrations corresponded to the range of known cytotoxic potential of the particular drug studied. According to the reported literature, doxorubicin, curcumin and betulinic acid exerts its cytotoxic potential in the range of 0.2-10µM (IC_{50} value), 10-100µM, 30-300µM respectively (Zuco et al., 2002), (Woo et al., 2003) and (Bache et al., 2011). All the three drugs in their free and nano encapsulated form has shown a dose dependent increase in cytotoxicity. Importantly, all the three modifications of PLGA nanoparticles surpassed the unmodified PLGA nanoparticles and the free drugs in terms in vitro therapeutic efficacy. The results of MTT viability assay clearly indicated that the cytotoxicity was most pronounced in cells exposed to drug loaded nanoparticles, while toxicity reduced to lower values when exposed to relatively equal concentration of drugs in their free form. The reduced antiproliferative effect of the native drugs obtained in our study could be correlated to its poor dissolution in physiological medium and the short duration of its intracellular retention. Free drugs are rapidly pumped off the cell cytosol by P-glycoprotein, which participates in the development of resistance to chemotherapy. Moreover, the availability of free drugs at its intracellular site of action is dependent on a passive diffusion mechanism. The limiting factors for this passive diffusion process are the low dissolution state of curcumin/betulinic acid and the high ionisation state of doxorubicin, respectively, at the physiological pH. In contrast, the greater toxicity of free drugs via the nano-sized particles means that there was a significant reversal of drug resistance as

explained above. Nanoparticles could reduce the MDR that characterizes many anticancer drugs, by lowering drug efflux from the cells through a mechanism of cell internalization called endocytosis.

In case of doxorubicin, among the three different modifications, glucosylated PLGA has shown the maximum cell death at lower concentration of 3.6µm while mucylated PLGA nanoparticles produced equivalent cell death at higher concentrations of 5.5µm, 9µM and 13µM respectively, as provided in Figure 32A. This was in correspondence to the rapid drug release and efficient uptake exhibited by glucosylated PLGA nanoparticles in comparison to the remaining doxorubicin loaded PLGA formulations. As PLGA based nanoparticle uptake is concentration dependent, the increased quantity of mucylated PLGA nanoparticles for producing higher drug concentration could possibly result in the uptake of more number of mucylated nanoparticles that subsequently release higher dose of drug within the cytoplasm of C6 cells (Davda and Labhasetwar, 2002). This explains for the equivalent cell death observed in case of mucylated PLGA nanoparticles at higher doxorubicin concentrations.

In case of curcumin the drug encapsulated nanoparticles exhibited almost double fold increase in cytotoxicity when compared to the free drug, as provided in Figure 32B. Among the three different modifications of PLGA nanoparticles, thiolated version has induced the maximum cell death at all the concentration ranges tested (except at 80µM). This again corresponds to the maximised release and uptake of thiolated PLGA nanoparticles. The release profile of PLGA and mucylated PLGA nanoparticles was almost similar that rationalised an

almost equivalent induction of cytotoxicity by these two different curcumin nanoformulations.

In case of betulinic acid, the cytotoxicity of both the free drug and nano encapsulated formulations were much less at low drug concentrations, as provided in Figure 32C. When the concentration of the drug was increased, an almost linear increase in the toxic potential of free and encapsulated form of betulinic acid was observed. This could be the combined result of the increase in the available drug concentration and increased uptake as PLGA based nanoparticles display concentration dependent increase in uptake. All the three modifications were successful in enhancing the cytotoxic profile of bare PLGA nanoparticles at concentrations of 40µM and 60µM of betulinic acid. Further, we observed a marginal increase in cytotoxicity of thiol and glucose modified PLGA nanoparticles when compared to mucylated PLGA nanoparticles. In accordance to doxorubicin and curcumin results, this observation could also be generalised in terms of higher release profile coupled with enhanced uptake. The data demonstrate higher in vitro therapeutic efficacy of both modified and unmodified PLGA nanoparticles when compared to the free betulinic acid.

The cytotoxicity analysis was performed on a range of drug concentrations in order to find the values closer to 50% cell death or IC_{50} value which corresponded to 12.5µM, 76µM and 80µM for Doxorubicin Curcumin and Betulinic Acid respectively. Here, instead of the released drug concentration, the free drug concentration was kept equal to the total drug encapsulated in the nanoparticles. This was justified as the actual drug released inside the cytoplasm can

vary from the theoretical value owing to the presence of enzymes and reductive cytoplasmic conditions which can definitely accelerate the release profile.

Hence, we conclude that the overall cytotoxic data was in accordance to the reports of Panyam et al that specified the therapeutic potential of nanoparticle encapsulated drug to be the product of nanoparticle uptake, intracellular distribution and the dose of drug release from the endocytosed nanoparticles within the cytosol (Panyam et al., 2002). This efficient uptake, high loading efficacy and rapid release can collectively contribute to the sensitization of drug resistant cancer cells and result in the higher therapeutic index of the drug loaded nanoparticles by overcoming the shortcomings of conventional doxorubicin, curcumin and betulinic acid formulations.

5.9.3.3 LIVE DEAD Assay

The loss of membrane integrity is a common indicator of cell death owing to the vital functions associated with the plasma membrane such as intracellular transport and permeability barrier. Darzynkiewicz has recognised the physical integrity of plasma membrane and the loss of transport function as the major features discriminating dead from the live cells (Darzynkiewicz et al., 1992). Pioneered by the early works of Brunning et al, several techniques using fluorescent dyes to determine cell viability and cytotoxicity has been established (Bruning et al., 1980). One such analysis of cell membrane integrity is based on the ability of the cells to extrude fluorescent dye compounds, which when applied at low concentrations do not pass through intact membranes. Nucleic acid stains are generally used in most of the membrane integrity analysis. This is based on the availability of high concentration of nucleic acids within the cells and the multifold

enhancement in the fluorescence of dye molecules following intercalation with nucleic acids. Hence clearly separates the dead from intact, living cells.

Among the wide diversity of impermeant nucleic acid stains, propidium iodide and ethidium bromide have been extensively used. EthD-1, a cationic plasma membrane impermeant dye, can only diffuse into cells with open pores or lesions that indicate damaged membranes of dying or dead cells. Following intercalation into double or single stranded nucleic acids with a double helical character, it displays a 40-fold enhancement of fluorescence, thereby staining the dead cells with bright red fluorescence (ex/em ~495 nm/~635 nm). EthD-1 undergoes rapid extrusion by the intact plasma membrane efflux pumps present in the live cells and hence is retained only by dead cells following nucleic acid intercalation.

Similarly for assessing cell viability, acetoxymethyl diacetyl ester of calcein, Calcein AM, a derivative of fluorscein, has emerged as the primary indicator following the replacement of Cr-release method. This was on account of the superior cell retention and relative insensitivity of calcein AM fluorescence towards pH gradient in the physiological range. Live cells are recognised by the presence of ubiquitous intracellular esterase activity that converts the virtually nonfluorescent cell-permeant calcein AM to the intensely fluorescent calcein. Subsequently, the lipophilic polyanionic calcein is retained only by live cells with intact plasma membrane as it inactivates the multidrug resistance protein. Dead or dying cells with damaged membrane rapidly leak the dye even though negligible esterase activity is retained. Hence only the live cells fluoresce with an intense uniform green colour (ex/em ~495 nm/~515 nm). As the loss of esterase activity is an early apoptotic event

that occurs before phosphatidyl serine exposure cum membrane lesions, the emitted green fluorescence strongly correlate to the number of living cells with active esterase activity. Hence Calcein AM functions as an activity and cell integrity probe that determine both enzymatic activity, which is necessary to activate their fluorescence and the cell membrane integrity, which is a prerequisite for the retention of intracellular fluorescence products.

In order to simultaneously detect live and dead cells, Molecular Probes have developed the Live Dead Viability/Cytotoxicity Assay kit for the determination of cell viability based on these physical and biochemical properties of cells. This assay facilitate a dual colour fluorescence based cell viability analysis, based on the simultaneous visualisation of live and dead cells using two complementary fluorescent reporter molecules that estimate the established indices of cell viability—intracellular esterase activity and plasma membrane integrity. In other words, it is a dye permeability assay based indication of intracellular enzyme activity and cell membrane integrity. Calcein AM and ethidium homodimer (EthD-1) functioned as the optimal dyes for this analysis. Sensitivity of this assay is high on account of minimal background fluorescence as the dyes are virtually non-fluorescent before interacting with the cells. The assay used these dyes in combination to simultaneously visualise the cells with intact membrane and active esterases though the green fluorescence and the cells with damaged membranes through red fluorescence. This red/green distinction was particularly easy to perceive by the eye in the fluorescence microscope.

According to Dive et al, conventionally the green positive and red negative cells are interpreted as viable while the red positive, green negative cells

are categorized as dead. Interestingly, a third population of cells was identified that displayed minimal green or red to orange fluorescence (Dive et al., 1990).

During apoptosis, cell membrane is subjected to a number of physical perturbations such as rapid loss of membrane extensions resulting in the smooth and round cell surface, lipid peroxidation, membrane fluidity and order changes etc that induced a gradual increase in permeability to vital stains such as ethidium bromide. Presumably, this step by step permeabilisation of plasma membrane corresponds to structural changes that progressively become more prominent. As a consequence, the access of ethidium bromide into cells is initially compromised modestly; resulting in a faint cellular fluorescence but eventually culminates in complete staining of the cell (Nelson et al., 2011). Further analysis on the kinetics of cell membrane permeability changes by Dive et al has specified that cells first lose green before acquiring red fluorescence. In addition, during intermediate membrane permeabilisation stages, Dive et al has mentioned about the selective passage of one probe rather than the other resulting in cell populations with more than red-green fluorescence extremes (Dive et al., 1990). Intercalating this reported literature, a possible explanation for the observed gradations in standard red-green fluorescence could be provided on the basis of the early exit of calcein followed by the gradual increase in access to external ethidium bromide, which resulted in the conversion of initial faint green fluorescence to orange in colour. This probably signifies the occurrence of early stage apoptosis in such cells. As the apoptosis progressed, gradual permeabilisation of cell membrane resulted in the accelerated entry of ethidium bromide that leads to the complete red fluorescence.

As an application of this assay, investigation of the qualitative determination of C6 cell viability following exposure to doxorubicin, curcumin and betulinic acid loaded modified and unmodified PLGA nanoparticles was performed and compared against the respective free drugs. The concentration closer to 50% cell death was selected from the previous MTT assay and it corresponded to 12.5µM for Doxorubicin, 76µM for curcumin and 41µM for betulinic acid. However, unlike MTT assay where the standard 24h time period was followed, live-dead assay had followed an increased time period of 30h. The time period was increased so as to permit the C6 cell population to undergo atleast one round of replication following nanoparticle exposure. During cell replication, an increase in the entry of drug and drug loaded nanoparticles into the nucleus can happen and this would definitely help to produce the maximum cytotoxicity as the doxorubicin and phytochemicals act on cell replication machinery. The control cells exposed to physiological buffer, PBS, displayed intense bright green fluorescence that established reasonable esterase activity in the cells under study. Subsequently, ruled out all possibilities of low esterase active cell populations produced by the C6 cell lines.

All the PLGA based doxorubicin and curcumin formulations displayed greater number and intense fluorescing dead cells in comparison to free drug as provided in Figure 33A and 33B. On the contrary, free doxorubicin and curcumin displayed dead cells with rather faint red fluorescence indicating early stage of apoptosis, while almost half of the population emitted bright green fluorescence from live cells. This directly indicates the availability of therapeutic doses of curcumin within the cytosol following the sustained release of drugs from the internalised nanoparticles. At the same time, free doxorubicin and curcumin

concentration failed to reach therapeutic levels within the cells due to the inability of passage of free drugs in solution through the plasma membrane. The thiolated PLGA nanoparticles produced the maximum population of bright red fluorescing dead cells, followed by mucylated PLGA nanoparticles in accordance to the MTT assay.

In case of betulinic acid, as provided in Figure 33C, the free drug resulted in more number of dead cells compared to the free curcumin, at a comparatively lower drug concentration. Nevertheless, all the PLGA based nanoencapsulated betulinic acid formulations displayed far better toxic effects as displayed by the red dead cells, in comparison to the free drug. The images confirmed the highest toxic potential of glucosylated nanoparticles followed by thiolated nanoparticles in accordance to the maximum bright red cells displayed.

Hence all the PLGA based drug formulations displayed greater number and intense fluorescing dead cells in comparison to the free drug. These differences in cytotoxicity had been highlighted in several literature reports based on the mechanism of cellular uptake. The free drug molecules enter the cells through passive diffusion, which is subjected to the efflux action of multidrug proteins and subsequently fails to maintain therapeutic concentrations. On the contrary, cellular uptake of drug encapsulated nanoparticles occur through non specific endocytic pathways which can circumvent this pumping action of multi drug resistant proteins which are always present in cancer cell plasma membranes.

Another significant observation was the comparatively large size of cells treated with free drugs and drug loaded PLGA based nanoformulations. Several lines of evidence from reported literature suggests about the mitotic catastrophe induced by the low doses of chemotherapeutic drugs such as doxorubicin

(Eom et al., 2005). Castedo et al has proposed that mitotic catastrophe is the cell death following abnormal mitosis in response to the combination of deficient cell cycle check points and cellular damage (Castedo et al., 2004). As cell death induced by plant phytochemicals proceeds through the cell cycle arrest, a causative factor of mitotic catastrophe, the enlarged size of betulinic acid and curcumin treated cells are not a surprise. The large size can be the result of abnormal mitosis induced multiple micro nuclei and decondensed chromatin and forms an irreversible trigger for the cell death. Alternatively, the large size can also be the result of influx of water molecules and extracellular ions which usually precedes the cell death process.

A direct correlation could be obtained between the MTT assay based cytotoxicity of nanoencapsulated drug formulations and the live dead assay based visualisation of this chemotherapeutic potential, at an invitro level. Hence, the current viability determination complimented the MTT assay and ensured that the results obtained in the colorimetric cytotoxicity assay was not an artefact. The consistency in the increased cytotoxicity of drug loaded nanoparticles when compared to free drugs was established with these multiple techniques.

5.9.3.4 Quantification of Cell Death by Flow Cytometry

Cytotoxicity generally refers to the cell death inducing potential of a chemical compound. This term does not specify any particular cell death mechanism. Nevertheless, strategically targeted cancer therapy through chemotherapeutic agents can elicit different cell death mechanisms such as autophagy, apoptosis, mitotic catastrophe, necrosis and senescence (Eom et al., 2005). Apoptosis has been considered as the basic mechanism of chemotherapy-induced cell death. This process refers to the naturally occurring developmental cell

death responsible for maintaining tissue homeostasis by regulating the equilibrium between cell proliferation and cell death. Cell membrane blebbing, cell shrinkage, chromatin condensation, and nucleosomal fragmentation characterise the morphological features of an apoptotic cell. Normal cells respond to the chemotherapeutic drug abuse by undergoing cell cycle arrest, DNA repair or in extreme conditions cell death by promoting apoptosis; all coordinated through the guardian of genome, p53 protein (Lowe and Lin, 2000). However, as majority of cancer cells have aberrant cell signalling pathways, such as of p53, which is a prerequisite for suppressing apoptosis during tumor development; it can lead to the concurrent reduction in the cancer cell sensitivity towards chemotherapeutic drugs. Hence alternative cell death pathways, such as necrosis are gaining importance in terms of improving treatment sensitivity.

Necrosis occurs when cells are subjected to drastic variance from physiological conditions and results in features such as the plasma membrane destruction. Under physiological conditions, toxic products and lytic viruses induce direct damage to the plasma membrane. This mechanism is initiated by the failure of plasma membrane to support homeostasis which leads to the progressive influx of water molecules and extracellular ions. Intracellular organelles, particularly mitochondria and the whole cell swell which culminate in the rupture or lysis of cell. As plasma membrane can no longer remain intact, leakage of cytoplasmic contents including lysosomal enzymes occurs. Emerging evidence suggests that necrosis is the preferred pathway of cell death for chemotherapy, under in vivo conditions as it elicits pro inflammatory response that recruits cytotoxic immune cells to the tumor

site. Hence quantifying the extent of necrosis can give a better estimation of the in vivo efficacy of chemotherapeutic drugs (Ricci and Zong, 2006).

However, it is worth mentioning that cell death induced by chemotherapeutics often do not have the classical features of either apoptosis or necrosis. Collins et al and Melamed et al had provided examples of cell death where the pattern of morphological and biochemical changes had features of both the apoptosis and necrosis, instead of resembling either of the typical process (Collins et al., 1992) & (Melamed et al., 1991). Additionally, Darzynkiewicz had stated that the death of epithelial type cells are more complex and difficult to categorise as exclusively apoptotic or necrotic (Darzynkiewicz et al., 1992). Further Wang et al has specified that C6 glioma cells treated with querceptin nano liposomes showed a cell death pattern associated with necrosis without apoptosis (Wang et al., 2012c). Based on these reported literature, the current investigation attempted to quantify cell death without discriminating apoptotic and necrotic cells.

The optimal method for estimation of cell death depends on several factors such as the cell system, nature of the cell death induced, mode of cell death, particular information required and the technical constrictions. Analysis of plasma membrane integrity through the exclusion of propidium iodide offer a simple and inexpensive method to determine both necrotic and cells advanced in apoptosis (Darzynkiewicz et al., 1992). This assay is based on the active effluxing of charged dyes such as propidium iodide in cells with intact plasma membrane, which results in the selective staining of dead cells alone, as live cells exhibit minimal dye uptake following short incubation with such dyes. However cells in their early stage of cell death (pertaining

to the faint green to orange fluorescing cells of live dead assay), are capable of effluxing propidium iodide owing to their intact plasma membrane. Hence such population of apoptotic cells might be erroneously considered as viable. Propidium iodide enter the cytoplasm through the membrane lesions in dead cells and upon binding the DNA, exhibit intense fluorescence with excitation at 536nm and emission at 617nm. Flow cytometry can provide a simple, rapid and quantitative estimation of cell death based on the fluorescence of DNA bound propidium iodide. The potential of flow cytometry for the rapid, individual analysis of vast number of cells enabled its choice as an ideally adapted technique for cell death quantification. Following the inspection of cell death through aforementioned fluorescent microscopy assisted live dead differentiation, further insight to the precise quantification of cell death becomes crucial in the context of determining the most efficient among the different drug encapsulated PLGA based modified nanoparticles, in terms of invitro chemotherapy.

The results of flow cytometry indicate that all the PLGA based nano encapsulated form of doxorubicin maintain the activity of the drug and is twice as effective as the free drug. The double fold increase in the cytotoxic potential of free curcumin and betulinic acid after PLGA nanoencapsulation were also confirmed by the flow cytometry. Moreover, the maximum toxic potential of doxorubicin, curcumin and betulinic acid became materialised through glucose, thiol and glucose modified PLGA nanoparticles respectively, as provided in Figure 34A, 34B and 34C. Here, the concentration of drugs varied from 12.5µM for doxorubicin to 76µM for curcumin and 41µM for betulinic acid respectively. However, another parameter has to be

considered here is the nanoparticle concentration. The most efficient formulation is the one that requires the minimal particle concentration to elicit the maximum cytotoxicity. Consideration of nanoparticle concentration will also help us to nullify the effect of varied drug concentration on the cytotoxicity profile. Then the scenario changes and it is the thiol modified doxorubicin loaded PLGA, mucin modified curcumin loaded PLGA and mucin modified betulinic acid loaded PLGA which turns out to be the most efficient formulation in terms of least nanoparticle concentration required.

The flow cytometric results were in agreement with the release profile, uptake experiments and MTT assay. An exception was found in the case of Doxorubicin, where thiol modified nanoparticles produced comparatively higher cell death when compared to mucylated PLGA nanoparticles that contradict the release and uptake data. However, the higher encapsulation efficiency of thiolated PLGA nanoparticles for Doxorubicin must not be forgotten, which in turn can produce higher dose of drug molecules from the internalised nanoparticles, in spite of lowered release. The drug released from the internalised thiolated particles can be more than the theoretical value as the electrostatic interactions which hold the surface adsorbed cationic doxorubicin to the anionic thiol moieties can become weaker in the reductive cellular cytoplasm. This can result in increased cytotoxicity even though uptake is lower.

Another interesting observation is the dissimilarity of cytotoxic values obtained through MTT assay and flow cytometry in case of mucin modified PLGA nanoparticles loaded with doxorubicin and curcumin respectively. This can be

explained on the basis of the growth curve of C6 cells, which doubles itself in every 30-40 hrs. An increased exposure time can lead to the selection and multiplication of the cancer resistant cell population and this can account for the decrease in observed cytotoxicity following increased duration of exposure.

Thus the three different modifications were equally efficient in enhancing the toxic potential of hydrophilic and hydrophobic drug encapsulated PLGA nanoparticles. The most efficient drug –particle combination in terms of higher cytotoxicity with least nanoparticle concentration turns out to be the doxorubicin encapsulated thiol modified PLGA nanoparticles, curcumin encapsulated mucin modified PLGA nanoparticles and betulinic acid encapsulated mucin modified PLGA nanoparticles respectively, as quantified by the flow cytometry. Furthermore, while determining the best among these three formulations, it is worth mentioning the reports of Zuco et al where a comparison between the therapeutic activity of betulinic acid and doxorubicin was provided (Zuco et al., 2002). The highlight was the selective antiproliferative activity of betulinic acid on neoplastic cells alone that induced minimal toxicity on normal cells while doxorubicin showed no such discrimination and proved damaging for healthy cells as well. Similarly, an interesting report by Ramachandran et al has signified the inhibition of proliferation of malignant as well as normal cells by curcumin, quite non- specifically, although the apoptotic effect is more pronounced in cancerous cells (Ramachandran et al., 2005). Although the percentage of cell death induced by betulinic acid was less when compared to curcumin, it should be acknowledged that the drug concentration was accordingly lower in case of betulinic acid. Most importantly, the p53 independent

cytotoxic action of betulinic acid, enable it to function as a broad spectrum chemotherapeutic drug. In fact, the lower potency of betulinic acid in comparison to doxorubicin become irrelevant in the context of its selective cytotoxicity and broad spectrum chemotherapeutic action against cell lines even clinically resistant to conventional antineoplastic drugs, such as melanoma. Considering all these factors, the current investigation concluded by projecting the mucin modified PLGA based nanoencapsulated formulation of the triterpene, betulinic acid, as the most efficient chemotherapeutic drug-particle combination, on an invitro chemotherapeutic scale. Concurrently the study projected the thiol modification as the most effective in terms of efficient encapsulation, intracellular uptake and release of hydrophilic as well as hydrophobic drugs from PLGA based nanoparticles evaluated in this study.

CHAPTER 6
SUMMARY AND CONCLUSION

6 SUMMARY and CONCLUSION

The drug resistant nature of cancer remains as a formidable challenge for the effectiveness of chemotherapy. Nanoparticle mediated drug delivery has been considered as a promising way of bypassing the chemo resistance. Injectable biodegradable and biocompatible copolymers of lactic and glycolic acid constitute an important advanced drug delivery system for week to month controlled release of both hydrophobic and hydrophilic drugs that display poor bioavailability. In fact, PLGA has the greatest clinical impact among the various controlled release polymer technologies. Thus, the need of the hour is the precise engineering of PLGA for encapsulating different therapeutics and thereby rendering them suitable for parenteral administration. Hence, potentially rescues an otherwise undeliverable drug. However, before developing an effective nanoparticle based drug carrier system for biomedical applications, an evaluation of several criteria including the precise control between biological, chemical and physical properties are necessary. Hence, the central dogma of drug delivery is to steer therapeutic carriers to target tissues or cells to achieve maximal therapeutic efficacy with minimal toxic effects. The success of each nanoparticle in meeting the clinical expectation is directly dependent on its hemocompatibility and the ability to overcome the host defence mechanism, the mononuclear phagocytic system. Despite the numerous advantages, PLGA suffers from several well characterised shortcomings that necessitated the modification of the polymer. In this context, emphasis was provided on the

potentiality of thiol, glucose and mucin as the surface modifiers that promoted the compatibility of PLGA nanoparticles, both in terms of physical and biological interactions. The dual role of thiol, glucose and mucin functionalities in bestowing the PLGA nanoparticles with adequate hemocompatibility parameters without compromising the ability to penetrate the cancer cells has been established. This enhanced compatibility cum cell penetrating capacity of the modified PLGA matrixes, prompted to determine its therapeutic potential when compared to unmodified PLGA nanoparticles, following chemotherapeutic drug encapsulation. Hence, the anti cancer activities of modified PLGA nanoparticles after encapsulating the chemotherapeutic drugs, doxorubicin, curcumin and betulinic acid were investigated. Three different chemotherapeutics of increasing hydrophobicity namely doxorubicin, curcumin and betulinic acid were chosen to analyse the interactions of these drugs to the hydrophobic core of PLGA matrix. The rationale for selecting doxorubicin, curcumin and betulinic acid for encapsulation inside PLGA and modified PLGA nanoparticles was based on the fact that nanoformulations are therapeutically active than the respective free drugs and also inhibit the development of MDR leading to increased antiproliferative activity in C6 cell lines. In their free form, frequent systemic administration of large doses of curcumin, betulinic acid and doxorubicin is necessary to achieve even a minimal therapeutic potential owing to the poor bioavailability and short half lives. Hence, the PLGA based nanoencapsulation of curcumin, betulinic acid and doxorubicin were attempted to determine the chemotherapeutic effectiveness of these different drug-nanoparticle combinations on exposure to glioma cells, C6 in vitro, after rendering the PLGA surface to varying hydrophilicity.

First of all, the amino groups of L-cysteine, glucosamine and mucin molecules were conjugated to the terminal carboxylic acid groups on PLGA to be followed by nanoparticle synthesis via standard solvent evaporation technique. Detailed in vitro experiments were performed to illustrate the significance of modified PLGA nanoparticles in terms of enhanced hemocompatibility and cellular uptake. All the three modifications were proved promising in controlling the PLGA nanoparticle-interactions with plasma proteins (opsonins) and blood components via hemolysis, thrombogenecity and complement activation experiments. Besides hemocompatibility, the modified and unmodified nanoparticles were also found to be cytocompatible with L929 and C6 cell lines. The fluorescent and confocal image analysis evaluated the extent of cellular uptake of nanoparticles into C6 cells. Specifically the combination of stealth properties and cellular internalization capacity of modified PLGA nanoparticles helped to propose it as a safe, efficient and multifunctional nanoplatform for disease specific intravenous drug delivery applications as far as in vitro experiments are concerned.

Subsequently, doxorubicin, curcumin and betulinic acid encapsulated nanoparticles were synthesised through solvent evaporation technique. Then the effect of modification on encapsulation efficiency and release kinetics of drugs from PLGA nanoparticles were considered. The physicochemical characteristics of the synthesised nanoparticles such as the size, polydispersity index, encapsulation efficiency and release kinetics were satisfactory in terms of drug delivery applications. Afterwards, the cellular uptake and cytotoxic potential of drug loaded PLGA nanoparticles on C6 cell lines, in correlation to the modification were

studied. The nanoencapsulation of drugs, doxorubicin, curcumin and betulinic acid within the PLGA based differently modified nanoparticles were successful in enhancing the therapeutic potential of the respective pure drugs in C6 cell lines, at in vitro scale. Finally, based on these characteristics, betulinic acid loaded mucin modified PLGA nanoparticles were identified as the most effective drug-particle combination in terms of in vitro chemotherapeutic activity, following the modification of the polymer, PLGA. Concurrently the study highlights the thiol based functionalisation of PLGA nanoparticles as the most effective modification in terms of efficient encapsulation, intracellular uptake and release of hydrophilic as well as hydrophobic drugs from PLGA based nanoparticles as evaluated in this study.

6.1 Future Prospects

In future, drug combination studies of curcumin with betulinic acid or doxorubicin could be attempted as the drug, curcumin, is considered to compromise the drug resistant nature of tumor cells. Also, the biodistribution of differently modified PLGA nanoparticles in comparison to control PLGA nanoparticles could be performed. Additionally, the in vivo pharmacokinetic parameters could be evaluated for the better understanding of the therapeutic benefits following modification.

REFERENCES

Acharya, S. & Sahoo, S. K. (2011) PLGA nanoparticles containing various anticancer agents and tumour delivery by EPR effect. *Advanced Drug Delivery Reviews,* 63**,** 170-183.

Aisha, A. F., Ismail, Z., Abu-Salah, K. M., Siddiqui, J. M., Ghafar, G. & Majid, A. M. A. (2013) Syzygium campanulatum korth methanolic extract inhibits angiogenesis and tumor growth in nude mice. *BMC complementary and alternative medicine,* 13**,** 168.

Albanese, A., Tang, P. S. & Chan, W. C. W. (2012) The Effect of Nanoparticle Size, Shape, and Surface Chemistry on Biological Systems. *Annual Review of Biomedical Engineering,* 14**,** 1-16.

Alexis, F. (2005) Factors affecting the degradation and drug-release mechanism of poly(lactic acid) and poly[(lactic acid)-co-(glycolic acid)]. *Polymer International,* 54**,** 36-46.

Alexis, F., Pridgen, E., Molnar, L. K. & Farokhzad, O. C. (2008) Factors affecting the clearance and biodistribution of polymeric nanoparticles. *Mol Pharm,* 5**,** 505-15.

Amoozgar, Z. & Yeo, Y. (2012) Recent advances in stealth coating of nanoparticle drug delivery systems. *Wiley Interdiscip Rev Nanomed Nanobiotechnol,* 4**,** 219-33.

Anand, P., Kunnumakkara, A. B., Newman, R. A. & Aggarwal, B. B. (2007) Bioavailability of curcumin: problems and promises. *Mol Pharm,* 4**,** 807-18.

Anand, P., Nair, H. B., Sung, B., Kunnumakkara, A. B., Yadav, V. R., Tekmal, R. R. & Aggarwal, B. B. (2010) Design of curcumin-loaded PLGA nanoparticles formulation with enhanced cellular uptake, and increased bioactivity< i> in vitro</i> and superior bioavailability< i> in vivo</i>. *Biochemical pharmacology,* 79**,** 330-338.

Anderson, J. M., Rodriguez, A. & Chang, D. T. (2008) Foreign body reaction to biomaterials. *Semin Immunol,* 20**,** 86-100.

Andersson, J., Ekdahl, K. N., Lambris, J. D. & Nilsson, B. (2005) Binding of C3 fragments on top of adsorbed plasma proteins during complement activation on a model biomaterial surface. *Biomaterials,* 26**,** 1477-1485.

Andrade, J. D. (1973) Interfacial phenomena and biomaterials. *Med Instrum,* 7**,** 110-9.

Aryal, S., Bkc, R., Dharmaraj, N., Bhattarai, N., Kim, C. H. & Kim, H. Y. (2006) Spectroscopic identification of SAu interaction in cysteine capped gold nanoparticles. *Spectrochimica Acta Part A: Molecular and Biomolecular Spectroscopy,* 63**,** 160-163.

Astete, C. E. & Sabliov, C. M. (2006) Synthesis and characterization of PLGA nanoparticles. *Journal of Biomaterials Science, Polymer Edition,* 17**,** 247-289.

Athanasiou, K. A., Niederauer, G. G. & Agrawal, C. M. (1996) Sterilization, toxicity, biocompatibility and clinical applications of polylactic acid/ polyglycolic acid copolymers. *Biomaterials,* 17**,** 93-102.

Avgoustakis, K., Beletsi, A., Panagi, Z., Klepetsanis, P., Karydas, A. & Ithakissios, D. (2002) PLGA–mPEG nanoparticles of cisplatin: in vitro nanoparticle

degradation, in vitro drug release and in vivo drug residence in blood properties. *Journal of controlled release,* 79**,** 123-135.

Bache, M., Zschornak, M. P., Passin, S., Keßler, J., Wichmann, H., Kappler, M., Paschke, R., Kaluderovic, G. N., Kommera, H. & Taubert, H. (2011) Increased betulinic acid induced cytotoxicity and radiosensitivity in glioma cells under hypoxic conditions. *Radiat Oncol,* 6**,** 111.

Barenholz, Y. C. (2012) Doxil®—the first FDA-approved nano-drug: lessons learned. *Journal of controlled release,* 160**,** 117-134.

Barichello, J. M., Morishita, M., Takayama, K. & Nagai, T. (1999) Encapsulation of hydrophilic and lipophilic drugs in PLGA nanoparticles by the nanoprecipitation method. *Drug development and industrial pharmacy,* 25**,** 471-476.

Beck, L. R., Pope, V. Z., Tice, T. R. & Gilley, R. M. (1985) Long-acting injectable microsphere formulation for the parenteral administration of levonorgestrel. *Adv Contracept,* 1**,** 119-29.

Bernacca, G. M., Gulbransen, M. J., Wilkinson, R. & Wheatley, D. J. (1998) In vitro blood compatibility of surface-modified polyurethanes. *Biomaterials,* 19**,** 1151-65.

Bertrand, N. & Leroux, J. C. (2012) The journey of a drug-carrier in the body: an anatomo-physiological perspective. *J Control Release,* 161**,** 152-63.

Besseling, N. (1997) Theory of hydration forces between surfaces. *Langmuir,* 13**,** 2113-2122.

Betancourt, T., Brown, B. & Brannon-Peppas, L. (2007) Doxorubicin-loaded PLGA nanoparticles by nanoprecipitation: preparation, characterization and in vitro evaluation.

Betancourt, T., Shah, K. & Brannon-Peppas, L. (2009) Rhodamine-loaded poly (lactic-co-glycolic acid) nanoparticles for investigation of in vitro interactions with breast cancer cells. *Journal of Materials Science: Materials in Medicine,* 20**,** 387-395.

Bodmeier, R. & Mcginity, J. (1988) Solvent selection in the preparation of poly (DL-lactide) microspheres prepared by the solvent evaporation method. *International journal of pharmaceutics,* 43**,** 179-186.

Bondioli, L., Costantino, L., Ballestrazzi, A., Lucchesi, D., Boraschi, D., Pellati, F., Benvenuti, S., Tosi, G. & Vandelli, M. A. (2010) PLGA nanoparticles surface decorated with the sialic acid,< i> N</i>-acetylneuraminic acid. *Biomaterials,* 31**,** 3395-3403.

Brigger, I., Dubernet, C. & Couvreur, P. (2002) Nanoparticles in cancer therapy and diagnosis. *Adv Drug Deliv Rev,* 54**,** 631-51.

Bruning, J. W., Kardol, M. J. & Arentzen, R. (1980) Carboxyfluorescein fluorochromasia assays. I. Non-radio actively labeled cell mediated lympholysis. *Journal of immunological methods,* 33**,** 33-44.

Budhian, A., Siegel, S. J. & Winey, K. I. (2007) Haloperidol-loaded PLGA nanoparticles: systematic study of particle size and drug content. *International journal of pharmaceutics,* 336**,** 367-375.

Cartiera, M. S., Johnson, K. M., Rajendran, V., Caplan, M. J. & Saltzman, W. M. (2009) The uptake and intracellular fate of PLGA nanoparticles in epithelial cells. *Biomaterials,* 30**,** 2790-2798.

Castedo, M., Perfettini, J.-L., Roumier, T., Andreau, K., Medema, R. & Kroemer, G. (2004) Cell death by mitotic catastrophe: a molecular definition. *Oncogene,* 23**,** 2825-2837.

Cavadas, M., Gonzalez-Fernandez, A. & Franco, R. (2011) Pathogen-mimetic stealth nanocarriers for drug delivery: a future possibility. *Nanomedicine,* 7**,** 730-43.

Cenni, E., Granchi, D., Avnet, S., Fotia, C., Salerno, M., Micieli, D., Sarpietro, M. G., Pignatello, R., Castelli, F. & Baldini, N. (2008) Biocompatibility of poly (d, l-lactide-< i> co</i>-glycolide) nanoparticles conjugated with alendronate. *Biomaterials,* 29**,** 1400-1411.

Ceonzo, K., Gaynor, A., Shaffer, L., Kojima, K., Vacanti, C. A. & Stahl, G. L. (2006) Polyglycolic acid-induced inflammation: role of hydrolysis and resulting complement activation. *Tissue engineering,* 12**,** 301-308.

Chang, J., Paillard, A., Passirani, C., Morille, M., Benoit, J.-P., Betbeder, D. & Garcion, E. (2012) Transferrin adsorption onto PLGA nanoparticles governs their interaction with biological systems from blood circulation to brain cancer cells. *Pharmaceutical research,* 29**,** 1495-1505.

Chaturvedi, P., Singh, A. P. & Batra, S. K. (2008) Structure, evolution, and biology of the MUC4 mucin. *FASEB J,* 22**,** 966-81.

Chen, S., Pieper, R., Webster, D. C. & Singh, J. (2005) Triblock copolymers: synthesis, characterization, and delivery of a model protein. *International journal of pharmaceutics,* 288**,** 207-218.

Chen, X., Lee, G. S., Zettl, A. & Bertozzi, C. R. (2004) Biomimetic engineering of carbon nanotubes by using cell surface mucin mimics. *Angewandte Chemie International Edition,* 43**,** 6111-6116.

Chittasupho, C., Xie, S. X., Baoum, A., Yakovleva, T., Siahaan, T. J. & Berkland, C. J. (2009) ICAM-1 targeting of doxorubicin-loaded PLGA nanoparticles to lung epithelial cells. *Eur J Pharm Sci,* 37**,** 141-50.

Choi, S. W., Kim, W. S. & Kim, J. H. (2003) Surface modification of functional nanoparticles for controlled drug delivery. *Journal of dispersion science and technology,* 24**,** 475-487.

Chouhan, R. & Bajpai, A. (2009) Real time in vitro studies of doxorubicin release from PHEMA nanoparticles. *J Nanobiotechnology,* 7**,** 5.

Chuah, L. H., Billa, N., Roberts, C. J., Burley, J. C. & Manickam, S. (2013) Curcumin-containing chitosan nanoparticles as a potential mucoadhesive delivery system to the colon. *Pharmaceutical development and technology,* 18**,** 591-599.

Clawson, C., Huang, C.-T., Futalan, D., Martin Seible, D., Saenz, R., Larsson, M., Ma, W., Minev, B., Zhang, F. & Ozkan, M. (2010) Delivery of a peptide via poly (d, l-lactic-< i> co</i>-glycolic) acid nanoparticles enhances its dendritic cell–stimulatory capacity. *Nanomedicine: Nanotechnology, Biology and Medicine,* 6**,** 651-661.

Cohen-Sela, E., Chorny, M., Koroukhov, N., Danenberg, H. D. & Golomb, G. (2009) A new double emulsion solvent diffusion technique for encapsulating hydrophilic molecules in PLGA nanoparticles. *Journal of controlled release,* 133**,** 90-95.

Collins, R. J., Harmon, B. V., Gobé, G. C. & Kerr, J. F. (1992) Internucleosomal DNA cleavage should not be the sole criterion for identifying apoptosis. *International journal of radiation biology,* 61**,** 451-453.

Croll, T. I., O'connor, A. J., Stevens, G. W. & Cooper-White, J. J. (2004) Controllable surface modification of poly(lactic-co-glycolic acid) (PLGA) by hydrolysis or aminolysis I: physical, chemical, and theoretical aspects. *Biomacromolecules,* 5**,** 463-73.

Csuk, R., Barthel, A., Sczepek, R., Siewert, B. & Schwarz, S. (2011) Synthesis, encapsulation and antitumor activity of new betulin derivatives. *Arch Pharm (Weinheim),* 344**,** 37-49.

Cu, Y. & Saltzman, W. M. (2009) Controlled surface modification with poly(ethylene)glycol enhances diffusion of PLGA nanoparticles in human cervical mucus. *Mol Pharm,* 6**,** 173-81.

Cui, Y., Xu, Q., Chow, P. K., Wang, D. & Wang, C. H. (2013) Transferrin-conjugated magnetic silica PLGA nanoparticles loaded with doxorubicin and paclitaxel for brain glioma treatment. *Biomaterials,* 34**,** 8511-20.

Dailey, L. A. & Kissel, T. (2005) New poly(lactic-co-glycolic acid) derivatives: Modular polymers with tailored properties. *Drug Discov Today Technol,* 2**,** 7-13.

Danhier, F., Ansorena, E., Silva, J. M., Coco, R., Le Breton, A. & Preat, V. (2012a) PLGA-based nanoparticles: an overview of biomedical applications. *J Control Release,* 161**,** 505-22.

Danhier, F., Ansorena, E., Silva, J. M., Coco, R., Le Breton, A. & Préat, V. (2012b) PLGA-based nanoparticles: an overview of biomedical applications. *Journal of controlled release,* 161**,** 505-522.

Darzynkiewicz, Z., Bruno, S., Del Bino, G., Gorczyca, W., Hotz, M., Lassota, P. & Traganos, F. (1992) Features of apoptotic cells measured by flow cytometry. *Cytometry,* 13**,** 795-808.

Das, J., Das, S., Samadder, A., Bhadra, K. & Khuda-Bukhsh, A. R. (2012) Poly (lactide-co-glycolide) encapsulated extract of< i> Phytolacca decandra</i> demonstrates better intervention against induced lung adenocarcinoma in mice and on A549 cells. *European Journal of Pharmaceutical Sciences,* 47**,** 313-324.

Davda, J. & Labhasetwar, V. (2002) Characterization of nanoparticle uptake by endothelial cells. *International journal of pharmaceutics,* 233**,** 51-59.

Davies, J. M. & Viney, C. (1998) Water–mucin phases: conditions for mucus liquid crystallinity. *Thermochimica acta,* 315**,** 39-49.

Derakhshandeh, K., Erfan, M. & Dadashzadeh, S. (2007) Encapsulation of 9-nitrocamptothecin, a novel anticancer drug, in biodegradable nanoparticles: factorial design, characterization and release kinetics. *European Journal of Pharmaceutics and Biopharmaceutics,* 66**,** 34-41.

Desai, M. P., Labhasetwar, V., Amidon, G. L. & Levy, R. J. (1996) Gastrointestinal uptake of biodegradable microparticles: effect of particle size. *Pharmaceutical research,* 13**,** 1838-1845.

Desai, M. P., Labhasetwar, V., Walter, E., Levy, R. J. & Amidon, G. L. (1997) The mechanism of uptake of biodegradable microparticles in Caco-2 cells is size dependent. *Pharmaceutical research,* 14**,** 1568-1573.

Desgouilles, S., Vauthier, C., Bazile, D., Vacus, J., Grossiord, J.-L., Veillard, M. & Couvreur, P. (2003) The design of nanoparticles obtained by solvent evaporation: a comprehensive study. *Langmuir,* 19**,** 9504-9510.

Dive, C., Watson, J. V. & Workman, P. (1990) Multiparametric analysis of cell membrane permeability by two colour flow cytometry with complementary fluorescent probes. *Cytometry,* 11**,** 244-252.

Diwan, M., Elamanchili, P., Cao, M. & Samuel, J. (2004) Dose sparing of CpG oligodeoxynucleotide vaccine adjuvants by nanoparticle delivery. *Current drug delivery,* 1**,** 405-412.

Dobrovolskaia, M. A., Aggarwal, P., Hall, J. B. & Mcneil, S. E. (2008a) Preclinical studies to understand nanoparticle interaction with the immune system and its potential effects on nanoparticle biodistribution. *Mol Pharm,* 5**,** 487-95.

Dobrovolskaia, M. A., Aggarwal, P., Hall, J. B. & Mcneil, S. E. (2008b) Preclinical studies to understand nanoparticle interaction with the immune system and its potential effects on nanoparticle biodistribution. *Molecular pharmaceutics,* 5**,** 487-495.

Dobrovolskaia, M. A. & Mcneil, S. E. (2013) Understanding the correlation between< i> in vitro</i> and< i> in vivo</i> immunotoxicity tests for nanomedicines. *Journal of controlled release,* 172**,** 456-466.

Duan, X. & Lewis, R. S. (2002a) Improved haemocompatibility of cysteine-modified polymers via endogenous nitric oxide. *Biomaterials,* 23**,** 1197-203.

Duan, X. & Lewis, R. S. (2002b) Improved haemocompatibility of cysteine-modified polymers via endogenous nitric oxide. *Biomaterials,* 23**,** 1197-1203.

Dufort, S., Sancey, L. & Coll, J.-L. (2012) Physico-chemical parameters that govern nanoparticles fate also dictate rules for their molecular evolution. *Advanced Drug Delivery Reviews,* 64**,** 179-189.

Duverger, E., Pellerin-Mendes, C., Mayer, R., Roche, A.-C. & Monsigny, M. (1995) Nuclear import of glycoconjugates is distinct from the classical NLS pathway. *Journal of cell science,* 108**,** 1325-1332.

Duvvuri, M. & Krise, J. P. (2005) Intracellular drug sequestration events associated with the emergence of multidrug resistance: a mechanistic review. *Front Biosci,* 10**,** 1499-1509.

Ekdahl, K. N., Lambris, J. D., Elwing, H., Ricklin, D., Nilsson, P. H., Teramura, Y., Nicholls, I. A. & Nilsson, B. (2011) Innate immunity activation on biomaterial surfaces: a mechanistic model and coping strategies. *Adv Drug Deliv Rev,* 63**,** 1042-50.

Endicott, J. A. & Ling, V. (1989) The biochemistry of P-glycoprotein-mediated multidrug resistance. *Annual review of biochemistry,* 58**,** 137-171.

Eom, Y.-W., Kim, M. A., Park, S. S., Goo, M. J., Kwon, H. J., Sohn, S., Kim, W.-H., Yoon, G. & Choi, K. S. (2005) Two distinct modes of cell death induced by doxorubicin: apoptosis and cell death through mitotic catastrophe accompanied by senescence-like phenotype. *Oncogene,* 24**,** 4765-4777.

Fadeel, B. (2012) Clear and present danger? Engineered nanoparticles and the immune system. *Swiss Med Wkly,* 142**,** w13609.

Farokhzad, O. C., Cheng, J., Teply, B. A., Sherifi, I., Jon, S., Kantoff, P. W., Richie, J. P. & Langer, R. (2006) Targeted nanoparticle-aptamer bioconjugates for cancer chemotherapy in vivo. *Proc Natl Acad Sci U S A,* 103**,** 6315-20.

Fields, R. J., Cheng, C. J., Quijano, E., Weller, C., Kristofik, N., Duong, N., Hoimes, C., Egan, M. E. & Saltzman, W. M. (2012) Surface modified poly (• amino ester)-containing nanoparticles for plasmid DNA delivery. *Journal of controlled release,* 164**,** 41-48.

Fischer, D., Li, Y., Ahlemeyer, B., Krieglstein, J. & Kissel, T. (2003) In vitro cytotoxicity testing of polycations: influence of polymer structure on cell viability and hemolysis. *Biomaterials,* 24**,** 1121-31.

Fonseca, C., Simoes, S. & Gaspar, R. (2002) Paclitaxel-loaded PLGA nanoparticles: preparation, physicochemical characterization and in vitro anti-tumoral activity. *Journal of controlled release,* 83**,** 273-286.

Fouad, H., Elsarnagawy, T., Almajhdi, F. N. & Khalil, K. A. (2013) Preparation and in vitro thermo-mechanical characterization of electrospun PLGA nanofibers for soft and hard tissue replacement. *Int J Electrochem Sci,* 8**,** 2293-304.

Frank, D., Tyagi, C., Tomar, L., Choonara, Y. E., Du Toit, L. C., Kumar, P., Penny, C. & Pillay, V. (2014) Overview of the role of nanotechnological innovations in the detection and treatment of solid tumors. *International journal of nanomedicine,* 9**,** 589.

Fredenberg, S., Wahlgren, M., Reslow, M. & Axelsson, A. (2011) The mechanisms of drug release in poly (lactic-co-glycolic acid)-based drug delivery systems—a review. *International journal of pharmaceutics,* 415**,** 34-52.

Frost, M. C., Reynolds, M. M. & Meyerhoff, M. E. (2005a) Polymers incorporating nitric oxide releasing/generating substances for improved biocompatibility of blood-contacting medical devices. *Biomaterials,* 26**,** 1685-93.

Frost, M. C., Reynolds, M. M. & Meyerhoff, M. E. (2005b) Polymers incorporating nitric oxide releasing/generating substances for improved biocompatibility of blood-contacting medical devices. *Biomaterials,* 26**,** 1685-1693.

Fulda, S. & Debatin, K.-M. (2000) Betulinic acid induces apoptosis through a direct effect on mitochondria in neuroectodermal tumors. *Medical and Pediatric Oncology,* 35**,** 616-618.

Gangwar, R. K., Tomar, G. B., Dhumale, V. A., Zinjarde, S., Sharma, R. B. & Datar, S. (2013) Curcumin conjugated silica nanoparticles for improving bioavailability and its anticancer applications. *Journal of agricultural and food chemistry,* 61**,** 9632-9637.

Garbayo, E., Ansorena, E., Lanciego, J. L., Blanco-Prieto, M. J. & Aymerich, M. S. (2011) Long-term neuroprotection and neurorestoration by glial cell-derived neurotrophic factor microspheres for the treatment of Parkinson's disease. *Movement disorders,* 26**,** 1943-1947.

Gaspar, R. & Duncan, R. (2009) Polymeric carriers: preclinical safety and the regulatory implications for design and development of polymer therapeutics. *Adv Drug Deliv Rev,* 61**,** 1220-31.

Gaucher, G., Asahina, K., Wang, J & Leroux, K. (2009) Effect of Poly (N-vinyl-pyrrolidone)-block-poly (d,l-lactide) as coating agent on the opsonisation, phagocytosis, and pharmacokinetics of biodegradable nanoparticles. Biomacromolecules, 10, 408-416.

Golub, J. S., Kim, Y.-T., Duvall, C. L., Bellamkonda, R. V., Gupta, D., Lin, A. S., Weiss, D., Taylor, W. R. & Guldberg, R. E. (2010) Sustained VEGF delivery

via PLGA nanoparticles promotes vascular growth. *American Journal of Physiology-Heart and Circulatory Physiology,* 298**,** H1959-H1965.

Gorbet, M. B. & Sefton, M. V. (2004) Biomaterial-associated thrombosis: roles of coagulation factors, complement, platelets and leukocytes. *Biomaterials,* 25**,** 5681-5703.

Gref, R., Domb, A., Quellec, P., Blunk, T., Müller, R., Verbavatz, J. & Langer, R. (1995a) The controlled intravenous delivery of drugs using PEG-coated sterically stabilized nanospheres. *Advanced Drug Delivery Reviews,* 16**,** 215-233.

Gref, R., Domb, A., Quellec, P., Blunk, T., Müller, R. H., Verbavatz, J. M. & Langer, R. (1995b) The controlled intravenous delivery of drugs using PEG-coated sterically stabilized nanospheres. *Advanced Drug Delivery Reviews,* 16**,** 215-233.

Gref, R., Luck, M., Quellec, P., Marchand, M., Dellacherie, E., Harnisch, S., Blunk, T. & Muller, R. H. (2000) 'Stealth' corona-core nanoparticles surface modified by polyethylene glycol (PEG): influences of the corona (PEG chain length and surface density) and of the core composition on phagocytic uptake and plasma protein adsorption. *Colloids Surf B Biointerfaces,* 18**,** 301-313.

Gref, R., Minamitake, Y., Peracchia, M. T., Trubetskoy, V., Torchilin, V. & Langer, R. (1994) Biodegradable long-circulating polymeric nanospheres. *Science,* 263**,** 1600-1603.

Gromnicova, R., Davies, H.A., Sreekanthredyy, P., Romero, I.A & Lund, T. (2013) Glucose coated gold nanoparticles transfer across human brain endothelium and enter astrocytes in vitro. *Plos One,* 12.

Guo, J., Gao, X., Su, L., Xia, H., Gu, G., Pang, Z., Jiang, X., Yao, L., Chen, J. & Chen, H. (2011) Aptamer-functionalized PEG–PLGA nanoparticles for enhanced anti-glioma drug delivery. *Biomaterials,* 32**,** 8010-8020.

Gupta, H., Aqil, M., Khar, R. K., Ali, A., Bhatnagar, A. & Mittal, G. (2010) Sparfloxacin-loaded PLGA nanoparticles for sustained ocular drug delivery. *Nanomedicine: Nanotechnology, Biology and Medicine,* 6**,** 324-333.

Gupta, S. C., Prasad, S., Kim, J. H., Patchva, S., Webb, L. J., Priyadarsini, I. K. & Aggarwal, B. B. (2011) Multitargeting by curcumin as revealed by molecular interaction studies. *Natural product reports,* 28**,** 1937-1955.

Hair, P. S., Echague, C. G., Rohn, R. D., Krishna, N. K., Nyalwidhe, J. O. & Cunnion, K. M. (2012) Hyperglycemic conditions inhibit C3-mediated immunologic control of Staphylococcus aureus. *J Transl Med,* 10**,** 35.

Hand, C. M., Vender, J. R. & Black, P. (1998) Chemotherapy in experimental brain tumor, part 1: in vitro colorimetric MTT assay. *Journal of neuro-oncology,* 36**,** 1-6.

Hatakeyama, H., Akita, H. & Harashima, H. (2011) A multifunctional envelope type nano device (MEND) for gene delivery to tumours based on the EPR effect: a strategy for overcoming the PEG dilemma. *Adv Drug Deliv Rev,* 63**,** 152-60.

Hatakeyama, H., Akita, H. & Harashima, H. (2013a) The polyethyleneglycol dilemma: advantage and disadvantage of PEGylation of liposomes for systemic genes and nucleic acids delivery to tumors. *Biol Pharm Bull,* 36**,** 892-9.

Hatakeyama, H., Akita, H. & Harashima, H. (2013b) The polyethyleneglycol dilemma: Advantage and disadvantage of pegylation of liposomes for systemic genes and nucleic acids delivery to tumors. *Biological and Pharmaceutical Bulletin,* 36**,** 892-899.

He, F., Li, J. & Ye, J. (2013) Improvement of cell response of the poly (lactic-co-glycolic acid)/calcium phosphate cement composite scaffold with unidirectional pore structure by the surface immobilization of collagen via plasma treatment. *Colloids and Surfaces B: Biointerfaces,* 103**,** 209-216.

Herrwerth, S., Eck, W., Reinhardt, S. & Grunze, M. (2003) Factors that determine the protein resistance of oligoether self-assembled monolayers-internal hydrophilicity, terminal hydrophilicity, and lateral packing density. *Journal of the American Chemical Society,* 125**,** 9359-9366.

Hersel, U., Dahmen, C. & Kessler, H. (2003) RGD modified polymers: biomaterials for stimulated cell adhesion and beyond. *Biomaterials,* 24**,** 4385-4415.

Higaki, M., Ishihara, T., Izumo, N., Takatsu, M. & Mizushima, Y. (2005) Treatment of experimental arthritis with poly (D, L-lactic/glycolic acid) nanoparticles encapsulating betamethasone sodium phosphate. *Annals of the rheumatic diseases,* 64**,** 1132-1136.

Higuchi, A., Shirano, K., Harashima, M., Yoon, B. O., Hara, M., Hattori, M. & Imamura, K. (2002) Chemically modified polysulfone hollow fibers with vinylpyrrolidone having improved blood compatibility. *Biomaterials,* 23**,** 2659-2666.

Hillaireau, H. & Couvreur, P. (2009) Nanocarriers' entry into the cell: relevance to drug delivery. *Cellular and Molecular Life Sciences,* 66**,** 2873-2896.

Hlady, V. V. & Buijs, J. (1996) Protein adsorption on solid surfaces. *Curr Opin Biotechnol,* 7**,** 72-7.

Holmlin, R. E., Chen, X., Chapman, R. G., Takayama, S. & Whitesides, G. M. (2001) Zwitterionic SAMs that resist nonspecific adsorption of protein from aqueous buffer. *Langmuir,* 17**,** 2841-2850.

Hu, K., Li, J., Shen, Y., Lu, W., Gao, X., Zhang, Q. & Jiang, X. (2009) Lactoferrin-conjugated PEG–PLA nanoparticles with improved brain delivery:< i> In vitro</i> and< i> in vivo</i> evaluations. *Journal of controlled release,* 134**,** 55-61.

Hua, J., Sakamoto, K. & Nagaoka, I. (2002) Inhibitory actions of glucosamine, a therapeutic agent for osteoarthritis, on the functions of neutrophils. *Journal of leukocyte biology,* 71**,** 632-640.

Hua, J., Suguro, S., Iwabuchi, K., Tsutsumi-Ishii, Y., Sakamoto, K. & Nagaoka, I. (2004) Glucosamine, a naturally occurring amino monosaccharide, suppresses the ADP-mediated platelet activation in humans. *Inflammation Research,* 53**,** 680-688.

Huang, J., Zhang, H., Yu, Y., Chen, Y., Wang, D., Zhang, G., Zhou, G., Liu, J., Sun, Z. & Sun, D. (2014) Biodegradable self-assembled nanoparticles of poly (D, L-lactide-co-glycolide)/hyaluronic acid block copolymers for target delivery of docetaxel to breast cancer. *Biomaterials,* 35**,** 550-566.

Hurtta, M., Pitkänen, I. & Knuutinen, J. (2004) Melting behaviour of D-sucrose, D-glucose and D-fructose. *Carbohydrate research,* 339**,** 2267-2273.

Hwang, W.-S., Chen, L.-M., Huang, S.-H., Wang, C.-C. & Tseng, M. T. (1993) Prediction of chemotherapy response in human leukemia using< i> in vitro</i> chemosensitivity test. *Leukemia research,* 17**,** 685-688.

Ishida, T., Atobe, K., Wang, X. & Kiwada, H. (2006) Accelerated blood clearance of PEGylated liposomes upon repeated injections: effect of doxorubicin-encapsulation and high-dose first injection. *Journal of controlled release,* 115**,** 251-258.

Jain, R. A. (2000a) The manufacturing techniques of various drug loaded biodegradable poly (lactide-< i> co</i>-glycolide)(PLGA) devices. *Biomaterials,* 21**,** 2475-2490.

Jain, R. A. (2000b) The manufacturing techniques of various drug loaded biodegradable poly(lactide-co-glycolide) (PLGA) devices. *Biomaterials,* 21**,** 2475-90.

Johansen, P., Men, Y., Audran, R., Corradin, G., Merkle, H. P. & Gander, B. (1998) Improving stability and release kinetics of microencapsulated tetanus toxoid by co-encapsulation of additives. *Pharmaceutical research,* 15**,** 1103-1110.

Johnson, K. T., Fath, K. R., Henricus, M. M. & Banerjee, I. A. (2009) Self-Assembly and Growth of Smart Cell-Adhesive Mucin-Bound Microtubes. *Soft Materials,* 7**,** 21-36.

Jokerst, J. V., Lobovkina, T., Zare, R. N. & Gambhir, S. S. (2011) Nanoparticle PEGylation for imaging and therapy. *Nanomedicine (Lond),* 6**,** 715-28.

Kamaly, N., Xiao, Z., Valencia, P. M., Radovic-Moreno, A. F. & Farokhzad, O. C. (2012) Targeted polymeric therapeutic nanoparticles: design, development and clinical translation. *Chem Soc Rev,* 41**,** 2971-3010.

Karmali, P. P. & Simberg, D. (2011) Interactions of nanoparticles with plasma proteins: implication on clearance and toxicity of drug delivery systems. *Expert Opin Drug Deliv,* 8**,** 343-57.

Kesimer, M., Makhov, A. M., Griffith, J. D., Verdugo, P. & Sheehan, J. K. (2010) Unpacking a gel-forming mucin: a view of MUC5B organization after granular release. *Am J Physiol Lung Cell Mol Physiol,* 298**,** L15-22.

Khalil, N. M., Do Nascimento, T. C., Casa, D. M., Dalmolin, L. F., De Mattos, A. C., Hoss, I., Romano, M. A. & Mainardes, R. M. (2013) Pharmacokinetics of curcumin-loaded PLGA and PLGA-PEG blend nanoparticles after oral administration in rats. *Colloids Surf B Biointerfaces,* 101**,** 353-60.

Khemani, M., Sharon, M. & Sharon, M. pH Dependent Encapsulation of Doxorubicin in PLGA.

Kiefer, T. L. & Becker, R. C. (2009) Inhibitors of platelet adhesion. *Circulation,* 120**,** 2488-2495.

Kim, D., El-Shall, H., Dennis, D. & Morey, T. (2005) Interaction of PLGA nanoparticles with human blood constituents. *Colloids Surf B Biointerfaces,* 40**,** 83-91.

Klugherz, B. D., Jones, P. L., Cui, X., Chen, W., Meneveau, N. F., Defelice, S., Connolly, J., Wilensky, R. L. & Levy, R. J. (2000) Gene delivery from a DNA controlled-release stent in porcine coronary arteries. *Nature biotechnology,* 18**,** 1181-1184.

Kocbek, P., Obermajer, N., Cegnar, M., Kos, J. & Kristl, J. (2007) Targeting cancer cells using PLGA nanoparticles surface modified with monoclonal antibody. *Journal of controlled release,* 120**,** 18-26.

Koh, L. B., Rodriguez, I. & Zhou, J. (2008) Platelet adhesion studies on nanostructured poly (lactic-co-glycolic-acid)–carbon nanotube composite. *Journal of Biomedical Materials Research Part A,* 86**,** 394-401.

Komarov, P., Ovchinnikov, M., Khizhnyak, S., Alekseev, V., Mikhailov, I. & Pakhomov, P. (2013) On Molecular Gelation Mechanism of L-Cysteine Based Hydrogel.

Kratz, F. & Elsadek, B. (2012) Clinical impact of serum proteins on drug delivery. *J Control Release,* 161**,** 429-45.

Kumar, R., Kulkarni, A., Nagesha, D. K. & Sridhar, S. (2012) In vitro evaluation of theranostic polymeric micelles for imaging and drug delivery in cancer. *Theranostics,* 2**,** 714-22.

Kumari, A., Yadav, S. K. & Yadav, S. C. (2010) Biodegradable polymeric nanoparticles based drug delivery systems. *Colloids Surf B Biointerfaces,* 75**,** 1-18.

Kutwin, M., Sawosz, E., Kurantowicz, N., Strojny, B. & Chwalibog, A. (2014) Structural damage of chicken red blood cells exposed to platinum nanoparticles and cisplatin. *Nanoscale Research Letters,* 9**,** 257.

Lee, D.-W., Shirley, S. A., Lockey, R. F. & Mohapatra, S. S. (2006) Thiolated chitosan nanoparticles enhance anti-inflammatory effects of intranasally delivered theophylline. *Respir Res,* 7**,** 112.

Lee, S.-Y., Cheng, J.-X. & Gad, S. C. 2010. Clearance of Nanoparticles During Circulation. *Pharmaceutical Sciences Encyclopedia.* John Wiley & Sons, Inc.

Lei, T., Srinivasan, S., Tang, Y., Manchanda, R., Nagesetti, A., Fernandez-Fernandez, A. & Mcgoron, A. J. (2011) Comparing cellular uptake and cytotoxicity of targeted drug carriers in cancer cell lines with different drug resistance mechanisms. *Nanomedicine: Nanotechnology, Biology and Medicine,* 7**,** 324-332.

Lestelius, M., Liedberg, B., Lundström, I. & Tengvall, P. (1994) In vitro Plasma protein adsorption and kallikrein formation on 3-mercaptopropionic acid, L-cysteine and glutathione immobilized onto gold. *Journal of biomedical materials research,* 28**,** 871-880.

Lewinski, N., Colvin, V. & Drezek, R. (2008) Cytotoxicity of nanoparticles. *Small,* 4**,** 26-49.

Li, T. & Takeoka, S. (2014) Enhanced cellular uptake of maleimide-modified liposomes via thiol-mediated transport. *Int J Nanomedicine,* 9**,** 2849-61.

Li, X., Radomski, A., Corrigan, O. I., Tajber, L., De Sousa Menezes, F., Endter, S., Medina, C. & Radomski, M. W. (2009) Platelet compatibility of PLGA, chitosan and PLGA-chitosan nanoparticles. *Nanomedicine,* 4**,** 735-746.

Li, Y.-P., Pei, Y.-Y., Zhang, X.-Y., Gu, Z.-H., Zhou, Z.-H., Yuan, W.-F., Zhou, J.-J., Zhu, J.-H. & Gao, X.-J. (2001) PEGylated PLGA nanoparticles as protein carriers: synthesis, preparation and biodistribution in rats. *Journal of controlled release,* 71**,** 203-211.

Li, Y., Wang, J., Wientjes, M. G. & Au, J. L. (2012) Delivery of nanomedicines to extracellular and intracellular compartments of a solid tumor. *Adv Drug Deliv Rev,* 64**,** 29-39.

Lindblad, M., Lestelius, M., Johansson, A., Tengvall, P. & Thomsen, P. (1997) Cell and soft tissue interactions with methyl-and hydroxyl-terminated alkane thiols on gold surfaces. *Biomaterials,* 18**,** 1059-1068.

Linnartz, B., Kopatz, J., Tenner, A. J. & Neumann, H. (2012) Sialic acid on the neuronal glycocalyx prevents complement C1 binding and complement receptor-3-mediated removal by microglia. *The Journal of Neuroscience,* 32**,** 946-952.

Liu, F.-C., Su, C.-R., Wu, T.-Y., Su, S.-G., Yang, H.-L., Lin, J. H.-Y. & Wu, T.-S. (2011) Efficient 1H-NMR Quantitation and Investigation of N-Acetyl-D-glucosamine (GlcNAc) and N, N'-Diacetylchitobiose (GlcNAc) 2 from Chitin. *International journal of molecular sciences,* 12**,** 5828-5843.

Liu, Y., Tan, J., Thomas, A., Ou-Yang, D. & Muzykantov, V. R. (2012a) The shape of things to come: importance of design in nanotechnology for drug delivery. *Therapeutic delivery,* 3**,** 181-194.

Liu, Y., Tan, J., Thomas, A., Ou-Yang, D. & Muzykantov, V. R. (2012b) The shape of things to come: importance of design in nanotechnology for drug delivery. *Ther Deliv,* 3**,** 181-94.

Loscalzo, J. (1992) Antiplatelet and antithrombotic effects of organic nitrates. *Am J Cardiol,* 70**,** 18B-22B.

Lowe, S. W. & Lin, A. W. (2000) Apoptosis in cancer. *Carcinogenesis,* 21**,** 485-495.

Lü, J.-M., Wang, X., Marin-Muller, C., Wang, H., Lin, P. H., Yao, Q. & Chen, C. (2009) Current advances in research and clinical applications of PLGA-based nanotechnology. *Expert Review of Molecular Diagnostics,* 9**,** 325-341.

Lu, J. M., Wang, X., Marin-Muller, C., Wang, H., Lin, P. H., Yao, Q. & Chen, C. (2009) Current advances in research and clinical applications of PLGA-based nanotechnology. *Expert Rev Mol Diagn,* 9**,** 325-41.

Lu, W. & Park, T. G. (1995) Protein release from poly (lactic-co-glycolic acid) microspheres: protein stability problems. *PDA Journal of Pharmaceutical Science and Technology,* 49**,** 13-19.

Maeda, H., Wu, J., Sawa, T., Matsumura, Y. & Hori, K. (2000) Tumor vascular permeability and the EPR effect in macromolecular therapeutics: a review. *J Control Release,* 65**,** 271-84.

Mahmoudi, M., Lynch, I., Ejtehadi, M. R., Monopoli, M. P., Bombelli, F. B. & Laurent, S. (2011) Protein-nanoparticle interactions: opportunities and challenges. *Chem Rev,* 111**,** 5610-37.

Makadia, H. K. & Siegel, S. J. (2011) Poly Lactic-co-Glycolic Acid (PLGA) as Biodegradable Controlled Drug Delivery Carrier. *Polymers (Basel),* 3**,** 1377-1397.

Markman, J. L., Rekechenetskiy, A., Holler, E. & Ljubimova, J. Y. (2013) Nanomedicine therapeutic approaches to overcome cancer drug resistance. *Adv Drug Deliv Rev,* 65**,** 1866-79.

Marradi, M., Chiodo, F., Garcia, I. & Penadés, S. (2013) Glyconanoparticles as multifunctional and multimodal carbohydrate systems. *Chemical Society Reviews,* 42**,** 4728-4745.

Martins, M. C. L., Ratner, B. D. & Barbosa, M. A. (2003) Protein adsorption on mixtures of hydroxyl-and methyl-terminated alkanethiols self-assembled monolayers. *Journal of Biomedical Materials Research Part A,* 67**,** 158-171.

Matsumura, Y. & Maeda, H. (1986) A new concept for macromolecular therapeutics in cancer chemotherapy: mechanism of tumoritropic accumulation of proteins and the antitumor agent smancs. *Cancer research,* 46**,** 6387-6392.

Maz•re, M., Pan•, A., • tefan, L., Silion, M., B•lan, M., Bandur, G. & Rusnac, L. Novel D-glucose Based Glycomonomers Synthesis and Characterization.

Mccarron, P. A., Marouf, W. M., Donnelly, R. F. & Scott, C. (2008) Enhanced surface attachment of protein-type targeting ligands to poly (lactide-co-glycolide) nanoparticles using variable expression of polymeric acid functionality. *Journal of Biomedical Materials Research Part A,* 87**,** 873-884.

Mehta, R. C., Thanoo, B. & Deluca, P. P. (1996) Peptide containing microspheres from low molecular weight and hydrophilic poly (< i> d</i>,< i> l</i>-lactide-co-glycolide). *Journal of controlled release,* 41**,** 249-257.

Melamed, M. R., Lindmo, T., Mendelsohn, M. L. & Bigler, R. D. (1991) Flow cytometry and sorting. *American Journal of Clinical Oncology,* 14**,** 90.

Mishra, S., Webster, P. & Davis, M. E. (2004) PEGylation significantly affects cellular uptake and intracellular trafficking of non-viral gene delivery particles. *European Journal of Cell Biology,* 83**,** 97-111.

Mittal, G., Sahana, D., Bhardwaj, V. & Ravi Kumar, M. (2007) Estradiol loaded PLGA nanoparticles for oral administration: Effect of polymer molecular weight and copolymer composition on release behavior< i> in vitro</i> and< i> in vivo</i>. *Journal of controlled release,* 119**,** 77-85.

Moghimi, S. M., Andersen, A. J., Ahmadvand, D., Wibroe, P. P., Andresen, T. L. & Hunter, A. C. (2011) Material properties in complement activation. *Adv Drug Deliv Rev,* 63**,** 1000-7.

Moghimi, S. M., Hunter, A. C. & Murray, J. C. (2001) Long-circulating and target-specific nanoparticles: theory to practice. *Pharmacol Rev,* 53**,** 283-318.

Moghimi, S. M., Hunter, A. C. & Murray, J. C. (2005) Nanomedicine: current status and future prospects. *FASEB J,* 19**,** 311-30.

Moghimi, S. M., Muir, I. S., Illum, L., Davis, S. S. & Kolb-Bachofen, V. (1993) Coating particles with a block co-polymer (poloxamine-908) suppresses opsonization but permits the activity of dysopsonins in the serum. *Biochimica et Biophysica Acta (BBA) - Molecular Cell Research,* 1179**,** 157-165.

Moghimi, S. M. & Szebeni, J. (2003) Stealth liposomes and long circulating nanoparticles: critical issues in pharmacokinetics, opsonization and protein-binding properties. *Prog Lipid Res,* 42**,** 463-78.

Mohammad, A. K. & Reineke, J. J. (2013) Quantitative detection of PLGA nanoparticle degradation in tissues following intravenous administration. *Mol Pharm,* 10**,** 2183-9.

Mohanty, C. & Sahoo, S. K. (2010) The< i> in vitro</i> stability and< i> in vivo</i> pharmacokinetics of curcumin prepared as an aqueous nanoparticulate formulation. *Biomaterials,* 31**,** 6597-6611.

Mollnes, T., Haga, H.-J., Brun, J., Nielsen, E., Sjöholm, A., Sturfeldt, G., Mårtensson, U., Bergh, K. & Rekvig, O. (1999) Complement activation in

patients with systemic lupus erythematosus without nephritis. *Rheumatology,* 38**,** 933-940.

Monsigny, M., Midoux, P., Mayer, R. & Roche, A.-C. (1999) Glycotargeting: influence of the sugar moiety on both the uptake and the intracellular trafficking of nucleic acid carried by glycosylated polymers. *Bioscience reports,* 19**,** 125-132.

Moros, M., HernáEz, B., Garet, E., Dias, J. T., SáEz, B., Grazú, V., GonzáLez-FernáNdez, A. F., Alonso, C. & De La Fuente, J. S. M. (2012) Monosaccharides versus PEG-functionalized NPs: influence in the cellular uptake. *ACS nano,* 6**,** 1565-1577.

Mosmann, T. (1983) Rapid colorimetric assay for cellular growth and survival: application to proliferation and cytotoxicity assays. *Journal of immunological methods,* 65**,** 55-63.

Mu, L. & Feng, S.-S. (2003) PLGA/TPGS nanoparticles for controlled release of paclitaxel: effects of the emulsifier and drug loading ratio. *Pharmaceutical research,* 20**,** 1864-1872.

Mukerjee, A. & Vishwanatha, J. K. (2009) Formulation, characterization and evaluation of curcumin-loaded PLGA nanospheres for cancer therapy. *Anticancer Res,* 29**,** 3867-75.

Mullauer, F. B., Van Bloois, L., Daalhuisen, J. B., Ten Brink, M. S., Storm, G., Medema, J. P., Schiffelers, R. M. & Kessler, J. H. (2011) Betulinic acid delivered in liposomes reduces growth of human lung and colon cancers in mice without causing systemic toxicity. *Anti-cancer drugs,* 22**,** 223-233.

Mundargi, R. C., Babu, V. R., Rangaswamy, V., Patel, P. & Aminabhavi, T. M. (2008) Nano/micro technologies for delivering macromolecular therapeutics using poly(d,l-lactide-co-glycolide) and its derivatives. *Journal of Controlled Release,* 125**,** 193-209.

Musumeci, T., Ventura, C. A., Giannone, I., Ruozi, B., Montenegro, L., Pignatello, R. & Puglisi, G. (2006) PLA/PLGA nanoparticles for sustained release of docetaxel. *International journal of pharmaceutics,* 325**,** 172-179.

Naahidi, S., Jafari, M., Edalat, F., Raymond, K., Khademhosseini, A. & Chen, P. (2013) Biocompatibility of engineered nanoparticles for drug delivery. *J Control Release,* 166**,** 182-94.

Nel, A. E., Madler, L., Velegol, D., Xia, T., Hoek, E. M. V., Somasundaran, P., Klaessig, F., Castranova, V. & Thompson, M. (2009) Understanding biophysicochemical interactions at the nano-bio interface. *Nat Mater,* 8**,** 543-557.

Nelson, J., Gibbons, E., Pickett, K. R., Streeter, M., Warcup, A. O., Yeung, C. H.-Y., Judd, A. M. & Bell, J. D. (2011) Relationship between membrane permeability and specificity of human secretory phospholipase A< sub> 2</sub> isoforms during cell death. *Biochimica et Biophysica Acta (BBA)-Biomembranes,* 1808**,** 1913-1920.

Ng, E. W., Shima, D. T., Calias, P., Cunningham, E. T., Guyer, D. R. & Adamis, A. P. (2006) Pegaptanib, a targeted anti-VEGF aptamer for ocular vascular disease. *Nature reviews drug discovery,* 5**,** 123-132.

Niu, X., Zou, W., Liu, C., Zhang, N. & Fu, C. (2009) Modified nanoprecipitation method to fabricate DNA-loaded PLGA nanoparticles. *Drug development and industrial pharmacy,* 35**,** 1375-1383.

Nobs, L., Buchegger, F., Gurny, R. & Allemann, E. (2003) Surface modification of poly(lactic acid) nanoparticles by covalent attachment of thiol groups by means of three methods. *Int J Pharm,* 250**,** 327-37.

O'hagan, D., Jeffery, H. & Davis, S. (1994) The preparation and characterization ofpoly (lactide-co-glycolide) microparticles: III. Microparticle/polymer degradation rates and the in vitro release of a model protein. *International journal of pharmaceutics,* 103**,** 37-45.

Okada, H. & Toguchi, H. (1995) Biodegradable microspheres in drug delivery. *Crit Rev Ther Drug Carrier Syst,* 12**,** 1-99.

Oliveira, M. F., Guimarães, P. P., Gomes, A. D., Suárez, D. & Sinisterra, R. D. (2013) Strategies to target tumors using nanodelivery systems based on biodegradable polymers, aspects of intellectual property, and market. *Journal of chemical biology,* 6**,** 7-23.

Ostuni, E., Chapman, R. G., Holmlin, R. E., Takayama, S. & Whitesides, G. M. (2001) A survey of structure-property relationships of surfaces that resist the adsorption of protein. *Langmuir,* 17**,** 5605-5620.

Owens, D. E., 3rd & Peppas, N. A. (2006) Opsonization, biodistribution, and pharmacokinetics of polymeric nanoparticles. *Int J Pharm,* 307**,** 93-102.

Owens Iii, D. E. & Peppas, N. A. (2006) Opsonization, biodistribution, and pharmacokinetics of polymeric nanoparticles. *International journal of pharmaceutics,* 307**,** 93-102.

Pan Ch, J., Tang, J. J., Weng, Y. J., Wang, J. & Huang, N. (2006) Preparation, characterization and anticoagulation of curcumin-eluting controlled biodegradable coating stents. *J Control Release,* 116**,** 42-9.

Panariti, A., Miserocchi, G. & Rivolta, I. (2012) The effect of nanoparticle uptake on cellular behavior: disrupting or enabling functions? *Nanotechnol Sci Appl,* 5**,** 87-100.

Panyam, J. & Labhasetwar, V. (2003) Biodegradable nanoparticles for drug and gene delivery to cells and tissue. *Advanced Drug Delivery Reviews,* 55**,** 329-347.

Panyam, J., Williams, D., Dash, A., Leslie-Pelecky, D. & Labhasetwar, V. (2004) Solid-state solubility influences encapsulation and release of hydrophobic drugs from PLGA/PLA nanoparticles. *J Pharm Sci,* 93**,** 1804-14.

Panyam, J., Zhou, W.-Z., Prabha, S., Sahoo, S. K. & Labhasetwar, V. (2002) Rapid endo-lysosomal escape of poly (DL-lactide-co-glycolide) nanoparticles: implications for drug and gene delivery. *The FASEB Journal,* 16**,** 1217-1226.

Papisov, M. I. (1998) Theoretical considerations of RES-avoiding liposomes: Molecular mechanics and chemistry of liposome interactions. *Advanced Drug Delivery Reviews,* 32**,** 119-138.

Park, J., Fong, P. M., Lu, J., Russell, K. S., Booth, C. J., Saltzman, W. M. & Fahmy, T. M. (2009) PEGylated PLGA nanoparticles for the improved delivery of doxorubicin. *Nanomedicine,* 5**,** 410-8.

Patel, M. M., Smart, J. D., Nevell, T. G., Ewen, R. J., Eaton, P. J. & Tsibouklis, J. (2003) Mucin/poly (acrylic acid) interactions: a spectroscopic investigation of mucoadhesion. *Biomacromolecules,* 4**,** 1184-1190.

Patil, Y., Sadhukha, T., Ma, L. & Panyam, J. (2009) Nanoparticle-mediated simultaneous and targeted delivery of paclitaxel and tariquidar overcomes tumor drug resistance. *J Control Release,* 136**,** 21-9.

Patil, Y. B., Swaminathan, S. K., Sadhukha, T., Ma, L. & Panyam, J. (2010) The use of nanoparticle-mediated targeted gene silencing and drug delivery to overcome tumor drug resistance. *Biomaterials,* 31**,** 358-365.

Peracchia, M. T., Harnisch, S., Pinto-Alphandary, H., Gulik, A., Dedieu, J. C., Desmaële, D., D'angelo, J., Müller, R. H. & Couvreur, P. (1999) Visualization of in vitro protein-rejecting properties of PEGylated stealth® polycyanoacrylate nanoparticles. *Biomaterials,* 20**,** 1269-1275.

Petros, R. A. & Desimone, J. M. (2010) Strategies in the design of nanoparticles for therapeutic applications. *Nat Rev Drug Discov,* 9**,** 615-27.

Prasad, S., Cody, V., Saucier-Sawyer, J. K., Saltzman, W. M., Sasaki, C. T., Edelson, R. L., Birchall, M. A. & Hanlon, D. J. (2011) Polymer nanoparticles containing tumor lysates as antigen delivery vehicles for dendritic cell–based antitumor immunotherapy. *Nanomedicine: Nanotechnology, Biology and Medicine,* 7**,** 1-10.

Qaddoumi, M. G., Ueda, H., Yang, J., Davda, J., Labhasetwar, V. & Lee, V. H. (2004) The characteristics and mechanisms of uptake of PLGA nanoparticles in rabbit conjunctival epithelial cell layers. *Pharmaceutical research,* 21**,** 641-648.

Qiu, L. Y. & Bae, Y. H. (2006) Polymer architecture and drug delivery. *Pharm Res,* 23**,** 1-30.

Rabuka, D., Parthasarathy, R., Lee, G. S., Chen, X., Groves, J. T. & Bertozzi, C. R. (2007) Hierarchical Assembly of Model Cell Surfaces: Synthesis of Mucin Mimetic Polymers and Their Display on Supported Bilayers. *Journal of the American Chemical Society,* 129**,** 5462-5471.

Rabuka, D., Forstner, M.B., Groves, J.T & Bertozzi, C.R. (2008) Non covalent cell surface engineering: Incorporation of bioactive sythetic glycopolymers into cellular membranes. *Journal of the American Chemical Society*, 18, 5947-5953.

Ramachandran, C., Rodriguez, S., Ramachandran, R., Nair, P. R., Fonseca, H., Khatib, Z., Escalon, E. & Melnick, S. J. (2005) Expression profiles of apoptotic genes induced by curcumin in human breast cancer and mammary epithelial cell lines. *Anticancer research,* 25**,** 3293-3302.

Ratner, B. D. (1993) New ideas in biomaterials science--a path to engineered biomaterials. *J Biomed Mater Res,* 27**,** 837-50.

Ratner, B. D., Hoffman, A. S., Schoen, F. J. & Lemons, J. E. 2013. Introduction - Biomaterials Science: An Evolving, Multidisciplinary Endeavor. *In:* LEMONS, B. D. R. S. H. J. S. E. (ed.) *Biomaterials Science (Third Edition).* Academic Press.

Ravi Kumar, M., Bakowsky, U. & Lehr, C. (2004) Preparation and characterization of cationic PLGA nanospheres as DNA carriers. *Biomaterials,* 25**,** 1771-1777.

Reddy, L. H. & Murthy, R. (2005) Etoposide-loaded nanoparticles made from glyceride lipids: formulation, characterization, in vitro drug release, and stability evaluation. *AAPS PharmSciTech,* 6**,** E158-E166.

Reddy, M. K., Wu, L., Kou, W., Ghorpade, A. & Labhasetwar, V. (2008) Superoxide dismutase-loaded PLGA nanoparticles protect cultured human neurons under oxidative stress. *Applied biochemistry and biotechnology,* 151**,** 565-577.

Remaut, K., De Smedt, S. C. & Demeester, J. (2012) Exploring the relation between the intracellular fate and biological activity of oligodeoxynucleotide containing nanoparticles. *Proceedings of the Belgian Royal Academies of Medicine,* 1**,** 140-156.

Ricci, M. S. & Zong, W.-X. (2006) Chemotherapeutic approaches for targeting cell death pathways. *The oncologist,* 11**,** 342-357.

Rieger, J., Passirani, C., Benoit, J. P., VanButsele, K., Jérôme, R. & Jérôme, C. (2006) Synthesis of Amphiphilic Copolymers of Poly(ethylene oxide) and Poly(ϵ-caprolactone) with Different Architectures, and Their Role in the Preparation of Stealthy Nanoparticles. *Advanced Functional Materials,* 16**,** 1506-1514.

Rosca, I. D., Watari, F. & Uo, M. (2004) Microparticle formation and its mechanism in single and double emulsion solvent evaporation. *J Control Release,* 99**,** 271-80.

Rosen, J. E. & Gu, F. X. (2011) Surface functionalization of silica nanoparticles with cysteine: a low-fouling zwitterionic surface. *Langmuir,* 27**,** 10507-10513.

S V, T. (2012) A HPLC Method for Determination of Ursolic Acid and Betulinic Acids from their Methanolic Extracts of Vitex Negundo Linn. *Journal of Analytical & Bioanalytical Techniques.*

Sah, H., Thoma, L. A., Desu, H. R., Sah, E. & Wood, G. C. (2013) Concepts and practices used to develop functional PLGA-based nanoparticulate systems. *International journal of nanomedicine,* 8**,** 747.

Sah, H., Toddywala, R. & Chien, Y. W. (1994) The influence of biodegradable microcapsule formulations on the controlled release of a protein. *Journal of controlled release,* 30**,** 201-211.

Sahoo, S. K. & Labhasetwar, V. (2005) Enhanced antiproliferative activity of transferrin-conjugated paclitaxel-loaded nanoparticles is mediated via sustained intracellular drug retention. *Molecular pharmaceutics,* 2**,** 373-383.

Sahoo, S. K., Panyam, J., Prabha, S. & Labhasetwar, V. (2002) Residual polyvinyl alcohol associated with poly (D, L-lactide-co-glycolide) nanoparticles affects their physical properties and cellular uptake. *Journal of controlled release,* 82**,** 105-114.

Salmaso, S. & Caliceti, P. (2013) Stealth properties to improve therapeutic efficacy of drug nanocarriers. *J Drug Deliv,* 2013**,** 374252.

Sandberg, T., Carlsson, J. & Ott, M. K. (2009a) Interactions between human neutrophils and mucin-coated surfaces. *Journal of Materials Science: Materials in Medicine,* 20**,** 621-631.

Sandberg, T., Karlsson Ott, M., Carlsson, J., Feiler, A. & Caldwell, K. D. (2009b) Potential use of mucins as biomaterial coatings. II. Mucin coatings affect the conformation and neutrophil-activating properties of adsorbed host proteins—Toward a mucosal mimic. *Journal of Biomedical Materials Research Part A,* 91**,** 773-785.

Sanna, V., Roggio, A. M., Posadino, A. M., Cossu, A., Marceddu, S., Mariani, A., Alzari, V., Uzzau, S., Pintus, G. & Sechi, M. (2011) Novel docetaxel-loaded

nanoparticles based on poly(lactide-co-caprolactone) and poly(lactide-co-glycolide-co-caprolactone) for prostate cancer treatment: formulation, characterization, and cytotoxicity studies. *Nanoscale Res Lett,* 6**,** 260.

Sarkar, S., Lee, G. Y., Wong, J. Y. & Desai, T. A. (2006) Development and characterization of a porous micro-patterned scaffold for vascular tissue engineering applications. *Biomaterials,* 27**,** 4775-4782.

Savla, R., Taratula, O., Garbuzenko, O. & Minko, T. (2011) Tumor targeted quantum dot-mucin 1 aptamer-doxorubicin conjugate for imaging and treatment of cancer. *Journal of controlled release,* 153**,** 16-22.

Semete, B., Booysen, L., Lemmer, Y., Kalombo, L., Katata, L., Verschoor, J. & Swai, H. S. (2010) In vivo evaluation of the biodistribution and safety of PLGA nanoparticles as drug delivery systems. *Nanomedicine: Nanotechnology, Biology and Medicine,* 6**,** 662-671.

Shah, S., Cha, Y. & Pitt, C. (1992) Poly (glycolic acid-co-DL-lactic acid): diffusion or degradation controlled drug delivery? *Journal of controlled release,* 18**,** 261-270.

Shahani, K. & Panyam, J. (2011) Highly loaded, sustained-release microparticles of curcumin for chemoprevention. *Journal of pharmaceutical sciences,* 100**,** 2599-2609.

Shaikh, J., Ankola, D., Beniwal, V., Singh, D. & Kumar, M. (2009) Nanoparticle encapsulation improves oral bioavailability of curcumin by at least 9-fold when compared to curcumin administered with piperine as absorption enhancer. *European Journal of Pharmaceutical Sciences,* 37**,** 223-230.

Shi, L., Ardehali, R., Caldwell, K. D. & Valint, P. (2000) Mucin coating on polymeric material surfaces to suppress bacterial adhesion. *Colloids and Surfaces B: Biointerfaces,* 17**,** 229-239.

Shi, L., Miller, C., Caldwell, K. D. & Valint, P. (1999) Effects of mucin addition on the stability of oil–water emulsions. *Colloids and Surfaces B: Biointerfaces,* 15**,** 303-312.

Shive, M. S. & Anderson, J. M. (1997) Biodegradation and biocompatibility of PLA and PLGA microspheres. *Adv Drug Deliv Rev,* 28**,** 5-24.

Shubhra, Q. T., Feczkó, T., Kardos, A. F., Tóth, J., Mackova, H., Horak, D., Dósa, G. & Gyenis, J. (2013) Co-encapsulation of human serum albumin and superparamagnetic iron oxide in PLGA nanoparticles: Part II. Effect of process variables on protein model drug encapsulation efficiency. *Journal of microencapsulation,* 31**,** 156-165.

Siegel, S. J., Kahn, J. B., Metzger, K., Winey, K. I., Werner, K. & Dan, N. (2006) Effect of drug type on the degradation rate of PLGA matrices. *Eur J Pharm Biopharm,* 64**,** 287-93.

Siepmann, J. & Siepmann, F. (2008) Mathematical modeling of drug delivery. *International journal of pharmaceutics,* 364**,** 328-343.

Simi, M., Leardi, S., Tebano, M., Castelli, M., Costantini, F. & Speranza, V. (1987) Raised plasma concentrations of platelet factor 4 (PF4) in Crohn's disease. *Gut,* 28**,** 336-338.

Simon, L. C. & Sabliov, C. M. (2013) Time Analysis of Poly (Lactic-Co-Glycolic) Acid Nanoparticle Uptake by Major Organs Following Acute Intravenous and Oral Administration in Mice and Rats. *Industrial Biotechnology,* 9**,** 19-23.

Singh, R. J., Hogg, N., Joseph, J. & Kalyanaraman, B. (1996) Mechanism of nitric oxide release from S-nitrosothiols. *J Biol Chem,* 271**,** 18596-603.

Smola, M., Vandamme, T. & Sokolowski, A. (2008) Nanocarriers as pulmonary drug delivery systems to treat and to diagnose respiratory and non respiratory diseases. *International journal of nanomedicine,* 3**,** 1.

Soica, C., Danciu, C., Savoiu-Balint, G., Borcan, F., Ambrus, R., Zupko, I., Bojin, F., Coricovac, D., Ciurlea, S. & Avram, S. (2014) Betulinic Acid in Complex with a Gamma-Cyclodextrin Derivative Decreases Proliferation and in Vivo Tumor Development of Non-Metastatic and Metastatic B164A5 Cells. *International journal of molecular sciences,* 15**,** 8235-8255.

Song, K. C., Lee, H. S., Choung, I. Y., Cho, K. I., Ahn, Y. & Choi, E. J. (2006) The effect of type of organic phase solvents on the particle size of poly (d, l-lactide-co-glycolide) nanoparticles. *Colloids and Surfaces A: Physicochemical and Engineering Aspects,* 276**,** 162-167.

Spenlehauer, G., Vert, M., Benoit, J. P. & Boddaert, A. (1989) In vitro and In vivo degradation of poly(D,L lactide/glycolide) type microspheres made by solvent evaporation method. *Biomaterials,* 10**,** 557-563.

Stevanovi•, M., Radulovi•, A., Jordovi•, B. & Uskokovi•, D. (2008) Poly (DL-lactide-co-glycolide) nanospheres for the sustained release of folic acid. *Journal of Biomedical Nanotechnology,* 4**,** 349-358.

Stevanovic, M. & Uskokovic, D. (2009) Poly (lactide-co-glycolide)-based micro and nanoparticles for the controlled drug delivery of vitamins. *Current Nanoscience,* 5**,** 1-14.

Sunoqrot, S., Bae, J. W., Pearson, R. M., Shyu, K., Liu, Y., Kim, D.-H. & Hong, S. (2012) Temporal control over cellular targeting through hybridization of folate-targeted dendrimers and PEG-PLA nanoparticles. *Biomacromolecules,* 13**,** 1223-1230.

Suresh, C., Zhao, H., Gumbs, A., Chetty, C. S. & Bose, H. S. (2012) New ionic derivatives of betulinic acid as highly potent anti-cancer agents. *Bioorganic & medicinal chemistry letters,* 22**,** 1734-1738.

Surolia, A. & Bachhawat, B. K. (1977) Monosialoganglioside liposome-entrapped enzyme uptake by hepatic cells. *Biochimica et Biophysica Acta (BBA) - General Subjects,* 497**,** 760-765.

Svensson, O. & Arnebrant, T. (2010) Mucin layers and multilayers—Physicochemical properties and applications. *Current Opinion in Colloid & Interface Science,* 15**,** 395-405.

Tahara, K., Sakai, T., Yamamoto, H., Takeuchi, H. & Kawashima, Y. (2008a) Establishing chitosan coated PLGA nanosphere platform loaded with wide variety of nucleic acid by complexation with cationic compound for gene delivery. *International journal of pharmaceutics,* 354**,** 210-216.

Tahara, K., Sakai, T., Yamamoto, H., Takeuchi, H. & Kawashima, Y. (2008b) Establishing chitosan coated PLGA nanosphere platform loaded with wide variety of nucleic acid by complexation with cationic compound for gene delivery. *Int J Pharm,* 354**,** 210-6.

Tang, L., Liu, L. & Elwing, H. B. (1998) Complement activation and inflammation triggered by model biomaterial surfaces. *Journal of biomedical materials research,* 41**,** 333-340.

Tewes, F., Munnier, E., Antoon, B., Ngaboni Okassa, L., Cohen-Jonathan, S., Marchais, H., Douziech-Eyrolles, L., Souce, M., Dubois, P. & Chourpa, I. (2007a) Comparative study of doxorubicin-loaded poly(lactide-co-glycolide) nanoparticles prepared by single and double emulsion methods. *Eur J Pharm Biopharm,* 66**,** 488-92.

Tewes, F., Munnier, E., Antoon, B., Ngaboni Okassa, L., Cohen-Jonathan, S., Marchais, H., Douziech-Eyrolles, L., Soucé, M., Dubois, P. & Chourpa, I. (2007b) Comparative study of doxorubicin-loaded poly (lactide-co-glycolide) nanoparticles prepared by single and double emulsion methods. *European Journal of Pharmaceutics and Biopharmaceutics,* 66**,** 488-492.

Thasneem, Y. M., Rekha, M. R., Sajeesh, S. & Sharma, C. P. (2013a) Biomimetic mucin modified PLGA nanoparticles for enhanced blood compatibility. *J Colloid Interface Sci,* 409**,** 237-44.

Thasneem, Y. M., Sajeesh, S. & Sharma, C. P. (2011) Effect of thiol functionalization on the hemo-compatibility of PLGA nanoparticles. *J Biomed Mater Res A,* 99**,** 607-17.

Thasneem, Y. M., Sajeesh, S. & Sharma, C. P. (2013b) Glucosylated polymeric nanoparticles: a sweetened approach against blood compatibility paradox. *Colloids Surf B Biointerfaces,* 108**,** 337-44.

Thevenot, P., Hu, W. & Tang, L. (2008) Surface chemistry influence implant biocompatibility. *Current topics in medicinal chemistry,* 8**,** 270.

Thomas, C., Rawat, A., Hope-Weeks, L. & Ahsan, F. (2011) Aerosolized PLA and PLGA nanoparticles enhance humoral, mucosal and cytokine responses to hepatitis B vaccine. *Molecular pharmaceutics,* 8**,** 405-415.

Tian, J. & Yu, J. (2011) Poly (lactic-co-glycolic acid) nanoparticles as candidate DNA vaccine carrier for oral immunization of Japanese flounder (< i> Paralichthys olivaceus</i>) against lymphocystis disease virus. *Fish & shellfish immunology,* 30**,** 109-117.

Tidwell, C. D., Ertel, S. I., Ratner, B. D., Tarasevich, B. J., Atre, S. & Allara, D. L. (1997) Endothelial Cell Growth and Protein Adsorption on Terminally Functionalized, Self-Assembled Monolayers of Alkanethiolates on Gold. *Langmuir,* 13**,** 3404-3413.

Tobio, M., Gref, R., Sanchez, A., Langer, R. & Alonso, M. (1998) Stealth PLA-PEG nanoparticles as protein carriers for nasal administration. *Pharmaceutical research,* 15**,** 270-275.

Tosi, G., Vergoni, A. V., Ruozi, B., Bondioli, L., Badiali, L., Rivasi, F., Costantino, L., Forni, F. & Vandelli, M. A. (2010) Sialic acid and glycopeptides conjugated PLGA nanoparticles for central nervous system targeting: In vivo pharmacological evidence and biodistribution. *J Control Release,* 145**,** 49-57.

Toti, U. S., Guru, B. R., Hali, M., Mcpharlin, C. M., Wykes, S. M., Panyam, J. & Whittum-Hudson, J. A. (2011) Targeted delivery of antibiotics to intracellular chlamydial infections using PLGA nanoparticles. *Biomaterials,* 32**,** 6606-6613.

Travo, A., Piot, O., Wolthuis, R., Gobinet, C., Manfait, M., Bara, J., Forgue-Lafitte, M. E. & Jeannesson, P. (2010) IR spectral imaging of secreted mucus: a promising new tool for the histopathological recognition of human colonic adenocarcinomas. *Histopathology,* 56**,** 921-931.

Tsai, Y. M., Chien, C. F., Lin, L. C. & Tsai, T. H. (2011) Curcumin and its nano-formulation: the kinetics of tissue distribution and blood-brain barrier penetration. *Int J Pharm,* 416**,** 331-8.

Ulbrich, W. & Lamprecht, A. (2009) Targeted drug-delivery approaches by nanoparticulate carriers in the therapy of inflammatory diseases. *Journal of The Royal Society Interface***,** rsif20090285.

Vauthier, C. & Bouchemal, K. (2009) Methods for the preparation and manufacture of polymeric nanoparticles. *Pharmaceutical research,* 26**,** 1025-1058.

Veerapandian, M., Jang, C.-H. & Yun, K. Year. Fabrication of glucosamine functionalized gold/silver glyconanoparticles from nanoclusters for biomedical nanotechnology: Multifunctional glyconanoparticles. *In:* Nanotechnology, 2009. IEEE-NANO 2009. 9th IEEE Conference on, 2009. IEEE, 469-472.

Verdugo, P. (2012) Supramolecular dynamics of mucus. *Cold Spring Harb Perspect Med,* 2**,** a009597.

Verma, A. & Stellacci, F. (2010) Effect of surface properties on nanoparticle–cell interactions. *Small,* 6**,** 12-21.

Vittaz, M., Bazile, D., Spenlehauer, G., Verrecchia, T., Veillard, M., Puisieux, F. & Labarre, D. (1996) Effect of PEO surface density on long-circulating PLA-PEO nanoparticles which are very low complement activators. *Biomaterials,* 17**,** 1575-1581.

Walczyk, D., Bombelli, F. B., Monopoli, M. P., Lynch, I. & Dawson, K. A. (2010) What the cell "sees" in bionanoscience. *Journal of the American Chemical Society,* 132**,** 5761-5768.

Wang, A. Z., Langer, R. & Farokhzad, O. C. (2012a) Nanoparticle delivery of cancer drugs. *Annu Rev Med,* 63**,** 185-98.

Wang, B., He, X., Zhang, Z., Zhao, Y. & Feng, W. (2012b) Metabolism of Nanomaterials in Vivo: Blood Circulation and Organ Clearance. *Accounts of Chemical Research,* 46**,** 761-769.

Wang, G., Wang, J. J., Yang, G. Y., Du, S. M., Zeng, N., Li, D. S., Li, R. M., Chen, J. Y., Feng, J. B. & Yuan, S. H. (2012c) Effects of quercetin nanoliposomes on C6 glioma cells through induction of type III programmed cell death. *International journal of nanomedicine,* 7**,** 271.

Wang, Y.-X., Robertson, J., Spillman, W., Jr. & Claus, R. (2004) Effects of the Chemical Structure and the Surface Properties of Polymeric Biomaterials on Their Biocompatibility. *Pharmaceutical Research,* 21**,** 1362-1373.

Williams, D. F. (2008) On the mechanisms of biocompatibility. *Biomaterials,* 29**,** 2941-53.

Wischke, C. & Schwendeman, S. P. (2008) Principles of encapsulating hydrophobic drugs in PLA/PLGA microparticles. *Int J Pharm,* 364**,** 298-327.

Wohlfart, S., Khalansky, A. S., Gelperina, S., Maksimenko, O., Bernreuther, C., Glatzel, M. & Kreuter, J. (2011) Efficient chemotherapy of rat glioblastoma using doxorubicin-loaded PLGA nanoparticles with different stabilizers. *PLoS One,* 6**,** e19121.

Woo, J.-H., Kim, Y.-H., Choi, Y.-J., Kim, D.-G., Lee, K.-S., Bae, J. H., Chang, J.-S., Jeong, Y.-J., Lee, Y. H. & Park, J.-W. (2003) Molecular mechanisms of curcumin-induced cytotoxicity: induction of apoptosis through generation of

reactive oxygen species, down-regulation of Bcl-XL and IAP, the release of cytochrome c and inhibition of Akt. *Carcinogenesis,* 24**,** 1199-1208.

Xie, J. & Wang, C. H. (2007) Encapsulation of proteins in biodegradable polymeric microparticles using electrospray in the Taylor cone-jet mode. *Biotechnology and bioengineering,* 97**,** 1278-1290.

Xie, X., Tao, Q., Zou, Y., Zhang, F., Guo, M., Wang, Y., Wang, H., Zhou, Q. & Yu, S. (2011) PLGA nanoparticles improve the oral bioavailability of curcumin in rats: characterizations and mechanisms. *Journal of agricultural and food chemistry,* 59**,** 9280-9289.

Xiong, S., Zhao, X., Heng, B. C., Ng, K. W. & Loo, J. S. C. (2011) Cellular uptake of Poly-(D, L-lactide-co-glycolide)(PLGA) nanoparticles synthesized through solvent emulsion evaporation and nanoprecipitation method. *Biotechnology journal,* 6**,** 501-508.

Xu, T., Zhang, N., Nichols, H. L., Shi, D. & Wen, X. (2007) Modification of nanostructured materials for biomedical applications. *Materials Science and Engineering: C,* 27**,** 579-594.

Yadav, A. K., Mishra, P., Mishra, A. K., Mishra, P., Jain, S. & Agrawal, G. P. (2007) Development and characterization of hyaluronic acid–anchored PLGA nanoparticulate carriers of doxorubicin. *Nanomedicine: Nanotechnology, Biology and Medicine,* 3**,** 246-257.

Yallapu, M. M., Gupta, B. K., Jaggi, M. & Chauhan, S. C. (2010) Fabrication of curcumin encapsulated PLGA nanoparticles for improved therapeutic effects in metastatic cancer cells. *J Colloid Interface Sci,* 351**,** 19-29.

Yang, X., Zhang, X., Liu, Z., Ma, Y., Huang, Y. & Chen, Y. (2008) High-efficiency loading and controlled release of doxorubicin hydrochloride on graphene oxide. *The Journal of Physical Chemistry C,* 112**,** 17554-17558.

Yoo, H. S., Lee, K. H., Oh, J. E. & Park, T. G. (2000) In vitro and in vivo anti-tumor activities of nanoparticles based on doxorubicin-PLGA conjugates. *J Control Release,* 68**,** 419-31.

Yoo, H. S. & Park, T. G. (2004) Folate-receptor-targeted delivery of doxorubicin nano-aggregates stabilized by doxorubicin–PEG–folate conjugate. *Journal of controlled release,* 100**,** 247-256.

Yoon, J. J., Nam, Y. S., Kim, J. H. & Park, T. G. (2002) Surface immobilization of galactose onto aliphatic biodegradable polymers for hepatocyte culture. *Biotechnology and bioengineering,* 78**,** 1-10.

Yu, D.-H., Lu, Q., Xie, J., Fang, C. & Chen, H.-Z. (2010) Peptide-conjugated biodegradable nanoparticles as a carrier to target paclitaxel to tumor neovasculature. *Biomaterials,* 31**,** 2278-2292.

Zentner, G. M., Rathi, R., Shih, C., Mcrea, J. C., Seo, M.-H., Oh, H., Rhee, B., Mestecky, J., Moldoveanu, Z. & Morgan, M. (2001) Biodegradable block copolymers for delivery of proteins and water-insoluble drugs. *Journal of controlled release,* 72**,** 203-215.

Zhang, Y., Chan, H. F. & Leong, K. W. (2013) Advanced materials and processing for drug delivery: the past and the future. *Adv Drug Deliv Rev,* 65**,** 104-20.

Zhao, L. & Feng, S. S. (2010) Enhanced oral bioavailability of paclitaxel formulated in vitamin E-TPGS emulsified nanoparticles of biodegradable polymers: In vitro and in vivo studies. *Journal of pharmaceutical sciences,* 99**,** 3552-3560.

Zuco, V., Supino, R., Righetti, S. C., Cleris, L., Marchesi, E., Gambacorti-Passerini, C. & Formelli, F. (2002) Selective cytotoxicity of betulinic acid on tumor cell lines, but not on normal cells. *Cancer letters,* 175**,** 17-25.

List of Publications

[1] **Y.M. Thasneem**, M.R. Rekha, S. Sajeesh, C.P. Sharma (2011) Biomimetic Mucin Modified PLGA nanoparticles for Enhanced Blood Compatibility. ***Journal of Colloid and Interface Science,*** 409, 237-44.

[2] **Y.M. Thasneem**, S. Sajeesh, C.P. Sharma (2013) Glycosylated polymeric nanoparticles; a sweetened approach against blood compatibility paradox. ***Colloids and Surfaces B: Biointerfaces***, 108, 337-44.

[3] **Y.M. Thasneem**, S. Sajeesh, C.P. Sharma (2013) Effect of thiol functionalisation on the hemocompatibility of PLGA nanoparticles. ***Journal of Biomedical Material Research –Part A***, 99A, 607-617.

[4] **Y.M. Thasneem**, Chandra P Sharma; Book Chapter entitled 'In Vitro Characterization of Cell-Biomaterials Interaction' in the book titled "***Characterization of Biomaterials***", edited by Bandhopadhyay and Bose, released 25th March, 2013

Conference Proceedings

1. **Oral Presentation**: "Functionalised PLGA nanoparticles for controlled chemotherapy" at **Tissue Engineering and Regenerative Medicine International Society-Asia Pacific** held at Shanghai & Wuzhen October 23-26, 2013.
2. **Oral Presentation**: "Biomimetic mucin modified PLGA nanoparticles for better blood compatibility" at the **International Conference on Design of Biomaterials** held at Indian Institute of Science, Bangalore December 9-11, 2012.
3. **Oral Presentation**: "Glucosylated PLGA nanoparticles: a sweetened approach against blood compatibility paradox" at the **9th World Biomaterials Congress** held at Chengdu, China on June 1-5, 2012.

4. **Oral Presentation:** “Thiol functionalisation of PLGA nanoparticles for controlled drug delivery” at the 25th Kerala Science Congress held at Techno Park, Thiruvananthapuram, Kerala, India held on January, 2013.

Curriculum Vitae

Education

PhD (2010 till date) **:** Enrolled in January 2010 at SCTIMST, Kerala, India.

Advisor : Dr. Chandra P Sharma, FBAO, FBSE

M.Sc (2007-2009) : Biochemical Technology with **72%.**

Madurai Kamaraj University, Madurai, India.

B.Sc (2003-2006) **:** Biotechnology with **70%.**

Mar Ivanios College**,** Kerala University, Kerala, India.

Home address

West Winds

XXII/492(D)

Bazar P.O

Near Vettakkaran Junction

Alleppy-688001